UNIVERSITÀ DEGLI STUDI DI MILANO

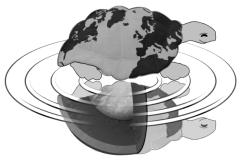

Dottorato di Ricerca in Scienze della Terra
Ciclo XXVII

The Tethys (Cismon core) and Pacific (DSDP Site 463) Ocean record of OAE1a: a taxonomic and quantitative analyses of planktonic foraminifera and their biological response across the Selli Level equivalent

Ph.D. Thesis

Alessia Barchetta
Matricola R09570

Tutore	**Anno Accademico**	*Coordinatore*
Dott. Maria Rose Petrizzo	**2013-2014**	**Prof.ssa Elisabetta Erba**

Alla mia Famiglia

"Nec me ulla res delectabit, licet sit eximia et salutaris, quam mihi uni sciturus sum. Si cum hac exceptione detur sapientia, ut illam inclusam teneam nec enuntiem, reiciam: nullius boni sine socio iucunda possessio est."

Lucius Annaei Senecae (Epistulae Morales ad Lucilium)

"No knowledge, though excellent, will give me any delight if I learn only for myself. If you grant me the wisdom with this limitation, to hold it inside me refusing to spread it, I will reject it: no joy comes from the possession of all good things, if you can not share them with others."

Lucio Annea Seneca (Letters to Lucilio)

CONTENTS

Abstract

The early Aptian (121 to 118 million years ago) represents a case history of excess CO_2 derived from a major volcanic episode, namely the emplacement of the Ontong Java Plateau. During this time-interval, oceans experienced a global phenomenon of widespread deposition of organic carbon-rich sediments under oxygen-depleted conditions, called the Oceanic Anoxic Event 1a (OAE1a). The sedimentary expression of the OAE1a is represented by the Selli Level, a regional marker-bed identified in the Umbria-Marche area (central Italy) consisting of laminated black shales rich in organic matter and low carbonate content, alternated with radiolarian silts.

This thesis is aimed at investigating the OAE1a across the Selli Level equivalents at DSDP Site 463 (Mid-Pacific Mountains) and in the Cismon core (Southern Alps, northern Italy) in order to provide a detailed and quantitative study of the planktonic foraminiferal assemblages, because a quantitative documentation in terms of species composition, variation in shell sizes and absolute abundances is still lacking. This study is performed on pelagic sediments and both sections are well-dated through bio-, magneto- and chemostratigraphy.

The project was divided in four distinct phases: 1) taxonomic and biostratigraphic analyses at the stereomicroscope, and SEM (Scanning Electron Microscope) to identify genera and species; 2) morphometric analyses of foraminifera to measure the variations in population size in washed residues (measure of the maximum diameter of each species using SEM images); 3) quantitative analyses to evaluate fluctuations in abundance at genera level (and species where possible) in thin sections and washed residues; 4) integration of results with geochemical, nannoplankton and sedimentological data and interpretations.

Taxonomic and biostratigraphic analyses reveal that planispiral (genus *Globigerinelloides*), trochospiral (genus *Hedbergella*), globigeriniform with globular chambers (genera *Gorbachikella* and *Gubkinella*) and pseudo-planispiral taxa with very elongate chambers (genus *Leupoldina*) occur at both studied sites, whereas trochospiral and planispiral taxa with elongate chambers (genera *Lilliputianella* and *Globigerinelloides*) are found only in the Cismon core.

Shell size measurements show a general increase from the base to the top of the studied interval at both sites (much higher at Cismon core) due to an increase of calcification. The group with the highest range of variation in shell size is represented by the Globigerinelloidids, followed by Lilliputianellids and then by Hedbergellids.

Planktonic foraminiferal abundances and comparison with the nannoconid abundance data reveal that both groups responded to variations in surface-water fertility, temperature and CO_2-induced acidification. In particular, when nannoconids underwent a biocalcification decline and crisis (started ~1 Ma before OAE1a), planktonic foraminifera decreased too.

At the onset of the OAE1a, both calcareous groups show a marked decline that can be related to widespread meso- to eutrophic conditions, combined with excess CO_2 in the ocean - atmosphere system. No extinctions within nannoconids and planktonic foraminifera have been observed in the OAE1a interval, and both calcareous groups can be considered as virtually absent. At Cismon core after the decline, nannoconids resume in the middle part of the Selli Level equivalent and continue to increase even above it, mirroring the $\delta^{13}C$ trend, but never become so abundant as before the OAE1a.

Planktonic foraminifera remain stable and start to increase significantly just above the Selli Level equivalent, where they become more abundant than before the OAE1a. The different timing recovery between the two calcareous groups could be justified by the higher susceptibility to dissolution of planktonic foraminifera than nannoconids.

Ecological interpretations of planktonic foraminifera reveal that: at both sites the genus *Hedbergella* is the most common component of the foraminiferal fauna across the studied interval and, thus, considered the most opportunistic taxon. The genus *Globigerinelloides* is a typical meso-oligotrophic taxon, while *Lilliputianella* and *Leupoldina* are meso-eutrophic taxa that likely proliferated in oxygen - depleted, deep and cool waters associated to a possible expansion of the OMZ (Oxygen Minimum Zone). The high values in abundances of the 3 groups of planktonic foraminifera, and their fluctuations in abundance above the Selli Level equivalent, can be related to the ecological competition among them, where planispirals resulted to be the most efficient and successful competitors compared to the pseudo-planispiral and trochospiral taxa.

The data and results presented here contribute to the understanding of the evolution of early Cretaceous (Barremian-Aptian) planktonic foraminifera, to the improving of the

biostratigraphic correlations on global scale, and provide additional and new interpretations of the response of planktonic foraminifera to ocean acidification.

My results emphasize the planktonic foraminiferal ability to evolve and diversify in a time-interval of complex and profound perturbation of the ocean-atmosphere system without undergoing extinction and, on the contrary, showing significant capacity of adaptation.

Chapter 1
Introduction

My PhD research project is focused on the study of the Barremian - Aptian planktonic foraminiferal assemblages across the OAE1a with the aim to model and quantify the planktonic foraminiferal response to ocean acidification across the Cretaceous OAEs (Oceanic Anoxic Events) and to understand if and/or to which extent the foraminiferal responses (e.g. shell size and composition changes) under excess CO_2 are comparable to those observed in the modern assemblages (e.g. Barker & Elderfield, 2002; Moy *et al*., 2009).

Planktonic foraminifera are marine heterotrophic protists with a calcium carbonate shell commonly divided into chambers that are added during growth. Cytoplasm inside the test contains eukaryotic cellular organelles, supplemented by fibrillar bodies, which allow to control the buoyancy (Hemleben *et al*., 1989). Outside the shell, cytoplasm is stretched into thin, anastomosing strands (rhizopodia), which serves to collect food particles and transport them toward the primary opening of the shell (aperture). The structure and composition of the test wall is important to the classification of the group and being foraminifera small, abundant and often extremely diverse, they are in many respects ideal biostratigraphic markers for marine rocks.

They are widespread in the global ocean, consist of both cosmopolitan and endemic taxa, have a very long evolutionary history, and are most sensitive to environmental change in the ocean-atmosphere system. For these reasons, planktonic foraminifera have been widely used in biostratigraphy and represent an useful tool to investigate the Cretaceous period (145 to 65 Ma), a particular time characterized by a prolonged greenhouse stage due to massive injection of carbon into the atmosphere-ocean system (Armstrong & Brasier, 2005).

The value of foraminiferal calcite in terms of recorder of chemical and isotopic signals was identified by Emiliani (1954a, 1954b) which understood that stable isotopic signals extracted from planktonic foraminifera could be a standard tool for the recognition of glacial cycles and orbital pacing of the ice-ages (Shackleton & Opdyke, 1973; Hays *et al.*, 1976).

The record of planktonic foraminiferal evolution through the Cretaceous is characterized by periods of diversification that alternate with periods of stasis when the assemblages apparently underwent little or no changes (Fig. 1.1).

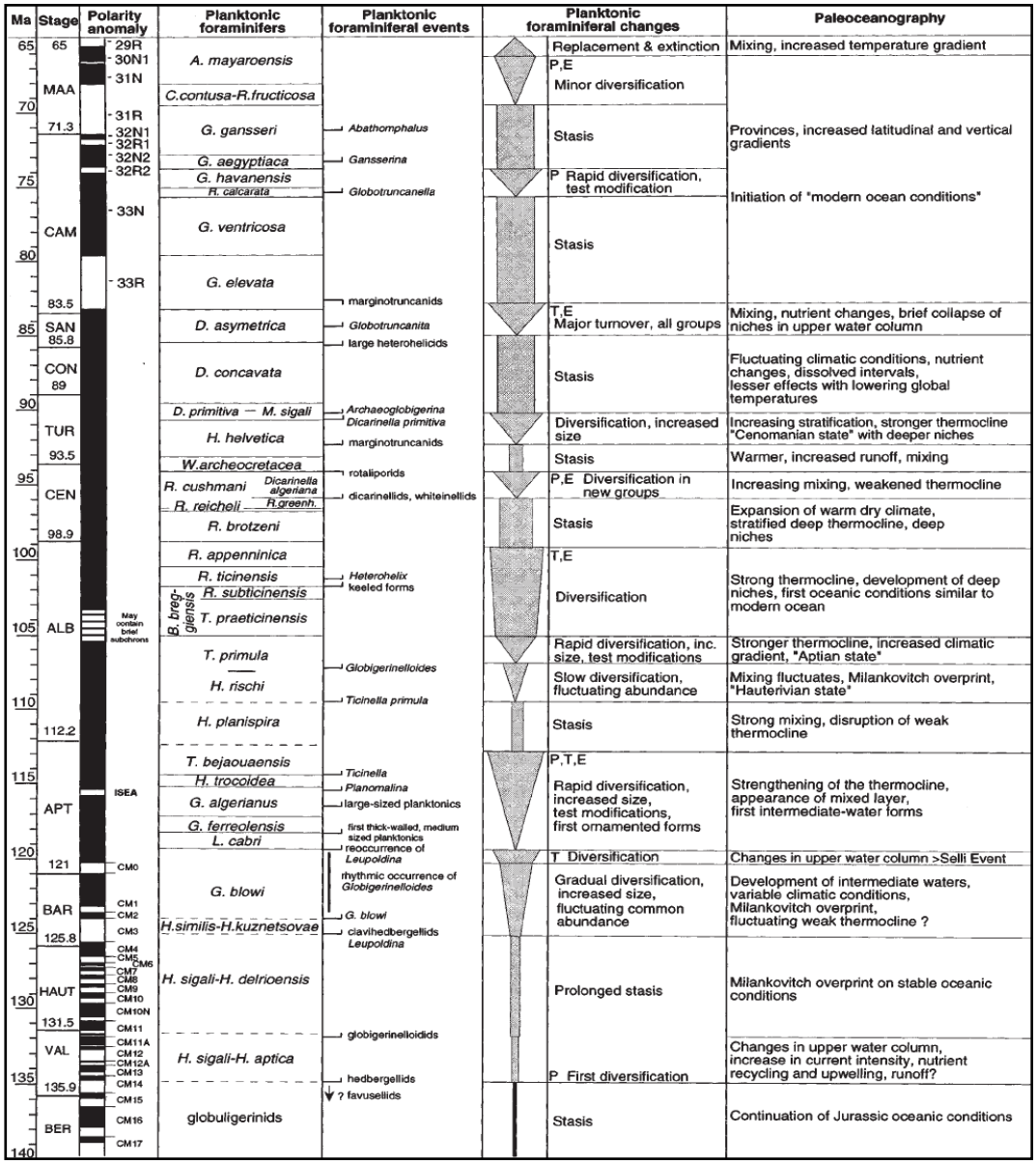

Figure 1.1. Planktonic foraminiferal evolutionary patterns and paleoceanographic changes through the Cretaceous plotted against planktonic foraminiferal zonal scheme and major stratigraphic events, magnetostratigraphy, and absolute age (from Erba *et al*., 1995, Channell *et al*., 1995). Arrows for evolutionary changes not in scale and exaggerated for changes in diversification. P: precursor events; T: turnover; E: extinctions. From Premoli Silva & Sliter, 1999.

Premoli Silva & Sliter (1999) recognize three principal intervals in terms of evolutionary and paleoceanographic changes:

a) the first interval extends from the first diversification in the early Valanginian until the uppermost Aptian showing a continuously increasing diversification that is interrupted by a single episode of moderate turnover near the Selli Event, an episode of organic carbon-rich (C_{org}-rich) sediment deposition greenhouse climate conditions in the late early Aptian (Coccioni *et al*., 1992; Erba, 1994).

b) the second interval starts from the Aptian/Albian boundary, another C_{org}-rich episode (Bréhéret *et al*., 1986; Tornaghi *et al*., 1989; Arthur *et al*., 1990) and extends until the latest Albian. New data from Petrizzo *et al*. (2012; 2013) and Kennedy *et al.* (2014) reveal that the interval labelled as a period of stasis (Fig. 1.1) by Premoli Silva & Sliter (1999) instead corresponds to an abrupt planktonic foraminiferal turnover across the Aptian/Albian boundary interval. The faunal turnover, recognized at the Col de Pré-Guittard section, in the Vocontian Basin (southeast France) occurs across the Kilian Level and is concomitant with a 1‰ negative $\delta^{13}C$ excursion in bulk carbonate. The Aptian-Albian planktonic foraminiferal turnover could be considered as the most dramatic event in the evolutionary history of Cretaceous planktonic foraminifera, with a change from large-sized and heavily ornamented species in the latest Aptian to small-sized globigeriniform specimens in the earliest Albian (Fig. 1.2).

c) The third interval, from near the top of the Albian until the end of the Cretaceous is characterized by short periods of rapid diversification and turnover separated by longer periods of stasis except around the C_{org}-rich Bonarelli Event (OAE2) near the Cenomanian/Turonian boundary (Arthur *et al*., 1990), when the cycles of alternation were strongly accelerated (two periods of diversification separated by a stasis within < 6 m.y.).

During the Cretaceous, the Earth system has experienced extreme environmental conditions resulting from the natural input of large amounts of CO_2. These perturbations appear to have been caused by major magmatic-tectonic episodes, perhaps augmented by release of gas hydrate reservoirs (Jenkyns, 2010). Under such extreme conditions, the oceans experienced prolonged global anoxia, known as Oceanic Anoxic Events (OAEs), when unusually large amounts of organic matter accumulated in marine sediments (Schlanger & Jenkyns, 1976).

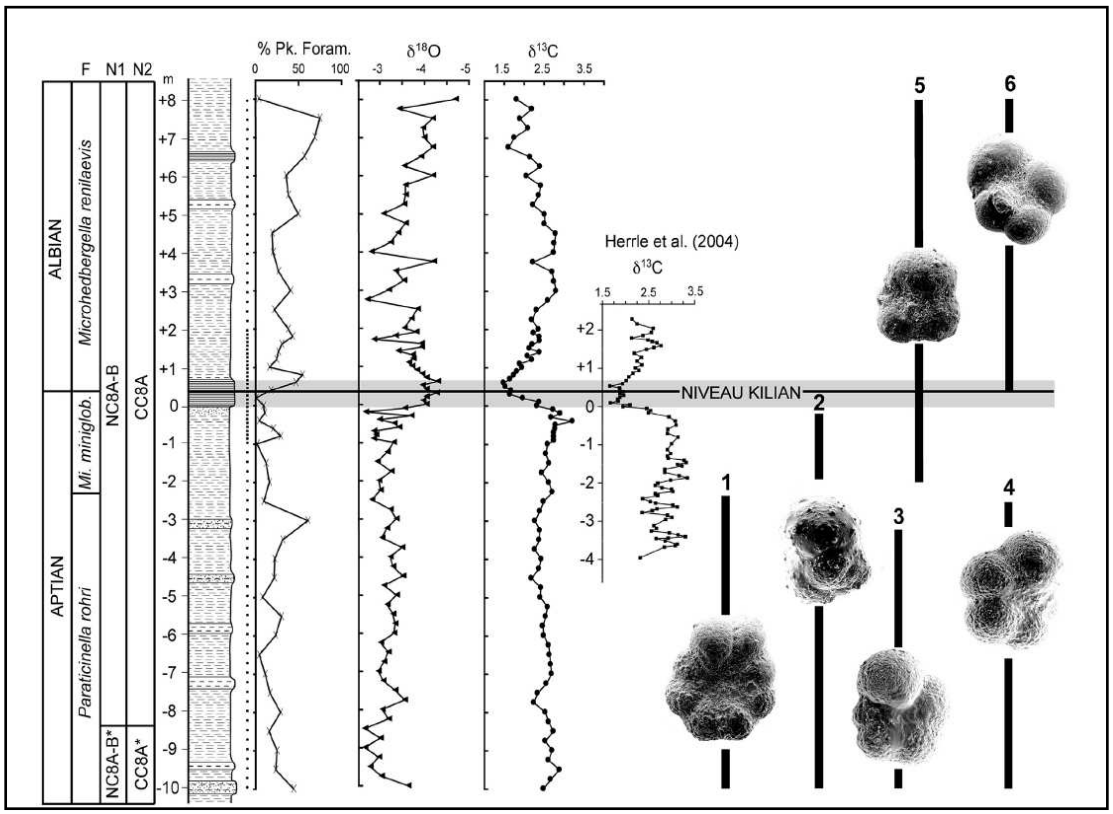

Figure 1.2. Abundance (%) of planktonic foraminifera and oxygen- and carbon stable isotope stratigraphy from Petrizzo *et al*. (2012), and carbon-isotope data from Herrle (2002) through the Niveau Kilian at Pré-Guittard. Species illustrated (not to scale) with their ranges include: 1: *Paraticinella rohri*; 2: *Pseudoguembelitria blakenosensis*; 3: *Hedbergella infracretacea*; 4: *Hedbergella aptiana*; 5: *Microhedbergella miniglobularis*; 6: *Microhedbergella renilaevis*. From Kennedy *et al*., 2014.

This thesis is aimed at investigating one of these extreme case-histories, namely the early Aptian Oceanic Anoxic Event 1a (OAE1a), in order to provide a detailed and quantitative study of the planktonic foraminiferal assemblages across the Selli Level equivalents at DSDP Site 463 (Mid-Pacific Mountains) and in the Cismon core (Southern Alps, northern Italy) because a quantitative documentation in terms of species composition, variation in shell sizes and absolute abundances is still lacking.

The project was divided in four distinct phases:

a) taxonomic and biostratigraphic analyses at the stereomicroscope, and SEM (Scanning Electron Microscope) to identify genera and species;

b) morphometric analyses of foraminifera to measure the variations in population size in washed residues (measure of the maximum diameter of each species using SEM images);

c) quantitative analyses to evaluate fluctuations in abundance at genera level (and species where possible) in thin sections and washed residues;

d) integration of results with geochemical, nannoplankton and sedimentological data and interpretations.

The data and results presented here contribute to the understanding of the evolution of early Cretaceous planktonic foraminifera, to the improving of the biostratigraphic correlations on a global scale, and provide additional and new interpretation of the response of planktonic foraminifera to ocean acidification.

Chapter 2
Oceanic Anoxic Events (OAEs)

During the Mesozoic and, in particular in the Cretaceous time, was observed a common occurrence of carbon cycle disturbances sometimes associated with the widespread development and deposition of organic-carbon rich sediments deposited in both shallow and deep marine environment. The dark colour, high organic carbon content, typical fine laminations, and lack of bioturbations that characterize most of these sediments, suggest unusual conditions of anoxia or near anoxia over the seafloor during the time of deposition (Arthur *et al.*, 1979).

More than 30 year ago, Schlanger & Jenkyns, (1976) during the Deep Sea Drilling Project (DSDP) expeditions in the Pacific, Atlantic and Indian Oceans, discovered black carbon-rich deposits in Cretaceous sediments accumulated on submarine volcanic plateaus (Shatsky Rise, Manihiki Plateau) that were identical in age with similar deposits cored from the Atlantic Ocean and known from outcrops in Europe, particularly in the geological record of the limestone-dominated Apennines chain in Italy. This evidence highlighted that these deposits were not of local significance and strictly controlled by local basin geometry, but widespread intervals which recorded highly unusual oxygen-depleted conditions in the world ocean during several distinct discrete periods of geological time: they called them "Oceanic Anoxic Events” (OAEs) that formed in a variety of paleo-bathymetric settings including oceanic plateaus and basins, continental margins and shelf seas (Schlanger & Jenkyns, 1976; Arthur *et al*., 1979) (Figure 2.1).

The OAEs were interpreted as the results of sea level rising (Late Cretaceous transgression) associated with an increase of the primary productivity, a reduced ocean circulation and the existence of an equable global climate. The consequence was the formation of an expanded oxygen-minimum layer and deposition of organic carbon-rich deposits on global scale (Schlanger & Jenkyns, 1976).

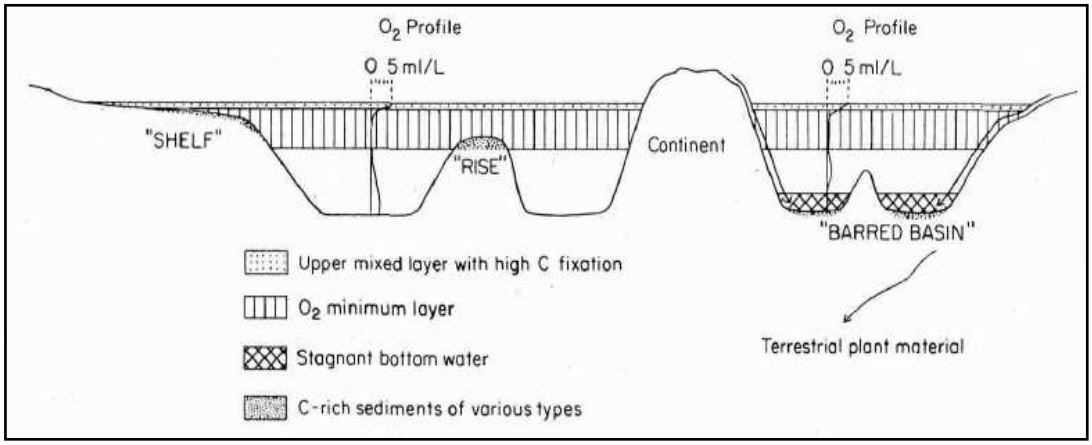

Figure 2.1. Stratification during an "Oceanic Anoxic Event" in three different environments : a) shelf type (these may be locally intensified by the introduction of terrestrial organic material from large rivers); b) rise type (these should be relatively free of terrestrial plant debris); c) barren basin type (contain abundant terrestrial plant debris delivered to these basins in their early opening stages by rivers and turbidity currents). From Schlanger & Jenkyns, 1976.

Several OAEs were recognized starting from the Jurassic Period as the Toarcian OAE (Posidonienschiefer Event, ~ 183 Ma) (Jenkyns 1985, 1988; McArthur *et al.*, 2000, 2008; Sabatino *et al.*, 2009), the Valanginian OAE (Weissert Event, ~ 136 Ma) (Scholle & Arthur, 1980; Cotillon & Rio, 1984; Arthur & Dean, 1986; Weissert, 1989; Lini *et al.*, 1992; Weissert & Erba 2004; Erba *et al.*, 2004), the Hauterivian OAE (Faraoni Event, ~ 130 Ma) (Cecca *et al.*, 1993; Baudin, 2005; Bodin *et al.*, 2007), the Early Aptian OAE1a (Selli Event, ~ 120 Ma), the early Albian OAE1b (Paquier Event, ~ 111 Ma, first recognized in the Vocontian Trough of the SE France), the OAE1c (which is probably regional, ~ 103 Ma), the late Aptian OAE1d (Breistroffer Event, ~ 100 Ma), the Cenomanian-Turonian OAE2 (Bonarelli Event, ~ 93 Ma) and the Coniacian-Santonian OAE3 (~ 86 Ma), (Jenkyns, 2010) (Figure 2.2).

All the Mesozoic OAEs are characterized by similar features, in fact they are represented by organic carbon-rich sediments, are poor in carbonate content, and are associated with major perturbations of the C-cycle recorded by δ13C anomalies both in carbonate and organic matter (Weissert, 1989; Arthur *et al.*, 1990; Weissert & Lini, 1991; Erba, 1994; Erbacher *et al.*, 1996; Weissert *et al.*, 1998; Jenkyns, 1999, 2003; Larson & Erba, 1999; Leckie *et al.*, 2002; Jenkyns, 2003) and in some areas they are characterized by abundant radiolarian sands.

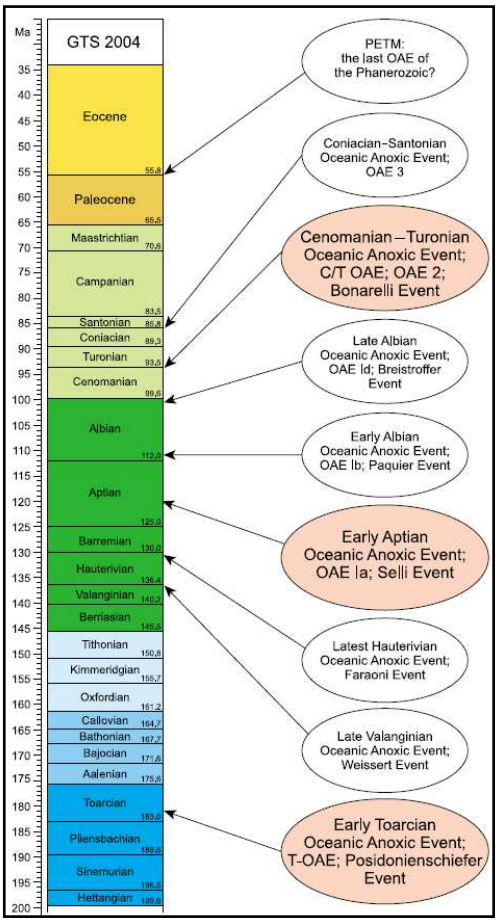

Figure 2.2. Stratigraphic position and nomenclature of OAEs. From Jenkyns, 2010.

Studies of Osmium and Strontium isotopes highlight that during the OAEs a relative paleotemperature maxima occurred, accompanied by an accelerated hydrological cycle and global increase in weathering rates (Jenkyns, 2003). Because Osmium is concentrated in organic-rich sediments, it is used as geochemical proxy to reconstruct changes in the composition of ancient seawater related to volcanic activity and/or continental weathering, as well as, Strontium isotope is used to understand the geologic history of chemical weathering, carbonate dissolution and hydrothermal activity at mid-ocean ridges.

As regard the $^{87}Sr/^{86}Sr$ excursions (Bralower *et al*., 1997; Jones & Jenkyns, 2001; Frijia & Parente, 2008) and the $^{187}Os/^{188}Os$ record (Peucker-Ehrenbrink & Ravizza, 2000; Cohen *et al*., 2004; Cohen & Coe, 2007; Turgeon & Creaser, 2008; Tejada *et al*., 2009), they reflects enhanced continental weathering and/or hydrothermal activity, and coincide with increased ocean crust production and large igneous provinces (LIPs)

emplacement (Larson, 1991a, 1991b; Kerr, 1998; Larson & Erba, 1999; Jenkyns, 1999; Leckie *et al*., 2002; Erba, 2004; Neal *et al*., 2008).

Obviously all these strong changes in the ocean-atmosphere system during the mid-Cretaceous OAEs have influenced the plankton marine assemblages that experienced accelerated rates of speciation and/or extinction near the major Cretaceous OAEs leading to a reorganization of plankton community structure (Leckie, 2002; Erba, 2004).

2.1 Oceanic Anoxic Event 1a

2.1.1 Lithological and geochemical features

The OAE1a (Early Aptian, 120-119 Ma) was identified by Wezel (1985) at the transition between the Maiolica and Marne a Fucoidi pelagic formations in the Umbria-Marche area (central Italy).

The lithological expression of OAE1a was called “Livello Selli” in honour of Raimondo Selli and defined as an “icthyolithic-bituminous-radiolaritic 1-3 m thick regional marker-bed consisting of laminated black shales rich in organic matter, alternated with radiolarian silts and a carbonate content close to zero” by Coccioni *et al*. (1987, 1989). The cyclic organic-rich and organic-poor sediments of the Selli Level were interpreted to be largely deposited during a time interval comprised between 500 kyr and 1 Myr (Menegatti *et al.,* 1998).

Coeval lithological expressions of OAE1a outside the type area are referred to as “Selli Level equivalent”. Selli Level equivalents have been identified and studied in many sections: in the northern Italy (Cismon, southern Alps; Bersezio, 1994; Erba *et al.*, 1999), southern Italy (Apulia and Sicily; Cobianchi *et al.*, 1999; Bellanca *et al.*, 2002), in the Pacific Ocean where it was recovered at several DSDP (Deep Sea Drilling Project) sites (Mid Pacific Mountain, Magellan and Shatsky Rises, and Manihiki Plateau) (Sliter, 1989; Erba, 1994; Baudin, 1996; Ando *et al.*, 2008), at DSDP and ODP (Ocean Drilling Program) sites in the North and South Atlantic (Bay of Biscay, Bermuda Basin, Galicia Bank, Angola basin, Falkland Plateau), in the Indian Ocean (Exmouth Plateau)

(Bralower *et al.*, 1994; Premoli Silva *et al.*, 1999; Leckie *et al.*, 2002), in the northern Caucasus (Baraboshkin, 1996), in the North Sea (Jenkyns, 1980) and in the southern France, where it is called "Niveau Goguel" (Bréhéret, 1988, 1994, 1997).

The geochemical data of the early Aptian OAE1a reveal interesting information: a pronounced negative carbon isotope excursion (n-CIE), that coincides with the lowest stratigraphic levels of the organic-rich black shale, is followed by a positive carbon isotope excursion in marine pelagic sediments, in shallow-water carbonates, in marine organic matter and in terrestrial higher-plant materials (Arthur *et al.*, 1979; Weissert *et al.*, 1985; Lini, 1994; Föllmi *et al.*, 1994; Menegatti *et al.*, 1998; Gröcke *et al.*, 1999; Hesselbo *et al.*, 2000; Jahren *et al.*, 2001; Heimhofer *et al.*, 2003; Van Breugel *et al.*, 2007). The n-CIE suggests a large input of isotopically light carbon in the ocean-atmosphere system either through methane liberation from gas-hydrate dissociation (Gröcke *et al.*, 1999; Hesselbo *et al.*, 2000; Jahren *et al.*, 2001; Beerling *et al.*, 2002; Heimhofer *et al.*, 2003; Van Breugel *et al.*, 2007) or volcanogenic CO_2 emissions during the Ontong Java and Manihiki Plateau emplacements (Larson, 1991a; Weissert & Lini, 1991; Bralower *et al.*, 1994; Erba, 1994; Weissert *et al.*, 1998; Menegatti *et al.*, 1998; Larson & Erba, 1999).

The general trend of the $^{87}Sr/^{86}Sr$ isotopes curve is characterized by a decline, closely with that of the negative carbon isotope excursion, implying that hydrothermal or other mantle-derived sources of strontium were becoming increasingly important in governing seawater chemistry (Jones & Jenkyns, 2001).

The $^{187}Os/^{188}Os$ profiles through the Livello Selli in Italy (Gorgo a Cerbara section) indicate a pulse of radiogenic osmium to the oceans interrupting a trend to lower values, linked to the eruption of submarine volcanic products with attendant hydrothermal activity (Tejada *et al.*, 2009) (Figure 2.3).

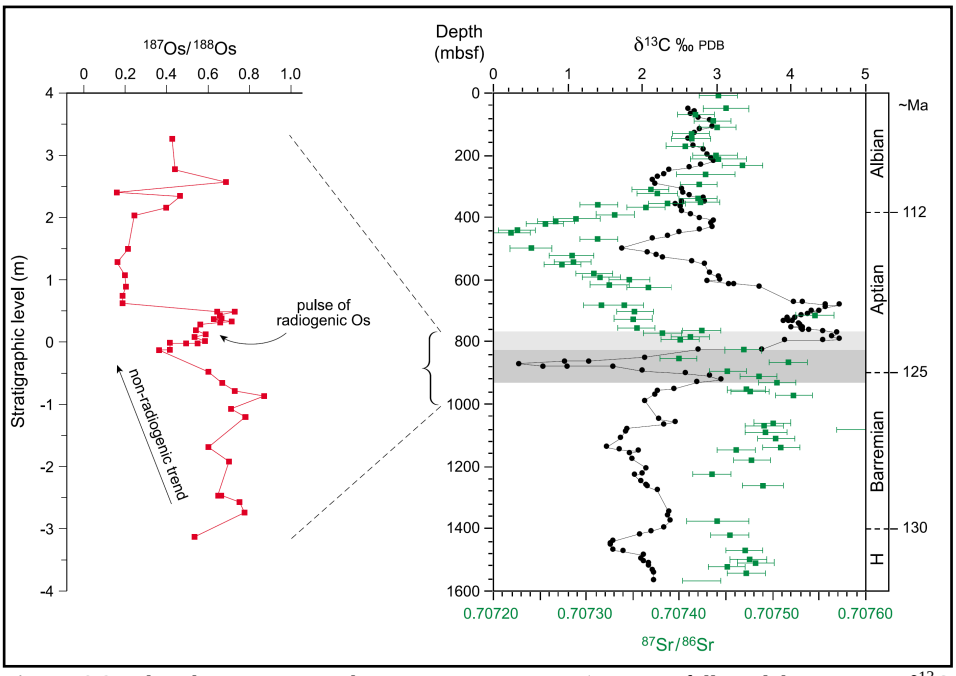

Figure 2.3. The characteristic carbon isotope signature (negative followed by positive $\partial^{13}C$ excursion) and strontium isotope profile through the 1.6 km shallow water platform carbonate section at the Resolution Guyot, Mid-Pacific Mountains (ODP Site 866). Accompanying osmium isotope data derive from an Aptian (OAE1a, Selli Level) pelagic black shale from central Italy (Tejada *et al.*, 2009). From Jenkyns, 2010.

At the onset of OAE1a the oxygen isotopes data (Menegatti *et al.*, 1998; Luciani *et al.* 2001; Price, 2003; Ando *et al.*, 2008) and TEX_{86} suggest high, but fluctuating temperatures (30-36°C) during deposition of the organic matter, with at least two episodes of cooling (Dumitrescu *et al.*, 2006) (Figure 2.4). This warming event, with the highest temperatures recorded in the core of the negative carbon-isotope interval, was recorded worldwide in the Tethys (e.g. Menegatti *et al.*, 1998; Hochuli *et al.*, 1999; Luciani *et al.*, 2001; Bellanca *et al.*, 2002; Jenkyns, 2003; Millán *et al.*, 2009; Erba *et al.*, 2010; Jenkyns, 2010; Keller *et al.*, 2011; Stein *et al.*, 2011; Bottini *et al.*, 2012; Hu *et al.*, 2012; Husinec *et al.*, 2012), Vocontian Basin (e.g. Moullade *et al.*, 1998; Kuhnt *et al.*, 2011), Boreal Realm (Mutterlose *et al.*, 2010; Bottini & Mutterlose, 2012; Pauly *et al.*, 2013; Mutterlose & Bottini, 2013), eastern European Russian Platform (Zakharov *et al.*, 2013), and Pacific Ocean (e.g. Jenkyns, 1995; Price, 2003; Schouten *et al.*, 2003; Ando *et al.*, 2008; Bottini *et al.*,2012) and documents the effects of volcanic and hydrothermal activity that produced a greenhouse climate mode, increased weathering rates and sea level rise (Haq *et al.*, 1988). This sea level rise is probably related to the lithospheric bulge produced by the rising "superplume" in the Pacific Ocean, the massive amount of

new midplate volcanism, and the contemporaneous increase in ridge spreading rates (Larson, 1991b).

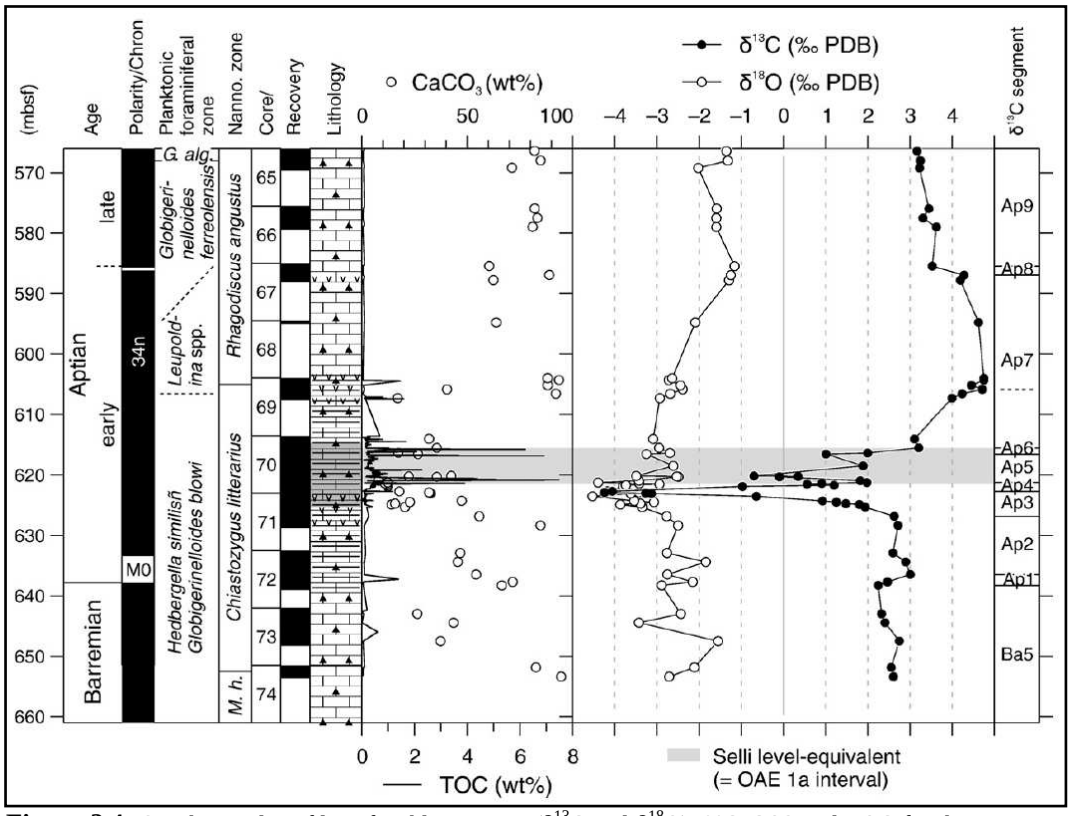

Figure 2.4. Geochemical profiles of stable isotopes ($\delta^{13}C$ and $\delta^{18}O$), %CaCO3 and TOC for the uppermost Barremian-lower upper Aptian pelagic limestones at the Mid-Pacific Mountains, DSDP Site 463. $\delta^{13}C$ segments are according to Ando *et al.*, 2008. From Ando *et al.*, 2008.

2.1.2 Calcareous plankton features

As regards the calcareous plankton assemblages, OAE1a falls within the *Leupoldina cabri* planktonic foraminifera Zone and *Chiastozygus litterarius* (C6) calcareous nannofossil Zone (Erba, 2004). Previous studies (Coccioni *et al.*, 1987, 1992; Bréhérét & Delamette, 1989; Sliter, 1989, 1992b; Bralower *et al.*, 1993, 1994; Weiss, 1995) attributed the Selli Level and equivalent black shales of OAE1a totally to the *Globigerinelloides blowi* Zone because no specimens of *L. cabri* were found below or within the Selli, although the first appearance of leupoldinids was reported in the middle lower Barremian at Rio Argos (Coccioni & Premoli Silva, 1994). An early appearance of

L. cabri has been reported in the Vocontian Basin by Magniez-Jannin *et al.* (1997), where *L. cabri* was found below the Goguel Level (OAE 1a equivalent in the SE France) in the *D. weissi* ammonite Zone of early Aptian age. This discrepancy in foraminiferal zonal attribution of OAE1a is due to the rarity of *L. cabri* at the beginning of its range and to its supposed susceptibility to diagenesis (Erba *et al.*, 1999).

It is worth mentioning the uncertainty of the stratigraphic position of the base of the *Leupoldina cabri* Zone as it is either placed at its FO level or at its acme level. However, the FO of *L. cabri* is well dated, through calibration to magnetostratigraphy, in the Cismon core (Erba *et al.*, 1999) and in the Gorgo a Cerbara section (Coccioni *et al.*, 2006) at an age of 124.47 Ma and 124.26 Ma, respectively.

According to previous studies the planktonic foraminiferal assemblages reveal interesting changes in morphology, shell size and diversification across the OAE1a at Cismon, where planktonic foraminifera are mainly preserved as siliceous moulds (Premoli Silva *et al.*, 1999), and in few other sections where they do occur (Bellanca *et al.*, 2002; Tarduno *et al.*, 1989; Cobianchi *et al.*, 1999; Coccioni *et al.*, 2006; Luciani *et al.*, 2006; Ando *et al.*, 2008).

So far data collected from the upper part of the *Globigerinelloides blowi* Zone to the top of the *Leupoldina cabri* Zone show that planktonic foraminifera are rather diverse and abundant before the onset of OAE1a. Peculiar changes in morphologies and sizes have been documented in this interval (Bellanca *et al.*, 2002), with diversification of clavate hedbergellids and leupoldinids with radially elongate and elongate bulbous chambers, respectively. Normally-shaped morphologies are either absent or alternate with “clavate” forms; in particular leupoldinids display an acme in abundance at the beginning of the C-isotopic recovery phase (Premoli Silva *et al.*, 1999; Bellanca *et al.*, 2002; Coccioni *et al.*, 2006). At the same time some new species showing an increase in test size and morphological complexity are documented within a long and progressive radiation episode following OAE1a (Leckie *et al.*, 2002). Calcareous nannoplankton assemblages show a decrease in nannoconids abundance (known as “nannoconid decline”, Erba, 1994; Erba *et al.*, 1999; Erba *et al.*, 2010) below the base of magnetic polarity zone CM0 which culminated with a "nannoconid crisis" just 40-100 kyr before the deposition of OAE1a black shales (Bralower *et al.*, 1993, 1994, 1999; Erba, 1994, 2004; Aguado *et al.*, 1997, 1999; Channell *et al.*, 2000; Bellanca *et al.*, 2002; Bersezio *et al.*, 2002; Erba & Tremolada, 2004). The "nannoconid crisis" occurred in an interval

characterized by a major rise in relative sea level, which started close to the Barremian/Aptian boundary (Haq *et al*., 1988).

Prior to the "nannoconid crisis" nannofloral assemblages display a speciation event (First Occurrence of *Flabellites oblongus, Rucinolithus irregularis, Nannoconus truittii*) that started in the latest Barremian, in addition, after the "nannoconid crisis" event, a short interval with a virtual absence of nannoconids and dominated by other nannofossils was observed.

Nannoconid decline and crisis seem to be synchronous with early Aptian volcanic eruptions (DSDP site 463 and ODP site 807) associated with the "superplume" episode (Larson, 1991a, 1991b) and related to the formation of the Ontong Java Plateau (Tarduno *et al*., 1991; Mahoney *et al.*, 1993, 1994), which induced high primary productivity (Erba, 1994, 2004) introducing a large amount of biolimiting metals (Sinton & Duncan, 1997; Larson & Erba, 1999; Leckie *et al*., 2002; Erba, 2004).

Chapter 3

Geological and stratigraphic setting

To perform this study the Lower Aptian stratigraphic interval recovered at two drill-sites were investigated (Figure 3.1), as follows:

1) Cismon core, located in the Belluno Basin (Northern Italy);
2) DSDP Site 463, situated in the Mid-pacific Mountains (Pacific Ocean).

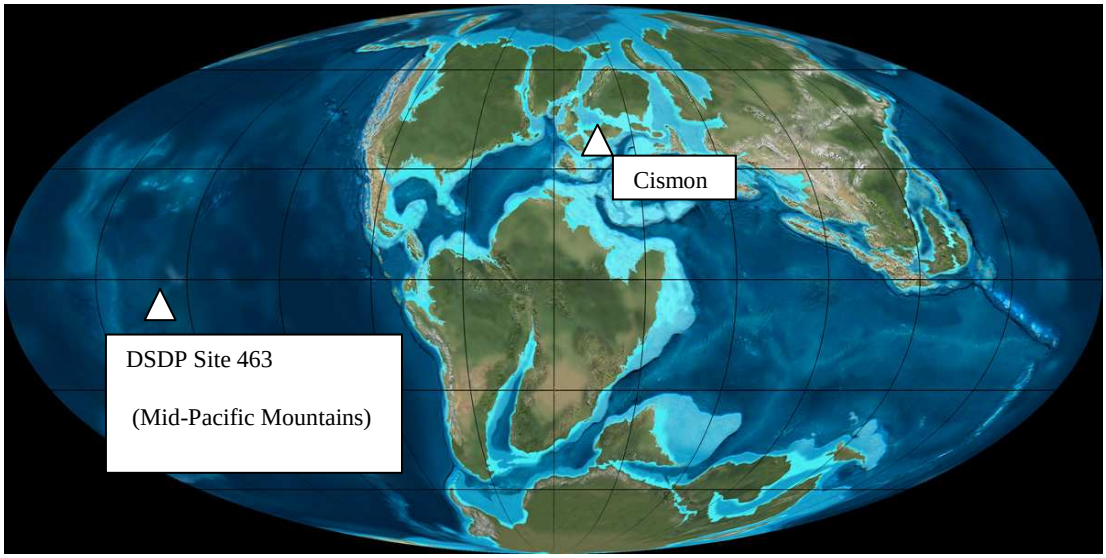

Figure 3.1. Paleogeographic location of the studied sections: Cismon core and DSDP Site 463. From Colorado Plateau Geosystem Inc. (http://www2.nau.edu/rcb7/120moll.jpg).

3.1 The Cismon core

The Cismon core drilling is part of a program called APTICORE (Larson *et al*., 1993) aimed to obtain a documentation of the global oceanic anoxic events, isotopic excursions of carbon and strontium, paleotemperatures in the oceans and fluctuations in terms of abundance and diversity of the planktonic flora and fauna. The Cismon core was studied for integrated cyclochronology and litho-, bio-, chemo- and magneto-stratigraphy

(Herbert, 1992; Erba *et al*., 1999; Premoli Silva *et al*., 1999; Larson & Erba, 1999; Channel *et al*., 2000; Erba & Tremolada, 2004; Van Breugel *et al*., 2007; Li *et al*., 2008; Malinverno *et al*., 2010).

The drill site is located in the Venetian Prealps (Southern Alps, NE Italy), west of the town of Feltre (Belluno Basin), along the Passo Rolle road, at km 52.6 (46°02'43.46"N; 11°45'46.85"E; 398 m altitude). The Venetian Prealps are part of the Southern Alps, which represent a portion of the southern margin of the Mesozoic Tethys on the eastward-deepening slope between the Trento Plateau and the Belluno Basin (Figure 3.2).

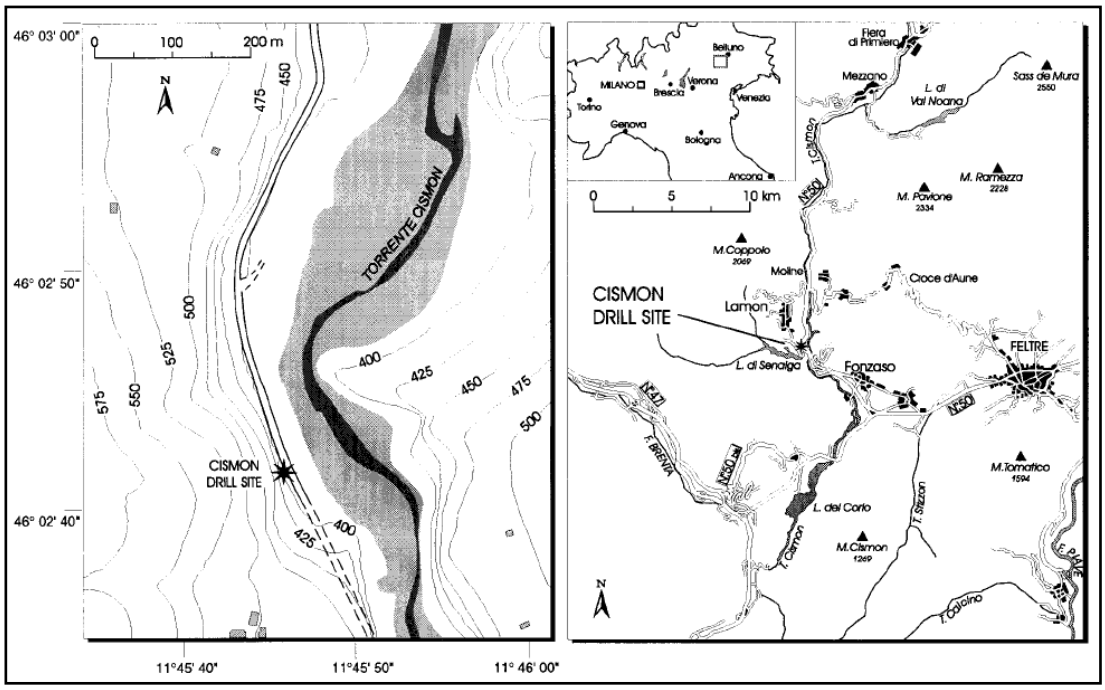

Figure 3.2. Location of the Cismon drill site in the Southern Alps (northern Italy, Belluno basin). From Premoli Silva *et al.*, 1999.

The Cismon core was drilled to a total depth of 131.8 mbwh (meters below well head), with dips to the north of 17-22 degrees from 0 to 60 mbwh and more variable dips below 60 mbwh. The significant dip throughout the core made necessary to convert the hole depths into stratigraphic thicknesses.

The cored interval extends from the upper Aptian to the lower upper Hauterivian and it is attributed to the Biancone Formation (Hauterivian-Barremian) and Scaglia Variegata Formation (Aptian), respectively the local equivalent of the Tethyan Maiolica Formation

and Scisti a Fucoidi Formation of the Umbria-Marche Basin (Erba & Larson, 1998). The Biancone Formation consists of dominant limestones with intercalated black shales and radiolarian-rich layers while the Scaglia Variegata Formation is characterized by marlstones, marly limestones, black shales and radiolarian beds.

The cored sequence was subdivided into 8 lithostratigraphic units based on carbonate content, dominant colours, occurrence of black shales, chert and radiolarian-rich levels (Erba *et al.*, 1999) and the sequence was deposited at an estimated paleo-depth of 1000-1500 m during the Early Cretaceous (Weissert & Lini, 1991; Erba & Larson 1998; Bernoulli & Jenkyns, 2009) (Figure 3.3).

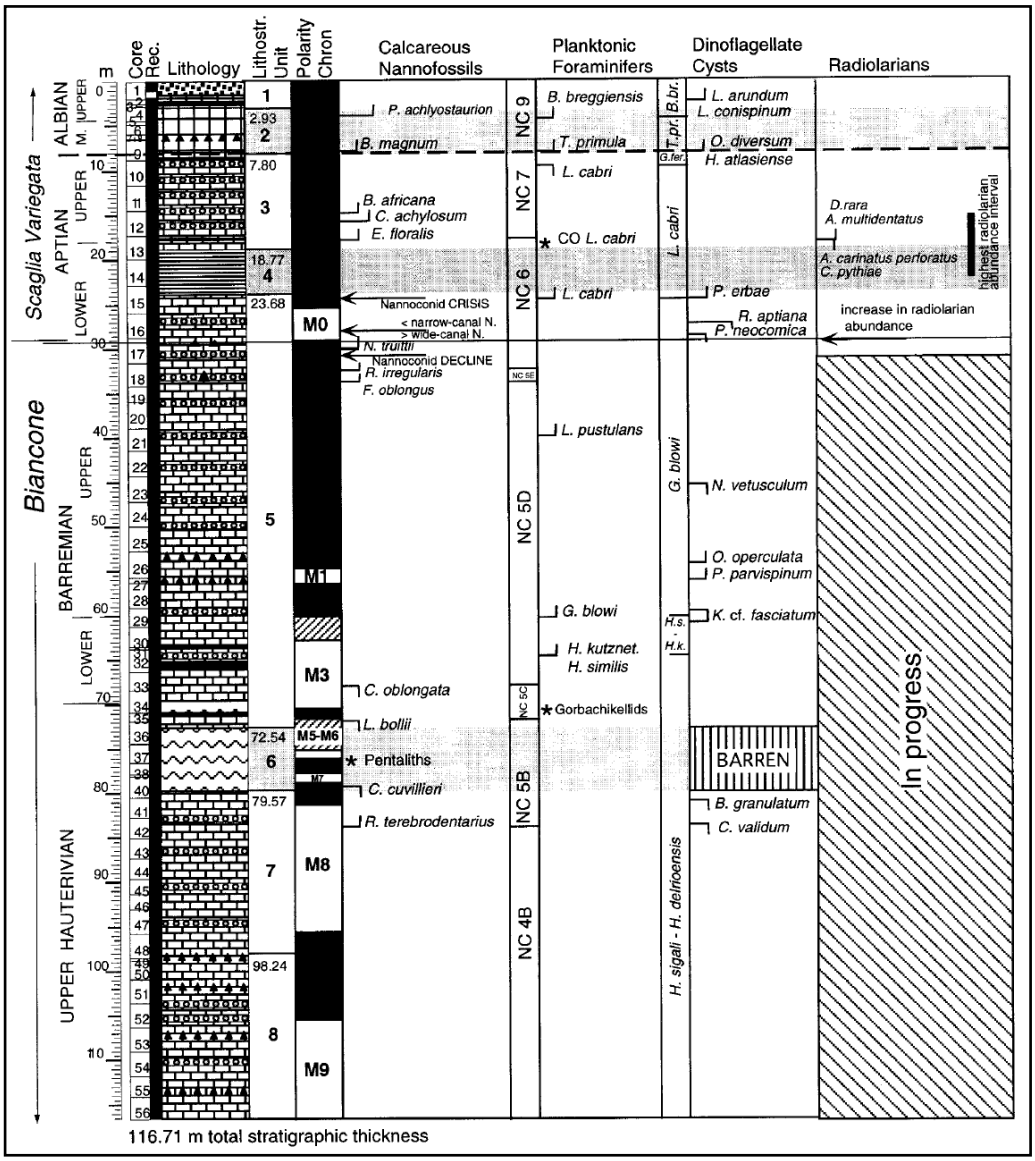

Figure 3.3. Magnetostratigraphy, calcareous nannofossil, planktonic foraminiferal, dinoflagellate and radiolarian events of the Cismon core. From Erba *et al.*, 1999.

The Selli Level is comprised within the Scaglia Variegata Formation between 23.68 and 18.77 stratigraphic meter depths and it is 4.91 m-thick. Lithologically it can be subdivided into three discrete intervals based on presence/absence of black shales: a lower interval, 1.32 m-thick (23.68–22.36 m), characterized by marlstone alternated with 1 cm-thick black shales and few discrete radiolarian beds; a middle interval, 1.95 m-thick (22.36-20.41 m), richer in carbonates and nearly devoid of black shale with rare radiolarian beds; and an upper interval (20.41-18.77 m), characterized by alternating marlstone, common radiolarian beds and black shales (Erba *et al*., 1999; Premoli Silva *et al.*, 1999).

At Cismon core the Selli Level equivalent occurs in the upper part of the nannofossil *Chiastozygus litterarius* Zone, and in the upper part of the radiolarian *Acanthocircus carinatus* Zone as well as in the upper part of the *A. carinatus perforatus* Subzone (Erba *et al*., 1999). In terms of planktonic foraminiferal biostratigraphy, the Selli Level equivalent is entirely comprised in the foraminiferal *Leopoldina cabri* Zone and it is marked by a $\delta^{13}C$ anomaly, consisting of a pronounced negative shift followed by a long positive excursion (Figure 3.4).

At Cismon core, across the magnetic chron M0, the $\delta^{13}C$ profile (From Erba *et al.*, 1999, Fig 3.4; see also Chapter 7, Fig. 7.5 a) shows a gentle decrease followed by an increase of values close to 3‰ (segments C1 and C2). Subsequently, a negative pronounced excursion (C3) at the base of the Selli Level equivalent (values range from ~ 3‰ to ~ 1.8‰) was documented. The middle part of the Selli Level eq., displays constant values close to 3 ‰ (C5), followed by a positive excursion that starts from the top of it (from 2.7 ‰ to 3.7‰, C6) and continues above it until maximum values of approximately 5‰ in the uppermost of the *Leupoldina cabri* Zone (C7) (Erba *et al.*, 1999).

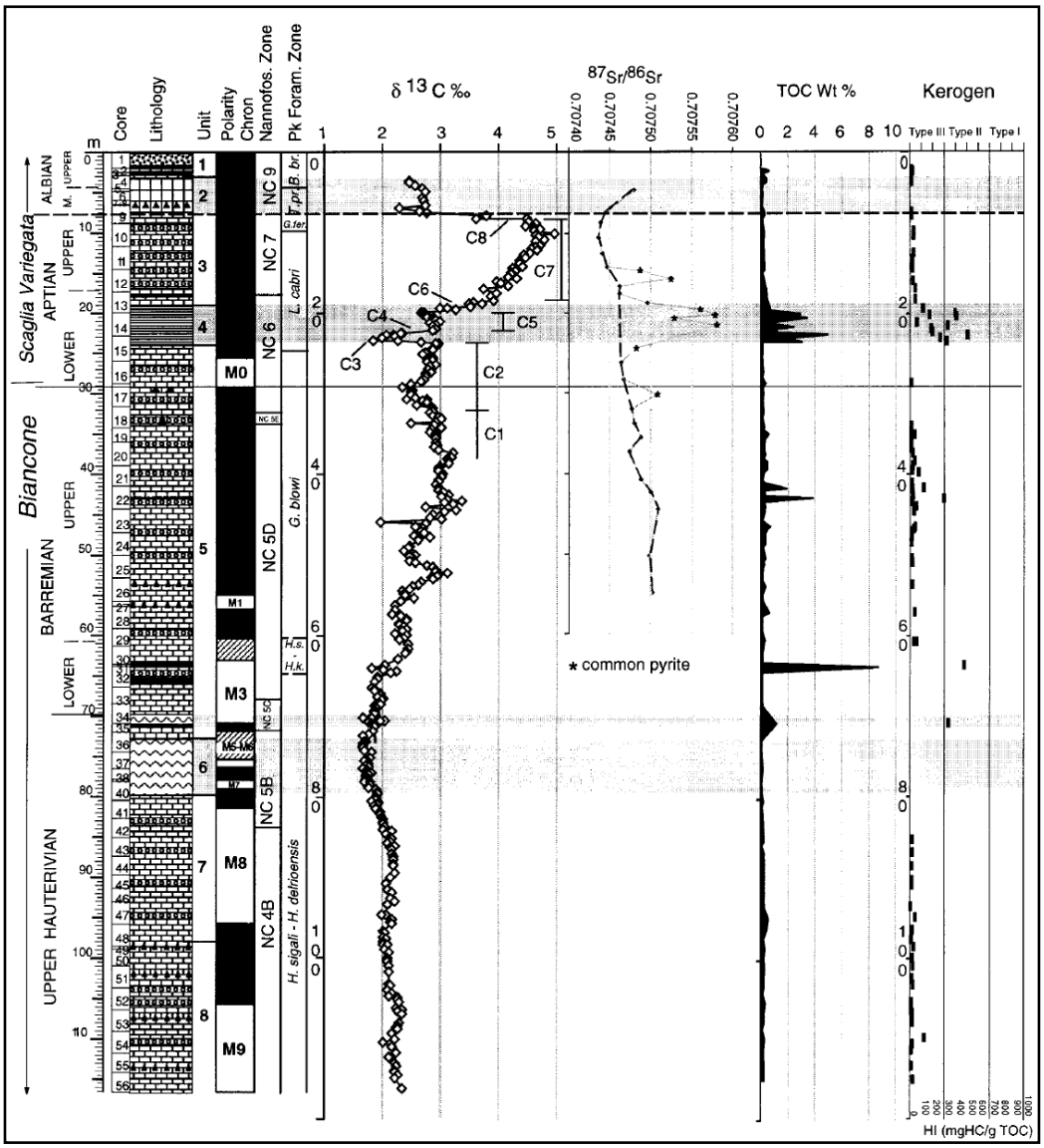

Figure 3.4. Magneto- and chemostratigraphy of the Cismon core. From Erba *et al.*, 1999.

3.2 DSDP Leg 62 Site 463

DSDP Site 463 was drilled at a water depth of 2525 meters in the western Mid-Pacific Mountains (21°21.01'N, 174°40.07'E), which consist of several segments thought to be part of an ancient fracture-zone-ridge-crest system that separated the North and South Pacific Plates (Figure 3.5). During the Early Cretaceous site 463 was situated roughly at

20°S and 150°W paleo-latitude (Lancelot, 1978), with a paleo-depth between few hundred meters (Mélières *et al*., 1978) and 1 km (Roth, 1981).

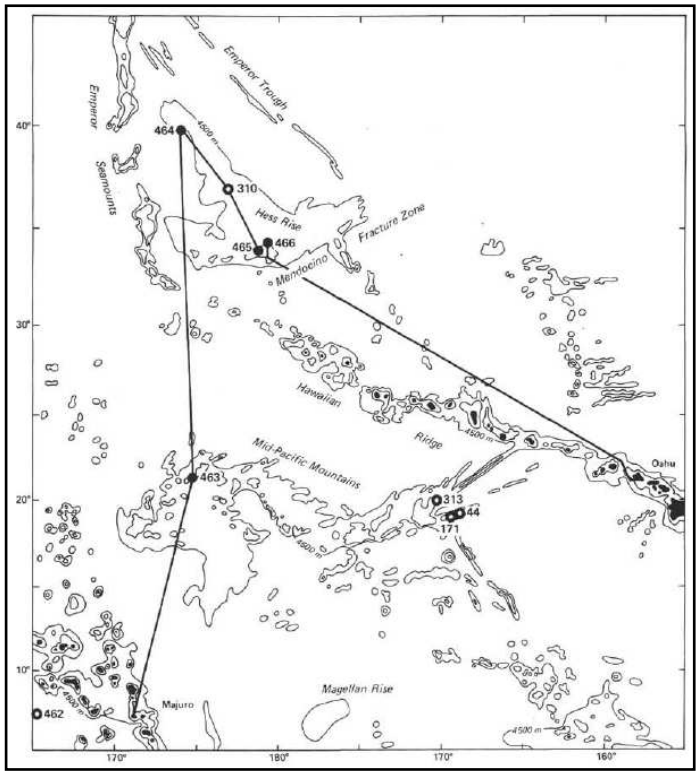

Figure 3.5 Location of the DSDP site 463 in the Mid-Pacific Mountains. From Thiede *et al.*, 1981.

The hole was continuously cored to a total sub-bottom depth of 822.5 meters, where it was abandoned because of bit destruction. The sedimentary sequence at Site 463 comprises Cenozoic ooze and Cretaceous (post-early Barremian) chalk and limestone (Thiede *et al.*, 1981). The section is subdivided into four lithologic units, based mainly on composition, sedimentary structures and diagenetic features (Figure 3.6):

- Sub-unit IA: Nannofossil Ooze (0-46.8 m); Sub-unit IB: Foraminifer Nannofossil Chalk and Nannofossil Foraminifer Chalk (46.8-452 m);
- Unit II: Multicolored Limestone and Silicified Limestone (452-587.7 m);
- Unit III: Tuffaceous and Carbonaceous Limestone (587.7-632.5 m);
- Unit IV: Interbedded Pelagic and Clastic Limestone (632.5-822.5 m).

As regard the Unit III, the limestone is highly silicified, and thin volcanic ash layers are present from 623.7 mbsf (meters below sea floor) to 606.7 mbsf, representing approximately 1 My (Dean & Thiede, 1978), possibly linked to Ontong Java Plateau volcanism. The altered-ash beds appear to be contemporaneous with the generation of basaltic basement farther east in the Mid-Pacific Mountains.

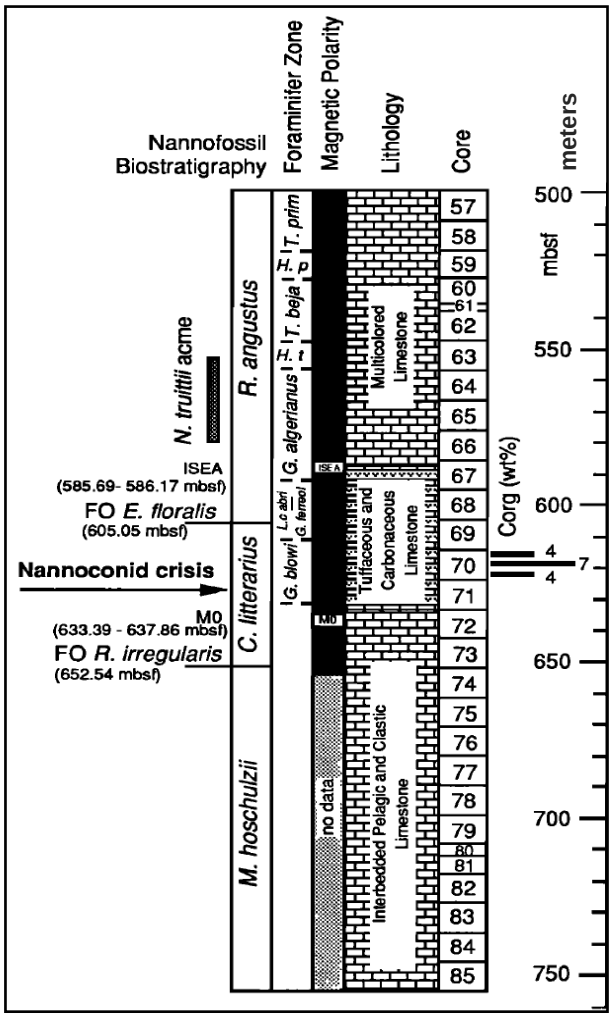

Figure 3.6. Litho- and biostratigraphy at DSDP Site 463 (modified from Erba, 1994).

The paleodepth of deposition (Figure 3.7) for oldest sediments at Site 463 is difficult to reconstruct because the sediments consist of pelagic limestones that are interbedded with layers rich in clastic, shallow-water calcareous components. Stromatolites, oolites, and mollusk fragments apparently were displaced from an adjacent neritic environment.

Dredge hauls from flanks of guyots in other parts of the Mid-Pacific Mountains contain shallow water fossils supporting the conclusion that many of the submarine volcanoes and guyots were islands surrounded by reefs or carbonate banks during much of the Cretaceous.

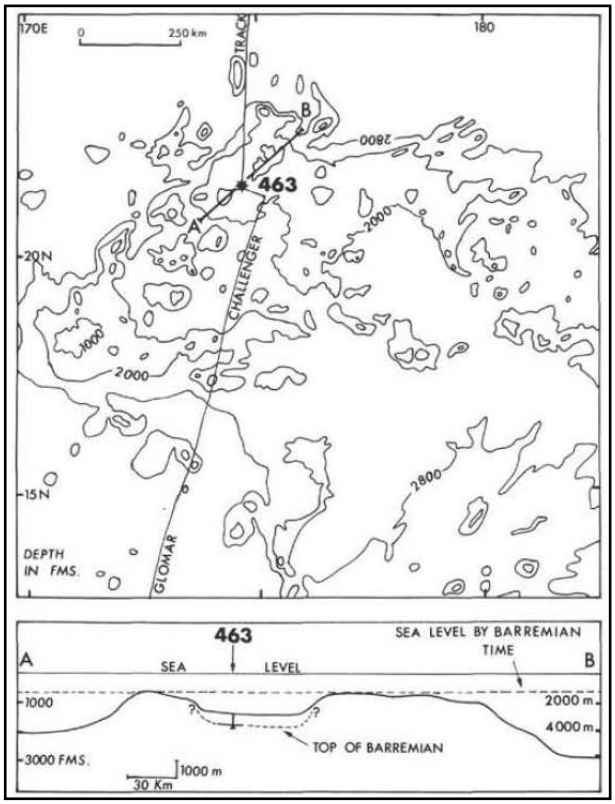

Figure 3.7. Bathymetric map of the western Mid-Pacific Mountains, and cross-section through Site 463. From Ferry & Schaaf, 1981.

Lithologically the Selli level equivalent at DSDP Site 463 is not represented by black shales (as at the Cismon core), and corresponds to ~12 m (between ca. 626-615 mbsf) of tuffaceous limestone containing a number of discrete organic-rich horizons with TOC up to 7 (wt%) (Thiede *et al.*, 1981; Erba, 1994). Other authors as Ando *et al.*, (2008) positioned the Selli Level equivalent between 621.45-615.53 mbsf, considering the increased hydrogen index of >150 mg HC/g C_{org} (the value typical of Type II Kerogen).

At DSDP site 463 the Selli Level occurs in the upper part of the nannofossil *Chiastozygus litterarius* Zone and the foraminiferal *Leopoldina cabri* Zone.

As regards the geochemical data, the Selli Level equivalent at DSDP Site 463 is marked by a $\delta^{13}C$ and $\delta^{18}O$ anomalies occurring immediately before OAE1a (Ando *et al.*, 2008) (Figure 3.8). The $\delta^{13}C$ values were nearly constant between 2.2‰ and 3.0‰ in the latest Barremian-earliest Aptian, then decreased dramatically by ~7‰ to a minimum value of - 4.2‰. After that, they increased again dramatically by 9.0‰ (from - 4.2‰ to 4.8‰) across OAE 1a until to reach values similar to the pre-excursion level of ~3‰.

The $\delta^{18}O$ values were typically ranging from -2 to -3‰ during the earliest Aptian and then shifted toward more negative values as low as - 4.5‰ just prior to OAE 1a. After that, they returned to ~ -3‰ during the CIE of the early Aptian, followed by a gradual increase to up to - 1.2‰ in the early late Aptian (Ando *et al.*, 2008).

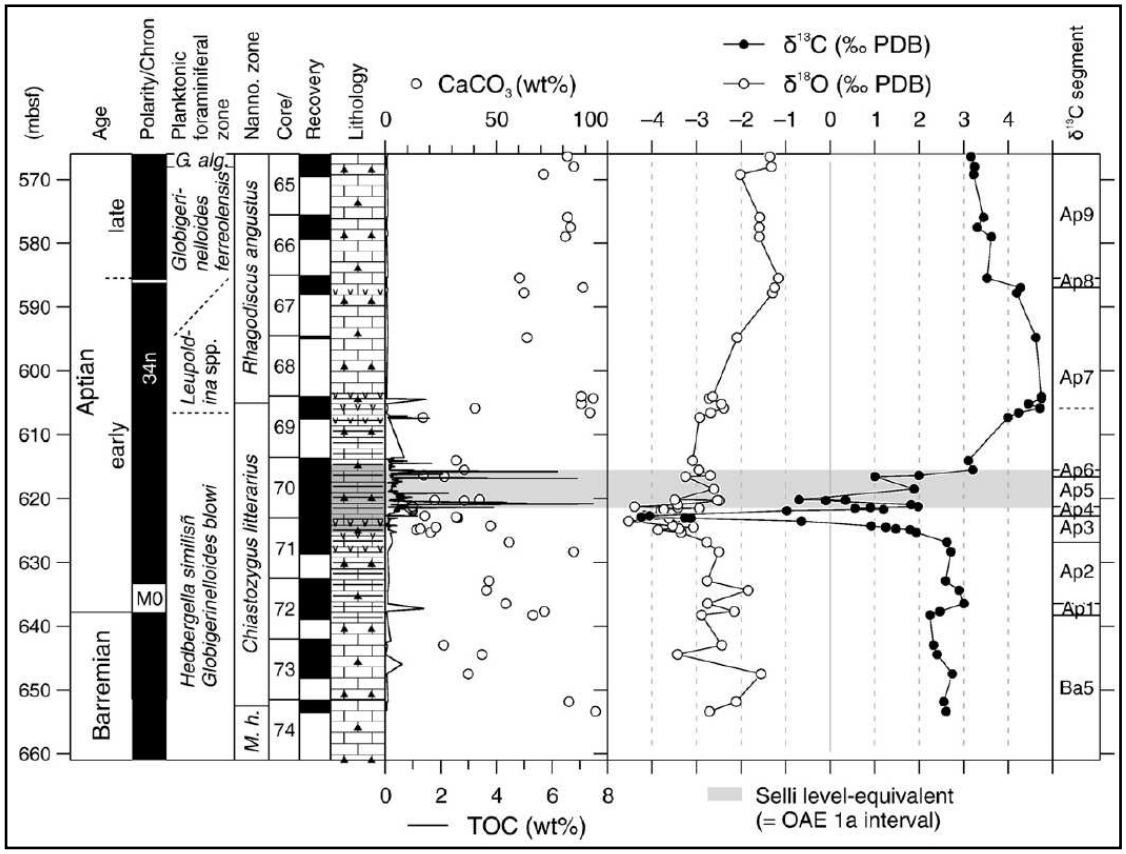

Figure 3.8. Geochemical profiles of stable isotopes ($\delta^{13}C$ and $\delta^{18}O$), %CaCO3 and TOC for the uppermost Barremian-lower upper Aptian pelagic limestones at the Mid- Pacific Mountains, DSDP Site 463. From Ando *et al*, 2008.

Chapter 4
Material and methods

Samples were processed using different methodologies due to the lithology and hardness of sediments. Planktonic foraminiferal and radiolarian analyses were conducted on washed residues and thin sections, following the standard micropaleontological procedure.

Samples studied from the Cismon core are 217, as follows: 112 washed residues with a sampling resolution from 5 to 50 cm, 105 thin sections with a sampling resolution from 5 to 20 cm within the Selli Level equivalent, and from 40 cm to about 1 m below and above it (see Table 1).

177 samples were studied at DSDP Site 463, in particular 76 in washed residues and 101 in thin sections. Considering that Site 463 is characterized by several intervals of no recovery, the sampling resolution is variable from core to core (see Table 2), as follows: 17 samples of core 73, 19 samples for core 72, 25 samples for the core 71, 48 samples for the core 70, 11 samples for the core 69, 3 samples for the core 68, and 6 samples for the core 67. Most of the samples were studied both in thin section and washed residue.

For the washed residues, being the sample rocks very small in size, samples were selected according to their content in planktonic foraminifera and after observation of the thin sections. Subsequently, I studied all the other samples and I continued to investigate the stratigraphic interval using a variable sampling resolution. Almost all samples were barren in planktonic foraminifera, except for few samples above the Selli Level equivalent characterized by soft carbonate lithologies and a high content of planktonic foraminifera and for few samples below the Selli Level equivalent with a low carbonate content and very rare planktonic foraminifera. The entire interval including the Selli Level equivalent is barren of planktonic foraminifera, except two samples (74c and 13a).

On the washed residues it was not possible to apply the same methods used in the Cismon core for producing quantitative analysis because of the rarity of planktonic foraminifera associated with the lower carbonate content and the hard lithologies.

4.1 Planktonic foraminiferal preparation

Planktonic foraminiferal preparation was conducted on washed residues and thin sections in both studied sites:

- Washed residues were prepared using standard preparation method (Figure 4.1):

a) Cismon core samples: hard siliceous samples were processed with hydrochloric acid to extract isolated radiolaria, while softer lithologies were soaked in hydrogen peroxide and desogene for few hours to extract isolated planktonic foraminifera. All samples were then washed, dried and sieved through a set of sieves (40 μm, 150 μm and 250 μm).

Previous studies on the Cismon core (Premoli Silva *et al*., 1999; Erba *et al*., 1999) revealed that washed residues initially processed for radiolaria were characterized by the presence of common siliceous moulds of planktonic foraminifera with a peculiar preservation, and for that reason, they have been studied.

b) DSDP Site 463 samples: soft lithologies have been soaked in hydrogen peroxide for several hours (about 5 to 24 hours), while lithified rocks have been processed using acetic acid (CH_3COOH) according to the procedure developed by Lirer (2000). The acid causes a very low reaction that allows disaggregating the rocks without destroying and corroding the fossil content.

Rock samples were broken into small fragments and sieved to obtain three fractions (> 250 μm , > 125 μm and >40 μm). Each size-fraction was placed in separate beakers, covered by a solution of 80% acetic acid and 20% H_2O for a time interval from 1 hour to 10 hours depending on the hardness of the rock sample. During the preparation process, samples were monitored until the maximum degree of disaggregation was reached and then removed from the solution. After this phase, the three fractions were washed under water, dried and used for the micropaleontological analyses.

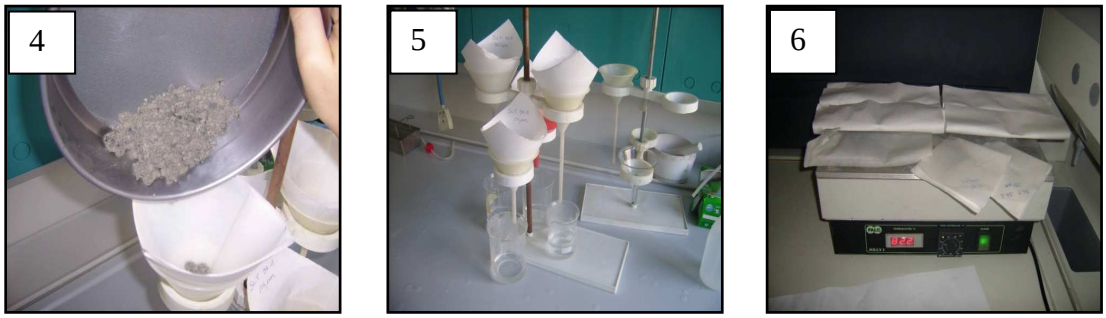

Figure 4.1. Pictures from 1 to 6 represent all steps necessary to obtain a washed residue.

Washed residues were examined under a stereomicroscope to select the significative and crucial species for biostratigraphic, taxonomic, morphometric and abundance analysis.

The most significant and best preserved specimens were observed and identified under the Scanning Electron Microscope (SEM) available at the Department of Earth Sciences "A. Desio" of the University of Milan.

- Thin sections for both sites were prepared starting from small rock fragments, then each of them was cut, polished (mechanically and then manually) and mounted on a glass slide. After this phase, it was made another cutting, followed by a manually thinning up to ca. 30 μm. To optimize the view of planktonic foraminifera, the thin sections were manually polished to a thickness of ~20 μm. The thin sections were studied under a microscope to perform quantitative analysis.

4.2 Taxonomic and biostratigraphic analyses

The results of the taxonomic analyses are presented in Chapter 6 and the SEM images of the most significant specimens are reported in Plates 5 to 23. All the species and genera identified during this study are reported in the taxonomic list in Chapter 5 "Taxonomy".

The results of the biostratigraphic analyses and the distribution charts ("Appendix", Table 3 and 4) are discussed and shown in Chapter 5. The presence/absence of planktonic

foraminiferal species and their relative abundance (total number of planktonic foraminifera in each sample) is plotted against the zonal schemes. The abundance of planktonic foraminifera is expressed in terms of frequency classes as follows:

0 specimen =barren (b),
1 specimen = very rare (vr);
2-3 specimens = rare (r);
4-5 specimens = rare to few (r/f);
6-8 specimens = few (f);
9-12 specimens = few to common (f/c);
13-16 specimens = common (c);
17-20 specimens = common to abundant (c/a);
21-25 specimens = abundant (a);
> 25 specimens = very abundant (va).

In all the studied sites the stratigraphic distribution of planktonic foraminifera has been calibrated to the nannofossil zonation and the magnetostratigraphic scale according to Erba *et al.*, 1999.

4.3 Planktonic foraminiferal morphometric analyses

The identification of the species has been followed by morphometric analyses carried out on SEM images. The maximum diameter of each trochospiral and planispiral species was measured starting from the last chamber of the last whorl (passing through the proloculus) and arriving to the opposite side (Figure 4.2). It was not possible to measure the pseudo-planispiral forms because of their high morphologic variability at species level. For instance, the pseudo-planispiral species can have elongated chambers with one ampulla, with two ampullae or the ampulla can be absent because broken. Actually, I have not found a unique method for measuring the maximum diameter in this group of

specimens that avoids mistakes in the measurements and enables to obtain comparable data. The globigeriniform taxa recognized in both sites (genera *Gorbachikella* and *Gubkinella*) have not been measured.

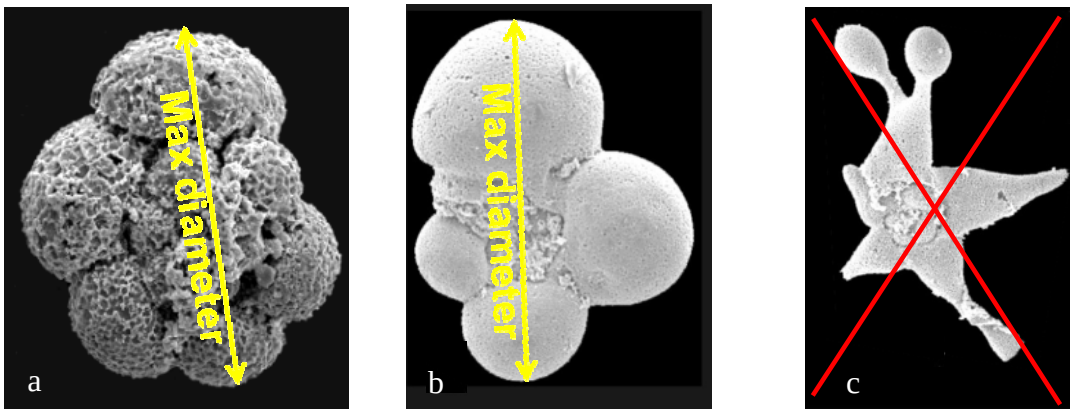

Figure 4.2. Measurement of the maximum diameter of throcospiral (a) and planispiral forms (b) but not pseudo-planispiral forms.

As regard the Cismon core the specimens assigned to each species have not been measured in each sample examined because of the discontinuous occurrences of the species. However, it has been possible to evaluate changes in test size within single species and changes in test size among species within genera across the studied stratigraphic interval. The data are discussed in the “Results” Chapter 6.

At DSDP Site 463 it was not possible to obtain a continuous record of planktonic foraminiferal shell size throughout the stratigraphic section being most of the samples barren of planktonic foraminifera.

4.4 Planktonic foraminiferal and radiolarian quantitative analyses

Quantitative analyses have been carried out by counting the total number of planktonic foraminifera and radiolaria in thin sections and the total number of planktonic

foraminifera in the washed residues with the aim to compare the results obtained using the two different methods.

Planktonic foraminifera and radiolaria were counted in each thin section in 40 fields of view randomly chosen (Figure 4.3) using a 125X magnification (1 field of view corresponds to an area of 2,0096 mm^2, thus the total area counted is 80,384 mm^2, Figure 4.4). For both studied sites I obtained two curves, one representing the total planktonic foraminiferal abundance and the other one the total radiolarian abundance (see "Results").

Being the amount of the washed residues very variable from sample to sample, I decided to analyse the same amount of residue for the three fractions of each sample from both sites. In this way I counted the total number of planktonic foraminifera observing always the same amount of residue. As regard DSDP Site, being most sample barren or containing very rare planktonic foraminifera, the amount of residue observed was higher than that used for the Cismon samples and highly variable from sample to sample.

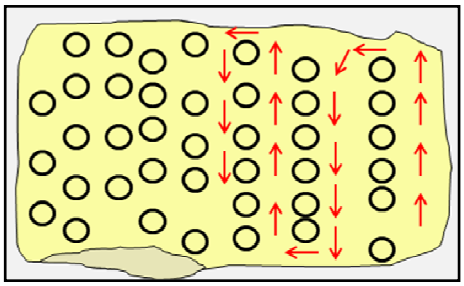

Figure 4.3. Schematic thin section with the 40 fields of view randomly chosen.

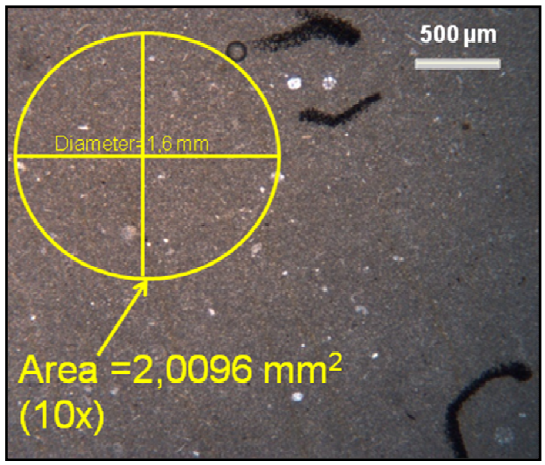

Figure 4.4. Schematic drawing of a field of view at 125X magnification.

4.5 Microfacies analyses

Using the Dunham classification (1962) (Figure 4.5) I recognized under the microscope all the different kinds of microfacies in the Cismon core and DSDP Site 463. The data obtained are shown in the "Results" Chapter 6.

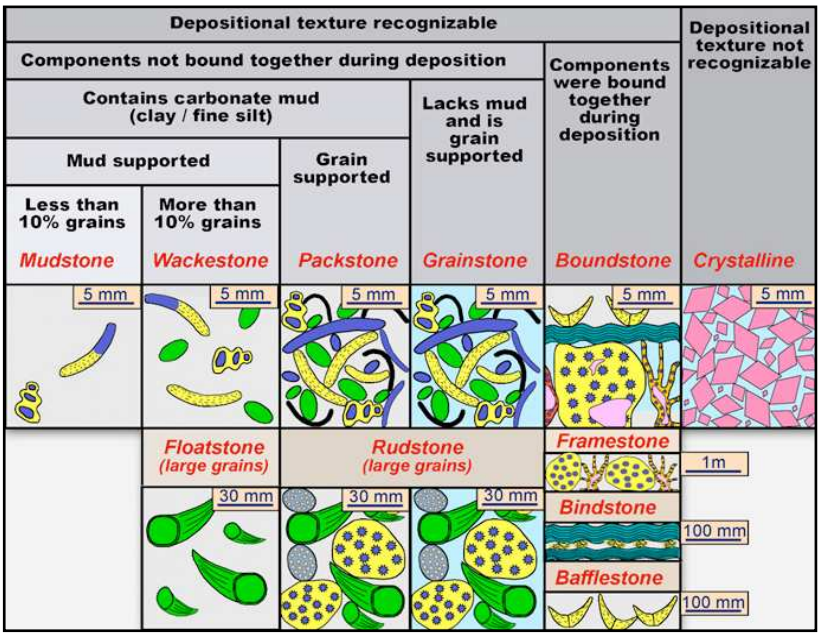

Figure 4.5. Dunham's carbonate rock texture classification (modified by Embry & Klovan, 1971).

4.6 Descriptive Statistics

To quantify the data obtained, two statistical methods were used:

- **Box Plots**: They display and compare the distribution of a parameter/variable across several groups. A boxplot (Fig. 4.6) depicts the central tendency of the variable in terms of the median of the values (the smallest box in black) that is the central half of the data roughly between the 25% and 75% points.

The variability of the values is represented in this plot by the quartiles (the 25^{th} and 75^{th} percentiles) and by the minimum and maximum values of the variable (the "whiskers" in the plot). Extreme values are plotted with a circle and called "Outliers" that are values "faraway" from the middle of the distribution.

The confidence interval considered around the median is 95% .

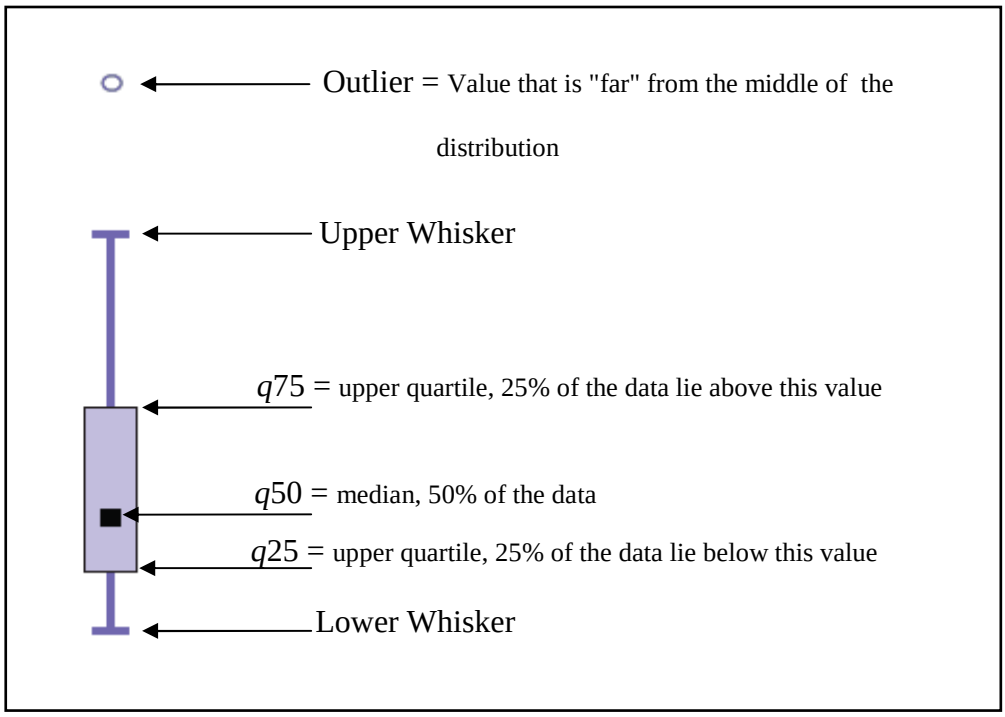

Figure 4.6. Schematic representation of Box plot elements.

In this work boxplots have been used to display and quantify the range of variation of planktonic foraminiferal test sizes within single species and among species within genera across the studied interval.

- **Pearson Coefficient (R):** in statistics the R Coefficient is a measure of the linear correlation (dependence) between two variables *X* and *Y*, giving a value between +1 and −1 inclusive, where 1 is total positive correlation between X and Y, 0 indicates no correlation, and −1 is total negative correlation (Fig. 4.7).

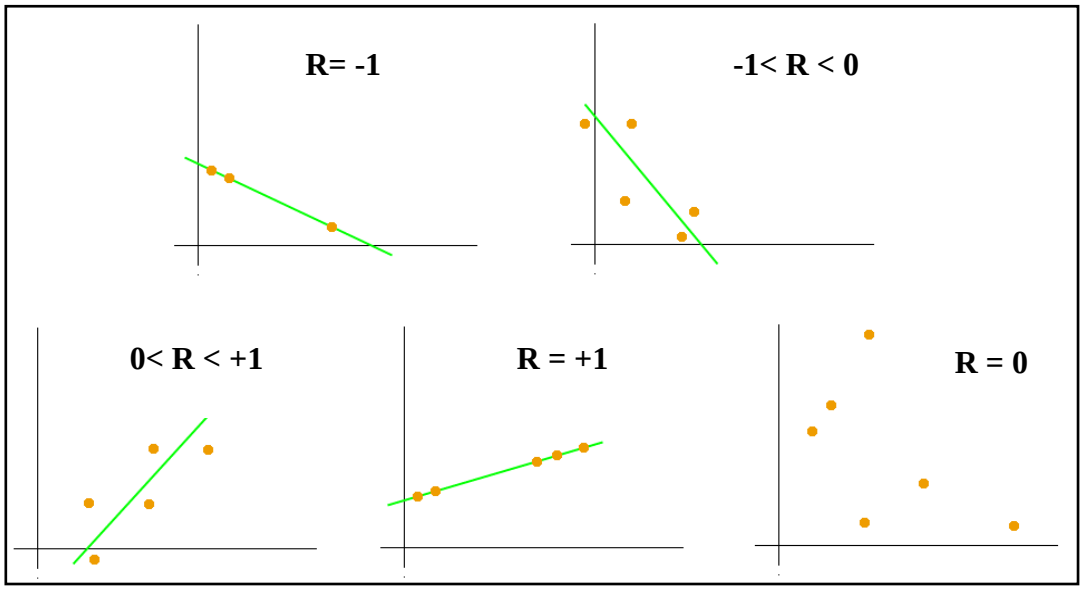

Figure 4.7. Examples of scatter diagrams with different values of correlation coefficient (R).

In particular, is it possible to quantify the strength of correlation as follows:

IF 0 < R < 0,3 and -0,3 < R < 0, the correlation is weak positive and negative, respectively;

IF 0,3 < R < 0,7 and -0,7 < R < -0,3, the correlation is moderate positive and negative, respectively;

IF R > 0,7 and R > - 0,7, the correlation is strong positive and negative, respectively.

IF R = 0, no correlation which means that the two variables are independent.

In this work Pearson's R has been used with the aim to quantify and analyze the relationships between the test size variations and stratigraphic depth (time interval).

Chapter 5

Taxonomy

5.1 Introduction

The classification of planktonic foraminifera has been always based entirely on the features of their external shells allowing the identification of Order, Superfamily, Family, Subfamily, Genus and Species. According to Loeblich & Tappan (1987), in the studied assemblages I recognized species belonging to the superfamilies Rotaliporacea (Sigal, 1958) and Planomalinacea (Bolli *et al.*, 1957).

Taxonomic concepts for genera and species identification in this research project follow Sigal (1977), Caron (1985), Banner & Desai (1988), Verga & Premoli Silva (2002, 2003 and 2005), Moullade *et al.* (2002, 2008), Huber & Leckie (2011), Ellis and Messina Foraminifera Catalogue (Micropaleontolgy Press, www.micropress.org) and CHRONOS online Mesozoic Planktonic Foraminiferal Taxonomic Dictionary (http://portal.chronos.org).

The taxonomic analysis highlights that all taxa belong to the Order Globigerinina and they have been assigned to three different genera on the basis of their coiling mode and shape of the chambers, as follows:

1) trochospiral taxa with globular chambers: genus *Hedbergella*;

2) trochospiral taxa with elongate chambers: genus *Lilliputianella*;

2) planispiral taxa with globular and elongate chambers: genus *Globigerinelloides*;

3) pseudo-planispiral taxa with very elongated chambers: genus *Leupoldina.*

All speciemens are characterized by a bad preservation of the original shell because of strong dissolution due to diagenesis that occurred during the OAE 1a. In particular, most of the Cismon core specimens show a peculiar preservation being characterized by siliceous moulds.

5.2 Description of species

Genera and species within genus are discussed in the text following the alphabetical order.

Comments are included for each examined species when necessary to clarify the taxonomic concept followed in this study and to note significant morphological features. Additional references are included when needed to support the species concepts here adopted.

All holotypes of species here treated are shown in Plates 1, 2, 3 and 4.

Order GLOBIGERININA Delage & Hérouard, 1896

Superfamily PLANOMALINACEA Bolli, Loeblich & Tappan, 1957

Family GLOBIGERINELLOIDIDAE Longoria, 1974

Subfamily GLOBIGERINELLOIDINAE Longoria, 1974

Genus ***Globigerinelloides*** Cushman & Ten Dam, 1948

Type species: *Globigerinelloides algeriana* Cushman & Ten Dam, 1948, p. 43, pl. 8, figs. 4-6.

Globigerinelloides aptiensis (Longoria, 1974)

(Pl. 1, 1a-b; Pl. 5, figs. 1a-b, 2a-b, 3a-b, 4a-b, 5a-b, 6a-b; Pl. 19, fig. 1a-b)

Planomalina escheri (Kaufmann), Bolli, 1959, p. 260, pl. 20, figs. 7-8.

Globigerinelloides aptiense Longoria, 1974, p. 79, pl. 4, figs. 9-10 (holotype); pl. 8, figs. 4-6, 17, 18.

Blowiella solida Krechmar & Gorbachik, 1986, p. 123, pl. 27, fig. 3.

Globigerinelloides aptiense (Longoria), Coccioni & Premoli Silva, 1994, p. 679, fig. 13.16-21.

Blowiella solida (Krechmar & Gorbachik), BouDagher-Fadel *et al*. 1997, p. 181, pl. 10.2, fig. 4.

Alanlordella aptiensis (Longoria), BouDagher-Fadel *et al*. 1997, p. 212, pl. 12.2, figs. 1-3.

Blowiella sp. 1, Moullade *et al.* 1998, p. 206, pl. 5, figs. 9-10.

Globigerinelloides (?) *aptiensis* (Longoria), Moullade *et al*. 2002, p. 131, fig. 4A-E.

Description: Test small in size, planispiral, evolute, equatorial periphery lobate, periphery outline subcircular to slightly lobate, 5.5–6.5 chambers in the last whorl, increasing gradually and slowly in size. Chambers spherical to subspherical and inflated, sutures straight to slightly curved, radial and depressed; umbilical area rather wide and shallow; aperture a low to medium arch.

Dimensions: holotype, maximum diameter 290 μm. Cismon, maximum diameter 86.75-211.90 μm. Site 463, maximum diameter 136.19 μm.

Distinguishing features: G*lobigerinelloides aptiensis* differs from *G. paragottisi* (Verga & Premoli Silva, 2003a) for its more numerous chambers (5.5-6.5 instead of 5-5.5) in the last whorl and a slower growth rate. Moreover, *G. aptiensis* can be easily distinguished from its descendant *Globigerinelloides ferreolensis* for its less numerous chambers (5.5-6.5 instead of 7-9), a slower growth rate and a hexagonal (instead of ovoid) test, and a more lobate equatorial periphery.

Remarks: *Globigerinelloides aptiensis* displays some morphological variability mainly regarding a) the number of chambers of the outer whorl (ranging from 5.5 to 6.5) and in b) the periphery outline, which can be more or less slightly lobate. The original wall texture is not preserved.

The Upper Aptian specimen from Trinidad described by Bolli (1959) as *Planomalina escheri* Kaufmann (illustrated in Bolli, 1959, pl. 20, figs. 7–8), is included here within the morphological variability of *G. aptiensis* as Bolli's description corresponds perfectly to Longoria's diagnosis.

The poorly illustrated holotype (umbilical view tilted) of *Blowiella solida* (Krechmar & Gorbachik, 1986, pl. 27, fig. 3) is a six-chambered specimen characterized by a slow

and gradual growth with a slightly lobate equatorial periphery. According to Verga & Premoli Silva (2003b) this morphotype has the same morphological features as *G. aptiensis* and, consequently, it is treated as its junior synonym.

The specimen illustrated as *Blowiella solida* by BouDagher-Fadel *et al.* (1997, pl. 10.2, figs. 5-6), clearly differs from the holotype of Krechmar & Gorbachik (1986) by possessing five chambers in the outer whorl and a much faster growth rate. This morphotype is assigned to *G. paragottisi* (Verga & Premoli Silva, 2003a).

Stratigraphic distribution: lower part of the Late Barremian-Aptian, from the lower part of the *Globigerinelloides blowi* Zone to the *Mi. miniglobularis* Zone.

Globigerinelloides blowi (Bolli, 1959)

(Pl. 1, 2a-b; Pl. 5, fig. 7a-b, 8a-b, 9a-b, 10a-b, 11a-b; Pl. 19, fig. 2a-b)

Globigerinelloides blowi Bolli, 1959, figs 9.7-13, 10.1-12.

Planomalina blowi Bolli, 1959, p. 260, pl. 20, fig. 2a, b (holotype), not fig. 3.

Globigerinella gottisi Chevalier, 1961 p. 32, pl. 1, figs. 9-13.

Globigerinelloides blowi (Bolli), Moullade, 1966, p. 129, pl. 8, fig. 25, not figs. 24, 26.

Not *Globigerinelloides blowi* (Bolli), Hermes, 1966 p. 161, text-figs. 1, 2.

?Globigerinelloides blowi (Bolli), Kuhry, 1971 p. 228, pl. 1, figs. 3a, b.

Globigerinelloides blowi (Boll), Longoria, 1974 p. 82, pl. 4, figs. 4, 11-13, not fig. 7.

Globigerinelloides blowi (Bolli), Caron, 1985, p. 47, fig. 29.10-11.

Not *Blowiella blowi* (Bolli), Banner & Desai, 1988, p. 170, pl. 4, figs. 5-7.

Globigerinelloides blowi (Bolli), Coccioni & Premoli Silva, 1994 p. 680, fig. 14.1-6.

Blowiella blowi (Bolli), BouDagher-Fadel *et al*. 1997, p. 179, pl. 10.1, figs. 1-4; fig. 10.1.

Blowiella maridalensis (Bolli), BouDagher-Fadel *et al*. 1997, p. 180, pl. 10.1, fig. 14.

Not *Blowiella blowi* (Bolli), Moullade *et al.* 1998, p. 205, pl. 3, figs. 5, 6.

Description: Test small to medium in size, planispiral, evolute to seminvolute, equatorial periphery slightly lobate, 5 chambers in the last whorl (rarely 4.5 or 6 chambers also reported) increasing gradually and slowly in size. Chambers from spherical to subglobular with the last chamber inflated and chambers slightly reniform in lateral view. Sutures straight, radial and depressed, umbilical area rather wide and deep, aperture a low to medium arch.

Dimensions: holotype, maximum diameter 310 μm. Cismon, maximum diameter 95.35-373.23 μm. Site 463, maximum diameter 87.30 μm.

Distinguishing features: *Globigerinelloides blowi* differs from *Globigerinelloides paragottisi* by having a markedly slower growth rate resulting in a circular and less lobate equatorial outline (instead of ovoid), and a more inflated last chamber.

Remarks: *Globigerinelloides blowi* displays a relatively wide morphological variability mainly regarding a) the number of chambers of the last whorl ranging from 4.5 to 6 (usually 5-5.5), b) the shape of the chambers from spherical to slightly reniform in lateral view, c) the more or less slightly lobate equatorial periphery, and d) the more or less depressed and wide umbilical area. The original wall texture is not preserved.

The specimens shown in Pl. 5, figs. 11a-b and Pl. 19, figs. 2a-b have been identified as *Globigerinelloides* cf. (= confer) *blowi* because morphologically similar to *Globigerinelloides blowi* but having the last chamber less inflated in lateral view.

The specimens illustrated by Bolli (1959, pl. 20, fig. 3) and by Banner & Desai (1988), pl. 4, figs. 5–7, do not correspond to the holotype of *G. blowi*, possessing four chambers in the outer whorl and a cross-shaped outline. According to Verga & Premoli Silva (2003a) these specimens should be included in the morphological variability of *Globigerinelloides duboisi*.

Moullade (1966) illustrated as *Globigerinelloides blowi* three specimens (only in spiral view), among them only one (pl. 8, fig. 25) corresponds to the holotype of the nominate taxon, whereas the other two possess four chambers (pl. 8, fig. 24) and five chambers (pl. 8, fig. 26) in the last whorl. According to Verga & Premoli Silva (2003a), these

specimens are close to *G. duboisi* (because of its cross-shaped outline) and possibly to *G. paragottisi* (because of its faster growth rate), respectively.

The seven-chambered form illustrated by Longoria (1974, pl. 4, fig. 7) as *Globigerinelloides blowi* does not correspond to the original diagnosis of this taxon ('with 5 or 6 chambers') reported by the Author. According to Verga & Premoli Silva (2003b), the large number of chambers, the depth of the umbilical area and the reniform chambers in lateral view are likely similar to a juvenile morphotype of *Globigerinelloides barri* (Bolli *et al*., 1957). According to Banner & Desai (1988), *Globigerinelloides blowi* identified by Kuhry (1971) does not belong to this species because of the very lobate periphery and higher number of chambers. The poor figures by Kuhry (1971) preclude a positive attribution to *G. blowi* or an agreement with Banner & Desai's opinion. Finally, the specimen illustrated by Moullade *et al.* (1998, pl. 3, fig. 5) as *Blowiella blowi* is assigned to *Globigerinelloides duboisi* because it has four outer chambers resulting in a cross-shaped test, and the specimen figured in Moullade *et al*. (1998, pl. 3, fig. 6) falls within the morphological variability of *Globigerinelloides paragottisi* because of its rapidly enlarging five outer chambers.

Stratigraphic distribution: middle Barremian-Aptian, from the *Globigerinelloides blowi* Zone to the *Mi. miniglobularis* Zone.

Globigerinelloides blowi lobatus (Verga & Premoli Silva, 2005)

(Pl. 1, 3a-b)

Globigerinelloides blowi lobatus Verga & Premoli Silva, 2005, p. 253-255, pl.2, figs. 1 (holotype), 2-14.

Description: Test medium in size, planispiral, evolute to seminvolute, laterally inflated, equatorial periphery subcircular to lobate, 5 to 6 chambers in the outer whorl, increasing in size rather slowly and gradually. Chambers globular to subglobular, progressively becoming radially elongate; sutures straight to slightly curved, radial and depressed, umbilicus broad and rather depressed; aperture straddling the periphery as a low arch.

Distinguishing features: *Globigerinelloides blowi lobatus* differs from *Globigerinelloides clavatus* in having a) a decidedly lower growth rate, b) less elongate chambers resulting in c) a circular (instead of ovoid), lobate (instead of substellate) test; this subspecies can be easily distinguished from *Globigerinelloides elongatus* for the same reasons and, in addition, in not having posteriorly elongate chambers.

Dimensions: holotype, maximum diameter 233.66 μm. Cismon, maximum diameter 196.08-336.00 μm.

Remarks: This subspecies shows a little morphological variability mainly concerning (a) the number of chambers in the last whorl and b) their elongation obviously resulting in (c) a more or less lobate test. The original wall texture is not preserved.

According to Verga & Premoli Silva (2005), *Globigerinelloides blowi elongatus* derives from *Globigerinelloides blowi* (Bolli 1959) from which differs only in developing slightly elongate chambers.

Stratigraphic distribution: Early Aptian-lower part of the Late Aptian, from the *Leupoldina cabri* Zone to the middle part of the *Globigerinelloides algerianus* Zone.

Globigerinelloides clavatus (Verga & Premoli Silva, 2005)

(Pl. 1, 4a-b; Pl. 8, figs. 2a-b, 3a-b)

Blowiella saundersi (Bolli), Gorbachik, 1986, pl. 27, fig. 4.

Claviblowiella saundersi (Bolli) BouDagher-Fadel *et al*., 1997, p. 181, pl. 10.2, figs 10-11, pl. 10.3, fig. 6.

Globigerinelloides paragottisi clavatus Verga & Premoli Silva, 2005, p. 256-257, Figs. 4.4 (holotype)-13, Fig.5.1-6.

Description: Test small to medium in size, planispiral, evolute to seminvolute, equatorial periphery ovoid and strongly lobate; 5 chambers (also 5.5 reported in the literature) in the outer whorl increasing rapidly and gradually in size as added. First chamber spherical to subspherical, the last two or three radially elongate and forward directed on both spiral and umbilical sides, laterally inflated; sutures straight to slightly

curved, radial and depressed, umbilical area rather small and shallow; aperture straddling the periphery as a low to medium arch.

Dimensions: holotype, maximum diameter 343.86 μm. Cismon, maximum diameter 115.33-377.08 μm.

Distinguishing features: This species differs from *Globigerinelloides elongatus* in having (1) laterally inflated chambers and, (2) not backward elongate chambers and from *Globigerinelloides blowi lobatus* by having a (1) faster growth rate resulting in an (2) ovoid, strongly lobate peripheral outline (instead of circular and moderately lobate).

Remarks: *Globigerinelloides clavatus* shows a small morphological variability mainly regarding (a) the number of chambers of the outer whorl ranging from 5 to 5.5, (b) the involution of the test (varying from evolute to slightly seminvolute), (c) the number of clavate chambers and (d) their elongation, and consequently (e) the shape of the periphery which can be more or less strongly lobate. The original wall texture is not preserved.

According to Verga & Premoli Silva (2005) *Globigerinelloides clavatus* evolves from *Globigerinelloides paragottisi* from which differs only in developing elongate chambers.

Stratigraphic distribution: Early Aptian-lower part of the Late Aptian, from the *Leupoldina cabri* Zone to the *Globigerinelloides algerianus* Zone.

Globigerinelloides duboisi (Chevalier, 1961)

(Pl. 1, 5a-b; Pl. 5, figs. 12a-b, 13a-b, 14a-b, 15a-b; Pl. 6, 1a-b, 2a-b, 3a-b, 4a-b, 5a-b, 6a-b, 7a-b, 8a-b; Pl. 19, 3a-b, 4a-b)

Globigerinella duboisi Chevalier, 1961, p. 33, pl. 1, figs. 14 (holotype), 15-17, not fig. 18.

Globigerinelloides blowi (Bolli), Moullade, 1966, p. 129, pl. 8, fig. 24.

Globigerinelloides duboisi (Chevalier), Longoria, 1974, pp. 83-84, pl. 11, figs. 12, 13; pl. 4, not figs. 15, 16.

Globigerinelloides gottisi (Chevalier), Longoria, 1974, p. 85, pl. 7, figs. 7, 8.

Blowiella duboisi (Chevalier), Banner & Desai, 1988, p. 172, pl. 8, figs. 10-12.

Blowiella duboisi (Chevalier), BouDagher-Fadel *et al*., 1997, p. 179, pl. 10.1, figs. 5-8.

Blowiella maridalensis (Bolli), BouDagher-Fadel *et al*., 1997, p. 180, pl. 10.1, figs. 15-16.
Blowiella blowi (Bolli), Moullade *et al*., 1998, p. 205, pl. 3, fig. 5.

Description: Test small to medium in size, planispiral, evolute to seminvolute, equatorial periphery cross-shaped, lobate to strongly lobate, 4-4.5 chambers in the last whorl increasing in size gradually but rather rapidly resulting in a very globular last chamber. Chambers globular to subglobular on both spiral and umbilical sides, inflated in lateral view; sutures straight, radial and depressed, umbilicus medium to wide and shallow; aperture as a low arch bordered by a thin lip.

Dimensions: holotype, maximum diameter 342 μm. Cismon, maximum diameter 91.10-358.16 μm. Site 463, maximum diameter 71.81-113.14 μm.

Distinguishing features: *Globigerinelloides duboisi* differs from *G. maridalensis* in having a symmetrical spiral view (instead of asymmetrical), inflated and globular to subglobular chambers (instead of laterally compressed and subglobular to elongate chambers tangentially in the direction of the coiling). It differs from the other 4/4.5-chambered specimens belonging to *G. sigali*, *G. elongatus* and *G. clavatus* by not having the last two or three chambers radially elongated.

Remarks: This taxon reveals a little morphological variability mainly concerning a) the number of chambers in the outer whorl (from 4 to 4.5), b) their shape from globular to subglobular, and consequently c) the shape of the test which can be slightly to strongly cross-shaped. In addition, d) a slight difference in the width of the umbilical area can be also recognized. The original wall texture is not preserved.

Moullade (1966), Risch (1971) and Caron (1985) considered *Globigerinelloides duboisi* a junior synonym of *G. blowi*. According to Longoria (1974), Banner & Desai (1988), Coccioni & Premoli Silva (1994) and BouDagher-Fadel *et al*. (1997) these forms are two distinct taxa on the basis of the morphological differences mentioned above.

The individual illustrated by Chevalier (1961, pl. 1, fig. 18) as *Globigerinelloides duboisi* does not correspond to the related description and is here assigned to *Globigerinelloides paragottisi.* According to Verga & Premoli (2003a), the specimen identified as *Globigerinelloides duboisi* by Longoria (1974, pl. 4, figs. 15-16), is not typical of this species, being strongly involute and exhibiting a faster growth rate (not cross-shaped outline). Finally, the 4-chambered specimens of *Globigerinelloides*

maridalensis illustrated by BouDagher-Fadel *et al*. (1997, pl. 10.1, figs. 15-16) are referred to *G. duboisi* because they have symmetrical and laterally inflated chambers.

Stratigraphic distribution: Early Aptian-lower part of the Late Aptian, from the uppermost part of the *Globigerinelloides blowi* Zone to the *Hedbergella trocoidea* Zone.

Globigerinelloides elongatus (Verga & Premoli Silva, 2005)

(Pl. 1, 6a-b; Pl. 8, fig. 4a-b)

Planomalina saundersi (Bolli), 1959, p. 262, pl. 20, fig. 9.

Claviblowiella saundersi (Bolli), BouDagher-Fadel *et al*., 1997, p. 181, pl. 10.2, fig. 6.

Globigerinelloides maridalensis elongatus Verga & Premoli Silva, 2005, p. 256, Fig. 5. 7-10, 11 (holotype), 11-12.

Description: Test small to medium in size, planispiral, seminvolute to evolute, equatorial periphery strongly lobate to stellate; 4.5 to 5.5 chambers in the outer whorl, increasing in size gradually but rather quickly as added. First chambers globular to subglobular, the last two or exceptionally three radially elongated, posteriorly directed, slightly compressed on both spiral and umbilical sides, slightly laterally compressed; sutures straight to slightly curved, radial and depressed; umbilicus rather small and shallow; aperture straddling the periphery as a low arch.

Dimensions: holotype, maximum diameter 252.94 μm. Cismon, maximum diameter 169.54-243.93 μm.

Distinguishing features: *Globigerinelloides elongatus* differs from *G. clavatus* in having chambers posteriorly directed (instead of forward) and from *G. sigali* because the latter doesn't have backward elongate chambers.

Remarks: This species has shown a moderate morphological variability mainly concerning (a) the number of chambers in the last whorl ranging from 4.5 to 5.5, (b) the elongation of the last two/three chambers and, consequently, (c) the shape of the test that can be more or less strongly lobate. The original wall texture is not preserved.

The individuals illustrated by Bolli (1959) in pl. 20, fig. 9 and by BouDagher-Fadel *et al.* (1997) in pl. 10.2, figs 10-11 and in pl. 10.3, fig. 6 (the same specimen reported by Bolli) possess backward directed, elongate last chambers respectively. According to Verga & Premoli Silva (2005), they fall in the morphological variability of *Globigerinelloides elongatus*. Moreover, *Globigerinelloides elongatus* evolves from *Globigerinelloides maridalensis* (Bolli 1959) by developing elongate chambers; thus the latter taxon is the only small planispiral morphotype yielding backward asimmetrycal chambers. This feature allow to clearly recognise *Globigerinelloides elongatus* from all the other clavate globigerinelloidids.

Stratigraphic distribution: Early Aptian-lower part of the Late Aptian, from the *Leupoldina cabri* Zone to the middle part of *Globigerinelloides algerianus* Zone.

Globigerinelloides maridalensis (Bolli, 1959)

(Pl. 1, 7a-b; Pl. 6, fig. 9a-b, 10a-b, 11a-b, 12a-b)

Planomalina maridalensis Bolli, 1959, p. 261, pl. 20, figs. 4-5, 6 (holotype).

Globigerinelloides maridalensis (Bolli), Longoria, 1974, p. 86, pl. 9, figs. 4-7, 10-13; not pl. 27, fig. 18.

Globigerinelloides maridalensis (Bolli), Masters, 1977, p. 406, pl. 11, fig. 3.

Blowiella maridalensis (Bolli), Banner & Desai, 1988, p. 172, pl. 9, figs. 2-3, not fig. 1.

Not *Planomalina* (*Globigerinelloides*) *maridalensis* Bolli, Salaj, 1990, pl. 18, fig. 6.

Globigerinelloides maridalensis (Bolli), Coccioni & Premoli Silva, 1994, p. 682, figs. 14. 11–14.

Blowiella moulladei BouDagher-Fadel, 1995, p. 146, pl. 4, figs. 1-2.

Blowiella maridalensis (Bolli); BouDagher-Fadel *et al.*, 1997, p. 180, pl. 10.1, fig.13, not figs. 14 16.

Blowiella moulladei BouDagher-Fadel; BouDagher-Fadel *et al.*, 1997, p. 180, pl. 10.2, figs. 1–3.

Description: Test small to medium in size, planispiral, evolute to seminvolute, equatorial periphery moderately lobate, 4-5 chambers in the outer whorl increasing fairly fast but gradually in size. Chambers subglobular to elongate tangentially in the direction of the coiling, asymmetrical in spiral view (more developed in their posterior part), laterally compressed; more or less cross-shaped in the 4-chambered morphotypes and ovoid in the 5-chambered specimens. The last chamber displays a crescentic shape in side view; sutures are straight, radial and rather depressed; umbilical area rather wide and shallow; aperture as low arch bordered by a thin lip.

Dimensions: holotype, maximum diameter 320 μm. Cismon, maximum diameter 78.29-292.45 μm.

Distinguishing features: *Globigerinelloides maridalensis* differs from the 4/5-chambered specimens belonging respectively to *Globigerinelloides duboisi* and *Globigerinelloides paragottisi* in having laterally compressed (instead of inflated) and subglobular to elongate chambers that are tangentially in direction of coiling, asymmetrical in spiral view (instead of symmetrical).

Remarks: *Globigerinelloides maridalensis* displays a rather small morphological variability mainly regarding a) the number of chambers in the last whorl (ranging from 4 to 5), b) their backward elongation degree, c) the shape of the test (cross-shaped to ovoid, more or less slightly lobate) and further small differences relating to d) the width of the umbilical area. The original wall texture is not preserved.

The specimen illustrated by Longoria (1974, pl. 27, fig. 18) cannot be referred to *G. maridalensis* because of its inflated chambers. The individual illustrated by Banner & Desai (1988, pl. 9, fig. 1a), re-figured by BouDagher-Fadel *et al.* (1997, pl. 10.1, fig. 14), belongs to *Globigerinelloides blowi* as supported by its slow growth rate, its circular test and uncompressed and symmetrical chambers. The 4-chambered specimens illustrated by BouDagher-Fadel *et al*. (1997, pl. 10.1, figs. 15–16) are referred to *Globigerinelloides duboisi* because of their globular, uncompressed chambers. Finally *Blowiella moulladei*, illustrated by BouDagher-Fadel (1995, pl. 4, figs. 1–2) and re-figured by BouDagher-Fadel *et al.* (1997, pl. 10.2, figs. 1–3), does not exhibit significant morphological characters which can distinguish this taxon from the 4-chambered specimens belonging to *Globigerinelloides maridalensis.*

Stratigraphic distribution: lower part of the Late Barremian-Aptian, from the *Globigerinelloides blowi* Zone to the *Mi. miniglobularis* Zone.

Globigerinelloides paragottisi (Verga & Premoli Silva, 2003a)

(Pl. 1, 8a-b; Pl. 6, figs. 13a-b, 14a-b, 15a-b; Pl. 7, 1a-b, 2a-b, 3a-b, 4a-b, 5a-b, 6a-b, 7a-b, 8a-b, 9a-b,10a-b, 11a-b,12a-b; Pl. 19, fig. 5a-b)

Globigerinella duboisi Chevalier, 1961, p. 32, pl. 1, fig. 18.

Globigerinelloides blowi (Bolli), Moullade, 1966, p. 129, pl. 8, fig. 26.

Globigerinelloides blowi (Bolli), Hermes, 1966, p. 161, text-figs. 1, 2.

Globigerinelloides gottisi (Chevalier), Longoria, 1974, p. 85, pl. 7, figs. 10, 13, not figs. 7, 8.

Globigerinelloides gottisi (Chevalier), Sigal, 1979, pl. 2, fig. 21.

Blowiella gottisi (Chevalier) Banner & Desai, 1988, p. 172, pl. 8, figs. 13-15.

Planomalina (Globigerinelloides) maridalensis Bolli, Salaj, 1990, pl. 18, fig. 7.

Globigerinelloides gottisi (Chevalier), Coccioni & Premoli Silva, 1994, p. 681, fig. 14.7-10.

Blowiella gottisi (Chevalier), BouDagher-Fadel *et al*., 1997, p. 180, pl. 10.1, figs. 9-12; fig. 10.1.

Blowiella solida (Krechmar & Gorbachik), BouDagher-Fadel *et al*., 1997, p. 181, pl. 10.2, fig. 5-6.

Blowiella blowi (Bolli), Moullade *et al*., 1998, p. 205, pl. 3, fig. 6.

Blowiella sp. 1., Moullade *et al*., 1998, p. 206, pl. 5, fig. 10, not fig. 9.

Globigerinelloides paragottisi, Verga & Premoli Silva, 2003a, p. 332-333, Fig. 6. 7-14, Figs. 7. 1-6, 7 (holotype), 8-14.

Description: Test small to medium in size, planispiral, equatorial periphery ovoid, moderately lobate, 5-5.5 (usually 5) chambers in the last whorl increasing rapidly in size. Chambers globular to subglobular on both spiral and umbilical sides, inflated in lateral view; sutures straight, slightly depressed and radial, umbilical area rather shallow and wide; aperture as a low arch bordered by a thin lip.

Dimensions: holotype, maximum diameter 222.32 μm. Cismon, maximum diameter 82.72- 427.71 μm. Site 463, maximum diameter 117.71 μm.

Distinguishing features: *Globigerinelloides paragottisi* differs from the five-chambered specimens belonging to *Globigerinelloides maridalensis* in having inflated (instead of laterally compressed), and symmetrical (instead of posteriorly developed) chambers. It differs also from *Globigerinelloides blowi* by having a markedly faster growth rate resulting in an ovoid equatorial outline (instead of circular and less lobate) and, a less last inflated chamber.

Remarks: *Globigerinelloides paragottisi* has a moderate morphological variability mainly regarding a) the shape of chambers from globular to subglobular, b) a more or less markedly lobate and ovoid outline, c) the number of chambers in the last whorls (ranging from 5 to 5.5), and further differences that concern d) the width of the umbilical area. The original wall texture is not preserved.

The morphotype identified as *Globigerinella duboisi* by Chevalier (1961, pl. 1, fig. 18), corresponds well to the diagnosis of *Globigerinelloides paragottisi*. Moreover, the five-chambered specimen illustrated by BouDagher-Fadel *et al.* (1997, pl. 10.2 figs. 5-6) as *Blowiella solida* clearly falls within the morphological variability of *G. paragottisi*. According to Verga & Premoli Silva (2003a) *G. paragottisi* comprises most of the specimens previously identified as *G. gottisi* except for the following: a) the specimens illustrated by Chevalier (1961, pl. 1, figs. 9-11, 13) as *Globigerinella gottisi* are here assigned to *G. blowi* (being characterized by a slower growth rate resulting in a subcircular-shaped test), while the individual reported by the same author (Chevalier, 1961, pl. 1, fig. 12) is assigned to *Globigerinelloides aptiense* because of its six spherical chambers, growing slowly and gradually, resulting in a hexagonal-shaped peripheral outline typical of the species of Longoria (1974); b) the specimens of *G. gottisi* illustrated by Longoria (1974, pl. 7, figs. 7-8) cannot be included in *G. paragottisi* because they possess four chambers and a cross-shaped test; they are attributable to *Globigerinelloides duboisi* Verga & Premoli Silva (2003a). On the basis of the general morphology the specimen of *G. blowi* illustrated by Moullade (1966, pl. 8, fig. 26) might belong to *G. paragottisi*, even though its growth rate is somewhat slower than in the latter taxon.

The specimen illustrated by BouDagher-Fadel *et al*. (1997, pl. 10.2 figs. 5-6) as *Blowiella solida* does not correspond to the original diagnosis of this taxon provided by Krechmar & Gorbachik (1986). In fact, this individual is characterised by only five chambers (instead of 6-7) on the outer whorl and a rather fast growth rate. According to Verga & Premoli Silva (2003a) it falls within the morphological variability of

Globigerinelloides paragottisi. Finally, the individual reported as *Blowiella* sp. 1 by Moullade *et al*. (1998, pl. 5, fig. 10) is assigned to *Globigerinelloides paragottisi* because of possessing five, rapidly enlarging, outer chambers, whereas the individual figured as *Blowiella* sp. 1 by the same authors (Moullade *et al*., 2002, pl. 5, fig. 9) appears to be close to *Globigerinelloides aptiense* Longoria, 1974.

Stratigraphic distribution: Uppermost Valanginian–lower part of the Late Aptian, from the middle part of the *Hedbergella sigali* Zone to the *Hedbergella trocoidea* Zone.

Globigerinelloides primitivus (Fuchs, 1971)

(Pl. 1, 9a-b; Pl. 13, fig. 13a-b; Pl. 8, fig. 1a)

Globigerinelloides primitivus Fuchs, 1971, p. 37, pl. 9, fig. 27 (holotype).
Globigerinelloides involutus Verga, 2004, p. 45, pl. 5.3, figs. 1-15.

Description: Test very small in size, planispiral, involute to slightly seminvolute, equatorial periphery rounded to lobate, laterally inflated; only 4 chambers in the outer whorl, arranged in two parallel rows, increasing slowly in size as added. Chambers globular to subglobular on both spiral and umbilical sides; sutures straight to slightly curved, radial and slightly depressed; umbilicus, when visible, small and rather shallow; aperture straddling the periphery as a very low arch.

Distinguishing features: *Globigerinelloides primitivus* differs from *Globigerinelloides duboisi* in having a) an involute to slightly seminvolute coiling mode (instead of evolute to semi-involute), b) chambers arranged on two subparallel rows resulting in c) a subrectangular (instead of cross-shaped), d) more compact test. For the same reasons it can be easily distinguished from the 4-chambered individuals of *G. maridalensis*, which, in addition, possesses a) laterally compressed chambers that are b) asymmetrical in their posterior part.

Dimensions: holotype, maximum diameter 250 μm. Cismon, maximum diameter 115.11-322.03 μm.

Remarks: This species shows a little morphological variability mainly concerning (a) the number of chambers in the last whorl that are only 4, (b) the involution of the test

(varying from totally involute to seminvolute), and (c) the shape of the periphery which can be more or less lobate. The original wall texture is not preserved.

The individual illustrated by Longoria as *Globigerinelloides duboisi* in pl. 4, figs 15-16 may be possibly included in the morphological variability of *Globigerinelloides primitivus*.

Stratigraphic distribution: lower middle-Barremian-uppermost part of Early Aptian, from *Globigerinelloides blowi* Zone to the *Leupoldina cabri* Zone.

Globigerinelloides sigali (Longoria, 1974)

(Pl. 1, 10a-b; Pl. 8, figs. 5a-b, 6a-b)

Globigerinelloides sigali Longoria, 1974, p. 88, pl. 3, fig. 1, pl. 7, figs 6, 9 (holotype).

Globigerinelloides saundersi (Bolli), Longoria, 1974, p. 88, pl. 3, figs 10-12.

Claviblowiella sigali (Longoria), Boudagher-Fadel *et al*., 1997, p. 182, pl. 10.3, figs 4-5.

Claviblowiella saundersi (Bolli), BouDagher-Fadel *et al*., 1997, p. 181, pl. 10.2, figs 7-9.

Globigerinelloides duboisi (Chevalier) *sigali* (Longoria), Verga & Premoli Silva, 2005, p. 255-256, Fig. 3.1-14, Fig. 4.1-3.

Description: Test small to medium in size, planispiral, evolute to seminvolute, equatorial periphery cross-shaped and strongly lobate, 4-4.5 chambers in the outer whorl increasing gradually and rather slowly in size except the last two or, exceptionally, three growing more rapidly. First chambers spherical to subspherical, the last two or three radially elongate and round; sutures straight to slightly curved, radial and depressed, umbilical area rather small and shallow; aperture straddling the periphery as a low to medium arch.

Dimensions: holotype, maximum diameter not specified; paratype, maximum diameter 140 μm. Cismon, maximum diameter 115.02-328.44 μm.

Distinguishing features: *Globigerinelloides sigali* differs from the 4-4.5-chambered specimens belonging to *G. clavatus* and *G. elongatus* by not having chambers respectively forward and posteriorly directed. It differs also from *G. duboisi* in having the last two or three chambers radially elongated.

Remarks: *Globigerinelloides sigali* displays a wide morphological variability mainly regarding a) the number of chambers of the outer whorl (ranging from 4 to 4.5), b) the involution of the test (varying from slightly seminvolute to evolute), c) the number of clavate chambers, d) their elongation and, consequently, e) the shape of the equatorial periphery that can be more or less strongly lobate. The original wall texture is not preserved.

Longoria (1974), in his original diagnosis, affirmed that the main morphological feature of *Globigerinelloides sigali* is its last, radially elongate chamber; however, the same author included in this species a specimen (pl. 3, fig. 1) exhibiting a cross-shaped test resulting from the elongation of the last three chambers.

According to Verga & Premoli Silva (2005) it appears that radial elongation may randomly occur on all the chambers of the outer whorl within the 4- 4.5 chambered planispiral plexus (see Figs. 3.1-14, 4.1-3). Consequently, it is possible to extend the morphological variability of *Globigerinelloides sigali* to include all the morphotypes mentioned above. The individual illustrated by Longoria (1974, pl. 3, figs. 10-12) as *Globigerinelloides saundersi* does not correspond to the original diagnosis of this taxon as it possesses four rounded chambers resulting in a cross-shaped test, and it falls within the morphological variability of *Globigerinelloides sigali*.

Stratigraphic distribution: Early Aptian- lower part of the Late Aptian, from the *Leupoldina cabri* Zone to the *Globigerinelloides algerianus* Zone.

Order GLOBIGERININA Delage & Hérouard, 1896

Superfamily ROTALIPORACEA Sigal, 1958

Family HEDBERGELLIDAE Loeblich & Tappan, 1961

Subfamily HEDBERGELLINAE Loeblich & Tappan, 1961

Genus ***Hedbergella*** Brönnimann & Brown, 1958

Type species: *Anomalina lorneiana* d'Orbigny var. *trocoidea* Gandolfi, 1942, p. 99, pl. 2, figs. 1a-c, pl. 4, figs. 2, 3, pl. 3, figs. 2a, b, 5a, b.

Hedbergella aptiana **(**Bartenstein, 1965)

(Pl. 2, 2a; Pl. 10, figs. 1a-b, 2a-b, 3a-b, 4a-b, 5a-b, 6a-b, 7a-b, 8a-b; Pl. 20, figs. 1a-b, 2a-b)

? *Globigerina* sp. D9 Hecht, 1938, p. 17, pl. 23, figs. 60 (holotype)-63.

Hedbergella aptiana Bartenstein, 1965, p. 347-348, text-figs. 4-6.

Hedbergella delrioensis (Carsey), Leckie, 1984, p. 598, pl. 1, fig. 12.

Blefuscuiana occulta (Longoria) *quinquecamerata* Banner & Desai, 1988, p. 162-163, pl. 7, figs. 9-11.

Blefuscuiana aptiana (Bartenstein) *aptiana* Banner, Copestake & White, 1993, p.9, pl. 6, figs. 4-6.

Blefuscuiana daminiae Banner, Copestake & White, 1993, p. 10, pl. 4, figs. 1a-b.

Blefuscuiana laculata Banner, Copestake & White, 1993, p. 13, pl. 3, figs. 2a-c.

Blefuscuiana laculata alobata Banner, Copestake & White, 1993, p. 13, pl. 3, figs. 3-5.

Blefuscuiana praesimilis Banner, Copestake & White, 1993, p. 14, pl. 8, figs. 4a-c, non figs. 5-6

Blefuscuiana aptiana (Bartenstein) *sensu strictu* Boudagher-Fadel *et al*., 1996, p. 252, fig. 4(1-5).

Blefuscuiana aptiana (Bartenstein) *sensu strictu* Boudagher-Fadel *et al*., 1997, p. 125, pl. 8.2, figs. 1-8.

Description: Test medium in size, coiled in a flat to low trochospire, equatorial periphery ovoid, slightly to moderately lobate, 5 to 5.5 chambers in the last whorl (rare juveniles with 4.5 chambers are reported in the literature) increasing rather rapidly in size. Spiral and umbilical sides with globular to sub-globular chambers and sutures depressed, radial to slightly curved; umbilical area shallow and moderately wide; aperture a low to medium arch sometimes bordered by a lip.

Dimensions: holotype, maximum diameter 242.77 μm. Cismon, maximum diameter 74.45-190.87 μm. Site 463, maximum diameter 71.27-94.66 μm.

Distinguishing features: *Hedbergella aptiana* differs from *H. infracretacea* by having a flat to slightly depressed spiral side and a faster growth rate of the chambers resulting in an ovoid (instead of sub-circular) test.

Remarks: This taxon shows a rather wide morphological variability mainly regarding the number of chambers in the final whorl, usually ranging from 5 to 5.5. Rare 4.5-chambered juveniles as well as few 6-chambered morphotypes have been signalled. The outline of the periphery or equatorial margin can be more or less slightly lobate. The original wall texture is not preserved.

The specimen shown in Pl. 10, figs. 8a-c, has been identified as *Hedbergella* cf. *aptiana* because morphologically similar to *Hedbergella aptiana* but slightly flat and deformed.

The individual figured as *Blefuscuiana daminae* by Banner, Copestake & White (1993) in pl. 4, figs. 1a-b (a paratype) exhibits five subglobular chambers coiled on a flat trochospire and resulting in an ovoid test; this specimen is here regarded as junior synonym of *Hedbergella aptiana* Bartenstein (1965). Similarly, the specimen of *Blefuscuiana laculata* illustrated by Banner, Copestake & White (1993) in pl. 3, figs. 2a-c (paratype) falls in the variability of *Hedbergella aptiana*. Again, the types of *Blefuscuiana laculata alobata*, reported by Banner, Copestake & White (1993) in pl. 3, figs. 3-5 shows the same general morphology of the species formalised by Bartenstein in 1965.

Stratigraphic distribution: lower part of the Early Barremian-Aptian, from the upper part of *Leupoldina cabri* Zone to the *Microhedbergella miniglobularis* Zone.

Hedbergella daminiae (Banner, Copestake & White, 1993)

(Pl. 2, 3a-c; Pl. 20, figs. 3a-b, 4a-b, 5a-b, 6a-b)

Blefuscuiana daminiae Banner, Copestake & White, 1993, p. 10, pl. 4, figs. 1a-b. (holotype)

Description: Test medium in size, coiled in a low trochospire, equatorial periphery subquadrangular, 5 chambers in the final whorl, increasing gradually in size. Chambers globular to subglobular in both spiral and umbilical sides, slightly depressed in the last whorl of the spire.

Sutures moderatly depressed and radial, umbilical small and deep, resulting from the distinct overhang of the chambers in the last whorl; the aperture appears to be a narrow slit.

Dimensions: holotype, maximum diameter 279.09 μm. Site 463, maximum diameter 70.83-79.45 μm.

Distinguishing features: *Blefuscuiana daminiae* differs from *Hedbergella infracretacea* by having a smaller and deeper umbilicus, an aperture that appears to be a narrow slit instead of a low to a medium arch and a more compact and subquadrangular test. The much more rapid chamber enlargement in the last whorl of this species, as seen dorsally, easily distinguishes it from *Blefuscuiana laculata* Banner, Copestake & White, 1993, s. l.

Remarks: This species displays low morphological variability mainly related to a) the number of chambers (five) and the shape of the last chamber from subglobular to slightly depressed. The original wall texture is not preserved.

The specimen shown in Pl. 20, figs. 6a-c has been identified as *Hedbergella* cf. *daminiae* because morphologically similar to *Hedbergella daminiae* but having a flatter trochospire and the last chamber in umbilical view not visible because covered by glue.

Stratigraphic distribution: Hauterivian-Barremian, from the upper part of *Hedbergella sigali* Zone to the *Globigerinelloides blowi* Zone.

Hedbergella excelsa (Longoria, 1974)

(Pl. 2, 4a-c; Pl. 11, figs. 1a-c, 2a-c, 3a-c, 4a-c; Pl. 20, 7a-c, 8a-c; Pl. 21, figs. 1a-c, 2a-c)

Hedbergella excelsa Longoria, 1974, p. 55-56, pl. 18, figs. 6-8, 9-11, 14-16 (holotype).

Hedbergella aff. *H. trocoidea* Leckie, 1984, p. 599, pl. 3, figs. 5-10.

Hedbergella aff. *H. trocoidea* Leckie, 1990, p., pl. 31, figs. 14-17.

Blefuscuiana excelsa cumulus Banner, Copestake & White, 1993, p. 11, pl. 6, figs. 1a-c, 2a-c.

Blefuscuiana excelsa (Longoria), Boudagher-Fadel *et al*., 1997, p. 126-127, pl. 8.5, figs. 4-6.

Blefuscuiana excelsa (Longoria) *cumulus* Banner, Copestake & White; Boudagher-Fadel *et al*., 1997, p. 126, pl. 8.5, figs. 7-12.

Description: Test small to medium in size, coiled in a high to very high trochospire, equatorial periphery circular to subcircular, slightly to moderately lobate, 5 to 6 chambers in the last whorl, increasing gradually in size. Spiral and umbilical side with globular to subglobular chambers and sutures depressed, radial to slightly curved; umbilical area medium and rather deep, aperture a low to medium arch.

Dimensions: holotype, maximum diameter 160 μm. Cismon, maximum diameter 71.45-172.41 μm. Site 463, maximum diameter 79.32-112.77 μm.

Distinguishing features: *Hedbergella excelsa* differs from *H. infracretacea* by having a higher trochospire, a smaller and deeper umbilical area. *Hedbergella ruka* is similar to *H. excelsa* in spire height but has a narrower umbilicus and only 4 chambers in the final whorl.

Remarks: *Hedbergella excelsa* displays a moderate morphological variability mainly regarding the a) number of chambers of the outer whorl (varying from 5 to 6), b) the height of the spiral side varying from convex to strongly convex. The original wall texture is not preserved.

Blefuscuiana excelsa cumulus Banner, Copestake & White (1993) is here regarded as junior synonym of *Blefuscuiana excelsa* Longoria (1974) being the differences reported by these authors (the number of outer chambers) too weak in differentiating these two

taxa. Moreover, the individuals (the holotype and two paratypes) figured by Longoria in pl. 18, figs. 6-11, 14-16 exhibit a final whorl with 5.5-6 chambers.

Stratigraphic distribution: upper part of the Late Barremian-Aptian, from the upper part of the *Globigerinelloides blowi* Zone to the *Microhedbergella miniglobularis* Zone.

Hedbergella gorbachikae (Longoria, 1974)
(Pl. 2, 5a-c)

Hedbergella gorbachikae Longoria, 1974, p. 56-58, pl. 15 figs. 11-13 (holotype).
Hedbergella gorbachikae (Longoria), Leckie, 1984, p. 598, pl. 4, figs. 9-11.
Hedbergella gorbachikae (Longoria), Gorbachik, 1986, p. 94, pl. 16, figs. 1-2.
Blefuscuiana gorbachikae (Longoria), Banner & Desai, 1988, p. 160, pl. 5, figs. 8-12.
Lilliputianella longorii Banner & Desai, 1988, p. 165-168, pl. 4, fig. 12.
Not *Blefuscuiana gorbachikae* (Longoria), Banner, Copestake & White, 1993, p. 11, pl. 6, figs. 3a-c.
Blefuscuiana gorbachikae (Longoria), Shanin, 1993, p. 422, pl. 5, fig. 4.
Blefuscuiana gorbachikae (Longoria), Boudagher-Fadel, 1995, p. 143, pl. 2, fig. 5.
Blefuscuiana gorbachikae (Longoria), Boudagher-Fadel *et al*., 1997, p. 127, pl. 8.6, figs. 1-6.

Description: Test medium in size, coiled in a flat to very slightly convex trochospire, periphery subcircular to ovoid, slightly to moderately lobate, 5 to 5.5 chambers in the outer whorl (rare juveniles with 4.5 chambers are also reported in the literature) increasing rather gradually and slowly in size. Chambers globular to subglobular with the last two or three tending to become subtrapezoidal on the spiral side, subrounded to subtriangular on the umbilical side with the last chamber protruding into the umbilicus and partly or completely covering it; chambers reniform in edge view. Sutures depressed, radial and straight; umbilical area small and shallow, aperture a low to medium arch.

Dimensions: holotype, maximum diameter 264 μm.

Distinguishing features: *Hedbergella gorbachikae* differs from all the other 5 to 6-chambered species of the genus *Hedbergella* by having a triangular last chamber protruding toward the umbilicus and totally or almost wholly covering it. In addition, it differs from *Hedbergella excelsa* in its lower spiral side and from *Hebergella aptiana* in its slower growth rate of the chambers resulting in a subcircular (instead of ovoid) test.

Remarks: *Hedbergella gorbachikae* shows a rather wide morphological variability mainly regarding a) the number of chambers in the final whorl (ranging from 4.5 to 5.5), b) the height of the spire (varying from flat to slightly convex), and c) the outline of the periphery, which can be more or less moderately lobate.

The specimen reported by Gorbachik (1986) in pl. 16, figs. 1-2, even probably deformed, falls in the variability of *Hedbergella gorbachikae* Longoria (1974).

The specimens reported by Banner & Desai (1988) in pl. 5, figs. 8-12 match the original description of this taxon; moreover, the specimen in pl. 5, fig. 9 testify that juveniles possessing 4.5 outer chambers ahave been already signaled in the literature.

The paratype of *Lilliputianella longorii*, reported in pl. 4, fig. 12 by Banner & Desai (1988) does not possesses radially elongate chambers but, conversely, high reniform chambers in lateral view. Besides a sligltly more lobulate peripheral outline, it exhibits the same general morphology of *Hedbergella gorbachikae* Longoria (1974) and is therefore included in the sinonimies of the latter taxon.

The specimen illustrated by Banner, Copestake & White (1993) in pl. 6, figs. 3a-c is here assigned to *Hedbergella hispaniae* Longoria (1974) based on the morphology of its six outer chambers resulting in a hexagonal, lobate test.

The individuals reported by BouDagher-Fadel *et al*. (1997) in pl. 8.6, figs. 1-6 testify the rather wide variability of the peripheral outline (ranging from more or less moderately lobate), which characterise this taxon.

Stratigraphic distribution: upper part of the Late Barremian-Aptian, from the middle-part of the *Globigerinelloides blowi* Zone to the *Microhedbergella miniglobularis* Zone.

Hedbergella kuznetsovae (Banner & Desai, 1988)

(Pl. 2, 6a-c)

Blefuscuiana kuznetsovae Banner & Desai, 1988, p. 156-158, pl. 3, fig. 10 (holotype), pl. 4, figs 1- 4.

No *Hedbergella kuznetsovae* (Banner & Desai), Coccioni & Premoli Silva, 1994, p. 676-677, figs 12.1-12 (= *Hedbergella primare*).

Blefuscuiana kuznetsovae (Banner & Desai), Boudagher-Fadel *et al.*, 1997, p. 124, pl. 8.1, figs. 1-5 (refigured holotype and 3 paratypes in one view).

Blefuscuiana kuznetsovae (Banner & Desai), Boudagher-Fadel *et al.*, 1997, p. 130, pl. 8.8, figs. 9-10.

Description: Test large in size, a low trochospire completely evolute (the spire opens slowly) and flat or slightly concave on the spiral side, equatorial periphery lobate, 6-8 chambers in the last whorl. Chambers globular to subglobular and inflated on the spiral and umbilical sides, equally biconvex on the lateral view. Sutures are moderately depressed and radial, umbilical area wide and shallow; the aperture is a low arch.

Dimensions: holotype, maximum diameter 292.63 μm. Cismon, maximum diameter 96.01-123.04 μm.

Distinguishing features: *Hedbergella kuznetsovae* differs from *H. luterbacheri* by having a wider umbilical area, a trochospire completely evolute and an equally biconvex profile. *Hedbergella kuznetsovae* differs from *H. primare* by having reniform chambers in edge view, a very depressed spire (close to *Globigerinelloides*) and an umbilicus rather large on both sides.

Remarks: *Hedbergella kuznetsovae* displays a moderate morphological variability mainly regarding a) the number of chambers of the outer whorl (from 6 to 8) and b) an evolute trochospire.

Stratigraphic distribution: uppermost Barremian-lower part of the Late Aptian, from the uppermost part the *Globigerinelloides blowi* Zone to the *Globigerinelloides algerianus* Zone.

Hedbergella infracretacea (Glaessner, 1937)

(Pl. 2, 7a-c; Pl. 11, figs. 5a-c, 6a-c, 7a-c; Pl. 12, figs. 1a-c, 2a-c, 3a-c, 4a-c; Pl. 21, figs. 3a-c, 4a-c, 5a-c, 6a-c)

Globigerina infracretacea Glaessner, 1937, p. 28, fig. 1 (holotype).

Globigerina aptica Agalarova 1951, p. 49, pl. 8, figs. 9-11.

Globigerina infracretacea (Glaessner) *trochoidea*, Moullade, 1960, p. 136, pl. 2, figs. 21, 23-25.

Globigerina infracretacea (Glaessner) *gargasiana* Moullade, 1961, p. 214.

Hedbergella beegumensis (Marianos & Zingula), 1966, p. 335, pl. 37, figs. 7a-c.

Hedbergella infracretacea (Glaessner), Glaessner, 1966, p. 179-184, pl. 1, figs. 1a-3c.

Hedbergella aptica (Agalarova), Gorbachik & Kretchmar, 1969, p. 50-51, pl. 1, figs. 1a-c.

Blefuscuiana cf. *aptica* (Agalarova), Banner & Desai, 1988, p. 160, pl. 3, figs. 4, 5a-b.

Hedbergella aff. *Hd. infracretacea* (Glaessner), Leckie, 1990, p. 321, pl. 2, figs. 1-18.

Blefuscuiana infracretacea (Glaessner) *sensu strictu* Banner, Copestake & White, 1993, p. 11, pl. 4, fig. 2, pl. 8, fig. 1.

Blefuscuiana infracretacea (Glaessner) *sensu strictu*, Boudagher-Fadel *et al*., 1997, p. 128-129, pl. 8.7, fig. 1-5, non figs. 6-8.

Blefuscuiana aptiana (Agalarova) *orientalis* BouDagher-Fadel *et al.*, 1997, p. 125, 126, pl. 1.1., figs. 3, 4; pl. 8.2, figs. 9–11, pl. 8.3, figs. 1-8.

Hedbergella infracretacea (Glaessner) *occidentalis* BouDagher-Fadel *et al*., 1997, p. 129, pl. 8.7, figs. 9-15.

Description: Test medium in size, coiled in a flat to slightly convex trochospire, equatorial periphery subcircular to ovoid, slightly to moderately lobate, 4.5–5.5 chambers in the final whorl, increasing gradually in size. Chambers globular to subglobular,

reniform when viewed laterally. Sutures depressed, radial to slightly curved; umbilical area rather wide and shallow; aperture as a low to medium arch.

Dimensions: holotype, maximum diameter 270.22 μm. Cismon, maximum diameter 67.89-193.32 μm. Site 463, maximum diameter 73.45-145.70 μm.

Distinguishing features: *Hedbergella infracretacea* differs from *H. aptiana* in having a slower growth rate of the chambers resulting in a subcircular (instead of ovoid) test. It can be easily recognised from *H. excelsa* by possessing a flatter spiral side and a shallower umbilical area.

Remarks: *Hedbergella infracretacea* displays a moderate morphological variability mainly regarding a) the number of chambers of the outer whorl (from 4.5 to 5.5), b) the height of the spiral side varying from almost flat to very slightly convex and c) in the chamber growth rate in the final whorl. The original wall texture is not preserved.

The specimen shown in Pl. 12, figs. 4a-c has been identified as *Hedbergella* cf. *infracretacea* because morphologically similar to *Hedbergella infracretacea* but having the last chamber ovoid instead of subglobular.

Stratigraphic distribution: upper part of the Late Barremian – Aptian, from the middle part of the *Globigerinelloides blowi* Zone to the *Mi. miniglobularis* Zone.

Hedbergella laculata (Banner, Copestake & White, 1993)

(Pl. 2, 8a-c; Pl. 12, fig. 5a-c; Pl. 21, figs. 7a-c, 8a-c)

Clavihedbergella eocretacea (Neagu), Sigal, 1979, p. 290, pl. 1, figs, 31, ?30.

Blefuscuiana laculata Banner, Copestake & White, 1993, p. 13, pl. 3, figs. 2a-c (holotype).

Hedbergella sigali (Moullade), Coccioni & Premoli Silva, 1994, Fig. 12.16-18.

Blefuscuiana praesimilis (Banner, Copestake & White), BouDagher-Fadel *et al*., 1997, p. 129, pl. 8.9, figs. 1-3.

Description: Test small to medium in size, coiled in a flat to weakly convex trochospire, equatorial periphery subquadrangular, 5 chambers in the last whorl, increasing gradually in size. Chambers subglobular in the penultimate whorl and

subglobular to slightly depressed in the last whorl. Sutures moderately depressed and radial; umbilical area broad and the aperture is a narrow slit.

Dimensions: holotype, maximum diameter 170 μm. Cismon, maximum diameter -μm. Site 463, maximum diameter 73.30-182.13 μm.

Distinguishing features: *H. laculata* differs from *H. sigali* for a) the number of chambers in the final whorl abutting the umbilicus (5 and 4-4.5 respectively) and b) by showing a slower increase in the growth of the spire in the last whorl.

Remarks: *Hedbergella laculata* displays a moderate morphological variability mainly regarding a) the number of chambers of the outer whorl (five), b) the height of the spiral side varying from almost flat to weakly concave and c) an equatorial periphery subquadrangular. The original wall texture is not preserved.

The specimen illustrated in Fig. 12, 16-18 as *H. sigali* from the Rio Argos section by Coccioni & Premoli Silva (1994) is very similar to *H. laculata* and is here regarded as a junior synonym. Moreover, in agreement with BouDagher-Fadel *et al* (1997), the holotype of *Blefuscuiana praesimilis* Banner *et al*. (1993) from the lower Barremian of the North Sea falls within the variability of *H. laculata*, is also considered a junior synonym.

Stratigraphic distribution: Early Barremian, upper Valhall Formation.

Hedbergella luterbacheri (Longoria, 1974)

(Pl. 2, 9a-c; Pl. 22, 1a-c, 2a-c, 3a-c)

Hedbergella luterbacheri Longoria, 1974, p. 61, pl. 19, figs. 21-26, pl. 26, figs. 15-17 (holotype).

Blefuscuiana kuznetsovae Banner & Desai, 1988, p. 156-158, pl. 3, fig. 10, pl. 4, figs. 1-4.

Blefuscuiana occulta (Longoria), Banner & Desai, 1988, p. 162, pl. 6, figs. 9-10.

Blefuscuiana multicamerata Banner & Desai, 1988, p. 165, pl. 6, figs. 7a-d.

Hedbergella kuznetsovae (Banner & Desai), Coccioni & Premoli Silva, 1994, p. 676-677, figs. 12.1-12.

Blefuscuiana kuznetsovae (Banner & Desai), Boudagher-Fadel *et al*., 1997, p. 124, pl. 8.1, figs. 1-5.
Blefuscuiana multicamerata (Banner & Desai), Boudagher-Fadel *et al*., 1997, p. 130, pl. 8.8, figs. 9-10.

Description: Test small to medium in size, coiled in a very low trochospire, equatorial periphery subcircular to ovoid, slightly lobate, 6 to 7.5 chambers in the last whorl increasing gradually but rather rapidly in size. Chambers globular to subglobular in the spiral and umbilical sides with the last two or three chambers possibly becoming slightly reniform in lateral view. Sutures depressed, radial to slightly curved; umbilical area wide and shallow; aperture a low to medium arch.

Dimensions: holotype, maximum diameter 300 μm. Cismon, maximum diameter 136.44-236.48 μm. Site 463, maximum diameter 94.23-210.61 μm.

Distinguishing features: *Hedbergella luterbacheri* differs from *H. kuznetsovae* by having a narrower umbilical area and an unequally biconvex profile.

Remarks: *Hedbergella luterbacheri* displays a moderate morphological variability mainly regarding a) the number of chambers of the outer whorl (from 6.5 to 7.5), b) the height of the spiral side varying from almost flat to weakly concave and the peripheral outline which can be more or less weakly lobate. The original wall texture is not preserved.

The specimen shown in Pl. 22, figs. 2a-c has been identified as *Hedbergella* cf. *luterbacheri* because morphologically similar to *Hedbergella luterbacheri* but is lacking of the umbilical view and for that reason is not possible to compare all features.

The specimen shown in Pl. 22, figs. 3a-c has been identified as *Hedbergella* cf. *luterbacheri* because morphologically similar to *Hedbergella luterbacheri* but it has six chambers instead of seven in the last whorl.

The holotype of *Blefuscuiana kuznetsovae* Banner & Desai (1988), illustrated in pl. 3, figs. 10, even possessing 7 outer chambers (instead of 7.5), shows the same general morphology of *Hedbergella luterbacheri* Longoria (1974) and is treated here as a junior synonym.

At the same, *Blefuscuiana multicamerata* Banner & Desai (1988) illustrated in pl. 6, figs. 7a-d does not display any meaningful differences from *Hedbergella luterbacheri* and is therefore included in the synonymy of the latter species.

Stratigraphic distribution: uppermost Barremian- lower part of the Late Aptian (from the uppermost part of *Globigerinelloides blowi* Zone to the *Globigerinelloides algerianus* Zone).

Hedbergella occulta (Longoria, 1974)

(Pl. 3, 1a-c; Pl. 12, figs. 6a-c, 7a-c, 8a-c; Pl. 13, figs. 1a-c, 2a-c, 3a-c, 4a-c)

Hedbergella occulta Longoria, 1974, p. 63, 64, pl. 11, figs. 1-3, 7, 8, pl. 20, figs. 5-7, 8-9 (holotype), 17, 18.

Hedbergella sp. 1 Leckie, 1984, p. 599, pl. 4, figs. 5-8, 12.

Hedbergella cf. *H. rischi* (Moullade), Leckie, 1984, p. 599, pl. 7, figs. 11,12.

? *Blefuscuiana aptica* (Agalarova), Banner & Desai, 1988, p. 160, pl. 5, fig. 7.

Blefuscuiana globigerinelloides (*Subbotina*) *lobulata* Banner & Desai, 1988, p. 164, pl. 6, figs. 1-3.

Blefuscuiana occulta perforocculta Banner, Copestake & White, 1993, p. 13, 14, pl. 8, figs. 2a-c, 3.

Hedbergella occulta (Longoria), Boudagher-Fadel *et al*., 1997, p. 130, pl. 8.8, figs. 11-12.

Description: Test medium in size, coiled in a low trochospire, equatorial periphery subcircular to ovoid, slightly lobate, 6 chambers in the last whorl increasing rather gradually and slowly in size. Chambers globular to subglobular, subtrapezoidal on the spiral side, tending to become subtriangular on the umbilical side with the last chamber inflated. Sutures depressed, radial to slightly curved; umbilical area slightly wide and rather deep; aperture a low to medium arch.

Dimensions: holotype, maximum diameter 251 μm. Cismon, maximum diameter 74.50-200.88 μm.

Distinguishing features: *Hedbergella occulta* differs from *Hd. praetrocoidea* by having a thinner test, a wider umbilical area and chambers less triangular in the umbilical side. It differs from *Hd. infracretacea* and *Hd. aptiana*, by having 6 chambers in the final whorl and from *Hd. excelsa* by having a low trochospire.

Remarks: *Hedbergella occulta* displays a rather wide morphological variability mainly regarding a) the height of the spiral side, which can be almost flat to slightly convex, and b) the peripheral outline ranging from subcircular to ovoid; c) other small differences can be detected in the outline of the peripheral margin which can be more or less weakly lobate. The original wall texture is not preserved.

The specimen shown in Pl. 13, figs. 4a-c has been identified as *Hedbergella* cf. *occulta* because morphologically similar to *Hedbergella occulta* but having five chambers instead of six in the last whorl and more globular chambers.

The specimen reported as *Blefuscuiana aptica* by Banner & Desai (1988) in pl. 5, fig. 7, even illustrated only in spiral view, seems to possess a general morhology very close to *Hedbergella occulta*.

Blefuscuiana globigerinelloides lobulata formalised by Banner & Desai (1988) and illustrated in pl. 6, figs 1-3, even showing a slightly more lobate peripheral outline, falls in the variability of *Hedbergella occulta* Longoria (1974).

The specimens reported as *Blefuscuiana occulta* by Banner & Desai (1988) in pl. 6, figs 9, and 12 characterized by having 7 globular chambers in the outer whorl increasing rather rapidly in size as added are here assigned to *Hedbergella luterbacheri* Longoria (1974).

Stratigraphic distribution: Aptian, from the uppermost part of the *Globigerinelloides blowi* Zone to the *Mi. miniglobularis* Zone.

Hedbergella praetrocoidea (Kretchmar & Gorbachik, 1986)

(Pl. 3, 2a; Pl. 13, figs. 5a-c, 6a-c, 7a-c, 8a-c; Pl. 22, figs. 4a-c, 5a-c, 6a-c, 7a-c, 8a-c; Pl. 23, figs. 1a-c, 2a-c, 3a-c, 4a-c, 5a-c, 6a-c, 7a-c)

Hedbergella praetrocoidea Kretchmar and Gorbachik (in Gorbachik), 1986, p. 95, pl. 16, figs. 3 (holotype)-5.

Blefuscuiana praetrocoidea (Kretchmar & Gorbachik), Boudagher-Fadel *et al*., 1997, p. 130-131, pl. 8.9, fig. 4, figs. 5-6, figs. 7, 9 and 12, figs 8, 10, 11 (= 4 paratypes).

Blefuscuiana rudis Banner, Copestake & White, 1993, p. 14, pl. 5, figs. 2, 5.

Blefuscuiana aptiana (Bartenstein) *implana*, Banner, Copestake & White, 1993, p. 10, pl. 7, fig. 2, non figs. 3-4.

1996 *Blefuscuiana aptiana* (Bartenstein) *orientalis*, Boudagher-Fadel *et al*, 1996, p. 252, fig. 2.11, figs. 3.1-2.

Blefuscuiana infracretacea (Glaessner), Boudagher-Fadel *et al*., 1996, p. 246-249, fig. 2.1-2.

Blefuscuiana aptiana (Bartenstein) *orientalis*, Boudagher-Fadel *et al.*, 1997, p. 125-126, pl. 8.2, fig. 11.

Description: Test medium to large in size, coiled in a low trochospire, equatorial periphery subcircular to ovoid, slightly lobate, 6 chambers in the last whorl (juveniles with 5.5 chambers are recognized in this study and species with 6.5 chambers are also reported in the literature) increasing gradually and slowly in size. Chambers subspherical to trapezoidal in the spiral side, subtriangular to triangular on the umbilical side, reniform in lateral view. Sutures depressed, radial to slightly curved; umbilical area medium and deep; aperture a low to medium arch.

Dimensions: holotype, maximum diameter 180 μm. Cismon, maximum diameter 71.22-183.16 μm. Site 463, maximum diameter 67-102.50 μm.

Distinguishing features: *Hedbergella praetrocoidea* can be easily differenciated from its ancestor *Hedbergella occulta* by possessing less triangular chambers in the umbilical side and a smaller umbilicus.

Remarks: *Hedbergella praetrocoidea* displays a slight morphological variability mainly regarding a) the number of chambers of the outer whorl (from 5.5 to 6.5) and b) the height of the spiral side varying from almost flat to weakly convex. The original wall texture is not preserved.

The specimens shown in Pl. 13, figs. 7a-c, 8a-c and Pl. 23, Fig. 7a-c have been identified as *Hedbergella* cf. *praetrocoidea* because morphologically similar to *Hedbergella praetrocoidea* but having 5-5 1/2 chambers instead of six in the last whorl.

Stratigraphic distribution: Early Hauterivian-Aptian, from the middle part of the *Hedbergella sigali* Zone to the *Mi. miniglobularis* Zone.

Hedbergella primare (Kretchmar & Gorbachik, 1986)

(Pl. 3, 3a; Pl. 14, fig. 1a-c)

Clavihedbergella primare Kretchmar & Gorbachik (in Gorbachik), 1986, p. 120-121, pl. 25, figs. 2 (holotype), 3.
Lilliputianella similis (Longoria), Banner, Copestake & White, 1993, p. 15, pl. 8, figs. 8a-c.
Blefuscuiana primare (Kretchmar & Gorbachik), Boudagher-Fadel *et al*., 1997, p. 131, pl. 8.10, figs. 1-3.

Description: Test medium in size, coiled on a very low trochospire; equatorial periphery circular to subcircular, lobulate, 6 to 7 chambers in the outer whorl increasing gradually and slowly in size. Chambers globular to subglobular, the last two or three becoming slightly reniform in lateral view; sutures depressed, radial to slightly curved, umbilical area extremely wide and shallow; aperture as a low to medium arch sometimes bordered by a lip.

Dimensions: holotype, maximum diameter 129 μm. Cismon, maximum diameter of 185.71 μm.

Remarks: *Hedbergella primare* displays a moderate morphological variability mainly regarding the number of chambers of the outer whorl (from 6 to 7) and the height of the spiral side varying from almost flat to weakly concave; other small differences are associated with the peripheral outline that can be more or less lobulate. The original wall texture is not preserved.

Hedbergella primare differs from *Lilliputianella maslakovae* Longoria (1974) mainly in not having radially elongate chambers; this species can be distinguished from *H. luterbacheri* Longoria (1974) a) by having a slower growth rate of the chambers, b) by

becoming reniform when laterally viewed, and (c by possessing a circular (instead of ovoid) test.

Stratigraphic distribution: Early Barremian-lower part of the Late Aptian (from the *Lilliputianella similis* Zone to the *Globigerinelloides algerianus* Zone).

Hedbergella sigali (Moullade, 1966)

(Pl. 3, 4a-b; Pl. 14, figs. 2a-c, 3a-c, 4a-c, 5a-c, 6a-c, 7a-c, 8a-c)

Hedbergella sigali Moullade, 1966, p. 87-88, pl. 7, figs. 20-23, 24-25 (holotype).

Praehedbergella sigali (Moullade), Banner, Copestake & White, 1993, p. 7, pl. 2, figs. 2a-c.

Hedbergella sigali (Moullade), Coccioni & Premoli Silva, 1994, p. 677-678, fig. 12.16-18, not figs. 12. 13-15, 12.19-21.

Praehedbergella sigali (Moullade), Boudagher-Fadel, 1995, p. 142, pl. 2, figs. 1, 2.

Praehedbergella sigali (Moullade); Boudagher-Fadel *et al*., 1997, p. 108, pl. 7.3, figs. 4-8, pl. 7.4, figs. 1-4.

Praehedbergella tatianae Banner & Desai; Boudagher-Fadel *et al*., 1997, p. 109, pl. 7.4, figs. 5-7.

Praehedbergella tuschepsensis (Antonova) *grigelisi* Banner & Desai, Boudagher-Fadel *et al*. 1997, p. 106, pl. 7.1, figs. 12-14.

Description: Test small to medium in size, coiled in a flat to weakly convex trochospire; equatorial periphery cross-shaped, slightly to strongly lobate, 4 to 4.5 chambers in the last whorl increasing slowly to rather rapidly in size. Chambers shape globular to subglobular on the spiral and umbilical sides, possibly becoming slightly reniform in lateral view. Sutures depressed, radial to slightly curved; umbilical area small/medium and deep, aperture a low to medium arch.

Dimensions: holotype, maximum diameter 230 μm. Cismon, maximum diameter 70.22-199.85 μm.

Distinguishing features: *Hedbergella sigali* differs from *Hedbergella tuschepsensis* by having a higher trochospire, an evident equatorial periphery cross-shaped.

Remarks: *Hedbergella sigali* displays a rather wide morphological variability mainly regarding a) the number of chambers of the outer whorl (from 4 to 4.5), b) the growth rate of the chambers, and c) the size of the umbilicus (ranging from small to medium). Other small differences can be detected in the height of the spiral side varying from almost flat to slightly convex. The original wall texture is not preserved.

The specimens shown in Pl. 14, figs. 6a-c, 7a-c and 8a-c have been identified as *Hedbergella* cf. *sigali* because morphologically similar to *Hedbergella sigali* but having a higher trochospire.

Stratigraphic distribution: Early Valanginian- Aptian (from the base of the *Hedbergella sigali* Zone to the *Mi. miniglobularis* Zone).

Hedbergella tuschepsensis (Antonova, 1964)

(Pl. 3, 5a-c; Pl. 3, 1a-c; Pl. 15, figs. 1a-c, 2a-c, 3a-c; Pl. 23, fig. 8a-c)

Globigerina tuschepsensis Antonova, 1964, p. 59-60, pl. 12, figs. 3a-c (holotype).

? *Clavihedbergella tuschepsensis* (Antonova), Gorbachik, 1986, p. 118-119, 236, pl. 25, fig. 1.

Not *Praehedbergella tuschepsensis* (Antonova), Banner, Copestake & White, 1993, p. 8-9, pl. 2, figs. 4a-c.

Praehedbergella tuschepsensis (Antonova), Boudagher-Fadel *et al.* 1997, p. 105-106, pl. 7.1, figs. 1-7.

Description: Test small to medium in size, coiled in a flat to weakly convex trochospire, equatorial periphery cross-shaped, slightly to strongly lobate, 4 chambers in the last whorl increasing slowly to rather rapidly in size (4.5 chambers are also reported in the literature).

Chambers globular to subglobular on the spiral and umbilical sides, possibly becoming slightly reniform in lateral view. Sutures depressed, radial to slightly curved, umbilical area small/medium and shallow; aperture a low to medium arch.

Dimensions: holotype, maximum diameter 229.16 μm. Cismon, maximum diameter 72.78-199.29 μm. Site 463, maximum diameter 67.97-104.85 μm.

Distinguishing features: *Hedbergella tuschepsensis* differs from *Hedbergella sigali* and *Hedbergella ruka* by having a very low trochospire and a shallower umbilical area.

Remarks: *Hedbergella tuschepsensis* displays a rather wide morphological variability mainly regarding a) the number of chambers of the outer whorl (from 4 to 4.5), b) the growth rate of the chambers, and c) the size of the umbilicus (ranging from small to medium). Other small differences can be detected in the height of the spiral side varying from almost flat to very slightly convex. The original wall texture is not preserved.

The specimens reported as *Hedbergella tuschepsensis* by Gorbachik (1986) in pl. 25, fig. 1, cannot be attributed to *Hedbergella tuschepsensis* being illustrated only in spiral view. The specimen reported as *Hedbergella tuschepsensis* by Banner, Copestake & White (1993) in pl. 2, figs. 4a-c is assigned here to *Hedbergella aptiana* because of its five outer chambers coiled in a flat trochospire and increasing rapidly in size as added, resulting in a ovoid, moderately lobate test. The same specimen was choosen as the holotype of *Praehedbergella yakovlaevae* by BouDagher-Fadel *et al*. (1993)

Stratigraphic distribution: Early Valanginian-Aptian, from the base of the *Hedbergella sigali* Zone to the *Mi. miniglobularis* Zone.

Order GLOBIGERININA Delage & Hérouard, 1896

Superfamily ROTALIPORACEA Sigal, 1958

Family PRAEHEDBERGELLIDAE BouDagher-Fadel,

Banner & Whittaker, 1997

Subfamily PRAEHEDBERGELLINAE BouDagher-Fadel,

Banner & Whittaker, 1997.

Genus ***Gorbachikella*** Banner & Desai, 1988

Type species: *Globigerina kugleri* Bolli, 1959, p.158-159, Pl. 23, figs. 3-5.

Gorbachikella kugleri (Bolli, 1959)

(Pl. 1, 11a-c; Pl. 19, fig. 6a-c),

Globigerina kugleri Bolli, 1959, p. 270, pl. 23, figs. 3-5 (holotype).

Caucasella hoterivica (Subbotina), Longoria, 1974, p. 49, pl. 11, figs 9-11, 14-16.

Gorbachikella kugleri (Bolli), 1988, Banner & Desai, p. 151, pl. 2, figs 1-2.

Gorbachikella kugleri (Bolli), 1995, BouDagher-Fadel *et al*., 1995, p. 188, pl. 2, figs 1-5.

Gorbachikella anteroapertura BouDagher-Fadel *et al*., 1995, p. 190-192, pl. 5, figs 1-6.

Globuligerina spiralis Maamouri and Salaj, 1995, p. 132, pl. 2, figs 3-6, pl. 3, figs 3-4, pl. 4, figs 1-2.

Gorbachikella kugleri (Bolli), BouDagher-Fadel *et al*., 1995, p. 142, pl. 1, figs 1-6.

Gorbachikella anteroapertura BouDagher-Fadel *et al*., 1995, p. 141, pl. 1, figs 11-12.

Gorbachikella kugleri (Bolli), BouDagher-Fadel *et al*., 1997, p. 87, pl. 6.1, figs 1-6, pl. 6.2, figs 1-6

Gorbachikella anteroapertura (BouDagher-Fadel), BouDagher-Fadel *et al*., 1997, p. 87, pl. 6.3, figs 1-10.

Gorbachikella grandiapertura (BouDagher-Fadel), BouDagher-Fadel *et al*.,1995, p. 88, pl. 6.6, fig. 4.

Description: Test small to medium, trochospirally coiled, globigeriniform, peripheral outline round and lobulate, dorsal side slightly to strongly convex, 4 chambers in the outer whorl increasing slowly and gradually in size. Chambers globular to subglobular on both spiral and umbilical sides; sutures depressed, radial, straight to slightly curved, umbilicus rather broad and shallow; aperture umbilical as a medium arch.

Dimensions: holotype, maximum diameter 280.00 μm. Cismon core, maximum diameter 83.75-116.52 μm. Site 463, maximum diameter 115.55 μm.

Distinguishing features: *Gorbachikella kugleri* differs from *Gubkinella graysonensis* mainly by possessing a wide umbilical area and an arch-like aperture.

Remarks: This species displays a moderate morphological variability regarding a) the number of species in the last whorl (four) and b) a dorsal side from slightly to strongly convex. The original wall texture is not preserved.

The specimens reported as *Gorbachikella anteroapertura* by BouDagher-Fadel *et al.* (1995) and illustrated in pl. 5, figs 1-6, are here included in the variability of *Gorbachikella kugleri* (Bolli, 1959). At the same, the individual described as *Gorbachikella anteroapertura* by BouDagher-Fadel *et al.* (1995) and illustrated in pl. 1, figs. 11-12 shows the same general morphology of *Gorbachikella kugleri* and are therefore here included in the variability of this latter taxon.

Stratigraphic distribution: Upper part of Valanginian-upper part of the lower Aptian, from the middle part of the *Hedbergella sigali* Zone to the *Leupoldina cabri* Zone.

Genus ***Lilliputianella*** Banner & Desai, 1988

Type species: *Lilliputianella longorii* Banner & Desai, 1988, p.158-159, pl. 4, figs 11-12.

Lilliputianella globulifera (Kretchmar & Gorbachik, 1971)

(Pl. 3, 11a-c; Pl. 16, figs. 1a-c, 2a-c, 3a-c, 4a-c, 5a-c, 6a-c, 7a-c, 8a-c; Pl. 17, figs. 1a-c, 2a-c)

Clavihedbergella globulifera Kretchmar & Gorbachik, 1971, p. 136, pl.30, fig. 1 a-c (holotype).

Lilliputianella globulifera (Kretchmar & Gorbachik), Banner & Desai, 1988, p. 170-171, pl. 8, figs. 1-4.

Lilliputianella globulifera (Kretchmar & Gorbachik), Bou-Dagher Fadel *et al*., 1997, p. 164-165, pl. 9.1, figs. 8-9.

Praehedbergella globulifera (Kretchmar & Gorbachik), Moullade *et al*., 2008, p. 24, pl. 7, figs. 2-7, 9-11, 15-17.

Description: Test small in size, coiled in a flat to weakly convex trochospire, test outline from rounded to oval, lobate; 5-5.5 chambers in the last whorl (also 6-7 chambers reported in the literature) increasing uniformly in size. Chambers in the first whorl are spherical, later chambers are oval in outline on the spiral and umbilical sides. Sutures straight and depressed, umbilical area wide and deep. Aperture bordered by a short lip.

Dimensions: holotype, maximum diameter 270.40 μm. Cismon, maximum diameter 83.75-221.08 μm.

Distinguishing features: *Lilliputianella globulifera* differs from *H. aptiana* by having more elongate chambers and a flatter trochospire, while it differs from *L. similis* by possessing less elongate chambers.

Remarks: This species displays a rather wide morphological variability mainly related to a) the number of elongate chambers (from 5 to 7) and to b) the chambers' elongation degree. The original wall texture is not preserved.

The individuals reported in Banner & Desai (pl.8, figs. 1-3, 1988) exhibit a last chamber more prominently radially elongate than the holotype. Bou-Dagher Fadel *et al.* (1997) illustrated a topotype (pl. 9, figs. 8-9) in which the spiral view is close to the holotype instead of the umbilical view that looks another species.

Stratigraphic distribution: Early Barremian-lower part of the Late Aptian, from the *Lilliputianella similis* Zone to the *Globigerinelloides algerianus* Zone.

Lilliputianella kuhryi (Longoria, 1974)

(Pl. 3, 12a-c; Pl. 17, figs. 3a-c, 4a-c)

Hedbergella kuhryi Longoria, 1974, p. 60, pl. 14, figs 1-3, 4-6 (holotype).
Lilliputianella kuhryi (Longoria), Banner & Desai, 1988, p. 169, pl. 8, fig. 5.
Lilliputianella kuhryi (Longoria), BouDagher-Fadel, 1995, p. 144, pl. 4, figs 7.
Lilliputianella kuhryi (Longoria), BouDagher-Fadel *et al*., 1997 p. 165, pl. 9.2, figs 7-10.

Description: Test medium to large in size, coiled in a flat trochospire, peripheral outline subcircular, strongly lobate to stellate; 5 chambers (5.5 to 6 chambers also reported in the literature) in the outer whorl, increasing rather fast in size. Chambers initially globular to subglobular on both spiral and umbilical sides, the last two or three tending to become radially elongate, laterally compressed and pointed at their end; spiral side flat tending to pseudoplanispirality; sutures straight to slightly curved on both spiral and umbilical sides; umbilicus broad and shallow; aperture as a low extraumbilical arch.

Dimensions: holotype, maximum diameter 310 μm. Cismon, maximum diameter 115.12-216.15 μm.

Distinguishing features: *Lilliputianella kuhryi* may be distinguished from *L. roblesae* mainly by its pointed (instead of round), sligtly compressed chambers; a wider and shallower umbilical area and because of its peculiar coiling mode tending to become planispiral.

Remarks: This species displays a moderate morphological variability regarding a) the number of chambers (5 to 6) in the outer whorl, b) their elongation degree and,

consequently, c) the peripheral outline which may be more or less strongly lobate; in addition d) the spiral side may range from flat to almost pseudoplanispiral. The original wall texture is not preserved.

The specimen poorly illustrated (only in umbilical view) by Banner & Desai in pl. 8, fig. 5 is probably an intermediate form between *Lilliputianella kuhryi* and *L. bizonae*; in fact, this specimen exhibits a growth rate which is closer to that of the latter species resulting in an ovoid test (instead of subcircular); however, this morphotype can be included here in the variability of *Lilliputianella kuhryi* because of its three globular, round initial chambers of the outer whorl.

Stratigraphic distribution: Early Aptian – lower part of the Late Aptian, from the *Leupoldina cabri* Zone to the *Globigerinelloides algerianus* Zone.

Lilliputianella labocaensis (Longoria, 1974)

(Pl. 4, 1a-c; Pl. 17, figs. 5a-c, 6a-c)

Hedbergella labocaensis Longoria, 1974, p. 60, pl. 16, figs 7-9, 22-24 (holotype).
Lilliputianella labocaensis (Longoria), BouDagher-Fadel *et al*., 1997 p. 165, pl. 9.2, figs 1-3.

Description: Test medium to large in size, coiled in a low trochospire, peripheral outline subcircular, strongly lobate, 5 to 6 chambers in the outer whorl, increasing very slowly and gradually in size. Chambers initially globular to subglobular on both spiral and umbilical sides, the last three or four tending to become slightly radially elongate, round at their end; sutures straight to slightly curved on both spiral and umbilical sides, umbilicus narrow and rather shallow; aperture as a low extraumbilical arch.

Dimensions: holotype, maximum diameter 291 μm. Cismon, maximum diameter 107.91-221.95 μm.

Distinguishing features: *Lilliputianella labocaensis* is quite similar to *L. maslakovae* Longoria (1974) from which differs mainly by its wider and slightly deeper umbilical area.

Remarks: This species displays a small morphological variability mainly regarding a) the number of chambers (5 to 6) in the outer whorl and b) their elongation degree. The original wall texture is not preserved.

The specimen illustrated by Longoria in pl. 16, figs 7-9 (the paratype), exhibiting only 5 chambers in the outer whorl, does not match the original diagnosis of this taxon given by Longoria ("six to seven chambers in the final whorl"); however, this individual possesses a general morphology which is very close to that of *Lilliputianella labocaensis*; on the other hand, none 7-chambered specimens has been reported in the literature and, therefore, on the basis of this observation *Lilliputianella labocaensis* is characterized by 5 to 6-chambered individuals.

Stratigraphic distribution: Early Aptian – lower part of the Late Aptian, from the *Leupoldina cabri* Zone to the *Globigerinelloides algerianus* Zone.

Lilliputianella maslakovae (Longoria, 1974)

(Pl. 4, 2a-b; Pl. 17, figs. 7a-c, 8a-c; Pl. 18, figs. 1a-c, 2a-c)

Hedbergella maslakovae Longoria, 1974 p. 61-63, pl. 20, figs 1-3, 14-16, pl. 24, figs 11-12 (holotype), 13, 14.

Hedbergella similis Longoria, 1974, p. 68-69, pl. 23, figs, 14-16.

Lilliputianella maslakovae (Longoria), Banner & Desai, 1988, p. 169, pl. 8, figs 6-7.

?*Lilliputianella bizonae* (Chevalier), Banner & Desai, 1988, p. 168, pl. 7, figs 13-14.

Lilliputianella similis (Longoria), Banner *et al*., 1993, p. 15, pl. 8, figs 8a-c.

Lilliputianella globulifera (Kretchmar & Gorbachik), BouDagher-Fadel *et al*., 1997, p. 164-165, pl. 9.1, figs 10-11, not figs 5-9, 12-15.

? *Lilliputianella bizonae* (Chevalier), BouDagher-Fadel *et al*., 1997, p. 164, pl. 9.3, 11-14.

Description: Test medium to large in size, trochospirally coiled; peripheral outline subcircular, strongly lobate, 6 to 6.5 chambers in the outer whorl, increasing very slowly and gradually in size. Chambers on both spiral and umbilical sides initially globular to subglobular, the last three or four tending to become slightly radially elongate, round at their end; spiral side very low to flat; sutures straight to slightly curved, umbilicus broad and shallow; aperture as a low extraumbilical arch reaching the periphery.

Distinguishing features: *Lilliputianella maslakovae* differs from *L. labocaensis* Longoria (1974) mainly by its a) wider and shallower umbilical area and by b) its low to flat spiral side; in addition it may be distinguished from *H. similis* Longoria (1974) by having a slower growth rate resulting in a less elongate final chamber.

Dimensions: holotype, maximum diameter 305 μm. Cismon, maximum diameter 115.35-204.11 μm.

Remarks: This species displays a small morphological variability mainly regarding the number of chambers (6 to 6.5) in the outer whorl, their elongation degree and the spiral side, which may range from low to flat. The original wall texture is not preserved.

The specimens shown in Pl. 17, 8a-c and Pl. 18, 2a-c have been identified as *Lilliputianella* cf. *maslakovae* because morphologically similar to *Lilliputianella maslakovae* but having less elongate chambers.

The specimen shown in Pl. 18, 1a-c has been identified as *Lilliputianella* cf. *maslakovae* because morphologically similar to *Lilliputianella maslakovae*but having more inflated chambers.

The specimen illustrated (only in umbilical view) by BouDagher-Fadel *et al*. in pl. 9.1, figs 5-7 (the holotype of *Clavihedbergella globulifera* Kretchmar & Gorbachik, 1971) and fig. 8 are here assigned to *Hedbergella aptiana* Bartenstein (1965) because they possess globular, non-elongate chambers; the individual in pl. 9.1, figs 12-15 is attributed to *Hedbergella similis* Longoria (1974) because of its slightly faster growth rate resulting in a more elongate last chamber, while the poorly illustrated (only in umbilical view) specimen in pl. 9.1, fig. 15 falls in the variability of *Hedbergella roblesae* Obregòn de la Parra (1959) on the account of its fast and gradual growth rate and of its decidedly elongate last two chambers.

Stratigraphic distribution: Early Aptian-lower part of the Late Aptian, from the *Leupoldina cabri* Zone to the *Globigerinelloides algerianus* Zone.

Lilliputianella roblesae (Obregòn de la Parra, 1959)
(Pl. 4, 3a-b)

Globigerina roblesae Obregòn de la Parra, 1959, p. 149, pl. 4, figs 4a-4b (holotype).

Hedbergella roblesae (Obregòn de la Parra), Longoria, 1974, p. 65-66, pl. 16, figs 1-3, 4-6, pl. 20, figs 10, 11.

Hedbergella semielongata Longoria, 1974, p. 66-68, pl. 21, figs 4-5.

?*Lilliputianella bizonae* (Chevalier), Banner & Desai, 1988, p. 168, pl. 7, figs 12, 15.

Clavihedbergella semielongata (Longoria), Coccioni & Premoli Silva, 1994, p. 670-671, figs 9.16-21, not figs 10.1-3.

Lilliputianella roblesae (Obregòn de la Parra), BouDagher-Fadel *et al.*, 1997, p. 165-166, pl. 9.3, fig. 1-7.

Description. Test medium to large in size, coiled in a flat trochospire, peripheral outline ovoid and strongly lobate; 5 chambers (rarely 4.5 to 6) in the outer whorl, increasing rapidly but gradually in size. Chambers on both spiral and umbilical sides initially globular to subglobular, the last two or three moderately to strongly elongate; chambers round at their end; spiral side low to medium-high; sutures straight to slightly curved on both spiral and umbilical sides; umbilicus rather wide and shallow; aperture a low extraumbilical arch.

Dimensions: holotype, maximum diameter 170 μm. Cismon, maximum diameter 105.23-231.78 μm.

Distinguishing features: *L. roblesae* differs from *L. globulifera* and *L. similis* mainly on the account of its more cilindric chambers.

Remarks: This species displays a rather wide morphological variability mainly regarding a) the number of chambers (4.5 to 6) in the outer whorl, b) the number of elongate chambers, c) their elongation degree, d) the peripheral outline which can be more or less strongly lobate, and e) the height of the spire which can range from low to moderately high.

The specimens reported by Coccioni & Premoli Silva (1994) in figs 9.16-21, even possessing 4.5 chambers in the outer whorl are assigned here to *Lilliputianella roblesae*

because of their fast and gradual growth rate of the chambers which are arranged in an ovoid test outline. Conversely, the specimen reported by the same authors in figs 10.1-3 does not fall in the variability of this taxon because of its very high spiral side.

Stratigraphic distribution: mid-Barremian – lower part of the Upper Aptian, through the upper part of the *Lilliputianella similis* Zone to the *Globigerinelloides algerianus* Zone.

Lilliputianella similis (Longoria, 1974)

(Pl. 4, 4a-c; Pl. 18, figs. 3a-c, 4a-c, 5a-c, 6a-c)

Hedbergella similis Longoria, 1974, p. 68-69, pl. 16, figs 10-11, 12-13, 14-18, 19-21 (holotype), pl. 18, figs, 12-13, pl. 23, not figs, 14-16.

Clavihedbergella eocretacea Neagu, 1974, p. 112-113, pl. 89, figs 3-4.

Lilliputianella similis (Longoria), Banner & Desai, 1988, p. 169-170, pl. 8, fig. 8, not fig. 9.

Not *Lilliputianella similis* (Longoria), Banner *et al*., 1993, p. 15, pl. 8, figs 8a-c.

Lilliputianella eocretacea (Neagu), Banner *et al*., 1993, p. 15, pl. 6, figs 8.

Hedbergella similis (Longoria), Coccioni & Premoli Silva, 1994, p. 678-679, figs 13.1-3, not figs 13.4-9.

Lilliputianella globulifera (Kretchmar & Gorbachik), BouDagher-Fadel *et al*., 1997, p. 165, pl. 9.2, figs 1-3.

Description: Test medium to large in size, coiled in a flat to weakly convex trochospire, peripheral outline ovoid, lobate, 5 chambers in the outer whorl (6 chambers are also reported in the literature), increasing slowly and gradually in size; on both spiral and umbilical sides chambers initially globular to subglobular, the last two or, exceptionally, three tending to become slightly radially elongate, in some specimens the final one may be more decidedly elongate (chambers round at their end). Spiral side low, sutures straight to slightly curved on both spiral and umbilical sides; umbilicus rather wide and shallow; aperture a low extraumbilical arch.

Dimensions: holotype, maximum diameter 261 μm. Cismon, maximum diameter 104.05-230.88 μm.

Distinguishing features: *Lilliputianella similis* is quite similar to *L. maslakovae* Longoria (1974) from which differs mainly in its slightly faster growth rate, in its slightly more elongate last two chambers (especially the final one) resulting in an ovoid (instead of subcircular) test. *Lilliputianella similis* also differs from *Lilliputianella globulifera* by having more elongate last two chambers (especially the final one).

Remarks: This species displays a rather wide morphological variability mainly regarding a) the number of chambers (5 to 6) in the outer whorl and b) their elongation, especially of the last one. The original wall texture is not preserved.

The specimens shown in Pl. 18, figs. 6a-c has been identified as *Hedbergella* cf. *similis* because morphologically similar to *Hedbergella similis* but having less elongated chambers.

The specimens reported by Longoria in pl. 23, figs. 14-16 (paratype), display a slightly slower growth rate and a less elongate last chambers if compared to the holotype of this taxon. Thus, this individual falls in the variability of *Lilliputianella maslakovae* Longoria (1974). The specimen illustrated by Longoria in pl. 16, figs 12-13 (paratype), yields a decidedly faster growth rate resulting in the last three strongly elongate chambers. This individual is not a typical *Lilliputianella similis*; even possessing six chambers in the outer whorl, its general morphology is rather close to *Lilliputianella roblesae* Obregòn de la Parra (1959) and, therefore, it is considered here as an intermediate form between the two taxa. For the same reason, the specimen illustrated by Banner & Desai (1988) in pl. 8, figs 9a-b is probably an intermediate form between the two species even though this individual exhibits a broken third chamber preventing its certain attribution.

The paratype of *Clavihedbergella eocretacea* Neagu (1975), reported in pl. 89, figs 4-5, possesses 5 outer chambers, the final one decidedly elongate and is therefore assigned to *Lilliputianella similis* Longoria (1974).

The specimens figured by Banner *et al.* (1993) in pl. 8, figs 8a-c falls here in the variability of *Lilliputianella maslakovae* Longoria (1974) by having a slower growth rate of the chambers, which are very slightly elongate, and a subcircular test.

The specimens reported by Coccioni & Premoli Silva in figs 13.4-6 and 13.7-9 are here assigned to *Lilliputianella roblesae* Obregòn de la Parra (1959) because of their rather fast growth rate and decidedly elongate last two chambers.

Stratigraphic distribution: Early Barremian - lower part of the Late Aptian, through the upper part of the *Lilliputianella similis* Zone to the *Globigerinelloides algerianus* Zone.

Order GLOBIGERININA Delage & Hérouard, 1896

Superfamily PLANOMALINACEA Bolli, Loeblich & Tappan, 1957

Family SCHACKOINIDAE Pokorný, 1958

Subfamily SCHACKOINIDAE Pokorný, 1958

Genus ***Leupoldina*** Bolli, 1957, emended Banner & Desai, 1988, newly emended.

Type species: *Leupoldina protuberans* Bolli, 1957, p. 277, pl. 2, figs 7, 7a .

PREMISE:

Several specimens within different species illustrated in Verga & Premoli Silva (2002) are considered not valid because they do not fit in the species' original descriptions and illustrations. However, the authors, through a verbal communication, explained the discrepancy between species' illustrations and descriptions as due to the wrong placement of the figure captions in the published paper. Therefore, figures and captions by Verga & Premoli Silva (2002) have been revised as follows:

Leupoldina cabri: Fig. 6.1-12; Fig. 7.1-6.

Leupoldina pustulans pustulans: Fig. 4.1-15; Fig. 8.1.

Leupoldina reicheli: Fig. 7.7-17.

Leupoldina pustulans quinquecamerata: Fig. 5.1-4; Fig. 8.2-12.

Leupoldina pustulans hexacamerata: Fig. 5.5-12.

Leupoldina cabri (Sigal, 1952)

(Pl. 3, 6a-b)

Schackoina cabri Sigal, 1952, p. 20, text-fig. 20.

Leupoldina protuberans Bolli, 1957, p. 277, pl. 2, figs 2, 5-13, not figs 1, 3, 3a, and 4. (Holotype Fig. 7, 7a).

Schackoina pustulans pustulans Bolli 1957, p. 274, pl. 1, figs 2, 4, and 5.

Schackoina pustulans quinquecamerata Bolli 1957, p. 274, pl. 1, fig. 6.

Schackoina cabri (Sigal), Sigal, 1959, p. 72, figs 19-46.

Leupoldina protuberans (Bolli), Bolli, 1959, p. 264, pl. 20, figs 20a, b.

Leupoldina protuberans (Bolli), Loeblich & Tappan, 1964, part C, vol. 2, C 658, fig. 526, 10 a, b.

Leupoldina protuberans (Bolli), Gorbachik, 1971, p. 125, pl. 30, figs 7a, b.

Leupoldina cabri (Sigal), Longoria, 1974, p. 90, pl. 2, figs 1-12.

Leupoldina pustulans (Bolli), Longoria, 1974, p. 90, pl. 3, fig. 3; pl.8, fig. 7.

Leupoldina protuberans (Bolli), Bartenstein & Bolli, 1977, p. 559, pl. 3, figs 15, 17, not fig. 16.

Leupoldina gr. *cabri* (Sigal), Banner & Desai, 1988, p. 176, pl. 10, fig. 7 not figs 1-6, and 8.

Leupoldina protuberans (Bolli), Loeblich & Tappan, 1987, p. 461, pl. 494, figs 14-15.

Not *Leupoldina cabri* (Sigal), Coccioni & Premoli Silva, 1994, p. 683, pl. 14, figs. 15-16.

Leupoldina cabri (Sigal), BouDagher-Fadel *et al*., 1995, p. 147, pl. 4, fig. 8, not fig. 9.

Schackoina cabri (Sigal), BouDagher-Fadel *et al*., 1997, p. 185, pl. 10.6, figs 8, 9, 14, not figs 10-13.

Leupoldina protuberans (Bolli), BouDagher-Fadel *et al*.,1997, p. 184, pl. 10.6, figs 1, 2, 6, and 7.

Not *Schackoina (Leupoldina) cabri* (Sigal), Moullade *et al*.,1998, p. 223, pl. 6, figs 9, 11-12.

Leupoldina cabri (Sigal), Verga & Premoli Silva, 2002, p. 200-203, Fig. 7.1-6, not 7.7-12; not Fig. 8.1-6.

Description: Test small to large in size, slightly trochospiral, seminvolute to involute, equatorial periphery irregular, strongly lobate to strongly stellate, 4 to 6 chambers in the last whorl increasing gradually and slowly in size. The first, second and exceptionally the third one pyriform or radially elongate, rarely globular, with a radial prolongation bearing a single ampulla; last chambers bi-, tri- or exceptionally quadrifurcated bearing consequently two or three ovoid to spherical ampullae; sutures radial, depressed, straight to slightly curved; umbilical area very small, shallow, partially visible only in the seminvolute morphotypes; aperture straddling the periphery as a low asymmetric arch bordered by a lip.

Dimensions: holotype, maximum diameter 401.50 μm.

Distinguishing features: *Leupoldina cabri* differs from *Leupoldina pustulans* and its subspecies by having an involute to seminvolute (instead of evolute) coiling mode and, in general, more branched chambers that lead to a more irregular shape of the test. It differs from *Leupoldina reicheli* by having an involute to seminvolute (instead of evolute, a more clearly trochospiral coiling mode, a bifurcated, squat, stout, and less radially elongate chambers.

Remarks: This species displays a wide morphological variability regarding the number of chambers in the last whorl (from 4 to 6), the degree of involution, the presence of chamber bifurcation and, consequently, the number of ampullae for each chamber. In particular, a wide range of intermediate morphotypes between the seminvolute, pseudoplanispiral individuals and strongly involute, clearly trochospiral, extremely branched specimens is observed.

According to Verga & Premoli Silva (2002), the morphotypes illustrated in pl. 1, figs. 2, 4, 5, as *Leupoldina pustulans pustulans* and in pl. 1, fig. 6 as *Leupoldina pustulans quinquecamerata* by Bolli (1957) seem to belong to *Leupoldina cabri* being involute, while the specimens identified as *Leupoldina protuberans* in pl. 2, figs. 1, 3 are assigned to *Leupoldina pustulans pustulans* as they display 4 chambers and an evolute coiling mode. As regard Bolli's specimens in pl. 2, fig. 4, provided with 5 chambers and an evolute coiling mode is a *Leupoldina pustulans quinquecamerata* instead of a *Leupoldina*

protuberans. The specimen illustrated by Gorbachik (1971) as *L. protuberans* is assigned to *Leupoldina cabri*, which is the senior synonym (Verga & Premoli Silva, 2002).

The individuals illustrated by Longoria (1974) as *L. pustulans* in pl. 3, fig. 3 and in pl. 8, fig. 7, being involute, are assigned to *L. cabri.*

The 5-chambered morphotype of Bartenstein & Bolli (1977) in pl. 3, fig. 16, even if poorly illustrated, seems to possess an evolute coiling, therefore is assigned here to *Leupoldina pustulans quinquecamerata.*

According to Verga & Premoli Silva (2002) the individuals illustrated by Banner & Desai (1988) as *Leupoldina* gr. *cabri* in pl. 10, figs. 1, 2, 4, 5, and 8 are assigned to *L. pustulans pustulans* as they possess an evolute coiling mode and 4 chambers; the extremely elongate specimen in figs. 3a, b, is *Leupoldina reicheli*; the one illustrated in fig. 6, in the same plate, is *Leupoldina pustulans quinquecamerata* being evolute and provided with 5 chambers.

The specimens illustrated by Coccioni & Premoli Silva (1994) in pl. 14, figs. 15, 16 can be attributed to *Leupoldina pustulans pustulans* as it exhibits an evolute coiling.

The morphotype described by BouDagher-Fadel (1995) as *Leupoldina cabri* and illustrated in pl. 4, fig. 9 seems to belong to the genus *Schackoina*.

The specimens *Schackoina cabri* described by BouDagher-Fadel *et al*. (1997) and illustrated in pl. 10.6, figs. 10, 12 could be attributed to *Leupoldina pustulans pustulans*, being evolute; the individual illustrated in the same pl., fig. 11 is a *Leupoldina reicheli* because of its evolute coiling and very elongate chambers, while the specimen illustrated in fig. 13 is a *L. pustulans quinquecamerata* having 5 chambers and an evolute coiling. Finally, the individuals illustrated as *Leupoldina protuberans* by BouDagher-Fadel *et al*. (1997) in pl. 10.6, figs. 1, 2, 6, and 7, are assigned by Verga & Premoli Silva (2002) to *Leupoldina cabri*, which is the senior synonym; the individuals illustrated in the pl. 10.6, figs. 3, 5, are referable to *L. pustulans pustulans*, while the specimen in pl. 10.6, fig. 4 is a *L. pustulans quinquecamerata.*

The individuals illustrated by Moullade *et al*. (1998) in pl. 6, figs. 9, 11-12 being evolute and provided with 4 chambers are assigned to *Leupoldina pustulans pustulans*.

Stratigraphic distribution: Early Aptian. The presence of *Leupoldina cabri* identifies its Total Range Zone. In the Cismon core the first appearance of this taxon is just below the Selli Level Equivalent, at the radiolarian level 15/164-170. At Cismon, the assemblages of the middle to the lower upper part of the *Leupoldina cabri* Zone contain also

morphotypes of *L. cabri* with 6 chambers in the outer whorl (no taxa with elongate chambers were found at DSDP Site 463).

Leupoldina pustulans hexacamerata (Verga & Premoli Silva, 2002)

(Pl. 3, 7a-c)

Leupoldina pustulans (Bolli) *hexacamerata,*Verga & Premoli Silva, 2002, p. 205, Fig. 5.5 (holotype)-12, not Fig. 6.5-12.

Description: Test medium to large, slightly trochospiral, evolute, equatorial periphery strongly stellate, 6 chambers in the last whorl increasing gradually and slowly in size, predominantly pyriform in shape throughout. Short, radial prolongations, bearing a single subspherical ampulla except the last one or two bifurcate (rarely trifurcate) chambers which bear two or exceptionally three ampullae; these ampullae exhibit different size and grow asymmetrically with respect to the coiling plane. Sutures radial, depressed, straight; umbilical area shallow and rather large, aperture straddling the periphery as a low asymmetrical arch bordered by a lip.

Dimensions: holotype, maximum diameter 366 μm;

Distinguishing feautures: *Leupoldina pustulans hexacamerata* differs from *L. pustulans pustulans, L. pustulans quinquecamerata*, *L. reicheli* by having 6 chambers in the outer whorl (mainly pyriform), instead of 4 or 5, and usually two asymmetrically developed ampullae in the last chamber.

Remarks: This subspecies displays a little morphological variability related to the subglobular shape of the first chambers in the last whorl, and the presence of bifurcation also in the penultimate chamber.

Stratigraphic distribution: Range restricted to the lower part of the *Leupoldina cabri* Zone (*sensu* Sigal, 1977 and Caron, 1985). In the Cismon core it ranges from the radiolarian level 13/119-127 up to the 12/209-214.

Leupoldina pustulans pustulans **(**Bolli, 1957)

(Pl. 3, 8a-b)

Schackoina pustulans pustulans Bolli, 1957, p. 274, pl. 1, figs. 1, 3, 3a (holotype), not figs 2, 4.

Leupoldina protuberans Bolli, 1957, p. 277, pl. 2, figs 1, 3, 3a.

Schackoina pustulans (Bolli), Sigal, 1959, p. 274, pl. 1, figs 1-7.

Leupoldina pustulans (Bolli), Gorbachick, 1971, pl. 30, figs 6a, b.

Leupoldina pustulans (Bolli), Longoria, 1974, p. 90, pl. 3, figs 4, 5 not fig. 3; pl. 8, not fig 7.

Globigerinelloides saundersi (Bolli), Longoria, 1974, p. 88, pl.3, figs 2, 6-9; pl. 9, figs 8, 9.

Schackoina pustulans pustulans (Bolli), Bartenstein & Bolli, 1977, p. 560, pl. 3, figs 20, 21.

Leupoldina pustulans (Bolli), Salaj, 1984, pl. 3, fig. 10.

Leupoldina gr. *cabri* (Sigal), Banner & Desai, 1988, p. 176, pl. 10, figs 1, 2, 4, 5, and 8.

Leupoldina pustulans (Bolli), Salaj, 1990, pl. 18, fig. 3; pl. 19 figs 11, 12.

Leupoldina pustulans (Bolli), Coccioni & Premoli Silva, 1994, p. 683, pl. 14, figs 17, 18.

Leupoldina cabri (Sigal), Coccioni & Premoli Silva, 1994, p. 683, pl. 14, figs.15-16.

Leupoldina protuberans (Bolli), BouDagher-Fadel, 1995, p.148, pl. 4, figs 3-5.

Schackoina cabri (Sigal), BouDagher-Fadel *et al*., 1997, p. 185, pl. 10.6, figs. 10, 12.

Leupoldina protuberans (Bolli), BouDagher-Fadel *et al*., 1997, p. 184, pl. 10.6, figs 3, 5.

Schackoina (Leupoldina) cabri (Sigal), Moullade *et al*., 1998, p. 223, pl. 6, figs 9, 11-12.

Leupoldina pustulans pustulans (Sigal), Verga & Premoli, 2002, p. 203, 205, Fig. 4.1-15; not Fig. 5.1.

Description: Test small to large in size, slightly trochospiral and evolute, equatorial periphery strongly stellate, rarely 4.5 chambers in the last whorl increasing gradually and slowly in size. The first and second chambers of the last whorl globular to slightly cylindrical or pyriform; last chambers pyriform, digitiform or tubular; mainly short, radial prolongations, bearing a single subspherical ampulla throughout or two bifurcate ampullae in the last and penultimate chambers. Sutures radial, depressed, straight to slightly curved; umbilical area shallow and rather large; aperture straddling the periphery as a low asymmetric arch bordered by a lip.

Dimensions: holotype maximum diameter 410 μm.

Distinguishing features: *Leupoldina pustulans pustulans* differs from *Leupoldina cabri* by having a evolute (instead involute to seminvolute) coiling mode and, in general, a more regular shape of the test. It differs from *Leupoldina pustulans quinquecamerata* and *Leupoldina pustulans hexacamerata* by having a lower number of chambers in the last whorl, 4 to 4.5 instead of 5 to 5.5 and 6.

Remarks: This subspecies displays a little variability regarding a) the number of chambers from 4 to 4.5, a more marked morphological variability concerning b) the shape of the chambers in the last whorl that ranges from subglobular or pyriform in the first chambers to pyriform, digitiform or tubular in the outer ones; c) the presence/absence of bifurcation in the last chambers, leading to bear one or two ampullae per chamber, and d) the degree of constriction that separates the ampullae from their respective chambers, abrupt to barely marked. In general, well-separated ampullae are associated with pyriform chambers, whereas in cylindrically shaped chambers constrictions are almost absent.

According to Verga & Premoli Silva (2002) the specimens illustrated by Longoria (1974) as *G. saundersi* in pl. 3, figs. 2, 6-9 and pl. 9, figs. 8, 9 fall within the morphological variability of *Leupoldina pustulans pustulans* as the chamber extensions, even broken, suggest the presence of bulb-shaped terminations.

Stratigraphic distribution: Upper Barremian-Upper Aptian, studies are in progress to better constain the stratigraphic distribution of the species.

Leupoldina pustulans quinquecamerata (Bolli, 1957)

(Pl. 3, 9a-b)

Schackoina pustulans quinquecamerata Bolli, 1957 p. 274, pl. 1, figs. 6, 7a, b (holotype).

Leupoldina protuberans Bolli, 1957 p. 277, pl. 2, fig. 4 (paratype only).

Not *Schackoina pustulans pustulans* (Bolli) Bartenstein & Bolli, 1977, p. 560, pl. 3, figs 22, 23.

Leupoldina gr. *cabri* (Sigal) Banner & Desai, 1988, p. 176, pl. 10, fig. 6.

Schackoina cabri Sigal: BouDagher-Fadel *et al*., 1997, p. 185, pl. 10.6, fig. 13.

Leupoldina protuberans (Bolli) BouDagher-Fadel *et al*., 1997, p. 184, pl. 10.6, fig. 4.

Leupoldina pustulans quinquecamerata (Bolli), Verga & Premoli Silva, 2002, Fig. 5.2-4, not 5.5-12; not Fig. 6.1-4.

Description: Test small to large in size, slightly trochospiral and evolute, equatorial periphery strongly stellate, 4 chambers in the last whorl (rarely 4.5) increasing gradually and slowly in size. The first and second chambers of the last whorl globular to slightly cylindrical or pyriform; last chambers pyriform, digitiform or tubular; mainly short, radial prolongations, bearing a single subspherical ampulla throughout or two bifurcate ampullae in the last and penultimate chambers. Sutures radial, depressed, straight to slightly curved; umbilical area shallow and rather large; aperture straddling the periphery as a low asymmetric arch bordered by a lip.

Dimensions: holotype maximum diameter 370 μm.

Distinguishing features: *Leupoldina pustulans quinquecamerata* differs from *Leupoldina pustulans pustulans* by having a higher number of chambers in the last whorl, 5 to 5.5 instead of 4 to 4.5. The two subspecies share the same features as well as the same morphological variability in terms of chamber shape, bifurcation, number and shape of ampullae and type of constrictions. However, cylindrical chambers are a less common feature in *L. pustulans quinquecamerata* than in *L. pustulans pustulans.*

Remarks: According to Verga & Premoli Silva (2002) the specimens illustrated by Bartenstein & Bolli (1977) in pl. 3 figs. 22, 23 as *Leupoldina pustulans quinquecamerata* do not display pyriform to tubular chambers bearing bulb-shaped extensions. These

individuals might fall in the morphological variability of *Lilliputianella roblesae* (Obregòn de la Parra, 1959).

Stratigraphic distribution: Early Aptian, at Cismon from the middle to the lower upper part of the *Leupoldina cabri* Zone.

Leupoldina reicheli (Bolli, 1957)

(Pl. 3, 10a-b)

Schackoina reicheli Bolli, 1957, p. 275, pl. 1, figs 8-10 (holotype).
Schackoina reicheli (Bolli), Sigal, 1959, p. 74, figs 48, 49.
Leupoldina reicheli (Bolli), Gorbachik & Kretchmar, 1969, pl. 2, figs 10 a-c.
Leupoldina reicheli (Bolli), Gorbachik & Kretchmar, 1970, p. 143, pl. 13, figs 3-6.
Leupoldina reicheli (Bolli), Gorbachik, 1971, p. 125, pl. 30, figs 8a, b.
Leupoldina pustulans (Bolli), Longoria, 1974 p. 92, pl. 27, fig. 17.
Leupoldina gr. *cabri* (Sigal), Banner & Desai, 1988, p. 176, pl. 10, figs 3a, b.
Not *Schackoina reicheli* (Bolli), BouDagher-Fadel *et al*., 1995, p. 148, pl. 4, figs 10, 11.
Schackoina cabri (Sigal), BouDagher-Fadel *et al*., 1997, p. 185, pl. 10.6, fig 11.
Leupoldina reicheli (Bolli), Verga & Premoli Silva, 2002, p. 205, 211, not Fig. 8.7-17.

Description: Test medium to large in size, pseudoplanispiral, evolute, equatorial periphery strongly stellate, 4 to 5 chambers in the last whorl increasing gradually and moderately in size; the first and the second pyriform, occasionally subglobular, then pyriform to tubular with very long radial prolongations bearing a single subspherical to ovoid ampulla. Very rare specimens display bifurcated prolongations; lateral profile subparallel to slightly asymmetrical with one side concave and the other convex; sutures radial, depressed, mainly straight; umbilical area very shallow and rather large; aperture straddling the periphery as a low asymmetrical arch bordered by a lip.

Dimensions: holotype, maximum diameter 520 μm.

Distinguishing features: For differences from the other leupoldinid species, see the descriptions above.

Remarks: This species shows a moderate morphological variability mainly regarding the number of chambers in the last whorl, from 4 to 5, the shape of the first chambers in the outer whorl, the elongation degree of the last chambers varying from moderately to strongly elongate, the shape of the ampullae from subspherical to ovoid, and the lateral profile from subsymmetrical to distinctly asymmetrical. In very rare specimens prolongations are bifurcated.

According to Verga & Premoli silva (2002), the specimens illustrated by BouDagher-Fadel (1995) in pl. 4 figs. 10, 11 do not belong to the genus *Leupoldina* but probably to the *Schackoina pentagonalis* group.

Stratigraphic distribution: Early Aptian, from the lower part of the *Leupoldina cabri* Zone to the lower part of the *Globigerinelloides ferreolensis* Zone.

Genus ***Gubkinella*** Suleymanov, 1955

Type species: *Gubkinella asiatica* Suleymanov, 1955

Gubkinella graysonensis (Tappan, 1940)

(Pl. 8, figs. 7a-c, 8a-c, 9a-c, 10a-c, 11a-c; Pl. 9, 1a-c, 2a-c, 3a-c, 4a-c, 5a-c; Pl. 19, figs. 7a-c, 8a-c, 9a-c)

Globigerina graysonensis Tappan, 1940, p. 122 pl. 19, figs. 15 (holotype)-17.

Gubkinella graysonensis (Tappan), Longoria, 1974, p. 50 pl. 1, figs. 1-12.

Gubkinella graysonensis (Tappan), Pflaumann & Krasheninnikov, 1977, p. 553 pl. 1, fig. 9-11.

Gubkinella graysonensis (Tappan), Leckie, 1984, p. 593 pl. 1, figs. 2-3.

Gubkinella graysonensis (Tappan), Leckie, 1990, Pl. 1, Figs. 1-7.

Description: Test tiny, coiled in a low to rather high trochospire, chambers from three to five in the last whorl, globular to subglobular and inflated in both spiral and umbilical sides; sutures distinct and depressed; aperture slit-like which extends toward the periphery.

Dimension: holotype, maximum diameter 210 μm. Cismon, maximum diameter 99.36-134.06 μm. 463 Site, maximum diameter 84.02-100.36 μm.

Distinguishing features: *Gubkinella graysonensis* differs from *Gorbachikella kugleri* mainly by possessing a narrower umbilical area and by the absence of an arch-like aperture.

Remarks: *Gubkinella graysonensis* displays some morphological variability regarding the a) number of chambers of the outer whorl (ranging from 3 to 5), and the b) height of the spiral side varying from slight to rather high. The original wall texture is not preserved.

The generic identification of this species is somewhat in doubt. It resembles *Globigerina* in being trochoid and in having nearly globular chambers, but differs somewhat in the feature of the aperture, as this species has an aperture that extends toward the periphery. This species is also considered a possible benthic form.

Stratigraphic distribution: lower part of the Late Barremian-middle Albian, from the middle-upper part of the *Globigerinelloides blowi* Zone to the *Ticinella primula Zone.*

Chapter 6

Results

6.1 Cismon core

The studied interval at Cismon core is 25 meters thick (from 32.49 m to 7.96 m) including the Selli Level equivalent. The major difficulties of my research project have been represented by the small size of the specimens occurring in this stratigraphic interval and by the overall poor preservation of the assemblages; in fact, within the Selli Level equivalent the very poor preservation in several samples did not allow the identification of all the specimens at species level.

6.1.1 Taxonomy

Taxonomic analyses reveal that the presence of thirty-five species belonging to six genera, as follows: genera *Hedbergella* (twelve species), *Lilliputianella* (six species), *Globigerinelloides* (ten species), *Leupoldina* (five species), *Gubkinella* (one species) and *Gorbachikella* (one species).

Two main groups have been identified based on chambers morphology:

1) trochospiral (genus *Hedbergella*), globigeriniform (genera *Gubkinella* and *Gorbachikella*) and planispiral taxa (genus *Globigerinelloides*) with globular chambers (Fig. 6.1);

2) trochospiral (genus *Lilliputianella*), planispiral (genus *Globigerinelloides*) and pseudo-planispiral taxa (genus *Leupoldina*) with “clavate” or elongate chambers (Fig. 6.2).

In general, planispiral, pseudo-planispiral and globigeriniform taxa are easily recognizable thanks to their morphology (e.g. *Globigerinelloides duboisi*, *Leupoldina reicheli* and *Gubkinella graysonensis*). On the contrary, trochospiral species show high morphological plasticity being characterized by having 4 to 8 chambers in the last whorl,

a low to very high trochospire, globular to elongate chambers (e.g. *H. sigali*, *H. aptiana*, *H. occulta*, *H. infracretacea*, and *Lilliputianella globulifera*), so that the identification at species level is sometimes very difficult also because the number of chambers is not always a useful criteria to discriminate species.

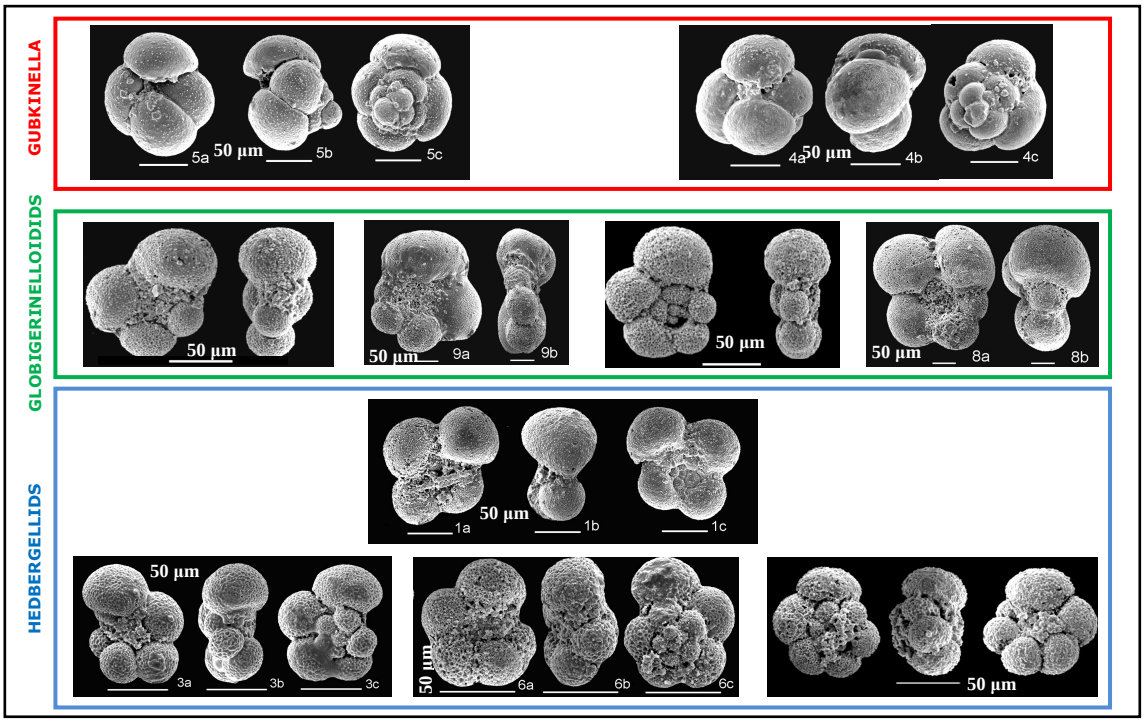

Fig. 6.1. Planktonic foraminifera with globular chambers identified at Cismon core.

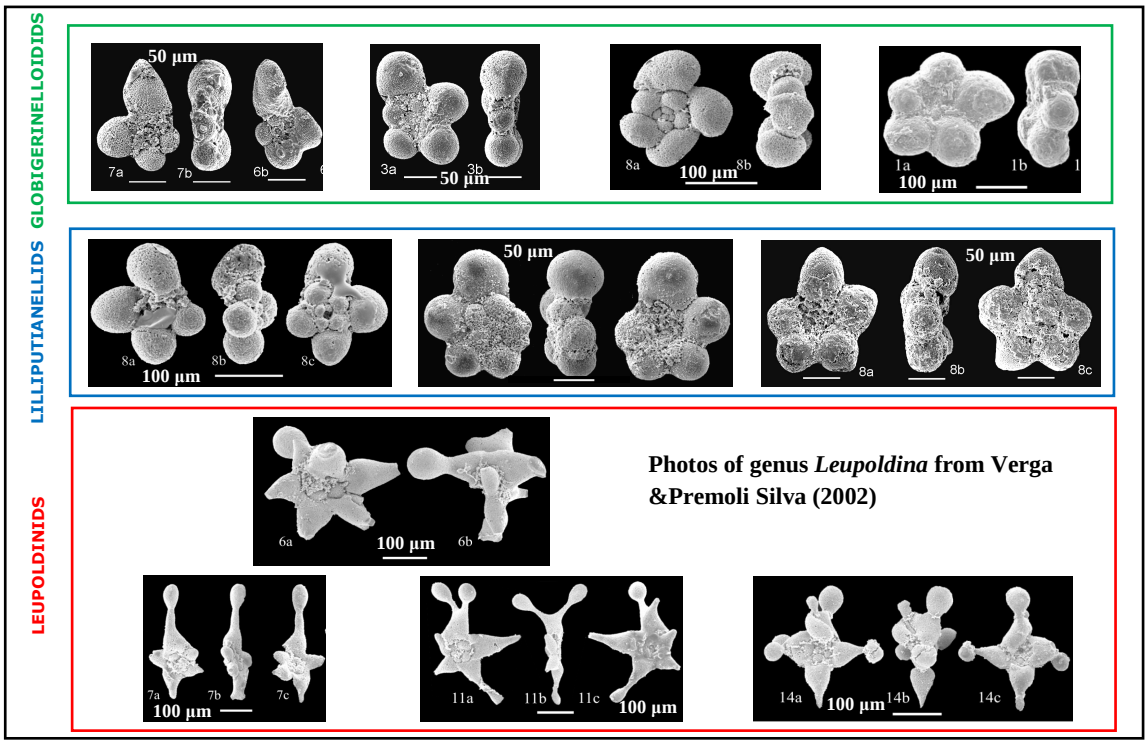

Fig. 6.2. Planktonic foraminifera with "clavate" or elongate chambers at Cismon core.

6.1.2 Planktonic foraminiferal assemblage composition

Figure 6.3 shows the composition of the assemblage in washed residues in terms of main morphologies: below the Selli Level eq. the trochospiral forms (mainly Hedbergellids) are the most abundant group, while the planispiral and pseudo-planispiral taxa are in suborder especially in some stratigraphic intervals.

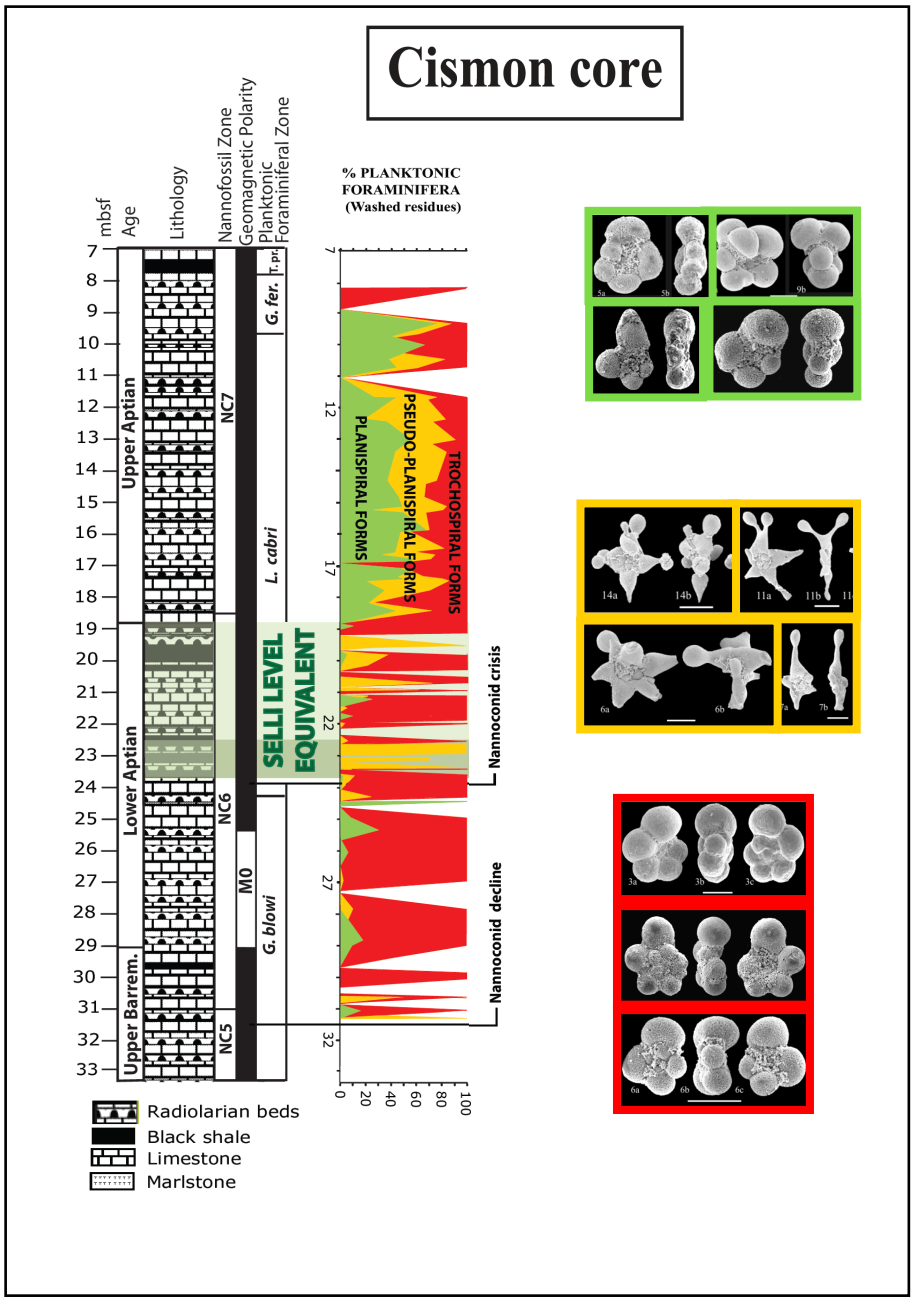

Fig. 6.3. Planktonic foraminiferal composition at Cismon core according to the morphology: trochospiral (red), pseudo-planispiral (yellow) and planispiral (green) forms. Nannofossil biostratigraphy is from Erba *et al.* (1999). Foraminiferal biostratigraphy is from Erba *et al.* (1999) and this study. Magnetostratigraphy is from Channell *et al.* (2000).

Within the Selli Level eq. the pseudo-planispiral, trochospiral (principally Hedbergellids) and globigeriniform forms are the most abundant groups while planispiral forms are very few; above it (from 18.43 m to the top) all the groups are equally distributed and, in particular, Globigerinelloidids and Leupoldinids become very common and abundant.

The stratigraphic distribution of taxa is quite discontinuous as reported in the distribution chart (Table 3, in Appendix):

1) Hedbergellids show the best continuous record across the entire studied interval (e.g. *H. aptiana*, *H. infracretacea* and *H. sigali*);

2) Lilliputianellids have a very discontinuous range below and within the Selli Level eq. (e.g. *L. similis*, *L. globulifera* and *L. labocaensis*), while they become enough common just above it.

3) Globigerinelloidids have a very discontinuous range from the base of the studied interval until the top of the Selli Level eq., while they become very common and abundant just above it (e.g. *G. duboisi*, *G. paragottisi* and *G. maridalensis*);

4) Leupoldinids have a discontinuous record until the top of the Selli Level eq., afterwards they become very common and abundant. It is important to underline that the data regarding this group have been integrated with those previously collected by Verga & Premoli Silva (2002).

5) The globigeriniform taxon *Gubkinella graysonensis* shows a stratigraphic distribution similar to the Hedbergellids.

In several cases, the low preservation did not allow the identification at species level (especially within the Selli Level eq.) making discontinuous the reconstruction of their stratigraphic distribution.

Figure 6.4 shows all types of wall preservation recognized in the Cismon core planktonic foraminiferal specimens:

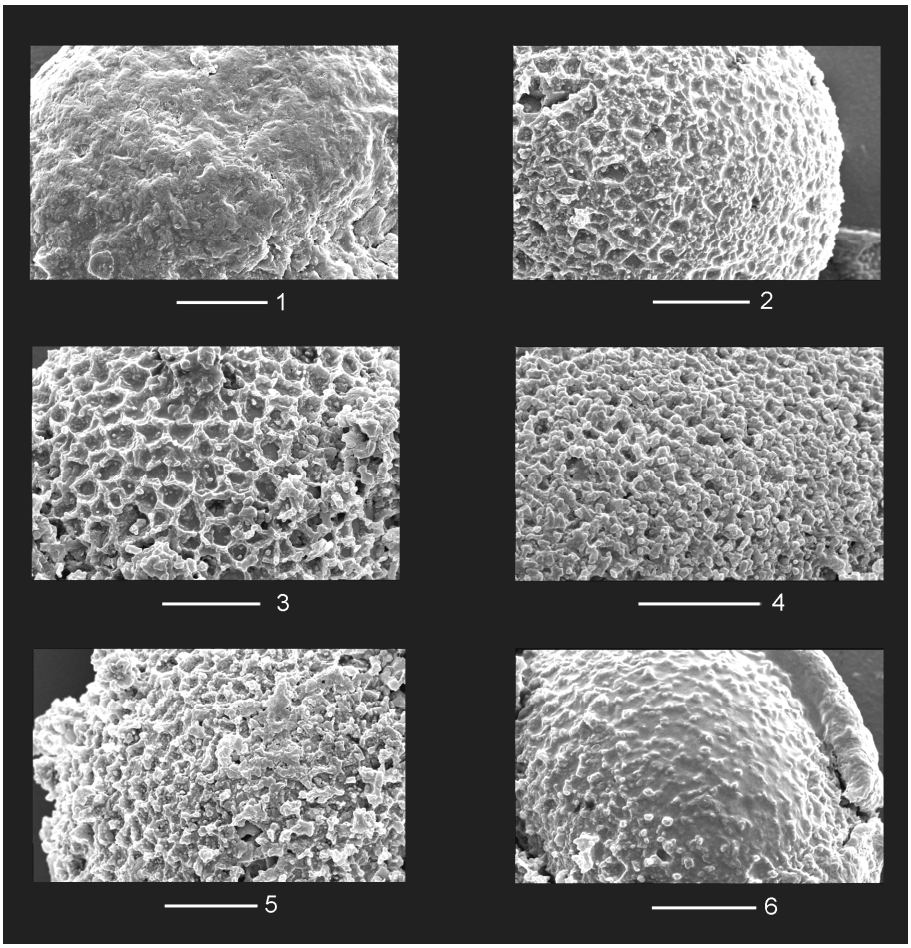

Fig. 6.4. Different types of wall texture recognized at Cismon core . 1: smooth wall texture, not dissolved; 2-3-4-5: different types of wall partially dissolved that simulates the faveolate wall texture typical of the favusellid group wall; 6: internal mold. All scale bars = 10 µm.

6.1.3 Planktonic foraminiferal relative abundance

The total abundance values (a) and species richness (b) of planktonic foraminifera are shown in Figure 6.5.

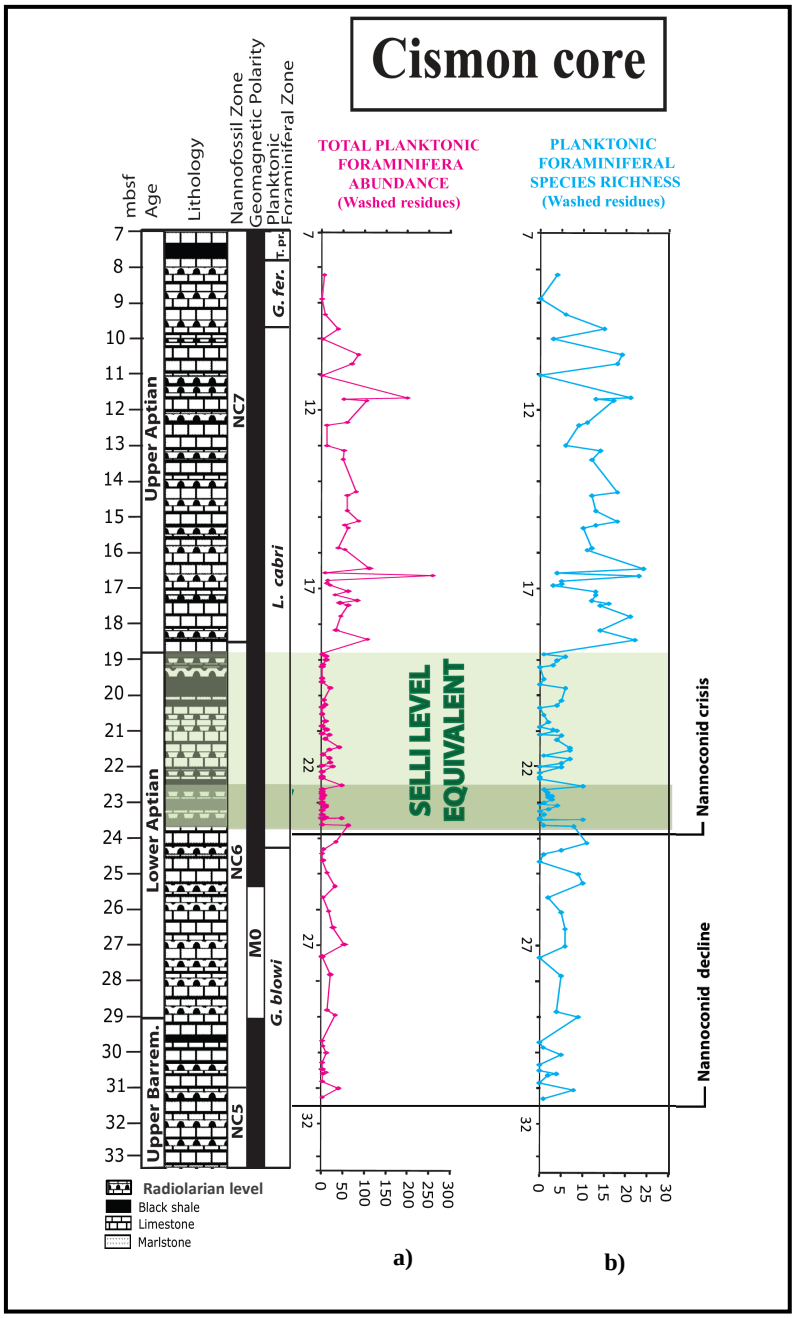

Fig. 6.5 Cismon core: comparison between the total number (a) and species richness (b) of planktonic foraminifera. Nannofossil biostratigraphy is from Erba *et al.* (1999). Foraminiferal biostratigraphy is from Erba *et al.* (1999) and this study. Magnetostratigraphy is from Channell *et al.* (2000).

Graph a) shows that the total abundance of planktonic foraminifera is moderate below the Selli Level equivalent (0 to 45 specimens for sample), then decreases within it (0 to 20) and become very high above it (0 to 254). A marked change in terms of number of specimens is observed from the first sample (RAD 37; 18.43 m) just above the Selli Level eq. upward.

Graph b) shows that the species richness is moderate below the Selli Level eq. (0 to 10 species in several samples), slightly lower within it (from 0 in several samples to 7-9 species) and high above it (from 0 in a couple of samples to 15-24 species).

The marked change observed from 18.43 m upward is mainly due to the appearance of clavate or elongate planispiral (Globigerinelloidids), trochospiral (Lilliputianellids) and pseudo-planispiral (Lilliputianellids) taxa and, at the same time, to an increase of the number of specimens in each sample of the three morphological groups.

6.1.4 Planktonic foraminiferal and radiolarian absolute abundances

The OAE1a is marked by a pronounced negative carbon isotope excursion preceding the $\delta^{13}C$ increase registered in marine pelagic and shallow-water carbonates, marine organic matter, and terrestrial higher-plant materials.

Figure 6.6 compares the $\delta^{13}C$ record (a) with planktonic foraminiferal (b) and radiolarian (c) abundances.

Three intervals have been recognized on the basis of the abundance values (Figs. 6.6b and 6.6c):

1) The interval below the Selli Level eq. is characterized by a low/moderate abundance of planktonic foraminifera (34 to 459 specimens) and a very low abundance of radiolaria (4-160), except for a couple of samples in which about 1000 specimens have been counted.

2) The abundance of planktonic foraminifera in the interval within the Selli Level eq. varies from very high at the onset of OAE1a to null values (0-479 specimens). Radiolaria show marked fluctuations in abundance from very low to very high (5-3177 specimens).

3) The last interval, above the Selli Level eq., is characterized by a marked correlation between foraminiferal and radiolarian abundances, as follows: a strong increase of the planktonic foraminiferal abundance (from 3 to 800 specimens) occurs when the radiolarian abundance (from 2617 to 3 specimens) decreases. In particular, an evident fluctuation in abundance of planktonic foraminifera characterizes the two meters above the Selli Level equivalent.

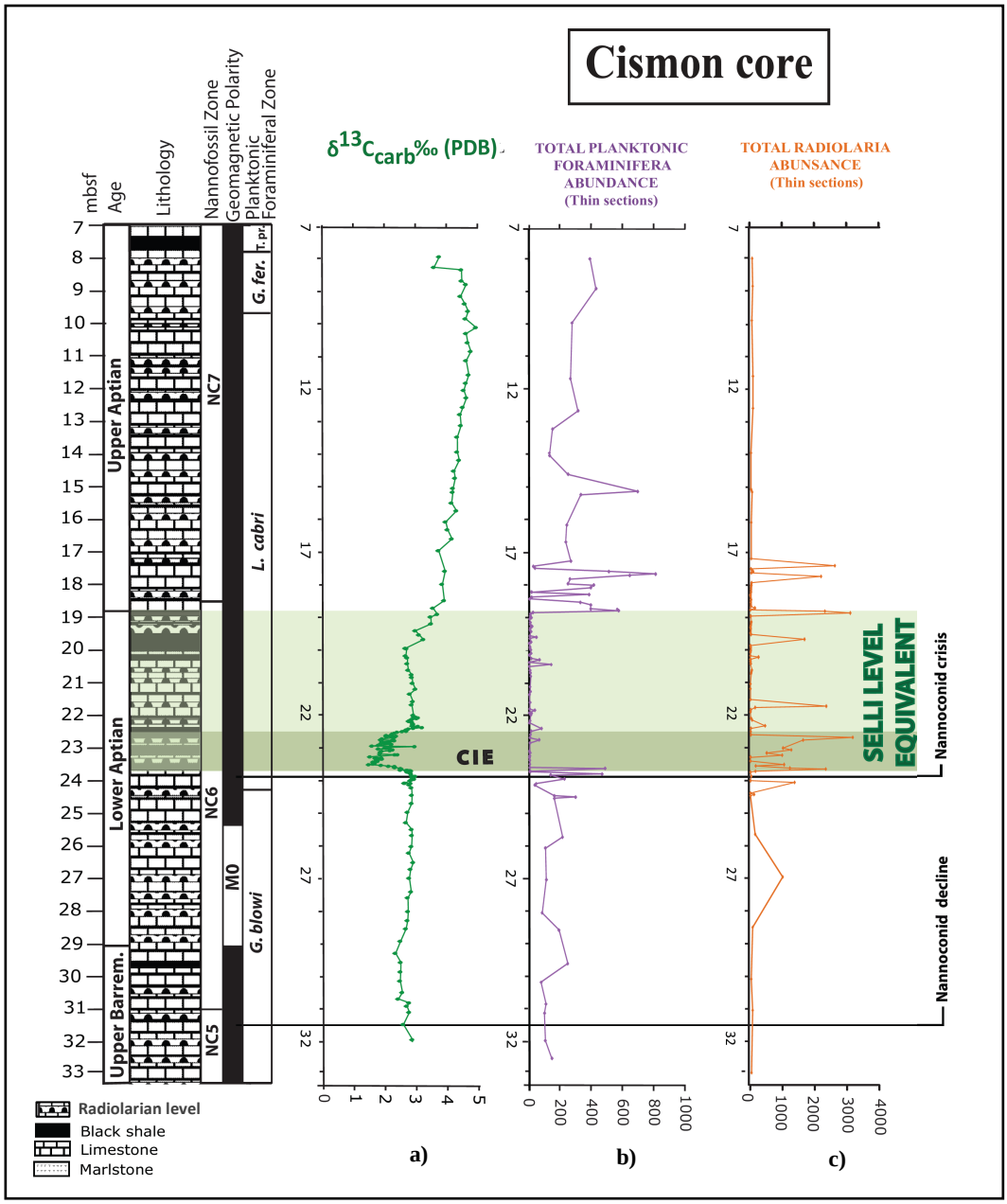

Fig. 6.6. Cimon core: comparison between the $\delta^{13}C$ record (a) and the total planktonic foraminiferal (b) and radiolarian (c) abundances. $\delta^{13}C$ is from Erba *et al.* (1999) and Mehày *et al.* (2009). Nannofossil biostratigraphy is from Erba *et al.* (1999). Foraminiferal biostratigraphy is from Erba *et al.* (1999) and this study. Magnetostratigraphy is from Channell *et al.* (2000).

Finally, comparing the planktonic foraminiferal data with the $\delta^{13}C$ curve, similarities and differences have been observed: at the onset of the OAE1a, planktonic foraminifera are characterized by a strong decrease of values which reflect the same behaviour of the $\delta^{13}C$ record. The negative carbon isotope shift is followed by a long positive excursion already within the Selli Level eq., but planktonic foraminiferal values remain still very low. They start to increase and become very high only from the first sample just above the Selli Level equivalent (18.72 m).

Comparing the radiolarian data with the $\delta^{13}C$ record an opposite trend was observed: at the onset of the OAE1a, radiolaria show an increase in abundance followed by a positive and negative fluctuations until to very low values in some intervals, while the $\delta^{13}C$ record show a negative shift followed by a long positive excursion.

6.1.5 Microfacies analyses

Microfacies analysis document eight different typologies, as follows (Figs 6.7-6.14):

1) Mudstone with few planktonic foraminifera and/or radiolaria;
2) Mudstone, locally wackestone due to accumulations of planktonic foraminifera;
3) Wackestone rich in planktonic foraminifera;
4) Wackestone very rich in planktonic foraminifera;
5) Wackestone very rich in radiolaria;
6) Packstone rich in radiolaria;
7) Wackestone with laminated organic matter (black shale);
8) Wackestone with no laminated organic matter (black shale).

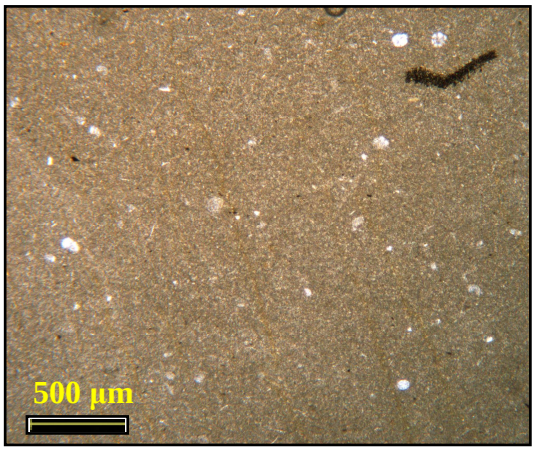

Fig. 6.7. Mudstone with few planktonic foraminifera and/or radiolaria

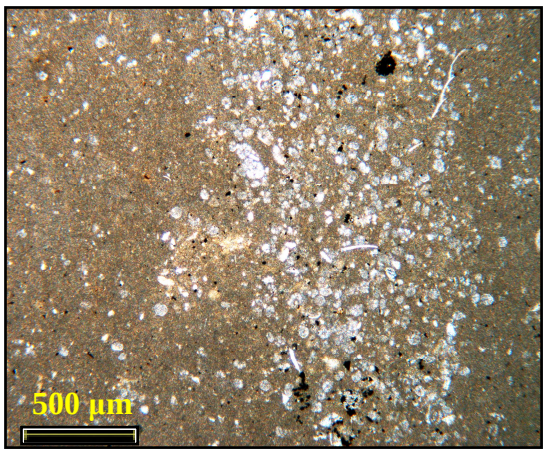

Fig 6.8. Mudstone, locally Wackestone very rich in planktonic foraminifera

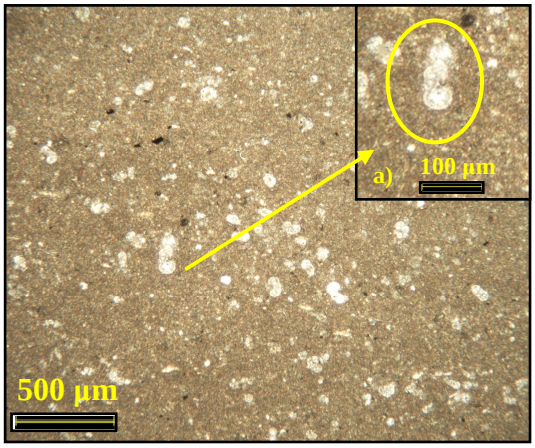

Fig. 6.9. Wackestone rich in planktonic foraminifera. In a) a perfect lateral cut of a trochospiral form.

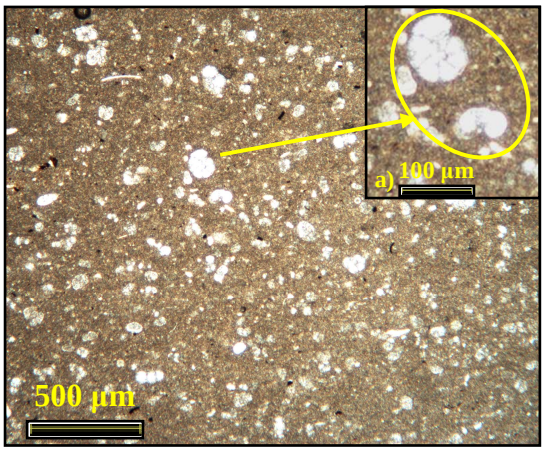

Fig. 6.10. Wackestone very rich in planktonic foraminifera. In a) a perfect equatorial and lateral cuts of planktonic foraminifera.

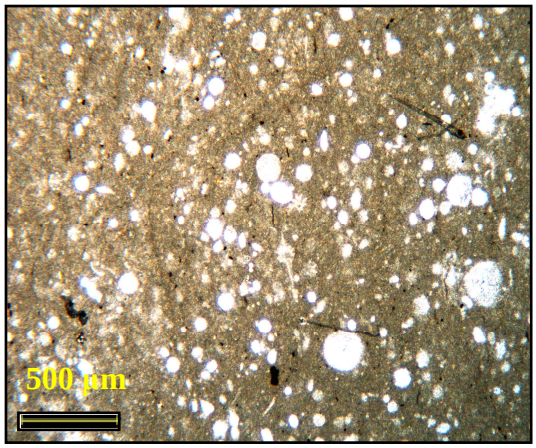

Fig. 6.11. Wackestone very rich in radiolaria of different test sizes.

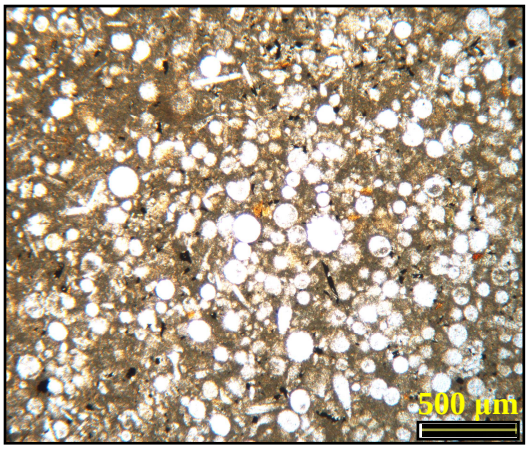

Fig. 6.12. Packstone rich in radiolaria with different morphology and test sizes.

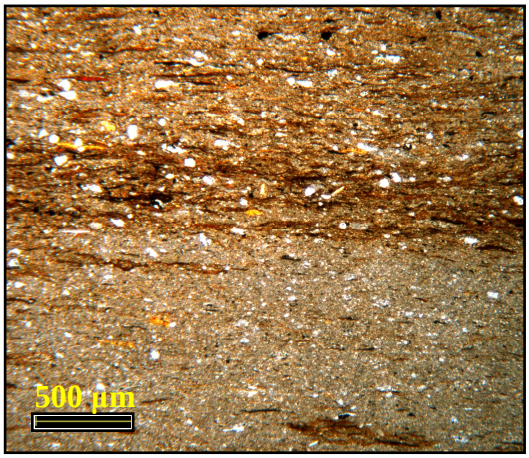

Fig. 6.13. Wackestone with laminated organic matter (black shale).

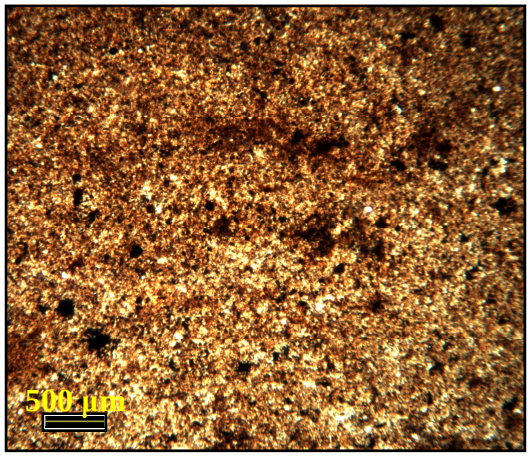

Fig. 6.14. Wackestone with no laminated organic matter (black shale).

By comparing the absolute abundances of planktonic foraminifera and radiolaria with the types of microfacies (Fig. 6.15) it is possible to observe:

1) the interval below the Selli Level eq. is typified by mudstone with planktonic foraminifera and/or radiolaria (A), mudstone locally wackestone with accumulations of planktonic foraminifera (B) (only one sample at 23.74 m), and wackestone rich in radiolaria (C);

2) the interval within the Selli Level eq. is characterized by mudstone locally wackestone with accumulations of planktonic foraminifera (B) (only one sample at 23.57 m), wackestone rich in radiolaria (C), wackestone with laminated (D) and not laminated (D1) organic matter, and packstone (E) rich in radiolaria;

3) above the Selli Level eq. the microfacies is represented by mudstone with planktonic foraminifera and/or radiolaria (A), mudstone locally wackestone with accumulations of planktonic foraminifera (B) (only one sample at 18.72 m), and wackestone from rich (B1) to very rich in planktonic foraminifera (B2).

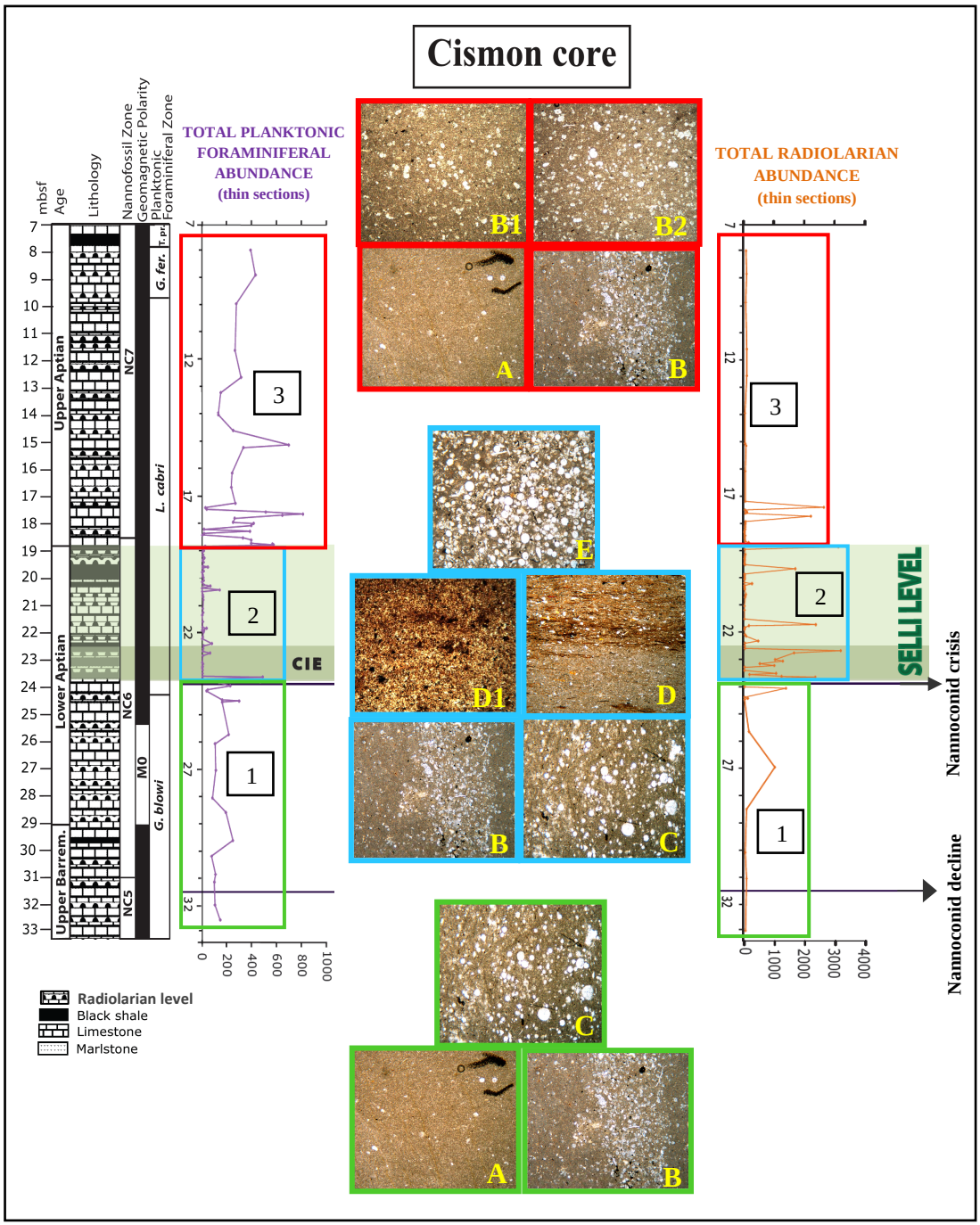

Fig. 6.15. Absolute abundances of planktonic foraminifera and radiolaria and microfacies types. INTERVAL 1 = low/moderate abundance of foraminifera and very low-moderate of radiolaria: microfacies type A, B and C (mudstone and wackestone); INTERVAL 2 = very high/low-null abundance of foraminifera and very low-very high of radiolaria: microfacies types B, C, D, D1, E (mudstone/wackestone, wackestone and packstone); INTERVAL 3 = moderate/high abundance of foraminifera and very high to very low of radiolaria: microfacies types A, B, B1, B2 (mudstone and wackestone). Nannofossil biostratigraphy is from Erba *et al.* (1999). Foraminiferal biostratigraphy is from Erba *et al.* (1999) and this study. Magnetostratigraphy is from Channell *et al.* (2000).

6.1.6 Planktonic foraminiferal morphometric analyses

A total of twenty-one species from 112 samples (washed residues) belonging to three different genera (*Hedbergella*, *Lilliputianella* and *Globigerinelloides*) were investigated for test sizes. Species with scarse data or incomplete record (e.g. *H. kuznetsovae*, *H. gorbachikae, H. luterbacheri, G. elongatus, G. blowi lobatus* and *Gorbachikella kugleri*) and species belonging to the genus *Leupoldina* and *Gubkinella* were excluded from the analyses (see Chapter 4.3).

The test size measurements for each species have been compared with the maximum diameter of the respective holotype.

Unfortunately, it was not possible to measure the same number of specimens for each species in all the studied samples because of the poor preservation of the assemblage. For instance, planktonic foraminifera are very rare or absent within the Selli Level eq. where the smallest shell size (53 µm) were measured.

Nonetheless, all the acquired data are presented and discussed since a quantitative documentation in terms of shell size has never been performed before the present study.

For each species the maximum diameter value is based on 1 to 5 measurements for sample, obtained by choosing the value of the smallest, biggest and intermediate specimen measured (Figs. 6.16 and 6.17).

In Figure 6.16 the test size data of Hedbergellids and Lilliputianellids (trochospiral forms) are reported: all species have been compared to the respective holotype. In general, the trochospiral species show the same behaviour as their test sizes are systematically lower than the size of their holotype; however, some exceptions are seen in two samples above the Selli Level eq.: the species *H. excelsa, H praetrocoidea, H. tuschepsensis* and *L. roblesae* display values very close to the holotype' test size.

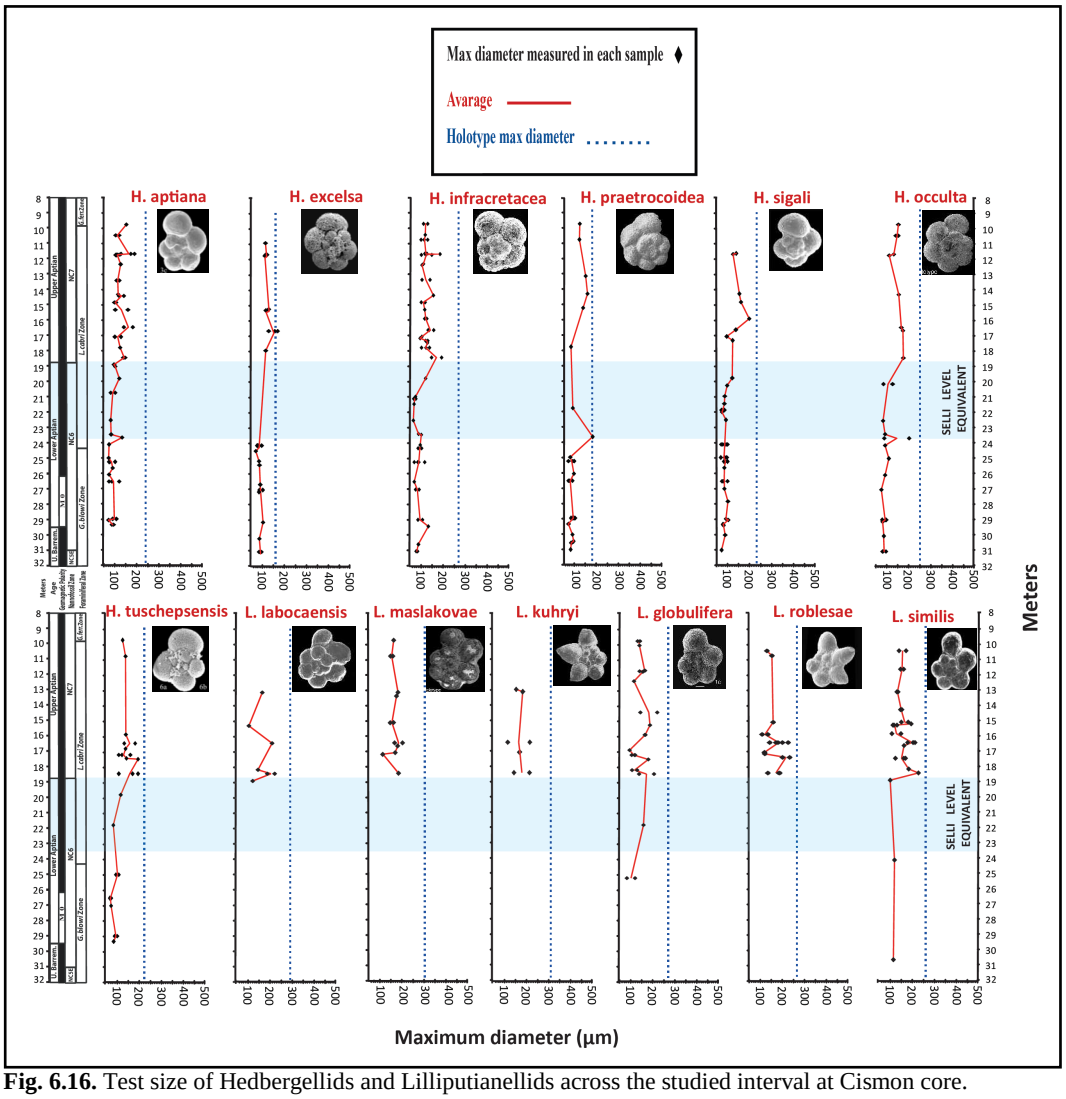

Fig. 6.16. Test size of Hedbergellids and Lilliputianellids across the studied interval at Cismon core.

Hedbergellids show the most complete record across the studied interval; in general, an increase in shell size from the base to the top is observed; in fact, the values displayed by the shell size are comparable below the Selli Level eq. (from 70 µm to 137 µm) and within it (from 68 µm to 125 µm), then they become slightly higher above it (from 84 µm to 236 µm). It is important to underline that even within the Selli Level eq. test sizes > 125 µm (15/96 W; 23.66 m) have been observed in three taxa only: *H. aptiana* (135.68 µm), *H. praetrocoidea* (183.16) and *H. occulta* (200.88 µm). Most interesting is that all the three species record a double value of test size compared to the previous sample (RAD 75; 24.12 m) and this feature happens at the onset of the Selli Level equivalent.

Furthermore, all Hedbergellids have the same range of variation across the studied interval except for *H. tuschepsensis* and *H. occulta* that show wider ranges.

Lilliputianellids have a less complete record because almost all species appear in the same sample above the Selli Level eq. (Sample RAD 37; 18,43 m) except for *Lilliputianella labocaensis, L. globulifera* and *L. similis*.

L. globulifera and *L. similis* show an increase in shell size from the base to the top while the other species show different trends. The shell sizes of the Lilliputianellids range from 83µm to 123 µm below the Selli Level eq., from 104µm to 158 µm within it (even if data are very few) and from 96 µm to 232 µm above it. The range of size variation is similar to the Hedbergellid group.

Figure 6.17 reports the results of the test size measurements of the Globigerinelloidids (planispiral forms): the comparison with the respective holotype shows different behaviours, as follows: species with test size systematically lower than the holotype (e.g. *G. aptiensis* and *G. duboisi*), species with test size higher than the holotype (e.g. *G. maridalensis*) and species with test size values comparable to the holotype (e.g. *G. blowi*); in addition, some species as *G. paragottisi, G. sigali* and *G. primitivus* show an irregular behaviour.

Globigerinelloidids do not have a complete record because only four species (*G. aptiensis, G. maridalensis, G. blowi* and *G. paragottisi*) do occur from the base of the studied interval, while the other species do occur either within (*G. duboisi* and *G. sigali*) or above (*G. primitivus, G. clavatus, G. blowi lobatus* and *G. elongatus*) the Selli Level equivalent.

Globigerinelloids' species are characterized by having different test size trends as follows, from the base to the top of the studied interval:

- *G. aptiensis* is the only species that shows an increase in test size comparable to the Hedbergelllids;
- *G. primitivus, G. duboisi* and G. *clavatus* instead show a decrease in test size;
- All other species do not have a single trend as they display a test size increases followed by a decrease (e.g. *G. maridalensis* and *G. paragottisi*). Species such as *G. blowi lobatus* and *G. elongatus* have too few data to make reliable considerations.

The range variation of the test size is moderate in species like *G. aptiensis* and very high in species like *G. maridalensis* and *G. blowi*.

The values displayed by the shell size are enough comparable below the Selli Level eq. (from 78 µm to 217 µm) and within it (from 85 µm to298 µm) and become higher above it (from 82 µm to 427 µm).

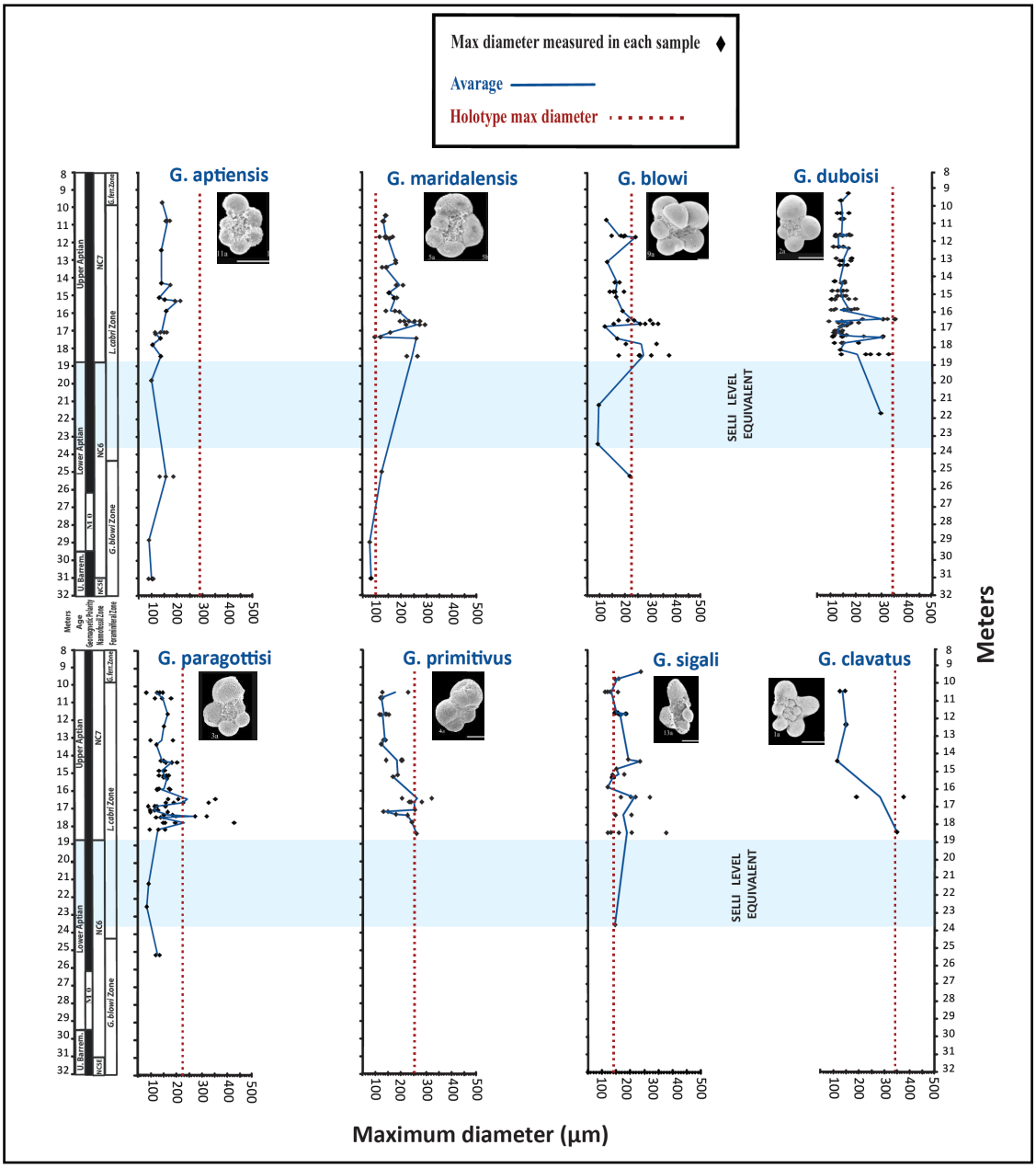

Fig. 6.17. Test size of Globigerinelloids across the studied interval at Cismon core.

The comparison between the trochospiral (Hedbergellids and Lilliputianellids) and the planispiral taxa (Globigerinelloidids) test size trends illustrated in Figure 6.16 and Figure 6.17 highlights the following similarities:

1) Several trochospiral and planispiral species show their lowest occurrence in the same sample (RAD 37; 18,43 m) and all of them possess elongate chambers;

2) Some trochospiral forms (*H. tuschepsensis*, *L. roblesae* and *L. similis*) show fluctuations of the test size just above the Selli Level eq. The same but wider trend is recorded within the planispiral group (*G. maridalensis*, *G. blowi*, *G. duboisi*, *G. paragottisi*, *G. primitivus* and *G. sigali*). However, the major changes in test size are concentrated above the Selli Level eq. likely because of a higher number of specimens per species in each sample (that allows more measures) and an increase of species richness.

3) By comparing the test size of the taxa that are first recorded below the Selli Level eq. we note that (from the base to the top) the trochospiral forms either became double (e.g. *H. aptiana*) or triple (e.g. *H. tuschepsensis* and *L. similis*) in size. On the contrary the planispiral species can either twice their size (e.g. *G. aptiensis*) or even quadruple it (e.g. *G. paragottisi*). Once again, Globigerinelloidids show wider variations in test size than Hedbergellids and Lilliputianellids.

To quantify the observed changes in test size within single species and among species within genera the acquired data have been statistically analysed and depicted in Figure 6.18. A box-plot for each species was plotted to illustrate the test size variation obtained subtracting the minimum value of test size from the maximum value measured for each species and for each sample. Graphically, it coincides with the *no-outlier range*, while the *outlier* values were not considered because they statistically do not appear to follow the distribution of the *no-outlier*.

Three groups have been recognized: 1) a group with a range of variation in test size below 100 µm, which is typical of some Hedbergellids and Lilliputianellids (e.g. *H. aptiana* and *L. maslakovae*); 2) a group with a range of variation in test size from 100 µm to 150 µm. Representative of the three genera (e.g. *H. tuschepsensis*, *L. globulifera* and *G. aptiensis*) fall in this group; 3) a group with a range of variation in test size > 150 µm represented only by Globigerinelloidids (e.g. *G. primitivus* and *G. maridalensis*).

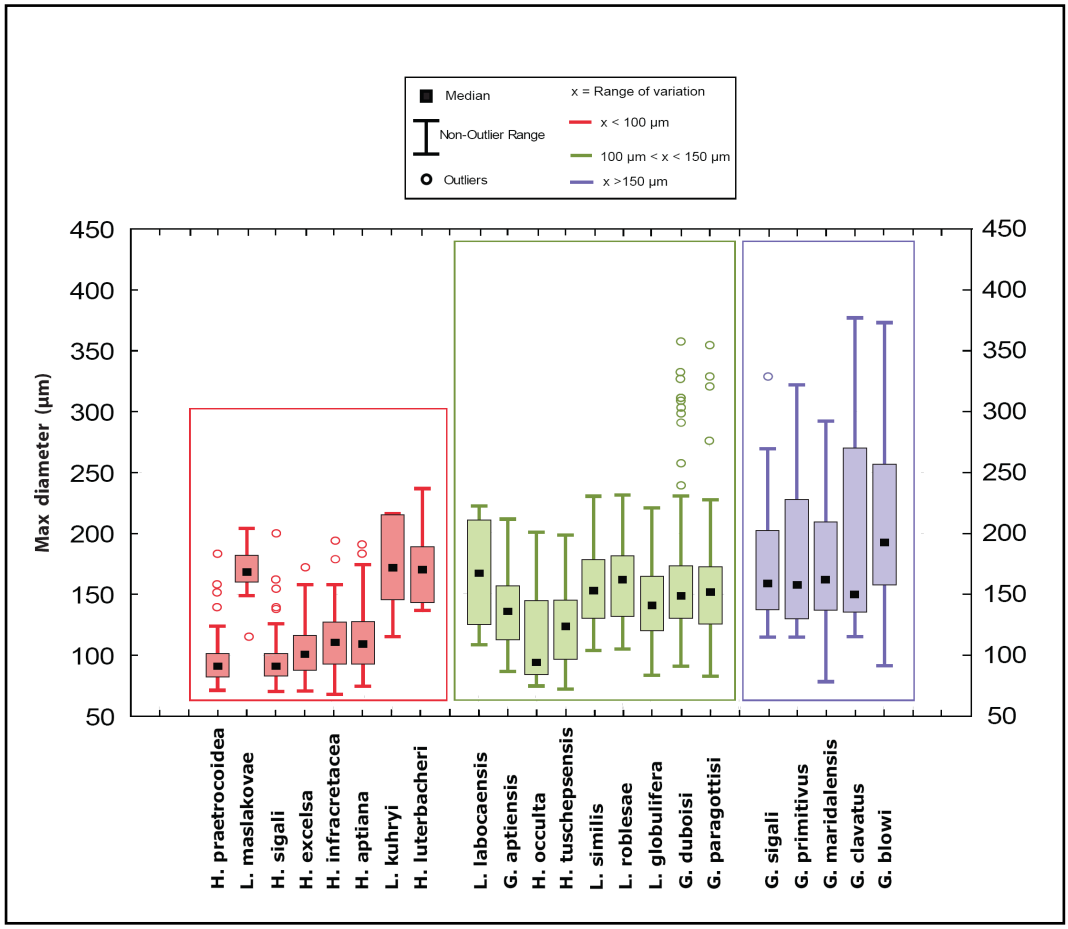

Fig. 6.18. Box plots of planktonic foraminifera test size across the Cismon core studied interval.

Finally, the observed increases and decreases of maximum diameters with depth (and time) have been quantified for all species by analysing the relationships between test size variations and depth through application of the Pearson correlation (R). First of all, the respective R-value, regression line and angular coefficient (β) were calculated for each species; subsequently, species belonging to the same genus were plotted against each other in order to understand if there were similarities or differences.

All graphs obtained are included in the Appendix chapter and only the most significant examples are illustrated and discussed herein by morphological group, as follows:

1) In general, considering the relationship between test size and depth, all Hedbergellids are characterized by moderate negative R values (from R= -0,508 to R= -0,700), by negative slopes and angular coefficients of the regression lines. It confirms that all taxa assigned to the Hedbergellids group show the same behaviour since there is a good negative correlation related to a constant increase of test size with the decrease of

depth and age. In other words there is an increase in test size from the older to the younger stratigraphic level. This increase could be likely linked to a higher number of specimens per sample and species richness that is observable just above the Selli Level equivalent.

Figure 6.19 shows two examples that summarize the main trends obtained for the Hedbergellids: *H. aptiana* vs. *H. praetrocoidea* (Fig. 19a) and *H. infracretacea* vs. *H. tuschepsensis* (Fig. 6.19b).

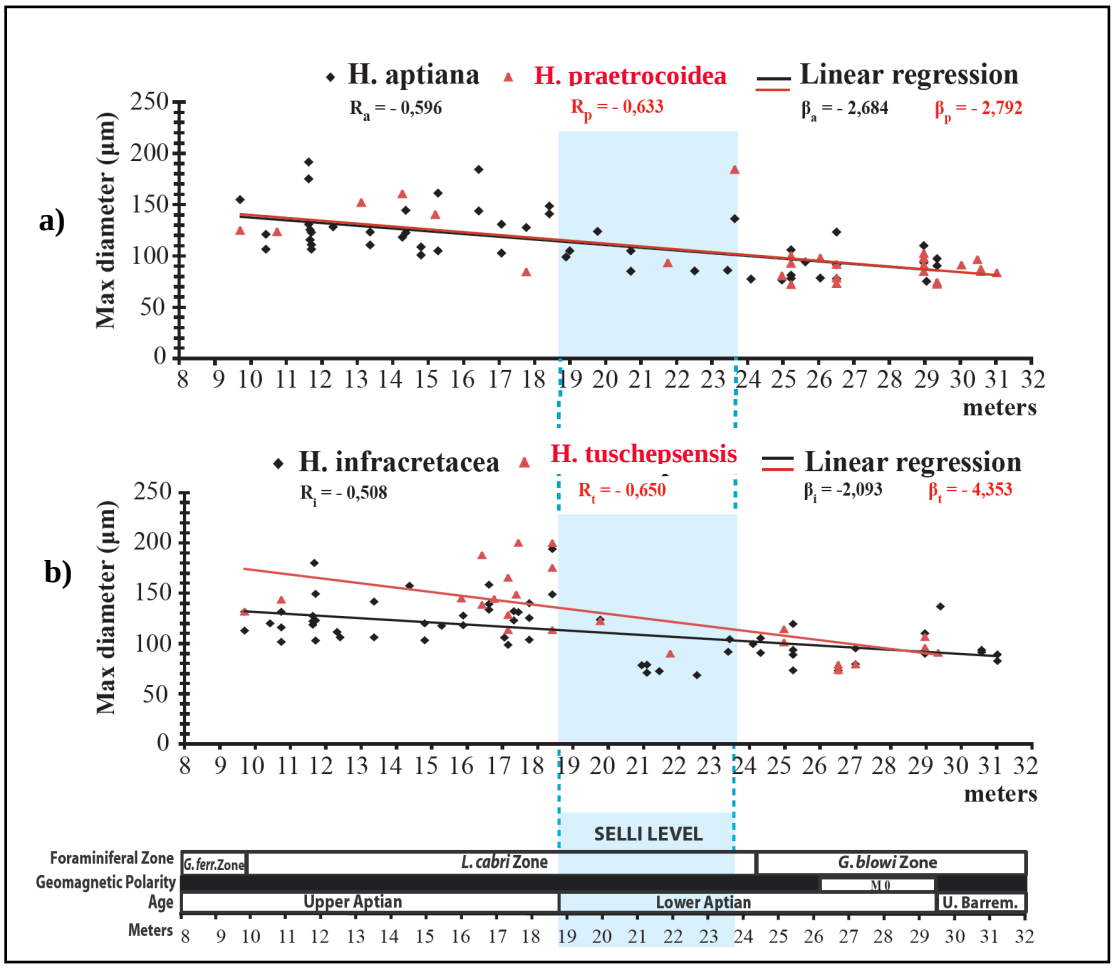

Fig. 6.19. Relationships between test size variations of Hedbergellids and depth. a) *H. aptiana* and *H. praetrocoidea*: Ra= Pearson's coefficient *H. aptiana*; Rp= Pearson's coefficient *H. praetrocoidea*; βa= angular coefficient *H. aptiana*; βp= angular coefficient *H. praetrocoidea*. b) *H. infracretacea* and *H. tuschepsensis*: Ri= Pearson's coefficient *H. infracretacea*; Rt= Pearson's coefficient *H. tuschepsensis*; βi= angular coefficient *H. infracretacea*; βt= angular coefficient *H. tuschepsensis*.

The variation in test size of *H. aptiana* and *H. praetrocoidea* ranges exactly in the same way as a function of depth (Fig. 19a); in fact, both species possess two similar negative R values, slopes and angular coefficients.

On the contrary, *H. tuschepsensis* shows a stronger relationship as function of depth, and a more negative slope and angular coefficient than *H. infracretacea* (Fig. 19b).

2) The results obtained on the Lilliputianellids are quite different compared to the Hedbegellids as the species show a very low positive and negative R value (from R=0,291 to R= -0, 268) confirming a weak correlation between test size variation and depth. Consequently, the slopes of the regression lines are both positive and negative. The results obtained by comparing the Lilliputianellids' species can be summarized using three examples (Fig. 6.20): *L. maslakovae* vs. *L. kuhryi* (Fig. 6.20a), *L. globulifera* vs. *L. similis* (Fig. 6.20b) and *L. globulifera* vs. *L. roblease* (Fig. 6.20c).

The correlation trends observed in Figure 6.20a and Figure 6.20b both display a weak correlation with depth, and with comparable values of R and β, respectively positive and negative.

The comparison between *L. globulifera* and *L. roblease* (Fig. 20c) demonstrates that the two taxa show an opposite trend as function of depth. For both species the relationship is weak and it is justified by the low R values (positive and negative) displayed.

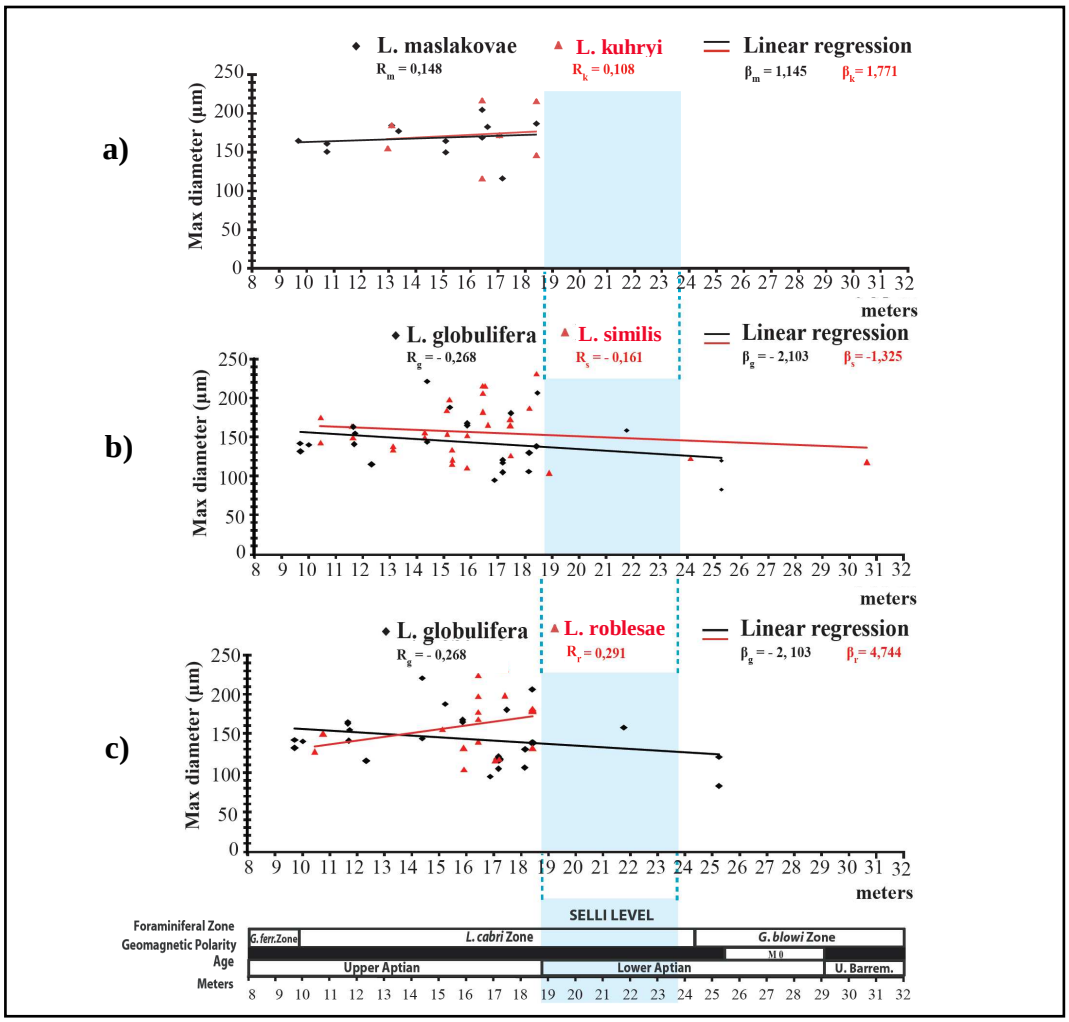

Fig. 6.20. Relationships between test size variations of Lilliputianellids and depth. a) *L. maslakovae* and *L. kuhryi*: Rm= Pearson's coefficient *L. maslakovae*; Rk= Pearson's coefficient *L. kuhryi*; βm= angular coefficient *L. maslakovae* ; βk= angular coefficient *L. kuhryi*. b) *L. globulifera* and *L. similis*: Rg= Pearson's coefficient *L. globulifera*; Rs= Pearson's coefficient *L. similis*; βg= angular coefficient *L. globulifera*; βs= angular coefficient *L. similis*. c) *L. globulifera* and *L.roblesae*: Rg= Pearson's coefficient *L. globulifera*; Rr= Pearson's coefficient *L. roblesae*; βg= angular coefficient *L. globulifera*; βs= angular coefficient *L.roblesae*.

3) The results obtained by comparing the Globigerinelloidids species vary from very low to moderate positive and negative R values (e.g. R=0,658, R=0,032 and R= -0,518) to confirm that some species have either a good positive correlation with depth (decrease in size paralleled by decrease in depth/time) or good negative correlation with depth (increase in size paralleled by the decrease in depth/time) while other taxa show a weak or null correlation.

Three examples are here discussed to summarize the results (Fig. 6.21): *G. duboisi* vs. *G. primitivus* (Fig. 6.21a), *G. maridalensis* vs. *G. paragottisi* (Fig. 6.21b), *G. aptiensis* vs. *G. duboisi* (Fig. 6.21c).

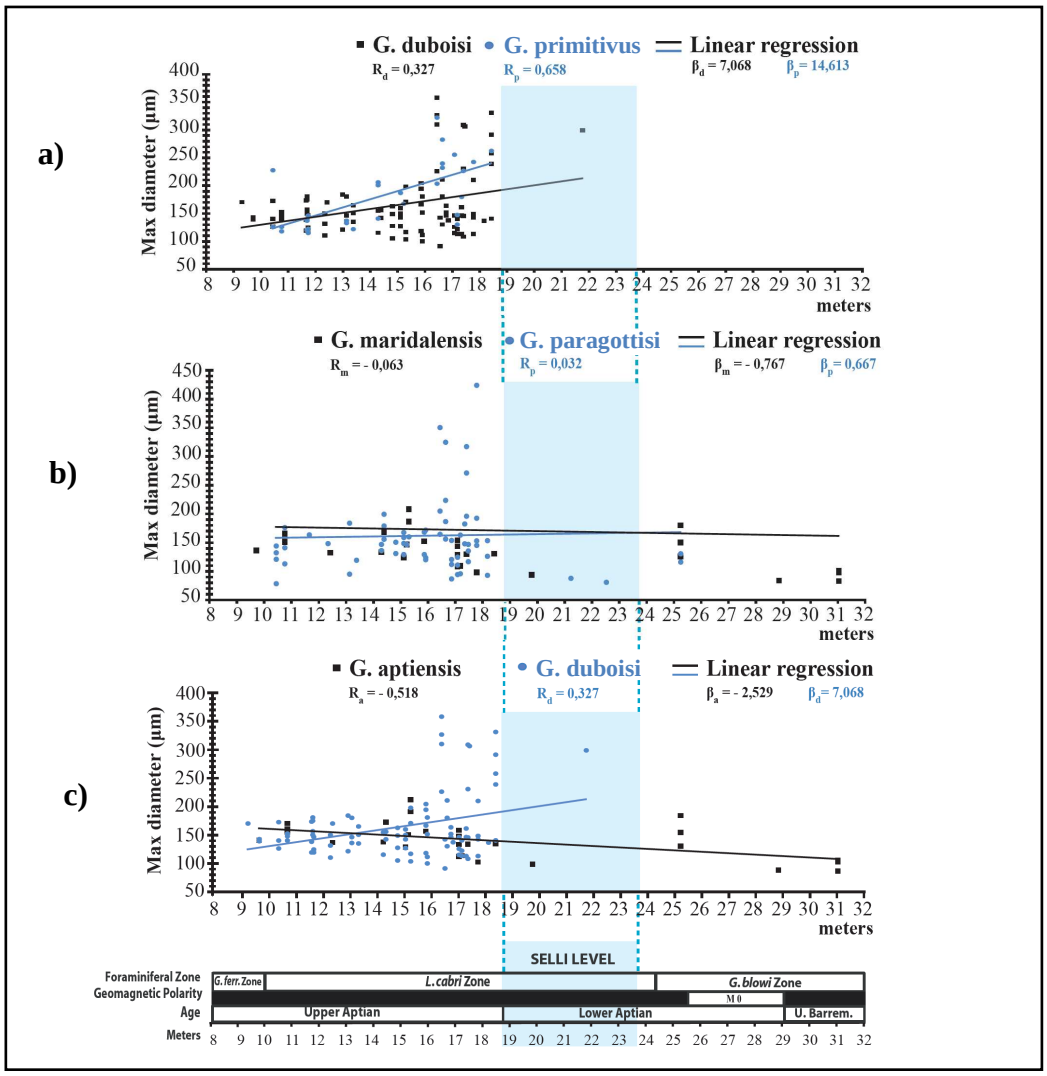

Fig. 6.21. Relationships between test size variations of Globigerinelloidids and depth. a) *G. duboisi* and *G.primitivus*: Rd= Pearson's coefficient *G. duboisi* ; Rp= Pearson's coefficient *G.primitivus*; βd= angular coefficient *G. duboisi* ; βp= angular coefficient *G.primitivus*. b) *G. maridalensis* and *G.paragottisi*: Rm= Pearson's coefficient *G. maridalensis*; Rp= Pearson's coefficient *G.paragottisi*; βm= angular coefficient *G. maridalensis*; βp= angular coefficient *G.paragottisi*. c) *G.aptiensis* and *G. duboisi*: Ra= Pearson's coefficient *G.aptiensis*; Rd= Pearson's coefficient *G. duboisi*; βa= angular coefficient *G.aptiensis*; βd= angular coefficient *G. duboisi*.

G. duboisi and *G. primitivus* are characterized by comparable values of R, positive slopes and angular coefficients; in fact, both species have a moderate positive correlation with depth (Fig. 6.21a). A null correlation with depth between *G. maridalensis* and *G. paragottisi* is shown in Figure 6.21b to indicate the absence of a linear (unidirectional) correlation, in fact both species have R values and angular coefficients close to zero. *G. aptiensis* and *G. duboisi* (Fig. 6.21c) show opposite trends as R values indicate a moderate correlation species-depth, negative and positive, respectively.

6.2 DSDP Site 463

The studied interval at DSDP Site 463 is about 62 meter thick (from 648 m to 586.53 m), including the Selli Level equivalent. Similar to the Cismon core, the major difficulties were represented by the small sizes of specimens and by the overall very poor preservation of the DSDP Site 463 assemblages.

Being most of washed residues barren in planktonic foraminifera, total abundances and test size curves were not plotted; in fact, it was possible to obtain only semi-quantitative data on test variations across the studied interval.

Planktonic foraminiferal and radiolarian abundances were obtained using thin sections.

6.2.1 Taxonomy

Taxonomic analyses reveal that at DSDP Site 463 most samples are barren in planktonic foraminifera and the assemblages are composed by fourteen species assigned to four genera characterized by having globular chambers (Fig. 6.22): genera *Hedbergella* (eight species), *Globigerinelloides* (four species), *Gorbachikella* (one species) and *Gubkinella* (one species). Forms with “clavate” or elongated chambers do not occur in the washed residues, but the possibility that rare to few forms belonging to the genus *Leupoldina* sp. could be present in the thin sections cannot be excluded.

In general, planispiral and globigeriniform taxa are easily recognizable thanks to their morphology (e.g. *Globigerinelloides duboisi*, *G. aptiensis*, *Gubkinella graysonensis* and *Gorbachikella kugleri*). On the contrary, identification at species level is sometimes very difficult for the trochospiral species characterized by having from 4 to 7 chambers in the last whorl, a low to very high trochospire, globular chambers (e.g. *Hedbergella tuschepsensis*, *H. infracretacea* and *H. excelsa*) also because the number of chambers is not always a useful criteria to discriminate among species.

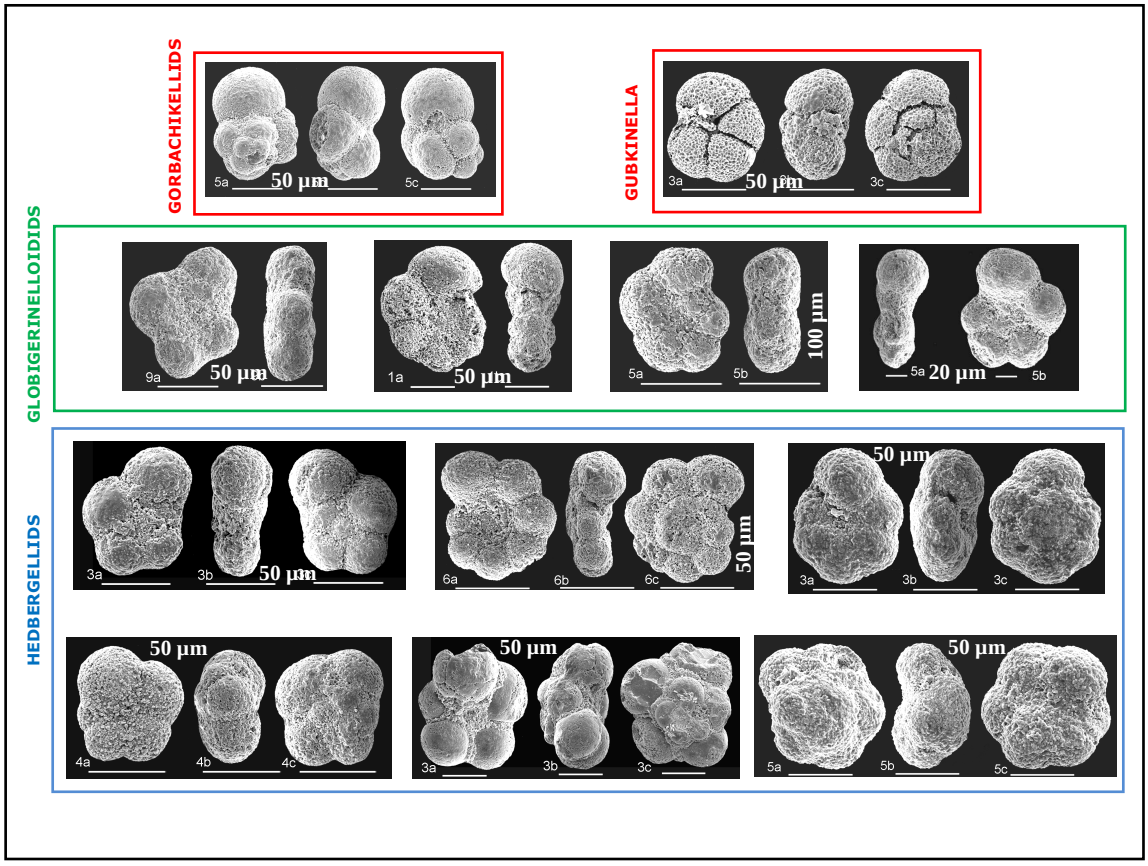

Fig. 6.22. Planktonic foraminifera with globular chambers recognized at DSDP Site 463.

6.2.2 Planktonic foraminiferal assemblage composition

In Figure 6.23 is shown the composition of the assemblage in washed residues in terms of main morphologies: across the studied interval Hedbergellids are the most common group and show a more continuous range, while planispiral, pseudo-planispiral and globigeriniform taxa occur only in some samples. Stratigraphic distribution of taxa is reported in the distribution chart (Table 4, in Appendix) in which is possible to observe that the record at DSDP Site 463 is very discontinuous also due to the very poor preservation that did not allow the identification at species level in several samples including the stratigraphic interval within the Selli Level equivalent (as seen in the Cismon core). For this reason, it was not possible to quantify the composition of the assemblage and plot the relative abundances of the morphological groups in percentage.

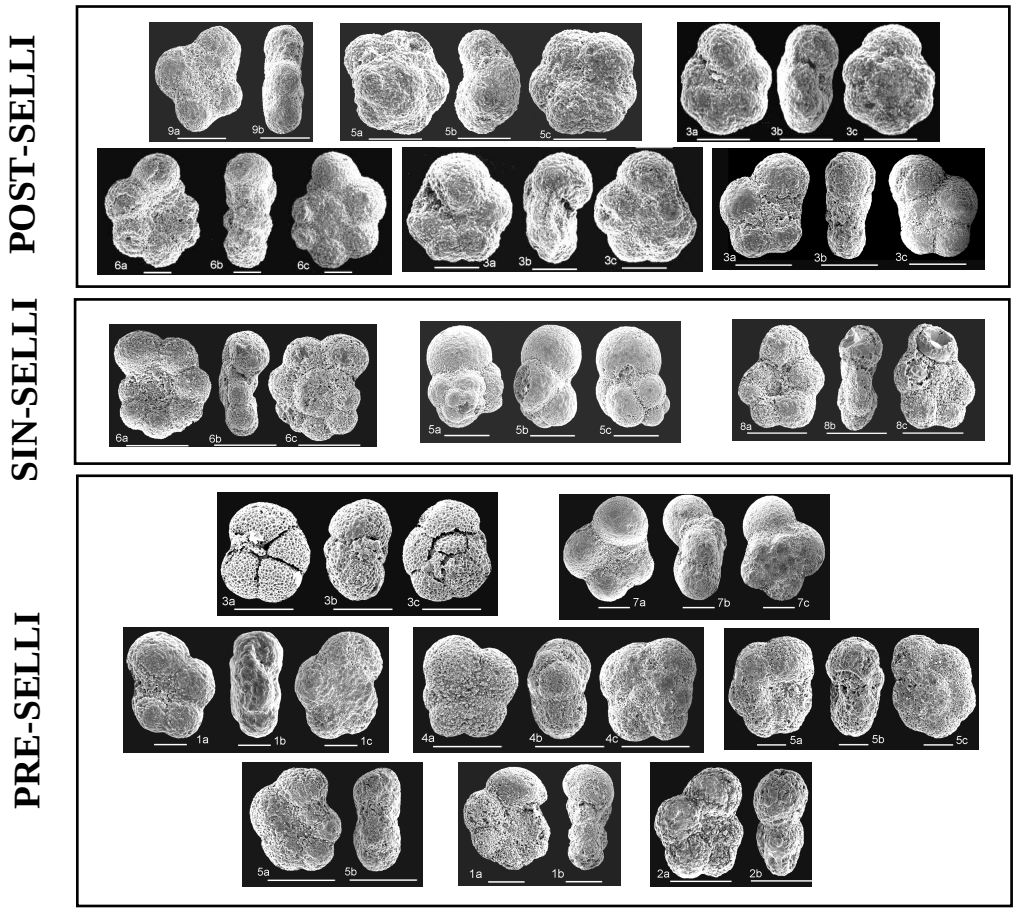

Fig. 6.23. Planktonic foraminiferal composition across the studied interval at DSDP Site 463 .

Figure 6.24 shows all types of wall preservation recognized at DSDP Site 463:

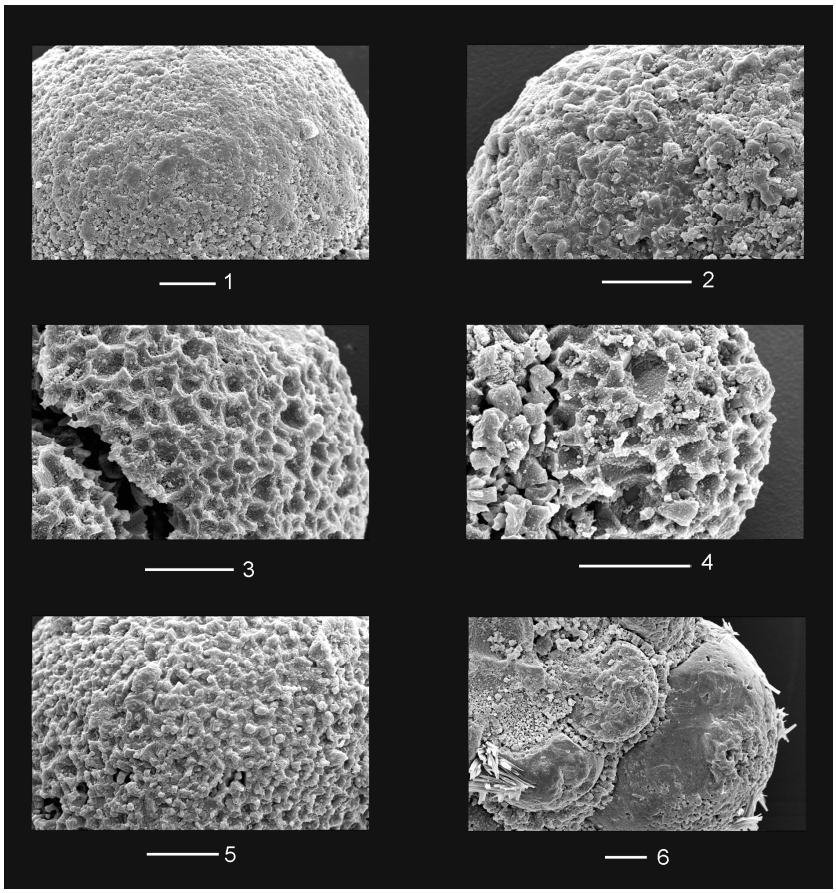

Fig. 6.24. Different types of wall texture recognized at DSDP Site 463 . 1-2 : smooth wall texture, not dissolved; 3-4-5: different types of wall partially dissolved that simulates the faveolate wall texture typical of the favusellid group wall; 6: internal mold. All scale bars = 10 µm.

6.2.3 Planktonic foraminiferal and radiolarian absolute abundances

At DSDP Site 463 a pronounced negative carbon isotope excursion at the onset of the Selli Level equivalent is recorded.

Figure 6.25 shows the comparison between the $\delta^{13}C$ record (a) and the planktonic foraminiferal (b) and radiolarian (c) abundances.

In Figures 6.25a and 6.25b three interval are highlighted according to variations in abundances:

1) The interval below the Selli Level eq. is characterized by low abundance of planktonic foraminifera (0 to 43 specimens) and a fluctuation from low to high values of radiolaria (104-3578 specimens).

2) The interval within the Selli Level eq. shows a decrease in abundance of planktonic foraminifera until to null values (0-4 specimens) in most of the samples and a fluctuation from low to very high values of radiolaria (170-5008 specimens).

3) The last interval, above the Selli Level eq., highlights a strong increase of the planktonic foraminiferal abundance (from 0 to 363 specimens) and a decrease until to very low/moderate values of radiolaria (from 4 to 1692 specimens), except for a couple of samples in which radiolaria reach values of about 3000 specimens. It is important to underline that the strong increase in planktonic foraminiferal abundance that occurs several meters above the Selli Level eq. (594.53 m) is probably related to the higher number of specimens in thin sections and to the low core recovery in the underlying stratigraphic level (Fig. 6.25).

Finally, comparing the planktonic foraminiferal data with the $\delta^{13}C$ curve, similarities and differences have been observed: at the onset of the OAE1a, the $\delta^{13}C$ record is characterized by a negative shift followed by a long positive excursion that falls already within the Selli Level equivalent, while planktonic foraminifera in the same interval are absent or very rare (from 0 to 4 specimens). Planktonic foraminifera start to increase and become very common only several meters above the Selli Level equivalent.

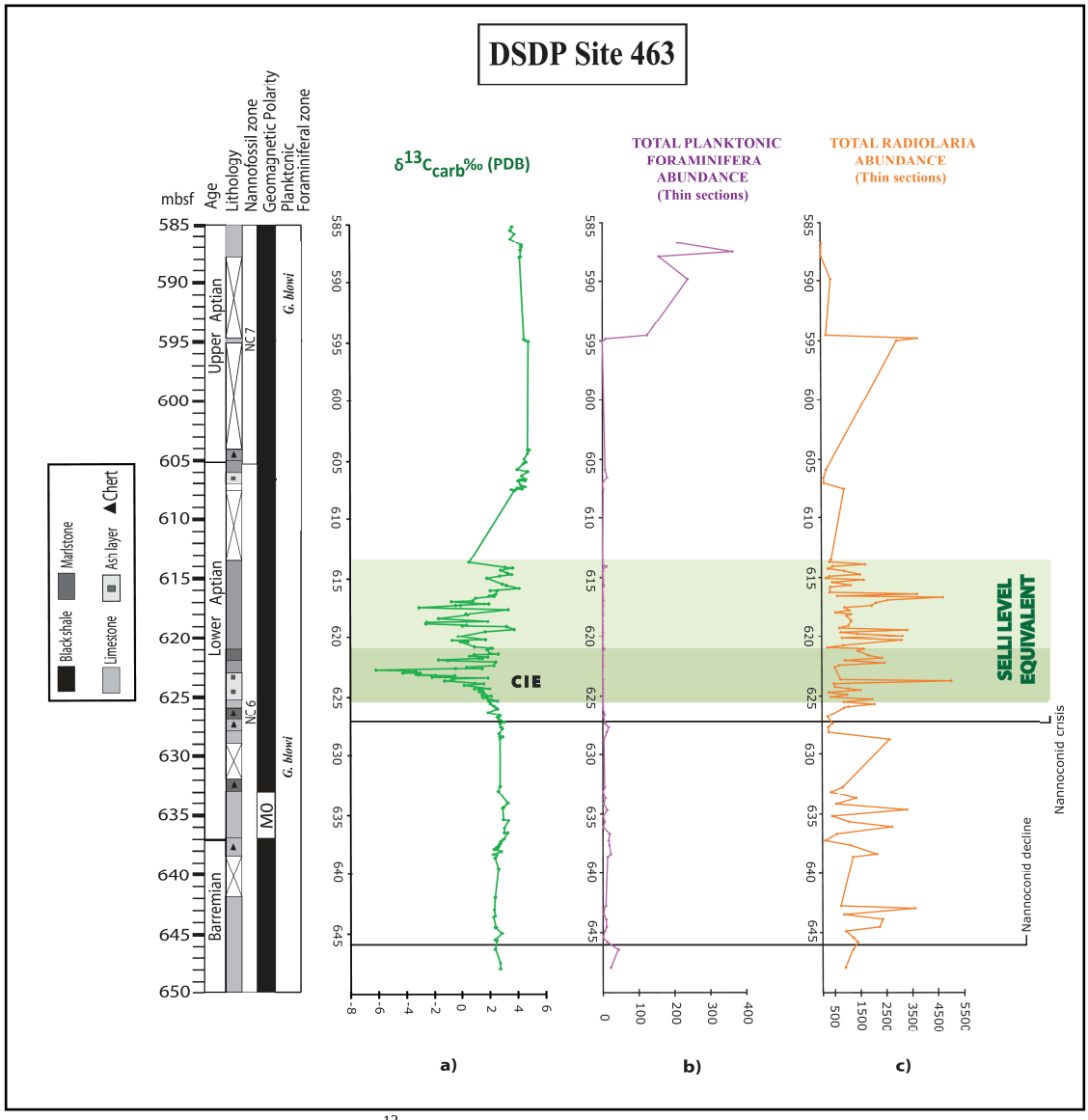

Fig. 6.25. Comparison between the $\delta^{13}C$ record (a) and the planktonic foraminiferal (b) and radiolarian (c) abundances at DSDP Site 463 Mid-Pacific Mountains. $\delta^{13}C$ modified after Bottini *et al.* (2012). Nannofossil biostratigraphy is from Erba (1994). Foraminiferal biostratigraphy is from this study. Magnetostratigraphy is from Tarduno *et al.* (1989).

Comparing the radiolarian data with the $\delta^{13}C$ curve an opposite trend was observed: at the onset of the OAE1a, radiolaria show an increase followed by fluctuations in abundance until to very low values above the Selli Level equivalent, while the $\delta^{13}C$ record displays a negative shift followed by a long positive excursion already within the Selli Level equivalent.

6.2.4 Microfacies analyses

Microfacies analysis document seven different typologies, as follows (Figs 6.26-6.32):

1) mudstone with few planktonic foraminifera and/or radiolaria;

2) wackestone rich in planktonic foraminifera;

3) wackestone rich in radiolaria;

4) wackestone very rich in radiolaria;

5) packstone rich in radiolaria;

6) wackestone with laminated organic matter (black shale);

7) wackestone with no laminated organic matter (black shale).

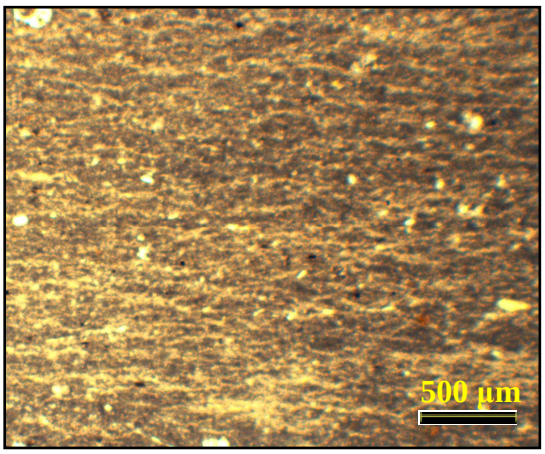

Fig. 6.26. Mudstone with few planktonic foraminifera and/or radiolaria

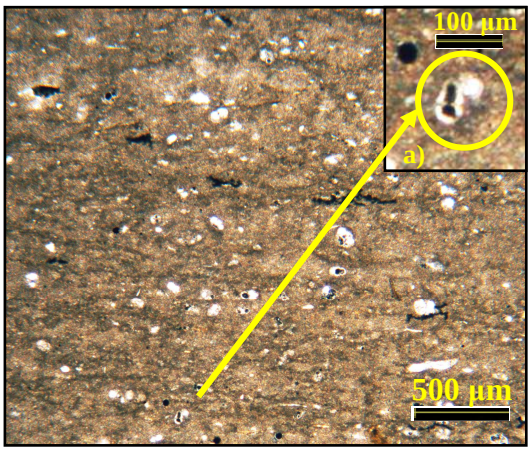

Fig. 6.27. Wackestone rich in planktonic foraminifera. In a) a perfect lateral cut of a trochospiral form.

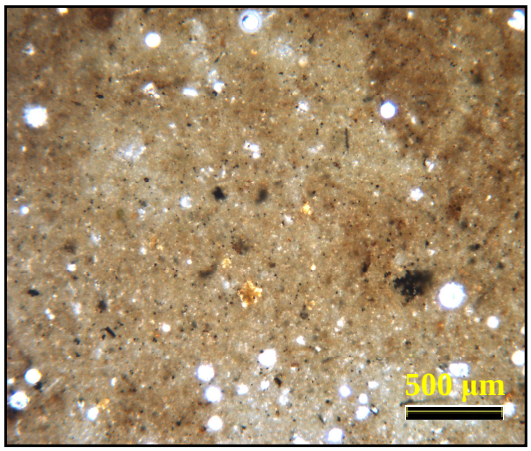

Fig. 6.28. Wackestone rich in radiolaria of different test sizes

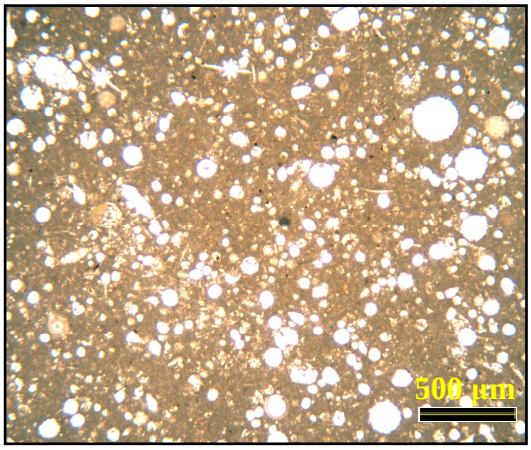

Fig. 6.29. Wackestone very rich in radiolaria of different test sizes and morphology

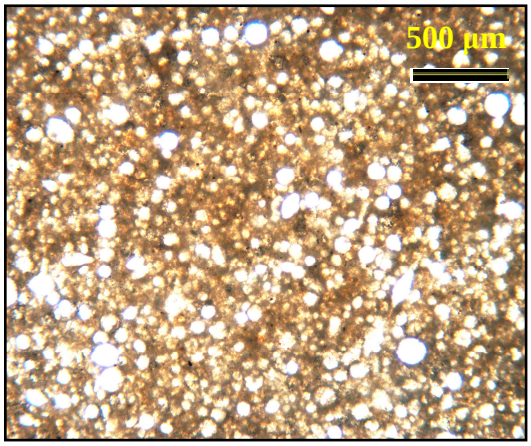

Fig. 6.30. Packstone rich in radiolaria with different morphology and test sizes

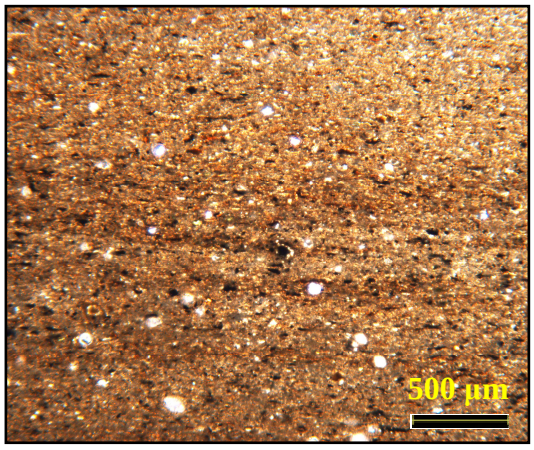

Fig. 6.31. Wackestone laminated organic matter (black shale)

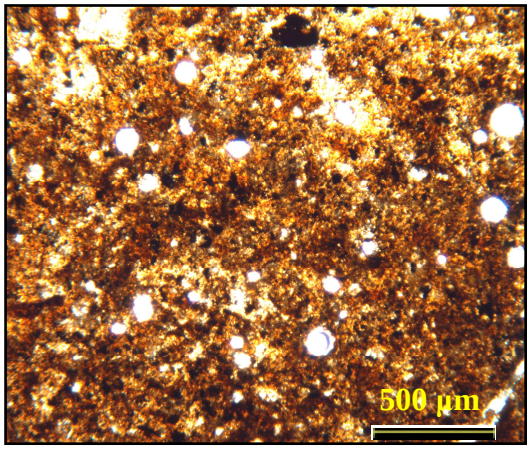

Fig. 6.32. Wackestone with no laminated organic matter (black shale)

Comparing the absolute abundances of planktonic foraminifera and radiolaria with the types of microfacies (Fig. 6.33) it is possible to observe:

1) the interval below the Selli Level eq. corresponds to a mudstone with few planktonic foraminifera and/or radiolaria (A) and to a wackestone very rich in radiolaria (C1);

2) the interval within the Selli Level eq. is characterized by wackestone with laminated (D) and not laminated (D1) organic matter, wackestone (C1) and packstone (E) very rich in radiolaria;

3) above the Selli Level eq. microfacies are represented by wackestone rich in radiolaria (C) and wackestone rich in planktonic foraminifera (B1).

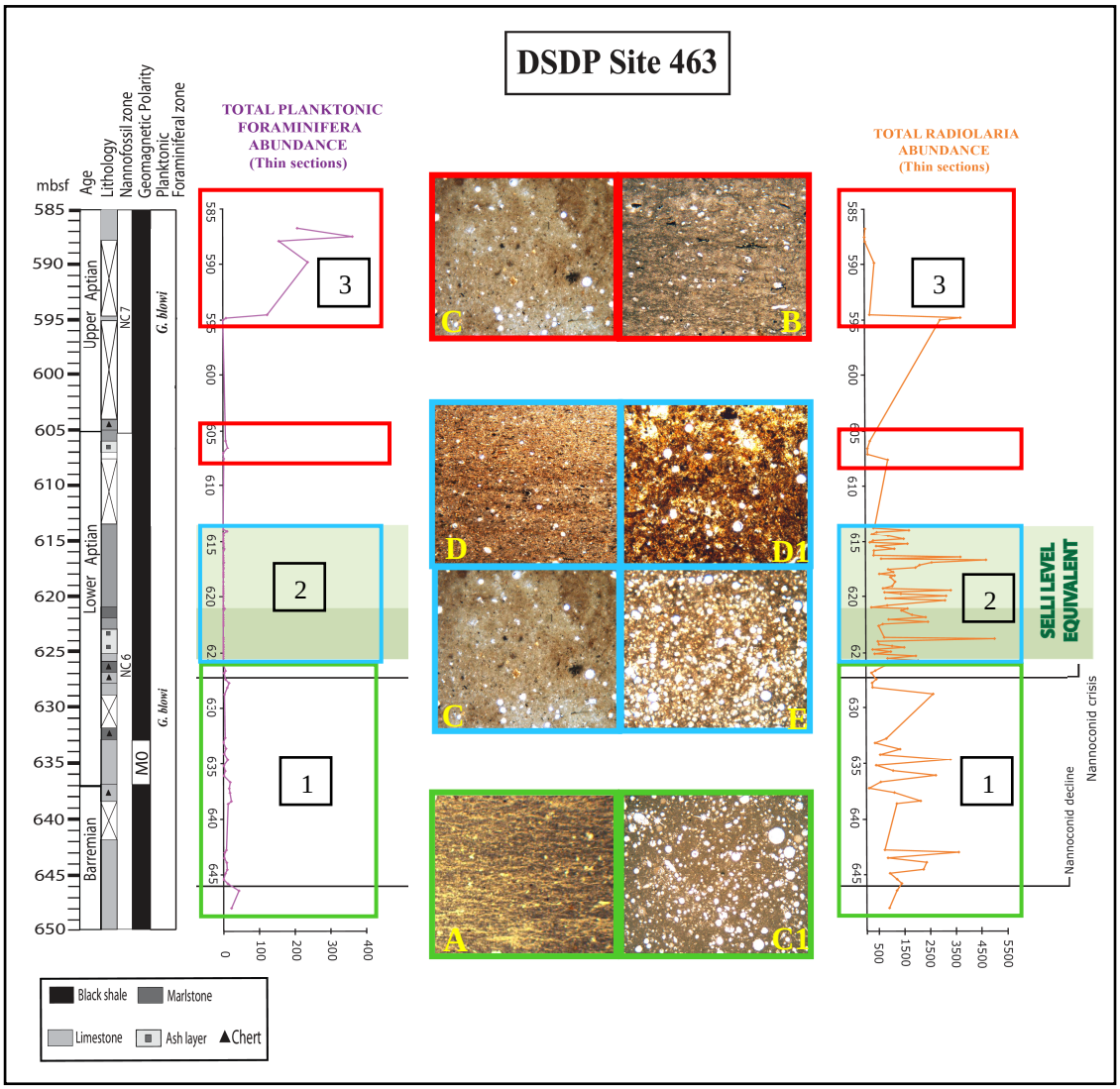

Fig. 6.33. Absolute abundances of planktonic foraminifera and radiolaria and microfacies types at 463 DSDP Site. INTERVAL 1 = low abundance of planktonic foraminifera and moderate-high abundance of radiolaria: microfacies types A and C1 (mudstone and wackestone); INTERVAL 2 = very low/null abundance of foraminifera and low-very high abundance of radiolaria: microfacies types C, D, D1, E (wackestone and packstone); INTERVAL 3 = high abundance of foraminifera and low-moderate abundance of radiolaria: microfacies types B and C (mudstone and wackestone). Nannofossil biostratigraphy is from Erba (1994). Foraminiferal biostratigraphy is from this study. Magnetostratigraphy is from Tarduno *et al*. (1989).

6.2.5 Planktonic foraminiferal morphometric analyses

Fourteen species belonging to four different genera (*Hedbergella*, *Gubkinella*, *Gorbachikella* and *Globigerinelloides*) were investigated for test sizes across the studied interval in 76 samples (washed residues). Being species characterized by a very incomplete record across the entire stratigraphic interval, only a semi-quantitative evaluation of test size variation was obtained and no test size curves were plotted.

Comparing the values before, within and above the Selli Level eq., a slight increase has been observed throughout the stratigraphic section:

1) Below the Selli Level eq., test sizes range from 61 µm to 146 µm;

2) Within it, test sizes range from 89 µm to 116 µm;

3) Above it, sizes range from 70 µm to 210 µm.

Chapter 7
Discussion

7.1 The biological response of planktonic foraminifera during the OAE1a

The Aptian Oceanic Anoxic Event 1a is considered one of the major perturbations in the Earth's history during the last 150 m.y. and is recorded on a global scale. The stratigraphic distribution of planktonic foraminifera in marine sediments and the relative abundance of different morphological groups are either related to their evolution and ecological response to environmental changes or to the sedimentation control such as dissolution, dilution and diagenesis (Luciani *et al*., 2001).

7.1.1 Composition, distribution and species richness of the planktonic foraminiferal assemblages

Coccioni & Premoli Silva (1994) reported the occurrence of Cretaceous planktonic foraminifera starting in the lowermost Valanginian in the Rio Argos succession and suggested a new zonal scheme for the Valanginian-Aptian interval.

After Coccioni & Premoli Silva (1994), other authors (Cobianchi *et al.*, 1999, Luciani *et al.*, 2001, Luciani *et al.*, 2006, Coccioni *et al.*, 2007) have collected data on planktonic foraminiferal assemblages from Lower Cretaceous sedimentary sequences. The most important planktonic foraminiferal Zones correlated to the Lower Cretaceous ammonite zonation are shown in Figure 7.1 (Coccioni *et al.*, 2007).

It is worth mentioning the uncertainty of the stratigraphic position of the base of the *Leupoldina cabri* Zone that is either placed at its FO level or at its acme level. However, the FO of *L. cabri* is well dated, through calibration to magnetostratigraphy, in the

Cismon core (Erba *et al.*, 1999) and in the Gorgo a Cerbara section (Coccioni *et al.*, 2006) at an age of 124.47 Ma and 124.26 Ma, respectively.

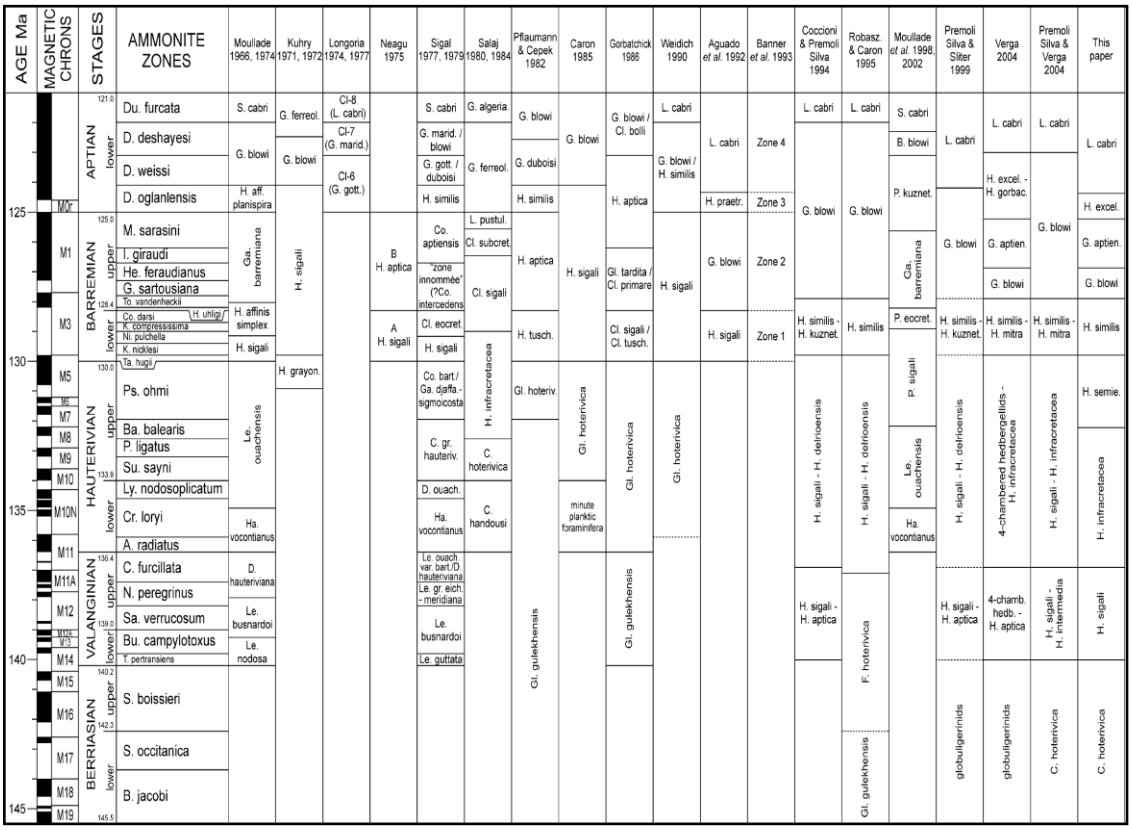

Fig. 7.1. Planktonic foraminifera biozonation according to various authors and plotted against the Lower Cretaceous ammonite zonation by Reboulet *et al*. (2006). Time scale after Gradstein *et al.* (2004). From Coccioni *et al.*, 2007.

The planktonic foraminiferal biological response to the OAE1a palaeoenvironmental perturbations in terms of changes in species richness, composition, abundance, and test size is documented in this work at Cismon core and at DSDP Site 463.

Considerations about the assemblage composition, distribution and species richness of planktonic foraminifera across the OAE1a are especially based, at both sites, on data from washed residues. In fact, the analysis in thin sections is hampered by a certain degree of uncertainty in assigning species names to different cuts (equatorial, oblique, lateral, etc.) of planktonic foraminiferal test. In several thin sections it was a problem to distinguish a planispiral from a trochospiral form when the cuts were not perfectly lateral or equatorial and there were "ghosts" of planktonic foraminifera. The differences in test thickness, morphology of the margin (e.g. forms with single or double keels) and type of wall

texture (e.g. forms with muricae) are important keys that help to discriminate planispiral from trochospiral taxa in the Late Cretaceous assemblages. Unfortunately, Barremian-Aptian taxa do not possess keels and muricae, and no differences in terms of wall thickness were observed to help in discriminate between planispiral and trochospiral taxa.

Therefore, only the absolute abundance data of planktonic foraminifera in thin sections are discussed for both sites.

In the washed residues, planktonic foraminifera have a general poor preservation and are evenly distributed across the studied interval, especially for the DSDP Site 463 where almost all samples are barren of foraminifera. Fortunately, at Cismon core planktonic foraminifera are more common and with a peculiar preservation as siliceous molds in the radiolarian beds.

At Cismon core globigeriniform taxa (genera *Gorbachikella* and *Gubkinella*), pseudo-planispiral with elongate chambers (genus *Leupoldina*) and both trochospiral and planispiral forms with globular (genera *Hedbergella* and *Globigerinelloides*) and elongate chambers (genera *Lilliputianella* and *Globigerinelloides*) were recognized. In Figure 7.2 is shown the percent abundance of these groups across the studied interval.

At DSDP Site 463 only globigeriniform (genera *Gorbachikella* and *Gubkinella*), planispiral and trochospiral taxa with globular chambers (*Globigerinelloides* and *Hedbergella*) were observed. Forms with “clavate” or elongate chambers do not occur in the washed residues, but the possibility that rare to few forms belonging to the genus *Leupoldina* sp. could be present in the thin sections cannot be excluded.

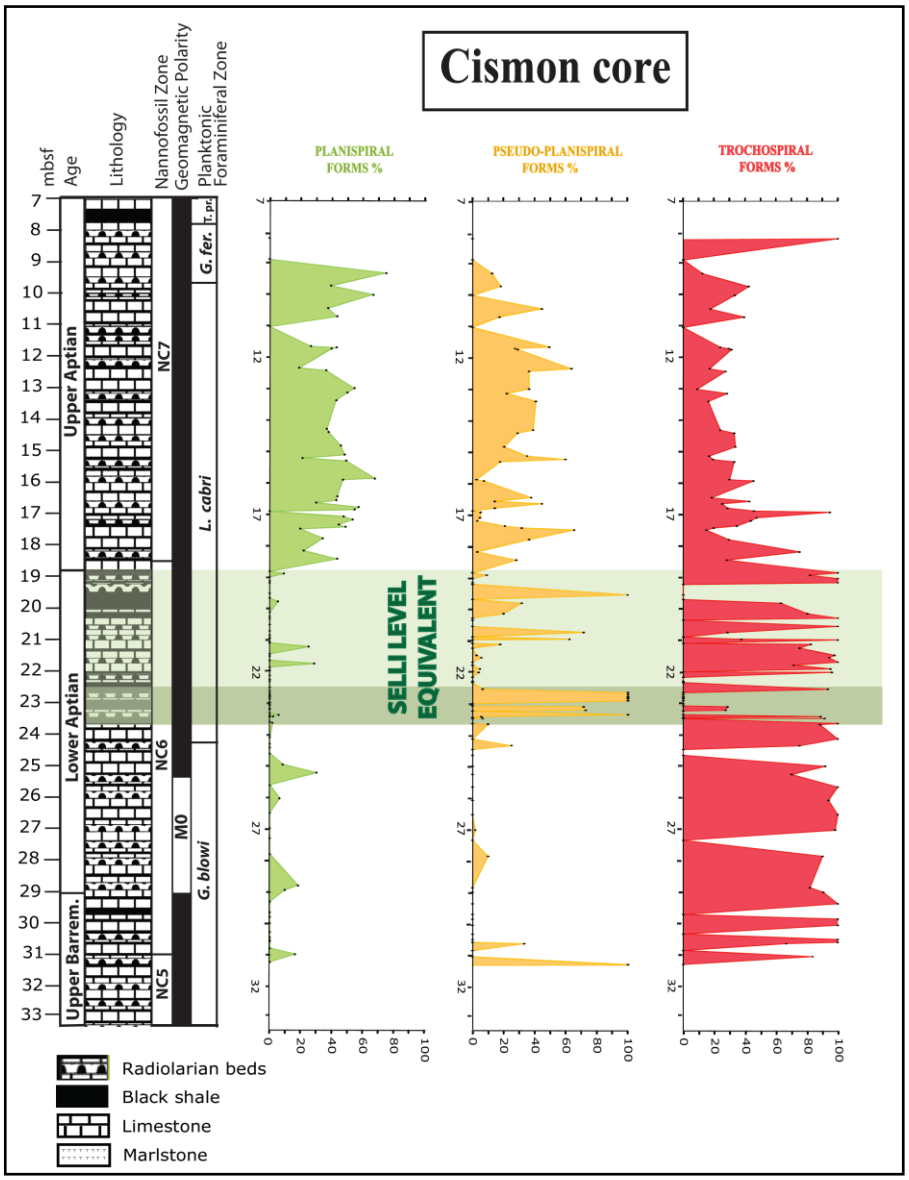

Fig. 7.2. Planktonic foraminiferal composition and percent abundance at Cismon core according to the morphology: planispiral (Genus *Globigerinelloides* with globular and clavate chambers = green), pseudo-planispiral (Genus *Leupoldina* = yellow) and trochospiral (Genera *Hedbergella*, *Lilliputianella*, *Gorbachikella* and *Gubkinella* = red) forms. Nannofossil biostratigraphy is from Erba *et al.* (1999). Foraminiferal biostratigraphy is from Erba *et al.* (1999) and this study. Magnetostratigraphy is from Channell *et al.* (2000).

The distribution of the planktonic foraminiferal assemblages is here discussed by morphological groups:

a) At both sites trochospiral forms with globular chambers (Hedbergellids) are the most common group across the studied interval and show the highest continuous record, when compared to the other groups. At Cismon core, the trochospirals were observed from the Upper Barremian (*Globigerinelloides blowi* Zone) until the top of the studied interval

(Upper Aptian, *Globigerinelloides algerianus* Zone). No variation in species composition across the studied interval has been observed: species recognized from the base of the section are also present until the top of the interval (e.g. *Hedbergella praetrocoidea*, *H. infracretacea* and *H. sigali*). Exceptions are the species *H. luterbacheri*, *H. laculata*, *H. gorbachikae* and *H. primare* that occur in very few samples, mainly above the Selli Level, where Hedbergellids are more common and abundant. In general, Hedbergellids shows a slight increase in test size from the base to the top of the interval; in fact, the values displayed by the shell size are comparable below the Selli Level eq. (from 70 µm to 137 µm) and within it (from 68 µm to 125 µm), then they become slightly higher above it (from 84 µm to 236 µm).

Moreover, trochospiral forms with clavate chambers (Lilliputianellids) are also recognized at this site from the *Globigerinelloides blowi* Zone to the *Globigerinelloides algerianus* Zone. Below and within the Selli Level eq., this group is very rare and represented principally by *Lilliputianella globulifera*, *Lilliputianella similis* and *Lilliputianella labocaensis*, while above it (from 18.43 m, RAD 37 upward) new clavate morphotypes do occur (*Lilliputianella roblesae*, *Lilliputianella maslakovae* and *Lilliputianella kuhryi*) and the group become more common.

Coccioni *et al.* (2004, 2006) record the first occurrence of Lilliputianellids (*Lilliputianella semielongata* and *Lilliputianella roblesae*) in the Upper Hauterivian, predating the onset of the Faraoni Event and its equivalent, at Rio Argos and in other localities of the Mediterranean Tethys (Fig. 7.3).

The shell sizes of the Lilliputianellids range from 83 µm to 123 µm below the Selli Level eq., from 104 µm to 158 µm within it (even if data are very few) and from 96 µm to 232 µm above it. The range of size variation is similar to the Hedbergellid group.

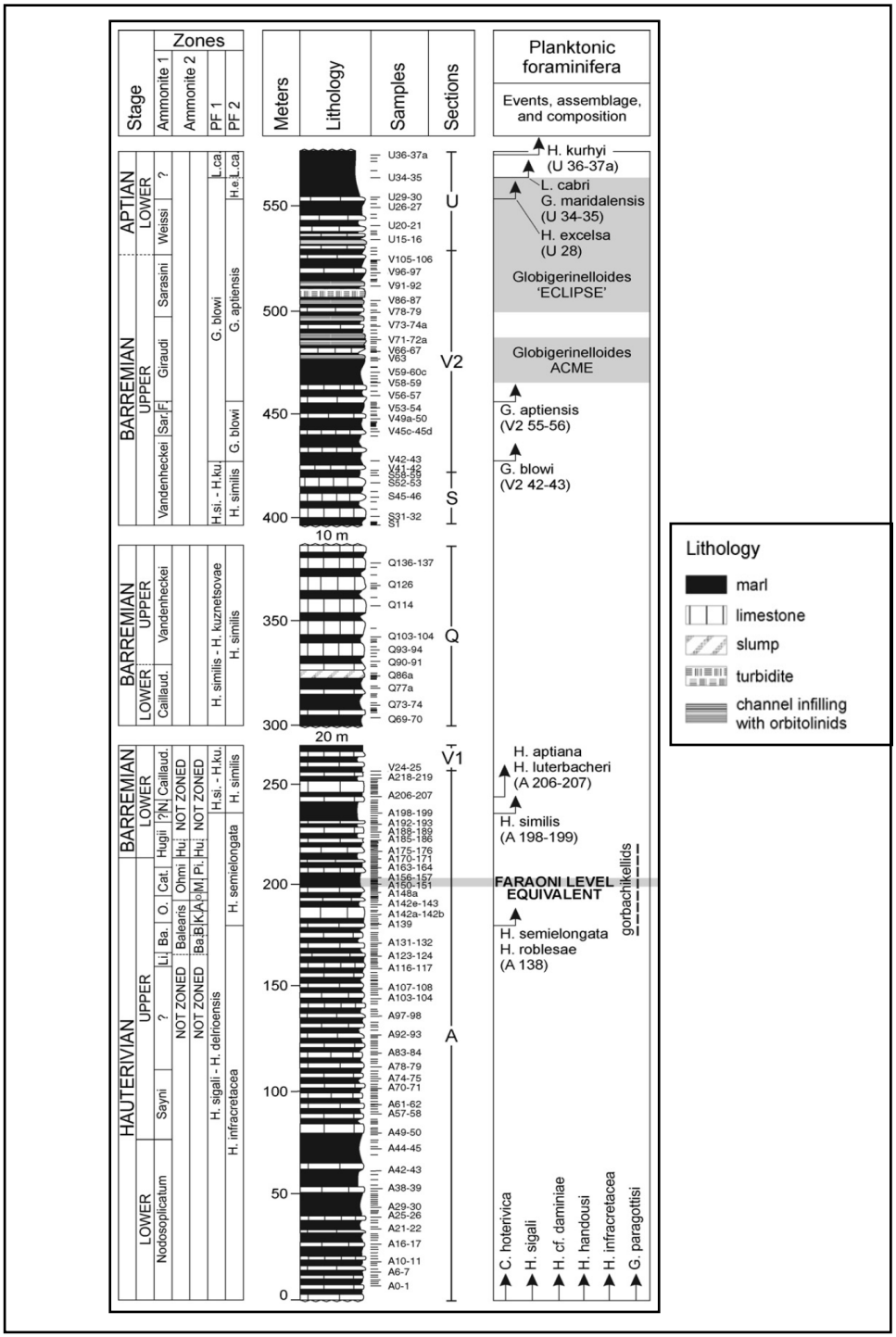

Fig. 7.3. Lithostratigraphic log with ammonite and planktonic foraminiferal zonations of sections A, V1, Q, S, V2, and U (lower Hauterivian–lower Aptian) plotted against the planktonic foraminiferal events, assemblages and composition at Rio Argos (modified after Coccioni & Premoli Silva, 1994 and Coccioni *et al*., 2004, 2006). Sections A, V1, S, and the lower part of Section V2 = Miravetes Formation; the upper part of Section V2 (from sample V2 63) and Section U = Argos Formation.

Ammonite zones: (1) Hoedemaeker, 2002; (2) Company *et al*., 2003a, 2003b. Planktonic foraminiferal (PF) zones: (1) Coccioni & Premoli Silva, 1994; (2) Coccioni *et al*., 2004, and Coccioni *et al*., 2007. Figure is modified after Coccioni *et al.*, 2007.

At DSDP Site 463 only trochospiral taxa with globular chambers (Hedbergellids) occur: they are, in general, rare and show a very discontinuous range. Only very rare specimens were recognized below and above the Selli Level equivalent (e. g. *Hedbergella praetrocoidea* and *Hedbergella infracretacea*) from the Upper Barremian (*Globigerinelloides blowi* Zone) until the Upper Aptian. Moreover, besides the presence of one specimen of *Globigerinelloides* cf. *blowi* (sample 473-73-3, 6-7 cm), the other zonal marker species were not recognized, so that planktonic foraminiferal Zones were not identified. For this reason, the comparison between the two studied sites, in terms of absolute abundances (see Chapter 7.1.2), is based on the $\delta^{13}C$ record (data from Erba *et al.*, 1999 and Méhay *et al.*, 2009 for Cismon core; data from Ando *et al*., 2008 and Bottini *et al*., 2012 for the DSDP Site 463).

The values displayed by the shell size are enough comparable below the Selli Level eq. (from 61 µm to 146 µm) and within it (from 89 µm to 116 µm), and become higher above it (from 70 µm to 210 µm).

b) Another important group that occurs in the studied interval is represented by Leupoldinids, pesudo-planispiral taxa with very elongate chambers and ampullae. The bulbose ampullae, appearing as small additional clavate chambers, considerably increase the surface/volume ratio of Leupoldinid tests. In particular, is possible that the branching ampullae, making better the contact with the surrounding water mass, improved buoyancy and may have been a better adaptation to flotation (Coccioni *et al*., 2004).

At Cismon core Leupoldinids are present below, within and especially above the Selli Level, where they are a common component of the assemblages (from RAD 37, 18.43 m upward). Data on the distribution and composition of this group acquired in this study are integrated with those by Verga & Premoli Silva (2002). The lowest occurrence of Leupoldinids with the FO of *Leupoldina pustulans pustulans* was observed in the Lower Barremian (Coccioni & Premoli Silva, 1994).

At DSDP Site 463 the Leupoldinid group has not been recognized in the washed residues but forms with “clavate” or elongate chambers belonging to the genus *Leupoldina* sp. could likely be present in the thin sections.

c) Planispiral taxa at Cismon core are represented by forms with clavate and globular chambers. The latter have a very discontinuous range below and within the Selli Level eq., while they become very abundant and common (e.g. *Globigerinelloides blowi* and *Globigerinelloides paragottisi*) from the first sample above it (RAD 37,18.43 m upward).

Planispiral taxa with clavate chambers occur from this sample upward (*Globigerinelloides blowi lobatus, Globigerinelloides clavatus, Globigerinelloides elongatus*), except for *Globigerinelloides sigali* that is present till the base of the Selli Level eq. (23.66 m).

The values displayed by the shell size are enough comparable below the Selli Level eq. (from 78 µm to 217 µm) and within it (from 85 µm to 298 µm) and become higher above it (from 82 µm to 427 µm).

At DSDP Site 463, only five planispiral specimens, all with globular chambers, were recognized in the washed residues across the entire interval. The values displayed by the shell size are from 71 µm to 136 µm below the Selli Level eq. and from 113 µm to 117 µm above it.

In general, the species richness increase upward through the Cismon core in agreement with the general trend described in previous studies (Coccioni *et al*., 1992; Coccioni & Premoli Silva, 1994; Premoli Silva & Sliter, 1997, 1999), that reported an increase in planktonic foraminiferal diversity in the early Valanginian through the Aptian.

At DSDP Site 463 no evident changes in terms of species richness are observed and data are too few to make reliable considerations.

Shell size measurements show a general increase from the base to the top of the studied interval at both sites (higher at Cismon core), probably due to an increase of calcification efficiency. However, the group with the highest range of variation is represented by Globigerinelloidids.

. 7.1.2 Comparison between planktonic foraminiferal and nannofossil absolute abundances

During the Early Cretaceous marine biota were strongly affected by wide global changes in the ocean-atmosphere system. In surface waters, changes in temperature, nutrients and the increase of pCO_2 and biolimiting metals, must have influenced the composition of biogenic sediments (Erba & Tremolada, 2004).

The comparison between the two studied sites, in terms of absolute abundances of planktonic foraminifera, is based on data of the $\delta^{13}C$ record, characterized by 8 chemostratigraphic segments (C1 to C8) defined by Menegatti *et al*. (1998), in the uppermost Barremian-Aptian interval.

At Cismon core, across the magnetic chron M0, the $\delta^{13}C$ profile (Fig. 7.4 a) shows a gentle increase of values close to 3‰ (segments C1 and C2), followed by a negative pronounced excursion (C3) at the base of the Selli Level equivalent (values range from ~3 ‰ to 1.5‰). The middle part of the Selli Level eq., displays constant values close to 3 ‰ (C5), followed by a positive excursion that starts from the top of it (from 2.7 ‰ to 3.7‰, C6) and continues above it until maximum values of approximately 5‰ in the uppermost part of the *Leupoldina cabri* Zone (C7) (Erba *et al.*, 1999; Méhay *et al.*, 2009).

At DSDP Site 463 (Fig. 7.4 d), a gentle increase was observed across the base of magnetic chron M0 (from 2.3‰ to 3.3‰, segment C1), followed by an interval with values ranging from 3.2‰ to ~ 2‰ (C2). The base of the Selli Level eq. is characterized by a very pronounced negative excursion of about -8‰ (from ~ 2‰ to -6‰), followed by a dramatic return to the near pre-excursion level by ~ 6‰ (from ~ -6.‰ to -0.43‰) and fluctuations of the values until the top of the Selli Level eq. (from -3‰ to 4‰, C4-C6). Above it, there are several meters of no recovery followed by values characterized first by an increase (from 0.53‰ to 4.8‰, C7), and then by a decrease (from 4.8‰ to ~ 4.3 ‰, C8) (Ando *et al*., 2008; Bottini *et al*., 2012).

At both sites, the interval C3-C6 identifies the Selli Level equivalent.

Considerations and comparison between the total planktonic foraminifera at both sites are made in thin sections, because of the few data in washed residues collected at DSDP Site 463 that do not allow plotting abundance curves.

Subsequently, to understand if there are or not similarities in the biological response of the planktonic foraminifera and other important microfossil group, such as the nannoconids among the calcareous nannofossils, a comparison between the respective abundance curves is made (using the abundance data acquired in thin sections).

In general, changes in abundance of planktonic foraminifera are similar and enough synchronous at two studied sites located in different oceans. In terms of behaviour we can describe the changes considering 3 intervals, as follows (Fig. 7.4, b and e):

1) Below the Selli Level equivalent (prior magnetic chron M0) nannoconids have values close to 1×10^4 specimens mm^{-2} at Cismon core (Fig. 7.4 c) and 2.5 x 10^3 specimens mm^{-2} at DSDP Site 463 (Fig. 7.4 f), then they decrease in abundance at about 1 Ma before the onset of the OAE1a (at 31 m at Cismon core and at about 646 m at DSDP Site 463). This decrease in abundance has been named "nannoconid decline" (Erba, 1994, 2004). In proximity of this biohorizon, planktonic foraminiferal abundances at Cismon core (Fig. 7.4 b) and DSDP Site 463 (Fig. 7.4 e) slightly decrease. Subsequently, nannoconids increase and then decrease again in abundance until to culminate in the "nannoconid crisis" (at 23.96 m at Cismon core and ~ 627m at DSDP Site 463; Erba, 1994; Erba *et al*., 1999). This second biohorizon has been documented worldwide below the Selli Level, in particular in the Tethyan realm, Boreal realm, and Atlantic and Pacific oceans (Bralower *et al*. 1994; Erba, 1994; Aguado *et al*. 1999; Bralower *et al*. 1999; Cobianchi *et al*., 1999; Erba *et al*. 1999; Habermann & Mutterlose, 1999; Larson & Erba, 1999; Premoli Silva *et al*. 1999).

In the stratigraphic interval above the decline of the nannoconids, the planktonic foraminifera show low amplitude fluctuations in abundances, followed by an abrupt decrease in abundances (much wider in the Cismon core) immediately below the nannoconid crisis level.

Approximately 25 to 30 thousand years (ky) after their crisis and just before the first OAE1a black shale, nannofossil assemblages show a relative increase in abundance of *Biscutum constans*, *Zeugrhabdotus erectus*, and *Discorhabdus Rotatorius* (represented by dwarfed specimens) and diversity, while planktonic foraminifera show only an increase in abundance (at Cismon core).

2) Within the Selli Level eq., planktonic foraminifera show moderate/high abundances at the onset of it, then the number of specimens become very low/null at Cismon core. At DSDP Site 463 planktonic foraminifera are always very low/null. More precisely, the

decrease in abundance at DSDP Site 463 starts a couple of meters before the onset of the OAE1a (627.37 m), while it starts at about ten centimetres after the onset of the event (23.54 m) in the Cismon core.

Nannoconid values reach a minimum within segment C3 of the carbon-isotope curve (C3), and are considered virtually absent. At Cismon core nannoconids resume and remain enough stable in the middle part of the Selli Level eq, while at DSDP Site 463 the interval between 624.24 m and 607.40 m (comprised within the Selli Level eq.) is totally devoid of nannoconids. In fact, they start to become abundant only several meters above the Selli Level equivalent.

Planktonic foraminiferal abundances remain very low/null for the entire interval across the OAE1a at both sites. However, it is important to underline that no extinctions within nannoconids or nannofossils and planktonic foraminifera have been observed in the OAE1a interval (Erba, 1994; Erba *et al*., 1999; Premoli Silva *et al*., 1999; Erba, 2004; Erba *et al*. 2010; Bottini *et al*., 2015).

3) Above the Selli Level eq., planktonic foraminiferal abundances are moderate/high at Cismon core from the first sample upward, whilst at DSDP Site 463 they are very low/null until to moderate at the top of the interval. Moreover, at Cismon core from the first sample (18.72 m) just above the Selli Level eq., a marked change in terms of abundance and diversity was documented.

In this time-interval nannoconids are characterized by moderate/high values at both sites, but they never become as abundant as before OAE1a (Erba, 2004). On the contrary, planktonic foraminifera reach values much higher than those recorded before the OAE1a; in particular, comparing abundance values before and after the Selli Level eq., they are almost two times higher in the Cismon core and eight times higher at DSDP Site 463.

The strong decrease of planktonic foraminifera during the early phase of OAE 1a could have the same significance documented for nannoconids. Planktonic foraminifera did not experience extinction and their virtual absence could be considered as the result of widespread meso- to eutrophic conditions, combined with excess CO_2 in the ocean - atmosphere system (e.g. Coccioni *et al*., 1992; Bralower *et al*., 1994; Erba, 1994; Premoli Silva *et al*., 1999; Erba, 2004; Erba & Tremolada, 2004; Erba *et al*., 2010).

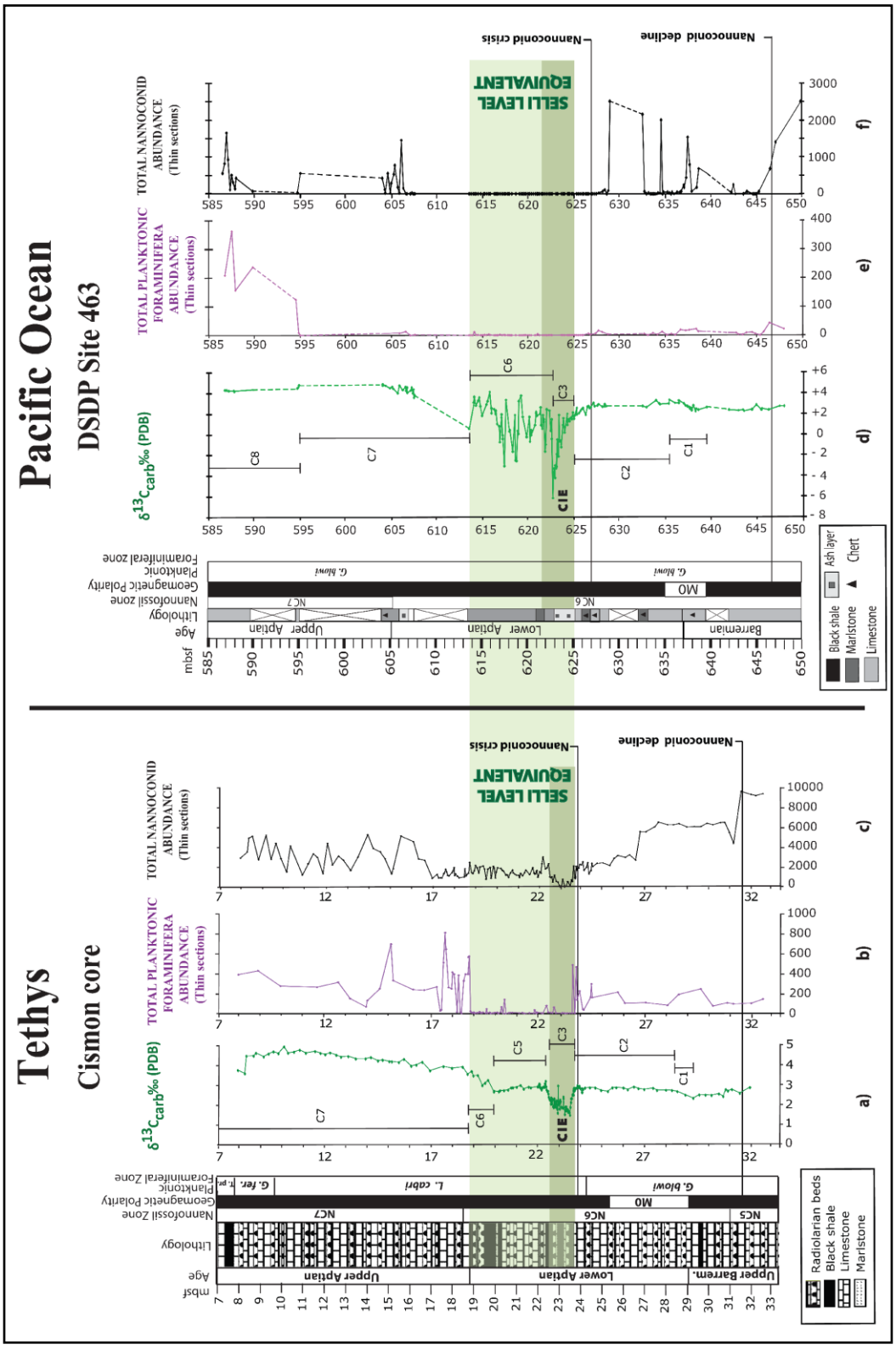

Fig. **7.4.** Planktonic foraminifera (a and e) and nannoconids (c and f) abundance data obtained in thin sections at Cismon core and DSDP Site 463. Abundance curves are compared with the $\delta^{13}C$ record (a and d). Abundance data are plotted with different scales to emphasize the data. Nannoconid data are from Bottini *et al.*, 2015. The $\delta^{13}C$ record of the Cismon core is according to Erba *et al.* (1999) and Méhay *et al.* (2009), while for the DSDP Site 463 data are from Ando *et al.* (2008) and Bottini *et al.* (2012).

The abundance values of the planispiral, pseudo-planispiral and trochospiral planktonic foraminifera are compared with the nannoconids in order to understand if there is a group of planktonic foraminifera displaying a life strategy similar to the nannoconids (Fig. 7.5). It is important to underline that at Cismon core, the abundances data of the Leupoldinids are collected from the washed residues (Fig. 7.5 b) as the data in thin sections could likely underestimate the real abundance of this group of foraminifera because of the high difficulty in identifying them in thin sections. All curves are compared with the Nannofossil Nutrient Index (NI) (Bottini *et al*., 2015) to understand if there are connections between abundances and water fertility.

Previous studies claim that nannoconids were adapted to oligotrophic conditions and specific to the lower photic zone, associated with a deep nutricline (Erba, 1994, 2004). Accordingly, Bottini *et al.* (2015) compared the nannoconids record with the nannofossil NI, to document the similarities between Cismon core and DSDP Site 463, as follows:

a) the earliest Aptian below the Selli Level eq. is characterized by low to intermediate NI values (Fig. 7.5, e and i) which suggest oligotrophic conditions, in fact, nannoconids show moderate/high abundances (Fig. 7.5, d and h). In particular, the relationship between the two peaks in the NI detected at the levels of the "nannoconid decline" (~1Ma before OAE 1a) and the "nannoconid crisis" is in agreement with the interpretation of nannoconids as oligotrophic taxa. In this time-interval planispiral (Fig. 7.5, a and f) and pseudo-planispiral (Fig. 7.5, b) planktonic foraminifera show low abundances too, while trochospirals are low (Fig. 7.5, g) and moderate (Fig. 7.5, c) in total abundance;

b) the onset of OAE1a was characterized by an increase in fertility (meso- to eutrophic conditions), which reached a maximum in the correspondence of the negative carbon-isotope excursion (segment C3, see Fig. 7.4) where nannoconids, planispiral and trochospiral taxa show a strong decrease in abundance at both sites. Leupoldinids are the principal foraminifera present at the base of the negative excursion and show a slight increase in abundance that was named acme of leupoldinids by Premoli Silva *et al*. (1999). Subsequently, NI decreases already within the Selli Level eq. and nannoconids resume from the middle part of it but only at Cismon core. Nannoconids from DSDP Site 463 and planktonic foraminifera of both sites, do not resume in this stratigraphic interval but start to become abundant only after the end of the OAE1a.

d) fertility starts to increase again just above the Selli Level equivalent (which suggest mesotrophic conditions) in agreement with the increase in abundance of nannoconids and planktonic foraminifera.

It is worth mentioning that at Cismon core we observe a discrepancy of the abundances values counted in thin section and in the washed residues of the planispiral taxa in the interval above the Selli Level equivalent: in the washed residues the planipirals are slightly more common and abundant than the trochospiral forms, while in thin sections they show an opposite trend. The reasons for such discrepancy could be various, for instance:

1) first of all, the samples studied for thin sections are not at the same stratigraphic levels of the washed residues samples;

2) the difficulty to discriminate between planispiral and trochospiral form in thin section could have underestimated or overestimated the real abundance of each group but not the total abundance of planktonic foraminifera, in fact the results of the two methods (counts in thin sections and washed residues) are similar and comparable;

3) the amount of material studied for thin sections is different from that analysed for the washed residues.

Anyway, besides the above-described discrepancy, the planispiral group have values in washed residues similar to the Leupoldinids, and always shows lower values within and below the Selli Level equivalent (both in thin sections and washed residues) when compared to the trochospiral group.

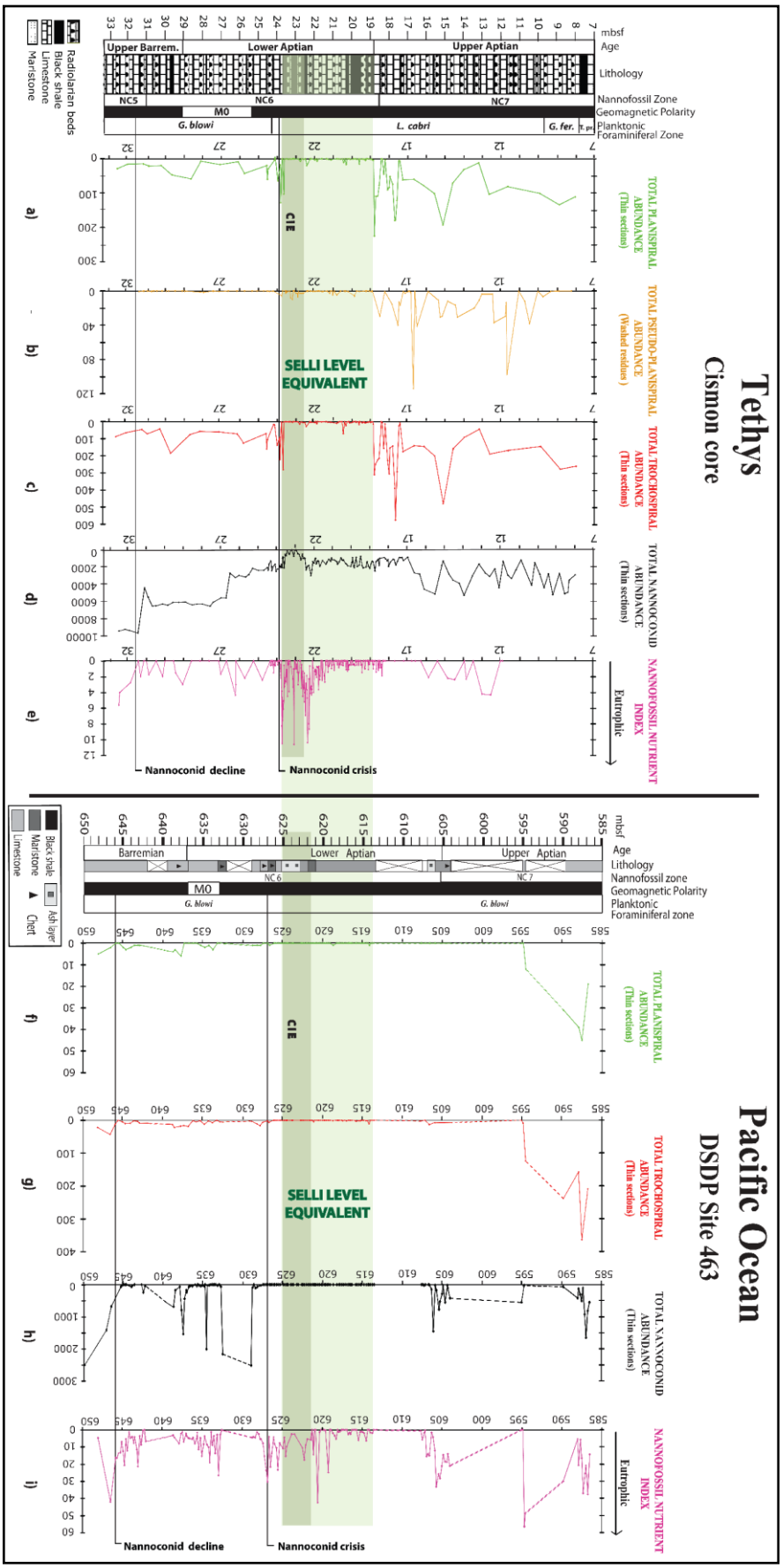

Fig. 7.5. Comparison between the Cismon core and DSDP Site 463. Total number of planispiral, pseudo-planispiral and trochospiral fpraminifera (a, b, c, f, and g). The total number of nannoconids (d and h) and Nannofossil Nutrient Index (NI) (e and i) are according to Bottini *et al.* (2015). Abundance data are plotted with different scales to emphasize the data.

7.1.3 Ecological/Paleoenvironmental inferences

The data collected in this study on the distribution, composition, species richness and abundances of planktonic foraminifera at Cismon core and DSDP Site 463, allow to make the following ecological/paleoenvironmental observations:

1) the genus *Hedbergella* is the most common component of the foraminiferal fauna across the studied interval at both sites. Being the Aptian interval characterized by strong changes in terms of temperature, salinity, nutrient and oxygen, Hedbergellids may have been able to change habitats in the water column and tolerate wide environmental variations. According to the ecological models developed so far, planktonic foraminifera populations composed by small-sized and thin-walled forms, are generally interpreted to be opportunistic, cosmopolitan and adapted to meso-eutrophic environments (Fig. 7.6) (Hart & Bailey, 1979; Leckie, 1987; Premoli Silva & Sliter, 1994, 1999; Hart, 1999; Luciani *et al*., 2001). In fact, *Hedbergella* proliferated in both open marine and epicontinental settings and in upwelling regions. It was present at different latitudes, dominating high-latitude assemblages and was living in a wide range of temperature-related habitats (Douglas & Savin, 1978; Corfield *et. al*., 1990; Norris & Wilson, 1998; Premoli Silva & Sliter, 1999; Petrizzo *et al*., 2008). For this reason, we can consider this group as R-mode strategist surface-dwellers (Caron & Homewood, 1983; Leckie, 1987, 1989; Premoli Silva *et al*., 1989; Coccioni *et al*., 1992; Premoli Silva & Sliter, 1994, 1999; Hart, 1999, among many others).

2) the genus *Globigerinelloides* with globular chambers is low to rare/null respectively below and within the Selli Level eq. at Cismon core and at DSDP Site 463. Above it, at Cismon core it becomes very abundant constituting a common component of the foraminiferal assemblages, while at DSDP Site 463 this genus is very rare in washed residues and more common in thin sections.

In particular, a crisis of this group, called the "*Globigerinelloides* eclipse", has been observed in the upper part of the *Globigerinelloides blowi* Zone in Spain (Coccioni & Premoli Silva, 1994), in the Umbria-Marche region (Coccioni *et al*., 1992), and in the Gargano Promontory (Cobianchi *et al*., 1997; Cobianchi *et al*., 1999). At Cismon core, even if Globigerinelloidids are very scarce/absent in the stratigraphic interval close to the Selli Level eq., a real *Globigerinelloides* eclipse event seems to be absent, while it is probably present and coinciding with the interval of the Selli Level eq., at DSDP Site 463.

This interval of crisis coincides with their temporary absence and has been interpreted as the biotic response to the critical conditions related to the Selli Event, possibly associated with a high-fertility episode. Moreover, the total abundances of this group, generally lower than trochospirals, seem to indicate the possibility that Globigerinelloidids are relatively specialized, possibly meso-oligotrophic forms (in between the two extremes, K-mode and R-mode strategist), probably intolerant to extreme eutrophic conditions, low oxygen content in the water and susceptible to dissolution during the late Early Aptian interval (e.g. Coccioni *et al*., 1992; Luciani *et al.*, 2001) (Fig. 7.6). Likely, *Globigerinelloides* is the group, among the planktonic foraminifera, with the nearest behaviour to nannoconids, in terms of trophic regime.

3) As regards the planispiral, pseudo-planispiral and trochospiral taxa with clavate forms (genera *Globigerinelloides*, *Leupoldina* and *Lilliputianella*), they were observed at Cismon core. The genus *Leupoldina* shows a more consistent stratigraphic distribution below and within the Selli Level eq., when compared to the other two genera. However, the three genera mentioned above become a common component of the planktonic foraminiferal assemblages just above the Selli Level eq. (from 18.43 m upward).

Previous studies (Coccioni & Premoli Silva, 1994) reported that starting from the Upper Hauterivian, planktonic foraminifera with clavate and radially elongate chambers became a consistent component of the foraminiferal assemblages at different stratigraphic levels in the lower Cretaceous, especially in coincidence or near the deposition of organic-rich layers (OAEs) (Magniez-Jannin, 1998). In particular, the elongation of the chambers has been interpreted as an adaptive response to low-oxygen conditions (Premoli Silva & Sliter, 1994; Boudagher-Fadel *et al*., 1997; Magniez-Jannin, 1998; Premoli Silva *et al.*, 1999). Moreover, at Cismon core at the base of the Selli Level eq. (from 23.35 m to 22.64 m), where meso- eutrophic conditions dominated, an acme of Leupoldinids (Premoli Silva *et al.*, 1999) is documented consisting in their predominance respect to the other taxa that are instead totally absent (except for 3-4 specimens of *Gubkinella graysonensis* in two samples at 23.20 m and 23.10 m). The Leupoldinids probably inhabited mesotrophic to slightly eutrophic water masses (Fig. 7.6) characterized by low oxygen content.

The increase of the Leupoldinids and of other elongate chambered forms (e.g. *Lilliputianella globulifera*, *L. similis* and *Globigerinelloides sigali*) recorded near the Early Aptian Selli Level equivalent from the Southern Alps (Premoli Silva *et al.*, 1999;

This study) and from Sicily (Bellanca *et al.*, 2002) resembles the increase of Schackoinids observed close to the Bonarelli Event (OAE2). Moreover, also the morphological similarity with the Eocene Hantkeninids, known to inhabit near oxygen-depleted sea surface waters (Boersma *et al.*, 1987; Coxall *et al.*, 2000, 2002), supports the interpretation that the paleoecological significance of these three groups are similar, because all of them prefer oxygen-depleted waters (Boudagher-Fadel *et al.*, 1997; Magniez-Jannin, 1998; Premoli Silva *et al.*, 1999).

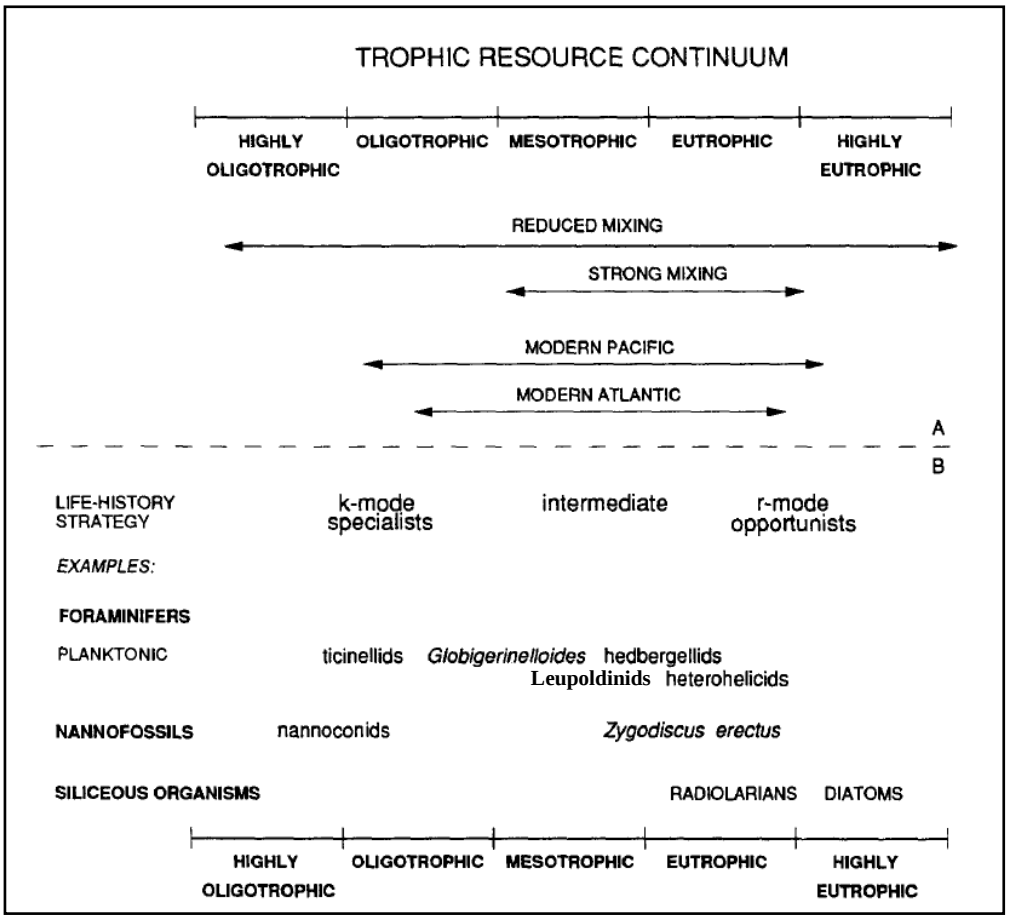

Fig. 7.6. A) Scheme of the oceanic surface-water trophic-resource continuum (TRC), comparing the modern Atlantic and Pacific with the inferred B) Lower Cretaceous life-history strategies and trophic resources. Modified from Coccioni *et al.*, 1992.

7.1.4 Final remarks and explanations

In agreement with the previous studies by Coccioni *et al.* (1992), Erba (1994, 2004), Premoli Silva *et al*. (1999), Luciani *et al.* (2001, 2006) and Bottini *et al.* (2015), the available data allow to interpret the Selli Level as a dramatic event of extremely high fertility during a period when meso-oligotrophic conditions prevailed. The maximum eutrophy, preceded and followed by transitional conditions, is indicated by the C organic-rich black shales of the OAE1a and by the presence of abundant radiolarians, which totally replaced the calcareous plankton (Coccioni *et al.*, 1992).

At both sites, planktonic foraminifera are unevenly distributed across the studied interval and show a decrease (stronger at Cismon core) at the onset of the OAE1a, followed by a recovery due to an increase of their abundances and diversity just above the Selli Level equivalent.

In the pre-OAE1a interval, the lower abundances and diversity of planktonic foraminifera respect those documented above the Selli Level eq. seem to contradict the interpretation of a dominant meso-oligotrophic environment and could be justified in two ways:

1) being the base of the studied sections near to the onset of the OAE1a, it is possible that abundance values already reflect the suffering of planktonic foraminifera, maybe started before the Upper Barremian. To verify this hypothesis it would be necessary to implement the sampling resolution below the Selli Level equivalent and study other samples from lower stratigraphic intervals;

2) a second possibility is that planktonic foraminifera start to suffer just in the interval below the Selli Level eq., as they show slight decrease and increase from layer to layer until they abruptly decline at the onset of it. This hypothesis is supported by previous works (Coccioni *et al.*, 1992; Coccioni & Premoli Silva, 1994) that document similar or even lower abundances of planktonic foraminifera from Lower Barremian and Valanginian sections than those documented in this work. Probably, the evolution and diversification of planktonic foraminifera was interrupted during the OAE1a by the very unstable conditions in the upper water column that could have disrupted the thermocline conditions (Premoli Silva & Sliter, 1999). The end of global anoxia, due to the cessation of volcanism and to a pronounced cooling (above the OAE1a, from the segment C7 of the $\delta^{13}C$ profile, Fig. 7.4), and the more suitable and much less stressed environmental

conditions could explain the high abundance and diversification of the 3 groups of planktonic foraminifera (planispirals, pseudo-planispirals and trochospirals). In particular, abundances range from very low to very high values, probably due to the ecological competition among them, where planispirals resulted to be the most efficient and successful competitors compared to the pseudo-planispirals and trochospirals. Moreover, planispiral taxa show the highest test size variations, a feature that is often directly related to reproductive potential (Hallock, 1985; Premoli Silva & Sliter, 1999).

In terms of diversification, the number of species become double from the first sample above the OAE1a upward (Fig. 7.7), mainly due to the appearance of new taxa having globular (*Hedbergella gorbachikae*, *H. kuznetsovae*, *H. luterbacheri*, *H. primare* and *Globigerinelloides primitivus*) and elongate or clavate chambers (*Leupoldina pustulans hexacamerata*, *Leupoldina pustulans quinquecamerata*, *Leupoldina reicheli*, *Lilliputianella kurhyi*, *Lilliputianella maslakovae*, *Lilliputianella roblease*, *Globigerinelloides blowi lobatus*, *Globigerinelloides clavatus* and *Globigerinelloides elongatus*).

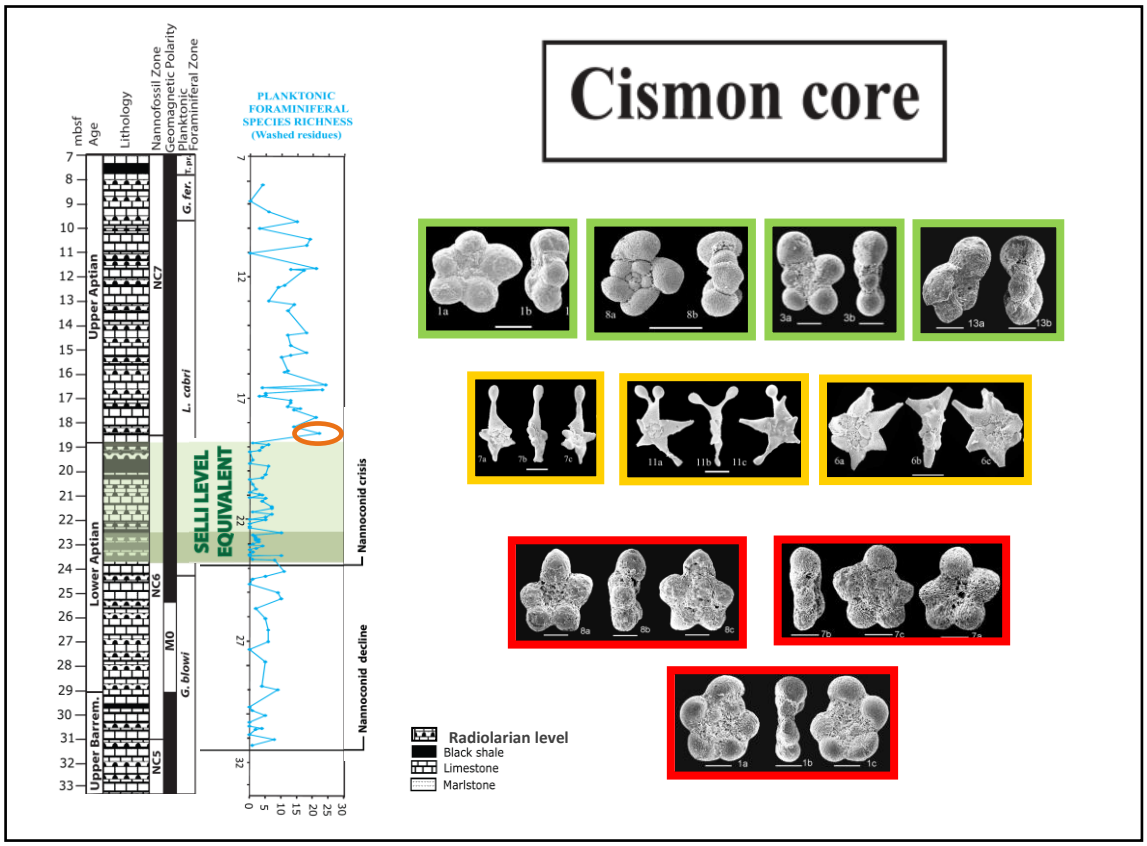

Fig. 7.7. Planktonic foraminiferal species richness at Cismon core. The orange circle in the graph represents the sample in which new globular and clavate species consistently occur upward section. Hedbergellids and Lilliputianellids are shown in red, Leupoldinids in yellow and Globigerinelloidids in green.

Remarkable is the high abundance of the Leupoldinid group and the appearance of new clavate and elongate morphotypes (both interpreted as taxa adapted to low oxygen waters) above the Selli Level eq., when the global anoxia was coming to an end and the mid-Aptian was characterized by high surface-water fertility and progressively decreasing temperatures, probably resulting from intense continental weathering drawing down pCO_2 (Bottini *et al.*, 2015).

This observation leads to an important question: Why the clavate (e.g. *Lilliputianella similis* and *Globigerinelloides sigali*) or elongate (e.g. *Leupoldina reicheli*) morphotypes are more abundant above the Selli Level eq. than below and/or within it?

Answering to this question is challenging as little is known about the ecology of digitate species because of their scarcity and patchy distribution in the geological record. Coxall *et al.* (2007) compared $\delta^{18}O$ and $\delta^{13}C$ values of digitate planktonic foraminifera species with those of normally-shaped planktonic and benthic taxa from the Cenomanian to the Holocene in seven different paleogeographic localities. Cretaceous, Eocene, Miocene, Pleistocene, and Holocene digitate forms consistently register the highest or close to the highest $\delta^{18}O$ values (implying the coolest calcification temperatures) and usually the lowest $\delta^{13}C$ of all planktonic foraminifera (Fig. 7.8).

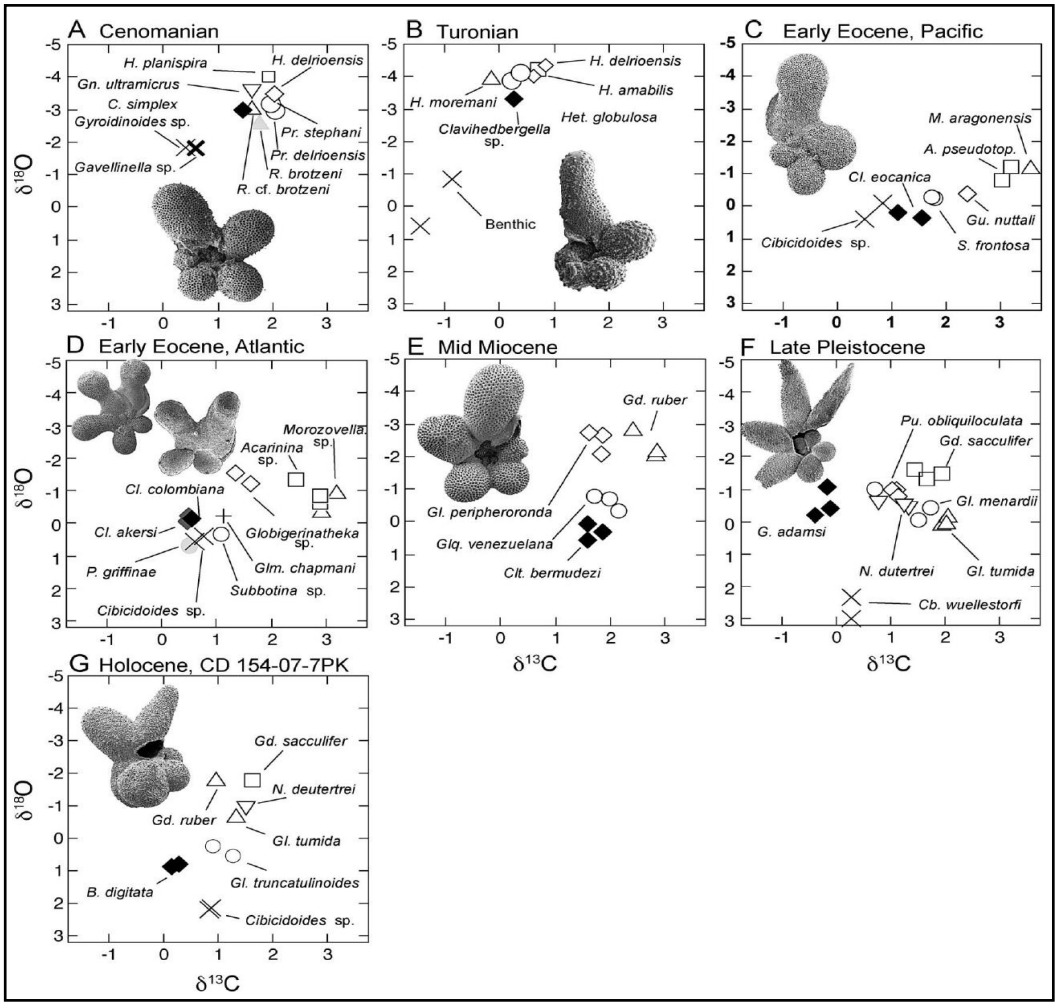

Fig. 7.8. Multispecies stable isotope arrays from seven sites showing the relative isotopic depth ranking of digitate homeomorphs (black and gray diamonds) compared with co-occurring planktonic and benthic species (where possible). **A**, DSDP Site 137-12-5, 4–6 cm. **B**, DSDP 144A-6R-1, 141–142.5 cm. **C**, ODP 865C-8H-3, 70–110 cm. **D**, Kane-9 Core-42, 470 cm. **E**. ODP 872C-9H-3, 95–97 cm. **F**, Box ERDC-92-5, 22–23 cm.
Generic abbreviations: *A.= Acarinina*; * *B.= Beella*; *C. = Clavihedbergella*; *Cb.= Cibicidoides*; *Cl. = Clavigerinella*; *Clt. = Clavatorella*; *G. = Globigerinella*; *Gd.= Globigerinoides*; * *Gl. = Globorotalia*; *Glm. = Globanomalina*; *Glq.= Globoquadrina*; *Gn. = Globigerinelloides*; *Gu. = Guembelitrioides*; *H. = Hedbergella*; * *Het. = Heterohelix*; * *M.= Morozovella*; * *N. = Neogloboquadrina*; *P. = Parasubbutina*; *Pr. = Praeglobotruncana*; *Pu. = Pulleniatina*; *R.= Rotalipora*; *S. = Subbotina*. *Inferred or known surface dwellers (Wilson *et al.* 2002; Boersma *et al*. 1987; Pearson, 1998; Berger *et al*. 1978; Hemleben *et al*. 1989). From Coxall *et al*., 2007.

These data suggest that all the investigated digitate species calcified their shells in a relatively cool and deepwater masses with high DIC (dissolved inorganic carbon) content, and below the surface mixed layer. The occurrence of modern digitates in deep-towed plankton nets supports this interpretation.

Considering Coxall *et al*. (2007) results and according to the assumption that species with similar digitate morphologies have comparable life strategies, we can infer that

clavate and elongate taxa likely proliferated in relatively cool, deep and low oxygen waters. Therefore, the increase in abundances and new appearances recorded above the Selli Level equivalent could indicate that they occupied the lowest depth below the surface mixed layer in a phase of a supposed expansion of the OMZ (Oxygen minimum Zone, Fig. 7.9).

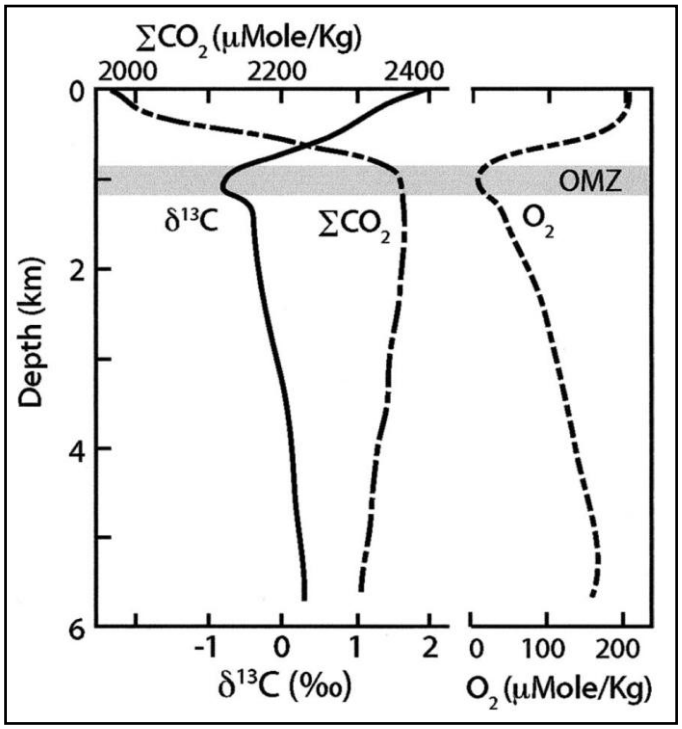

Fig. 7.9. Typical vertical profile of seawater dissolved inorganic carbon (*p*CO2), $\delta^{13}C$, and dissolved O_2 from the North Pacific (Kroopnick, 1985) to aid interpretation of carbon isotopes. OMZ, Oxygen minimum Zone. From Coxall *et al.*, 2007.

Chapter 8
Conclusion

This study provides a detailed biostratigraphic and quantitative analysis of the Barremian-Aptian planktonic foraminiferal assemblages recovered in two different localities, in the Tethys (Cismon core, Southern Alps) and Pacific (DSDP Site 463, Mid-Pacific Mountains) Oceans.

Micropaleontological analysis (absolute and relative abundances, and morphometric analysis) performed on pelagic sediments have contributed to the understanding of the evolution of early Cretaceous planktonic foraminifera, have improved biostratigraphic correlations on global scale, and have provided new insights in the interpretation of the response of planktonic foraminifera to ocean acidification in the studied time-interval.

The results obtained and their interpretations are the following:

1) Taxonomic analyses reveal that:

a) at Cismon core, planispiral and trochospiral taxa with globular and clavate chambers (genera *Globigerinelloides Hedbergella* and *Lilliputianella*), pseudo-planispiral with very elongate chambers (genus *Leupoldina*) and globigeriniform taxa (genera *Gubkinella* and *Gorbachikella*) occurred. Species richness increase upward through the interval, in agreement with the general trend described in previous studies (Coccioni *et al*., 1992; Coccioni & Premoli Silva, 1994; Premoli Silva & Sliter, 1999), that reported an increase in planktonic foraminiferal diversity in the early Valanginian through the Aptian. Just above the Selli Level equivalent a marked change in the composition is recorded, mainly due to the appearance of new taxa having globular (*Hedbergella gorbachikae, H. kuznetsovae, H. luterbacheri, H. primare* and *Globigerinelloides primitivus*) and clavate chambers (*Leupoldina pustulans hexacamerata, Leupoldina pustulans quinquecamerata, Leupoldina reicheli, Lilliputianella kurhyi, Lilliputianella maslakovae, Lilliputianella roblease, Globigerinelloides blowi lobatus, Globigerinelloides clavatus* and *Globigerinelloides elongatus*).

b) At DSDP Site 463, planispiral (genus *Globigerinelloides*), trochospiral (genus *Hedbergella*) and globigeriniform taxa (genera *Gorbachikella* and *Gubkinella*) with only globular chambers were documented. Possible morphotypes belonging to the *Leupoldina* sp. were recognized. No evident changes in species richness have been observed, probably because of the presence of some intervals of no recovery and of several samples barren in planktonic foraminifera that do not allow reliable considerations.

2) Shell size measurements show a general increase from the base to the top of the studied interval at both sites (much higher at Cismon core) due to an increase of calcification efficiency. The group with the highest range of variation in shell size is represented by the Globigerinelloidids, followed by Lilliputianellids and then by Hedbergellids.

3) Absolute abundance of planktonic foraminifera in thin sections show that: below the Selli Level eq., abundances are moderate at Cismon and low at DSDP Site 463, then they decrease in both sites at the onset of the OAE1a. Values remain stable and very low/null within it, until to a strong increase above it. In particular at Cismon core, the general trend of the planktonic foraminiferal abundance values observed in washed residues mirror the data acquired in thin sections: the two different methods have provided very similar results, different only in the scale of the numbers.

Abundances increase across the studied interval as well as test sizes.

4) Ecological intepretations of planktonic foraminifera reveal that: at both sites the genus *Hedbergella* is the most common component of the foraminiferal fauna across the studied interval and, thus, considered the most opportunistic taxon. The genus *Globigerinelloides* is a typical meso-oligotrophic taxon, while *Lilliputianella* and *Leupoldina* are meso-eutrophic taxa that likely proliferated in oxygen - depleted, deep and cool waters associated to a possible expansion of the OMZ (Coxall *et al.*, 2007).

Above the Selli Level eq., where the abundances fluctuate from very low to very high values, probably due to the ecological competition among the 3 groups, planispirals resulted to be the most efficient and successful competitors compared to the pseudo-planispirals and trochospirals. Moreover, the highest test size variations observed in the planispiral taxa is a

feature often directly related to reproductive potential (Hallock, 1985; Premoli Silva & Sliter, 1999).

5) The comparison between planktonic foraminiferal and nannoconid abundances highlights that:

a) When nannoconids underwent a biocalcification decline and, thus, decreased in abundance at about ~ 1 Ma before OAE1a, planktonic foraminifera slightly decreased too;

b) At the nannoconid crisis level documented before the onset of the OAE1a, planktonic foraminifera of Cismon core decrease in abundances prior to this biohorizon and increase after it until the onset of the OAE1a. At DSDP Site 463 only a constant decrease in abundances is observed starting before this biohorizon. At the onset of OAE1a both calcareous groups show a marked decline that can be related to widespread meso- to eutrophic conditions, combined with excess CO_2 in the ocean - atmosphere system. No extinctions within nannoconids and planktonic foraminifera have been observed in the OAE1a interval, both calcareous groups are considered virtually absent (e. g. Coccioni *et al*., 1992; Erba, 1994; Erba *et al*., 1999; Premoli Silva *et al*., 1999; Erba, 2004; Erba *et al*. 2010; Bottini *et al*., 2015).

c) At Cismon core nannoconids resume in the middle part of the Selli Level equivalent and increase until to the top of the interval but never become as abundant as before of the OAE1a (Erba, 2004), although their abundances still mirror the $\delta^{13}C$ trend. Planktonic foraminifera, after the decline within the Selli Level equivalent remain stable. They start to increase significantly just above the Selli Level equivalent, becoming more abundant than before the OAE1a. The different timing recovery could be justified by the higher susceptibility to dissolution of planktonic foraminifera than nannoconids (Cita, 1970).

The increase in abundance of planktonic foraminifera after the OAE1a is possible due to the termination of the widespread anoxia-dysoxia coincided with the end of the main emplacement of the Ontong Java Plateau, and the development of a more mesotrophic environment suitable to the proliferation of all planktonic foraminifera.

In conclusion, this study has implemented the current knowledge on planktonic foraminifera during the OAE1a by documenting their ability to evolve and diversify in a time-interval of complex and profound perturbation of the ocean-atmosphere system without undergoing extinction but, on the contrary, showing significant capacity of adaptation.

References

AGALAROVA, D. A., 1951. *Studies of Microfauna from Cretaceous Deposits of Azerbaijan*. In: Dzhafarov, D. I. & Kalilov, D. M., Aznefteizdat, Baku, 128 pp.

AGUADO, R., COMPANY, M., SANDOVAL, J., TAVERA, J. M., 1997. *Biostratigraphic events at the Barremian–Aptian boundary in the Beltic Cordillera (Southern Spain)*. Cretaceous Res., v. 18, pp. 309-329.

AGUADO, R., CASTRO, J. M., COMPANY, M., DE GEA, G. A., 1999. *Aptian bio-events-an integrated biostratigraphic analysis of the Almadich formation, inner Prebetic Domain, SE Spain*. Cretaceous Res., v. 20, pp. 663-683.

ANDO, A., KAIHO, K., KAWAHATA, H., KAKEGAWA, T., 2008. *Timing and magnitude of early Aptian extreme warming: Unraveling primary $\delta^{18}O$ variation in indurated pelagic carbonates at Deep Sea Drilling Project Site 463, central Pacific Ocean*. Palaeogeogr., Palaeoclimatol., Palaeoecol., v. 260, pp. 463-476.

ANTONOVA, Z. A., SHMIGINA, T. A., GNEDINA, A. G., BALUGINA, O. M., 1964. *Neokom i Apt Mezhduretsiya rafiyu i litologii Mezozoiskikh i Kainozoiskikh oltozhenii Kransnodarskogo Kraya*. Trudy Vsesoyuznogo Neftegazovogo Nauchnoissledovatel'skogo Instituta (VNII), Krasnodarskiy Filial, v. 12, pp. 3-72.

ARMSTRONG, H. A., BRASIER, M. D., 2005. *Microfossils.* Blackwell Publishing Ltd (2th edition), Malden, USA, 296 pp.

ARTHUR, M. A., SCHLANGER, S. O., 1979. *Cretaceous "oceanic anoxic events" as causal factors in development of reef-reservoired giant oil fields*. Am. Assoc. Pet. Geol. Bull., v. 63, pp. 870-885.

ARTHUR, M. A., DEAN, W. E., 1986. *Cretaceous paleoceanography*. In: B.E, Tucholke & P.R. Vogt, (eds), Decade of North American Geology, Western North Atlantic Synthesis Volume, Geol. Soc. Spec. Publ., v. 15, pp. 527-559.

ARTHUR, M. A., JENKYNS, H. C., BRUMSACK, H. J., SCHLANGER, S. O., 1990. *Stratigraphy, geochemistry and paleoceanography of organic carbon-rich Cretaceous sequences*. In: R.N. Ginsburg & B. Beaudoin (eds.), Cretaceous Resources, Events and Rhythms. Kruwer Academic Publisher, pp. 75-119.

BANNER, F. T., DESAI, D., 1988. *A review and revision of the Jurassic-Early Cretaceous Globigerinina, with especial reference to the Aptian assemblages of Speeton (North Yorkshire, England)*. J. Micropalaeont., v. 7, pp. 143-185.

BANNER, F. T., COPESTAKE, P., WHITE, M. R., 1993. *Barremian–Aptian Praehedbergellidae of the North Sea area: a reconnaissance*. Bull. Nat. Hist. Mus., London (Geology), v. 49, pp. 1-30.

BARABOSHKIN, E. J., 1996. *Aptian anoxic events of the Russian Platform and adjacent area.* Abstract, IGCP 343 and 369 Peri-Tethys Workshop, Moscow.

BARKER, S., ELDERFIELD, H., 2002. *Foraminiferal calcification response to glacial–interglacial changes in atmospheric CO_2.* Science, v. 297, pp. 833-836.

BARTENSTEIN, H., 1965. *Taxionomische Revision and Nomenklator zu Franz E, Hecht "Standard-Gliederung der Nordwest-deutschen Unterkreide nach Foraminiferen" (1938). Teil 4, Alb, mit Beschreibungen von Arten aus verschiedenen Unterkreide-Niveaus*. Senckenbergiana Lethaea, v. 46, pp. 327-366.

BARTENSTEIN, H., BOLLI, H. M., 1977. *The Foraminifera in the Lower Cretaceous of Trinidad W.I. Part 4: Couche Formation, upper part; Leupoldina protuberans Zone*. Eclogae Geol. Helv., v. 70, pp. 543-573.

BAUDIN, F., 1996. *Enregistrement de l'événement anoxique Aptien inférieur dans les faciés péritidaux du Guyot Resolution (Océan Pacifique NW).* Comptes Rendus de l'Académie des Sciences, v. 323, II, 3, pp. 221-228.

BAUDIN, F., 2005. *A Late Hauterivian short-lived anoxic event in the Mediterranean Tethys: The 'Faraoni event'* , C. R. Geosci., v. 337, pp. 1532-1540.

BELLANCA, A., ERBA, E., NERI, R., PREMOLI SILVA, I., SPROVIERI, M., TREMOLADA, F., VERGA, D., 2002. *Paleoceanographic significance of the Tethyan "Livello Selli" (Early Aptian) from the Hybla Formation, northwestern Sicily: biostratigraphy and high-resolution chemostratigraphic records.* Palaeogeogr., Palaeoclimatol., Palaeoecol., v. 185, pp. 175-196.

BERGER, W. H., KILLINGLEY, J. S., VINCENT, E., 1978. *Stable isotopes in deep-sea carbonates: Box Core ERDC-92, Western Equatorial Pacific*. Oceanologica Acta, v. 1, pp. 203-216.

BERNOULLI, D., JENKYNS, H. C., 2009. *Ancient oceans and continental margins of the Alpine-Mediterranean Tethys: deciphering clues from Mesozoic pelagic sediments and ophiolites.* Sedimentology, v. 56, pp. 149-190.

BERSEZIO, R., 1994. *Stratigraphic framework and sedimentary features of the Lower Aptian "Livello Selli" in the Lombardy Basin (Southern Alps, Northern Italy).* Riv. Ital. Paleont. Stratig., v. 99 (1993), pp. 569-589.

BERSEZIO, R., ERBA, E., GORZA, M., RIVA, A., 2002. *Berriasian – Aptian black shales of the Maiolica Formation (Lombardian Basin, Southern Alps, Northern Italy): local to global events.* Palaeogeogr., Palaeoclimatol., Palaeoecol., v. 180, pp. 253-275.

BODIN, S., GODET, A., MATERA, V., STEINMANN, P., VERMEULEN, J., GARDIN, S., ADATTE, T., COCCIONI, R., FÖLLMI, K. B., 2007. *Enrichment of redox-sensitive trace metals (U, V, Mo, As) associated with the late Hauterivian Faraoni oceanic anoxic event.* Int. J. Earth Sci., v. 96, pp. 327-341.

BOERSMA, A., PREMOLI SILVA, I., SHACKLETON., N. J., 1987. *Atlantic Eocene planktonic foraminiferal paleohydrographic indicators and stable isotope paleoceanography*. Paleoceanography, v. 2, pp. 287-331, doi: 10.1029/PA002i003p00287.

BOLLI, H. M., LOEBLICH, A. R., TAPPAN, E., 1957. *Planktonic foraminiferal families Hantkeninidae, Orbulinidae, Globorotaliidae and Globotruncanidae.* In: Loeblich, A. R., Jr. (eds.), Studies in Foraminifera. U. S. National Museum Bulletin, v. 215, pp. 3-50.

BOLLI, H. M., 1959. *Planktonic foraminifera from the Cretaceous of Trinidad, B.W.I.* Bulletins of American Paleontology, v. 39 (179), pp. 257-277.

BOTTINI, C., MUTTERLOSE, J., 2012. *Integrated stratigraphy of Early Aptian black shales in the Boreal Realm: calcareous nannofossil and stable isotope evidence for global and regional processes*. Newsl. Stratigr., v. 45, pp. 115-137.

BOTTINI, C., COHEN, A. S., ERBA, E., JENKYNS, H. C., COE, A. L., 2012. *Osmium-isotope evidence for volcanism, weathering and ocean mixing during the early Aptian OAE 1a*. Geology, v. 40, pp. 583-586.

BOTTINI, C., ERBA, E., TIRABOSCHI, D., JENKYNS, H. C., SCHOUTEN, S., SINNINGHE DAMSTÉ, J. S., 2015. *Climate variability and ocean fertility during the Aptian Stage*. Clim. Past. (cp-2014-10), in press.

BOUDAGHER-FADEL, M. K., 1995. *The planktonic foraminifera of the Early Cretaceous of Tunisia compared to those of western and central Tethys*. Palaeopelagos, v. 5, pp. 137-160.

BOUDAGHER-FADEL, M. K., 1996. *Re-evaluation of the phylogeny of Early Cretaceous planktonic foraminifera (Praehedbergellidae).* Cretaceous Res., v. 17, pp. 767-771.

BOUDAGHER-FADEL, M. K., BANNER, F. T., WHITTAKER, J. E., SIMMONS, M. D., 1997. *The Early Evolutionary History of Planktonic Foraminifera*. British Micropalaeontological Society Publications Series. Chapman and Hall, London, 269 pp.

BRALOWER, T. J., SLITER, W. V., ARTHUR, M. A., LECKIE, R. M., ALLARD, D. J., SCHLANGER, S. O., 1993. *Dysoxic/anoxic episodes in the Aptian–Albian (Early Cretaceous).* In: Pringle, M., *et al.* (eds.), The Mesozoic Pacific: Geology, Tectonics and Volcanism. AGU Geophys. Monogr., v. 77, pp. 5-37.

BRALOWER, T. J., ARTHUR, M. A., LECKIE, R. M., SLITER, W. V., ALLARD, D. J., SCHLANGER, S. O., 1994. *Timing and paleoceanography of oceanic dysoxia/anoxia in the Late Barremian to early Aptian.* Palaios, v. 9, pp. 335-369.

BRALOWER, T. J., FULLAGAR, P. D., PAULL, C. K., DWYER, G. S., LECKIE, R. M., 1997. *Mid-Cretaceous strontium-isotope stratigraphy of deep-sea sections*. Geol. Soc. Am. Bull. v. 109, pp. 1421-1442.

BRALOWER, T. J., COBABE, E., CLEMENT, B., SLITER, W. V., OSBURNE, C., LONGORIA, J., 1999. *The record of global change in mid-Cretaceous, Barremian –Albian sections from the Sierra Madre, northeastern Mexico*. J. Foraminiferal Res., v. 29, pp. 418-437.

BRÉHÉRET, J. G., CARON, M., DELAMETTE, M., 1986. *Niveaux riches en matière organique dans l'Albien Vocontien; quelques caractères du paléoenvironnement; essai d'interpretation génétique (Layers rich in organic matter from the Vocontian Albian; some paleoenvironmental characteristics; a tentative of genetic interpretation)*. Docum. du Bureau de Recherc. Géol. et Min., no. 110, pp. 141-191.

BRÉHÉRET, J. G., 1988. *Episodes de sèdimentation riche en matièere organique dans les marnes bleues d'ages Aptien et Albien de la partie pèlagique du bassin Vocontien.* B. Soc. Geol. Fr., v. 4, pp. 349-356.

BRÉHÉRET, J. G., DELAMETTE, M., 1989. *Les nodules barytiques d'âge Crétacé moyen dans le domaine Vocontien (SE France), marqueurs de discontinuités sédimentaires en série*

marneuse de bassin. C.R. Acad. Sci. Paris II, v. 308, pp. 1369-1374.

BRÉHÉRET, J. G., 1994. *The mid-Cretaceous organic-rich sediments from the Vocontian Zone of the French Southeast Basin.* In: Mascle, A.(ed.), Hydrocarbon and petroleum geology of France, Europ. Assoc. Geosci., Series 4, pp. 295-320.

BRÉHÉRET, J. G., 1997. *L'Aptien et l'Albien de la fosse vocontienne (des bordures au bassin). Evolution de la sèdimentation et enseignemnts sur les événements anoxiques.* Publication de la Soci. Géol. Nord 25, pp. 614.

BRÖNNIMANN, P., BROWN, N. K., 1958. *Hedbergella, a new name for a Cretaceous planktonic foraminiferal genus*. Washington Academy Science Journal, v. 48, pp. 15-17.

CARON, M., HOMEWOOD, P., 1983. *Evolution of early planktic foraminifers.* Marine Micropaleontology, v. 7, pp. 453-462.

CARON, M., 1985. *Cretaceous planktic foraminifera*. In: Bolli, H. M., Saunders, J. B., Perch-Nielsen, K. (eds.), Plankton Stratigraphy. Cambridge University Press, Cambridge, UK, pp. 17-86.

CARSEY, D. J., 1926. *Foraminifera of the Cretaceous of central Texas.* Bulletin of the University of Texas, Bureau of Econ. Geol. and Techn., pp. 1-56.

CECCA, F., MARINI, A., PALLINI, G., BAUDIN, F., BEGOUEN, V., 1993. *A guide-level of the uppermost Hauterivian (Lower Cretaceous) in the pelagic succession of Umbria-Marche (Central Italy): The Faraoni Level*, Riv. Ital. Paleontol. Stratigr., v. 99, pp. 551-568.

CHANNELL, J. E. T., ERBA, E., NAKANISHI, M., TAMAKI, K., 1995. *Late Jurassic-Early Cretaceous Time Scales and oceanic magnetic anomaly block models.* In: Berggren, W. A., Kent, D. V., Aubry, M. P., and Hardenbol, J. (eds.), Geochronology time scales and global stratigraphic correlation: Soc. Econ. Paleontol. Mineral. Spec. Publ., no. 54, pp. 51-63.

CHANNELL, J. E. T., ERBA, E., MUTTONI, G., TREMOLADA, F., 2000. *Early Cretaceous magnetic stratigraphy in the APTICORE drill core and adjacent outcrop at Cismon (Southern Alps, Italy), and correlation to the proposed Barremian/Aptian boundary stratotype.* Geol. Soc. Am. Bull., v. 112, pp. 1430-1443.

CHEVALIER, J., 1961. *Quelques nouvelles espèces de Foraminifères dans le Crétacé inférieur méditerranéen*. Rev. Micropal., v. 4, pp. 30-36.

CITA, M. B., 1970. *Observations sur quelques aspects paléoécologiques de sondages subocéaniques effectués dans l'Atlantique Nord.* Rev. Micropal., v. 12, pp. 187-201.

COBIANCHI, M., LUCIANI, V., BOSELLINI, A., 1997. *Early Cretaceous nannofossils and planktonic foraminifera from northern Gargano (Apulia, southern Italy).* Cretaceous Res., v. 18, pp. 249-293.

COBIANCHI, M., LUCIANI, V., MENEGATTI, A., 1999. *The Selli Level of the Gargano Promontory, Apulia, southern Italy: foraminiferal and calcareous nannofossil data*. Cretaceous Res., v. 20, pp. 255-269.

COCCIONI, R., NESCI, O., TRAMONTANA, M., WEZEL, C. F., MORETTI, E., 1987. *Descrizione di un livello guida "Radiolaritico-Bituminoso-Ittiolitico" alla base delle Marne a*

Fucoidi nell'Appennino Umbro-Marchigiano. Boll. Soc. Geol. Ital., v.106, pp. 183-192.

COCCIONI, R., FRANCHI, R., NESCI, O., WEZEL, F. C., BATTISTINI, F., PALLECCHI, P., 1989. *Stratigraphy and mineralogy of the Selli Level (Early Aptian) at the base of the Marne a Fucoidi in the Umbrian-Marchean Apennines (Italy).* In: Wiedmann, J. (ed.), Cretaceous of the Western Tethys. 3rd International Cretaceous Symposium. Schweizerbartsche, Stuttgart, Germany, pp. 563-584.

COCCIONI, R., ERBA, E., PREMOLI SILVA, I., 1992. *Barremian-Aptian calcareous plankton biostratigraphy from the Gorgo a Cerbara section (Marche, Central Italy) and implication for plankton evolution*. Cretaceous Res., v. 13, pp. 517-537.

COCCIONI, R., PREMOLI SILVA, I., 1994. *Planktonic foraminifera from the Lower Cretaceous of Rio Argos sections (Southern Spain) and biostratigraphic implications*. Cretaceous Res., v. 15, pp. 645-687.

COCCIONI, R., MARSILI, A., VENTURATI, A., 2004. *Chamber elongation in Early Cretaceous planktonic foraminifera: a case study from the Lower Hauterivian-Lower Aptian Rio Argos succession (southern Spain).* In: Coccioni, R., Galeotti, S., Lirer, F. (eds.), Proceedings of the First Italian Meeting on Environmental Micropaleontology, 9. Grzybowski foundation special publication, pp. 37-47.

COCCIONI, R., LUCIANI, V., MARSILI, A., 2006. *Cretaceous oceanic anoxic events and radially elongated chambered planktonic foraminifera: Paleoecological and paleoceanographic implications.* Palaeogeogr., Palaeoclimatol., Palaeoecol., v. 235, pp. 66-92.

COCCIONI, R., PREMOLI SILVA, I., MARSILI, A., VERGA, D., 2007. *First radiation of Cretaceous planktonic foraminifera with radially elongate chambers at Angles (Southeastern France) and biostratigraphic implications*. Rev. Micropal., v. 50, pp. 215-224.

COHEN, A. S., COE, A. L., HARDING, S. M., 2004. *Osmium isotope evidence for the regulation of atmospheric CO_2 by continental weathering*. Geology, v. 32, pp.157-160.

COHEN, A. S., COE, A. L., 2007. *The impact of the Central Atlantic Magmatic Province on climate and on the Sr- and Os-isotope evolution of seawater*. Palaeogeogr. Palaeoclimatol. Palaeoecol., v. 244, pp. 374-390.

COMPANY, M., AGUADO, R., JIMENEZ DE CISNEROS, C., SANDOVAL, J., TAVERA, J. M., VERA, J. A., 2003a. *Biotic changes at the Hauterivian/Barremian boundary in the Mediterranean Tethys. Field-trip guide to Agost (K/T) and Rio Argos (Hauterivian/Barremian) sections. Bioevents: their stratigraphical records, patterns and causes*. Caravaca de la Cruz 2003, June 3rd-8th, pp. 15-28.

COMPANY, M., SANDOVAL, J., TAVERA, J. M., 2003b. *Ammonite biostratigraphy of the uppermost Hauterivian in the Betic Cordillera (Southeastern Spain).* Geobios, v. 36, pp. 685-694.

CORFIELD, R. M., HALL, M. A., BRASIER, M. D., 1990. *Stable isotope development for foraminiferal habitats during the development of the Cenomanian-Turonian oceanic anoxic event*. Geology, v. 8, pp. 175-178.

COTILLON, P., RIO, M., 1984. *Cyclic sedimentation in the Cretaceous of DSDP Sites 535 and 540 (Gulf of Mexico), 534 (Central Atlantic) and in the Vocontian Basin (France).* Initial Reports of the DSDP, Washington D.C. (U. S. Government Printing Office), v. 77, pp. 339-376.

COXALL, H. K., PEARSON, P. N., SHACKLETON, N. J., HALL, A. H., 2000. *Hantkeninid depth adaptation: an evolving life strategy in a changing ocean*. Geology, v. 28, pp. 87-90.

COXALL, H. K., WILSON, P. A., PEARSON, P. N., 2002. *Paleoecology of some extreme 'clavate' planktonic foraminifera from the Cretaceous to Recent.* Newsl. Micropal., v. 66, pp. 14.

COXALL, H. K., WILSON, P. A., PEARSON, P. N., SEXTON, P. F., 2007. *Iterative evolution of digitate planktonic foraminifera*. Paleobiology, v. 33, pp. 495-516.

CUSHMAN, J. A., TEN DAM, A. T., 1948. *Globigerinelloides, a new genus of the Globigerinidae.* Contributions from the Cushman Laboratory for Foraminiferal Research, v. 24, pp. 42-43.

DEAN, W. A., THIEDE, J., 1978. *Origin of organic-carbon-rich mid-Cretaceous limestones Mid-Pacific Mountains and southern Hess Rise*. In: Initial Reports of the Deep Sea Drilling Project., Washington (U. S. Government Printing Office), v. 62, pp. 877-890.

DELAGE, Y., HÉROUARD, E., 1896. *Traité de Zoologie Concrète. La Cellule et les Protozoaires.* Paris, Schleicher Frères, v. 1, 670 pp.

DICKENS, G. R., O'NEIL, J. R., REA, D. C., OWEN, R. M., 1995. *Dissociation of oceanic methane hydrate as a cause of the carbon isotope excursion at the end of the Palaeocene*. Paleoceanography, v. 10, pp. 965-971, doi: 10.1029/95PA02087.

DICKENS, G. R., CASTILLO, M. M., WALKER, J. C. G., 1997. *A blast of gas in the latest Paleocene: simulating first-order effects of massive dissociation of oceanic methane hydrate*. Geology, v. 25, pp. 259-262.

DICKENS, G. R., 2000. *Methane oxidation during the Late Palaeocene Thermal Maximum*. Bull. Soc. Géol. France, v. 171, pp. 37-49.

DICKENS, G. R., 2001. *On the fate of past gas: what happens to methane released from a bacterially mediated gas hydrate capacitor?*. Geochem. Geophys. Geosyst., v. 32, pp.1179-1193.

DOUGLAS, R. G., SAVIN, S. M., 1978. *Oxygen isotopic evidence for the depth stratification of Tertiary and Cretaceous planktic foraminifera*. Mar. Micropal., v. 3, pp. 175-196.

DUMITRESCU, M., BRASSELL, S. C., SCHOUTEN, S., HOPMANS, E. C., SINNINGHE DAMSTÉ, J. S., 2006. *Instability in tropical Pacific sea-surface temperatures durinf the early Aptian*. Geology, v. 34, pp. 833-866.

DUNHAM, R. J., 1962. *Classification of carbonate rocks according to depositional texture.* In*:* Ham, W.E. (ed.), Classification of carbonate rocks. Amer. Assoc. Petr. Geol., Memoir., v. 1, pp. 108-121.

ELDHOLM, O., THOMAS, E., 1993. *Environmental impact of volcanic margin formation*. Earth Plan. Sci. Lett., v. 117, pp. 319-329.

EMBRY, A. F., KLOVAN, J. E., 1971. *A late Devonian reef tract on northeastern Banks Island, N.W.T.*: Bull. Canad. Petrol. Geol., v. 19, pp. 730-781.

EMILIANI, C., 1954a. *Depth habitats of some species of pelagic foraminifera as indicated by oxygen isotopes ratios.* Amer. J. Science, v. 252, pp. 411-419.

EMILIANI, C., 1954b. *Temperatures of Pacific bottom waters and polar superficial waters during the Tertiary.* Science, v. 119, pp. 853-855.

ERBA, E., 1994. *Nannofossils and superplumes: the early Aptian "nannoconid crisis"***.** Paleoceanography, v. 9, pp. 483-501, doi: 10.1029/94PA00258.

ERBA, E., PREMOLI SILVA, I., WILSON, P. A., PRINGLE, M. S., SLITER, W. V., WATKINS, D. K., ARNAUD VANNEAU, A., BRALOWER, T. I., BUDD, A. F., CAMOIN, G. F., MASSE, J. P., MUTTERLOSE, J., SAGER, W. V., 1995. *Synthesis of stratigraphies from shallow-water sequences at Sites 871 through 879 in the Western Pacific Ocean (Leg 144)*. In: Haggerty, J. A., Premoli Silva, I., Rack, F., and McNutt, M. K.,(eds.), Proceedings Ocean Drilling Program, Scientific Results, Volume 144: College Station, Texas, Ocean Drilling Program, pp. 873-885.

ERBA, E., LARSON, R. L., 1998. *The Cismon Apticore (Southern Alps, Italy): "Reference section" for the Lower Cretaceous at low latitudes.* Riv. Ital. Paleont. Stratig., v. 104, pp. 181-192.

ERBA, E., CHANNELL, J. E. T., CLAPS, M., JONES, C., LARSON, R., OPDYKE, B., PREMOLI SILVA, I., RIVA, A., SALVINI, G., TORRICELLI, S., 1999. *Integrated stratigraphy of the Cismon Apticore (Southern Alps, Italy): a "reference section" for the Barremian–Aptian interval at low latitudes*. J. Foraminiferal Res**.,** v. 29, pp. 371-392.

ERBA, E., 2004. *Calcareous nannofossils and Mesozoic oceanic anoxic events*. Mar. Micropal.., v. 52, pp. 85-106.

ERBA, E., TREMOLADA, F., 2004. *Nannofossil carbonate fluxes during the Early Cretaceous: phytoplankton response to nutrification episodes, atmospheric CO_2, and anoxia.* Paleoceanography, v. 19, pp. 1008.

ERBA, E., BARTOLINI, A., LARSON, R. L., 2004. *Valanginian Weissert oceanic anoxic event.* Geology, v. 32, pp. 149-152.

ERBA, E., BOTTINI, C., WEISSERT, J. H., KELLER, C. E., 2010.: *Calcareous Nannoplankton Response to Surface-Water Acidification Around Oceanic Anoxic Event 1a*. Science, v. 329, pp. 428-432.

ERBACHER, J., THUROW, J., LITTKE, R., 1996. *Evolution patterns of radiolarian and organic matter variations: a new approach to identify sea-level changes in mid-Cretaceous pelagic environments.* Geology, v. 24, pp. 499-502.

FERRY, S., SCHAAF, A., 1981. *The early Cretaceous environment at Deep Sea Drilling Project Site 463 (mid-Pacific Mountains), with reference to the Vocontian trough (French Subalpine ranges)*. In: Winterer, E.L., Sager, W.W., Firth, J.V. & Sinton, J.M. (eds.), Proceedings of the Ocean Drilling Program, Scientific Result, p. 669.

FÖLLMI, K. B., WEISSERT, H., BISPING, M., FUNK, P., 1994. *Phosphogenesis, carbon isotope stratigraphy and carbonate-platform evolution along the Lower Cretaceous northern Tethyan margin*. Bull. of the Geol. Soc. of Amer., v. 106, pp. 729-746.

FRIJIA, G., PARENTE M., 2008. *Strontium isotope stratigraphy in the upper Cenomanian shallow-water carbonates of the southern Apennines: Short-term perturbations of marine $^{87}Sr/^{86}Sr$ during the oceanic anoxic event 2*. Palaeogeogr. Palaeoclimatol. Palaeoecol, v. 261, pp. 15-29.

FUCHS, W., 1971. *Eine alpine Foraminiferenfauna des tieferen Mittel-Barrême aus den Drusbergschichten von Ranzenberg bei Hohenems in Vorarlberg.* Abhandlungen der Geologischen Bundesanstalt, Wien, v. 27, pp. 1-49.

GANDOLFI, R., 1942. *Ricerche micropaleontologiche e stratigrafiche sulla scaglia e sui flysch Cretacici dei dintorni di Balerna (Canton Ticino).* Riv. Ital. Paleont., Memoria, v. 4, pp. 1-160.

GLAESSNER, M. F., 1937. *Planktonforaminiferen aus der Kreide und den Eozen Und ihre Stratigraphische Bedetung*. Moscow University, Paleontological Laboratory Pubblications, Studies in Micropaleontology 1/1, pp. 27-52.

GLAESSNER, M. F., 1966. *Notes on foraminifera of the genus Hedbergella.* Eclogae Geol. Helv., v. 59, pp. 179-184.

GORBACHIK, T. N., KRECHMAR, V. , 1969. *Raschlenene Apt-Albskikh Otlozheny Krymapo Planktonnym Foraminiferam (Planktonic foraminifera of Aptian-Albian deposits of Crimea):* Vesthik Moskowskogo Universiteta, v. 3, pp. 46-56.

GORBACHIK, T. N., KRECHMAR, V., 1970. *Osobennosti Socheneniya Kamer u Rokovin Roda Leupoldina (Foraminifera) [Features of chambers articulation in test of the genus Leupoldina]*. Paleontologicheskiy Zhurnal, v. 3, pp. 143-146.

GORBACHIK, T. N., 1971. *On Early Cretaceous Foraminifera from Crimea*. Voprosy Mikropaleontologii, v. 14, pp. 125-139.

GORBACHIK, T. N., 1986. *Jurassic and Early Cretaceous planktonic foraminifera of the south of the USSR.* Akademia Nauk SSSR, Nauka, Moscow, pp. 239.

GRÖCKE, D. R., HESSELBO, S. P., JENKYNS, H. C., 1999. *Carbon-isotope composition of Lower Cretaceous fossil wood: ocean–atmosphere chemistry and relation to sea-level change*. Geology, v. 27, pp. 155-158.

HABERMANN, A., MUTTERLOSE, J., 1999. *Early Aptian black shales from NW Germany: calcareous nannofossil and their paleoceanographic implications*. Geol. Jahrbuch A, v. 212, pp. 379-400.

HALLOCK, P., 1985. *Why are larger Foraminifera large?* Paleobiology, v. 11, pp. 195-208.

HAQ, B. U., HARDENBOL, J., VAIL, P. R., 1988. *Mesozoic and Cenozoic chronostratigraphy and cycles of sea-level change*. In: C. K. Wilgus, B. S. Hastings, C. G. St. C. Kendall, H. W. Posamentier, C. A. Ross & J. C. Van Wagoner, (eds), Sea-Level Changes: An integrated Approach Special Publication of the Soc. Econ. Palaeont. Mineral., v. 42, pp. 72-108.

HART, M. B., BAILEY, H. W., 1979. *The distribution of planktonic Foraminiferida in the mid-Cretaceous of NW Europe*. In: Wiedmann, J., (ed.), Aspekte der Kreide Europas: Stuttgart, Intern. Un. Geol. Sci., Ser. A, v. 6, pp. 527-542.

HART, M. B., 1999. The *evolution and biodiversity of Cretaceous planktonic Foraminiferida*. Geobios, v. 32, pp. 247-55.

HAYS, J. D., IMBRIE, J., SHACKLETON, N. J., 1976. *Variations in the Earth's orbit: Pace maker of the ice ages*. Science, v. 104, pp. 1121-1132.

HECHT, F. E., 1938. *Standard-Gliederung der Norwestdeutschen Unterkreide nach Foraminiferen.* Abhandlungen von der Seckenbergischen Naturforschenden Gesellschaft, v. 443, pp. 3-42.

HEIMHOFER, U., HOCHULI, P. A., BURLA, S., ANDERSEN, N., WEISSERT, H., 2003. *Terrestrial carbon-isotope records from coastal deposits (Algarve, Portugal): A tool for chemostratigraphic correlation on an intrabasinal and global scale*. Terra Nova, v. 15, pp. 8-13.

HEMLEBEN, C., SPINDLER, M., ANDERSON, O. R., 1989. *Modern planktonic foraminifera.* New York, Springer,. 363 pp.

HERBERT, T. D., 1992. *Paleomagnetic calibration of Milankovitch cyclicity in Lower Cretaceous sediments*. Earth Plan. Sci. Lett. Amsterdam, v. 112, pp. 15-28.

HERMES, J. J., 1966 *Lower Cretaceous planktonic foraminifera from the Subbetic of southern Spain.* Geol. Mijnb., v. 45, pp. 35-66.

HERRLE, J. O., 2002. *Palaeoceanographic and palaeoclimatic implications on mid-Cretaceous black shale formation in the Vocontian Basin and Atlantic: evidence from calcareous nannofossils and stable isotopes*. Tübinger Mikropaläontologische Mitteilungen, v. 27, p. 114.

HESSELBO, S., GROCKE, D., JENKYNS, H. C., BJERRUM, C. J., FARRIMOND, P., MORGANS BELL, H. S., GREEN, O., 2000. *Massive dissociation of gas hydrate during a Jurassic oceanic anoxic event*. Nature, v. 406, pp. 392-395.

HOCHULI, P. A., MENEGATTI, A. P., WEISSERT, H., RIVA, A., ERBA, E., PREMOLI SILVA, I., 1999. *Episodes of high productivity and cooling in the early Aptian Alpine Tethys.* Geology, v. 27 (7), pp. 657-660.

HOEDEMAEKER, P. J., 2002. *Correlating the uncorrelatables: a Tethyan-Boreal correlation of pre-Aptian Cretaceous strata*. In: Michalik, J. (ed.), Tethyan/Boreal Cretaceous correlation. Publishing House of the Slovak Academy of Sciences, Bratislava, pp. 235-283.

HU, X., KUIDONG, Z., YILMAZ, I. O., YONGXIANG, L., 2012. *Stratigraphic transition and palaeoenvironmental changes from the Aptian oceanic anoxic event 1a (OAE1a) to the oceanic red bed 1 (ORB1) in the Yenicesihlar section, central Turkey*, Cretaceous Res., v. 38, pp. 40-51.

HUBER, B. T., LECKIE, R. M., 2011. *Planktic foraminiferal species turnover across deep-sea Aptian/Albian boundary sections*. J. Foraminiferal Res., v. 41, pp. 53-95.

HUSINEC, A., HARMAN, C. A., REGAN, S. P., MOSHER, D. A., SWEENEY, R. J., READ, J. F., 2012. *Sequence development influenced by intermittent cooling events in the Cretaceous Aptian greenhouse, Adriatic platform, Croatia*. AAPG Bulletin, v. 96, pp. 2215-2244.

JAHREN, A. H., ARENS, N. C., SARMIENTO, G., GUERRERO, J., AMUNDSON, R., 2001. *Terrestrial record of methane hydrate dissociation in the Early Cretaceous*. Geology, v. 29, pp. 159-162.

JENKYNS, H. C., 1980. *Cretaceous anoxic events: from continents to oceans.* J. Geol. Soc. London, v. 137, pp. 171-188.

JENKYNS, H. C., 1985. *The Early Toarcian and Cenomanian-Turonian anoxic events in Europe: Comparisons and contrasts*. Geol. Rundsch., v. 74, pp. 505-518.

JENKYNS, H. C., 1988. *The early Toarcian (Jurassic) anoxic event: Stratigraphic, sedimentary, and geochemical evidence.* Am. J. Sci., v. 288, pp. 101-151.

JENKYNS, H. C., 1995. *Carbon-isotope stratigraphy and paleoceanographic significance of the Lower Cretaceous shallow-water carbonates of Resolution Guyot, Mid-Pacific Mountains*. In: Winterer, E. L., Sager, W. W., Firth, J. V., Sinton, J. M., (eds.), Proceedings of the Ocean Drilling Program Scientific Results, College Station, Texas, v. 143, pp. 99-104.

JENKYNS, H. C., 1999. *Mesozoic anoxic events and paleoclimate*. Zbl. Geol. Palaönt. Teil, pp. 943-949.

JENKYNS, H. C., 2003. *Evidence for rapid climate change in the Mesozoic-Palaeogene greenhouse world.* Philos. Trans. R. Soc., Ser. A 361, pp. 1885-1916.

JENKYNS, H. C., 2010. *Geochemistry of oceanic anoxic events.* Geoch.., Geoph., Geosys., v. 11, pp. 1-30.

JOHN, C. M., BOHATY, S. M., ZACHOS, J. C., SLUIJS, A., GIBBS, S., BRINKHUIS, H., BRALOWER, T. J., 2008. *North American continental margin records of the Paleocene-Eocene thermal maximum: Implications for global carbon and hydrological cycling*. Paleoceanography, v. 23, doi:10.1029/207PA001465.

JONES, C. E., JENKYNS, H. C., 2001. *Seawater strontium isotopes, oceanic anoxic events, and seafloor hydrothermal activity in the Jurassic and Cretaceous*. Am. J. Sci., v. 301, pp. 112-149.

KELLER, C. E., HOCHULI, P. A., WEISSERT, H., BERNASCONI, S. M., GIORGIONI, M., GARCIA, T. I., 2011. *A volcanically induced climate warming and floral change preceded the onset of OAE1a (Early Cretaceous).* Palaeogeogr. Palaeocl., Paleoecol., v. 305, pp. 43-49.

KENNEDY, W. J., GALE, A. S., HUBER, B. T., PETRIZZO, M. R., BOWN, P., BARCHETTA, A., JENKYNS, H. C., 2014. *Integrated stratigraphy across the Aptian/Albian boundary at Col de Pré-Guittard (southeast France): A candidate Global Boundary Stratotype Section*. Cretaceous Res., v. 51, pp. 248-259.

KERR, A. C., 1998. *Oceanic plateau formation: a cause of mass extinction and black shale deposition around the Cenomanian-Turonian boundary*. J. Geol. Soc. London, v. 155, pp. 619-626.

KRECHMAR, V., GORBACHIK, T. N., 1971. *On Early Cretaceous Foraminifera from Krimea*. In: Gorbachik, T. N., (ed.),. Voprosy Mikropaleontologii, v. 14, pp. 125-139.

KRECHMAR, V., GORBACHIK, T. N., 1986. *Jurassic and Early Cretaceous Planktonic Foraminifera of the Southern SSSR*. Akademia Nauk SSSR, ‘‘Nauka’’, Moscow, pp. 239.

KROOPNICK, P. M., 1985. *The distribution of ^{13}C in the world oceans.* Deep-Sea Research, v. 32, pp. 57-84.

KUHNT, W., HOLBOURN, A., MOULLADE, M., **2011.** *Transient global cooling at the onset of early Aptian oceanic anoxic event (OAE) 1a*. Geology, v. 39, pp. 323-326.

KUHRY, B., 1971. *Stratigraphy and micropaleontology of the Lower Cretaceous in the Subbetic south of Caravaca (Province of Murcia, SE Spain)*. I and II. Koninklijk Nederlands Akademie van Wetenschappen Proceedings B , v. 75, pp. 193-222.

KURTZ, A. C., KUMP, L. R., ARTHUR, M. A., ZACHOS, J. C., PAYTAN, A., 2003. *Early Cenozoic decoupling of the global carbon and sulphur cycles.* Paleoceanography, 18, doi: 10.1029/2003PA000908.

LANCELOT, Y., 1978. *Relations entre evolution sédimentaire et tectonique de la plaque Pacifique depuis le Cretacee inferieur.* Soc. Geol. France Mem. N.S., p. 134.

LARSON, R. L., 1991a. *Latest pulse of Earth Evidence for a mid-Cretaceous superplume*. Geology, v. 19, pp. 547-550.

LARSON, R. L., 1991b. *Geological consequences of superplumes*. Geology, v. 19, pp. 963-966.

LARSON, R. L., FISCHER A. G., ERBA, E., PREMOLI SILVA, I., 1993. *APTICORE-ALBICORE: a workshop Report on Global Events and Rhythms of the mid-Cretaceous.* 4-9 October 1992, Perugia, Italy, p. 56, Washington D.C.

LARSON, R. L., ERBA, E., 1999. *Onset of the Mid-Cretaceous greenhouse in the Barremian-Aptian: Igneous events and the biological, sedimentary, and geochemical responses.* Paleoceanography, v. 14, pp. 663-678.

LECKIE, R. M., 1984. *Mid Cretaceous planktonic foraminiferal biostratigraphy of Central Morocco, Deep Sea Drilling Project Leg 79, Sites 545 and 547*. In: Initial Reports of Deep Sea Drilling Project, 79: Washington (U. S. Government Printing Office), pp. 579-620.

LECKIE, R. M., 1987. *Paleoecology of mid-Cretaceous planktonic Foraminifera: A comparison of open ocean and epicontinental sea assemblages*. Micropaleontology, v. 33, pp. 164-176.

LECKIE, R. M., 1990. *Mid-Cretaceous planktic foraminifera of the Antarctic margin: Hole 693A, ODP Leg 113*. In: Barker, P. F., Kennett, J. P. *et al.*, (eds.), Proceedings of the Ocean Drilling Program, Scientific Results, v. 113: Ocean Drilling Program, College Station, Texas, pp. 319-324.

LECKIE, R. M., BRALOWER, T. J., CASHMAN, R., 2002. *Oceanic anoxic events and plankton evolution: biotic response to tectonic forcing during the mid-Cretaceous.* Paleoceanography, v. 17, doi: 10.1029/2001PA000623.

LI, Y. X., BRALOWER, T. J., MONTAÑEZ, I. P., OSLEGER, D. A., ARTHUR, M. A., BICE, D. M., HERBERT, T. D., ERBA, E., PREMOLI SILVA, I., 2008. *Toward an orbital chronology for the early Aptian oceanic anoxic event (OAE1a, ~120 Ma).* Earth Plan. Sci. Lett., v. 271, pp. 88-100.

LINI, A., WEISSERT H., ERBA, E., 1992. *The Valanginian carbon isotope events: A first episode of greenhouse climate conditions during the Cretaceous*. Terra Nova v. 4, pp. 374-384.

LIRER, F., 2000. *A new technique for retrieving calcareous microfossils from lithified lime deposits*. Micropaleontology, v. 46, no. 4, pp. 365-369.

LOEBLICH, A. R. Jr., TAPPAN, H., 1961. *Cretaceous planktonic foraminifera*: *Part 1. Cenomanian*. Micropaleontology, v. 7, pp. 257-304.

LOEBLICH, A. R. Jr., TAPPAN, H., 1964. *Protista 2. Sarcodina chiefly 'Thecamoebians' and Foraminiferida.* In: Moore, R. C., (ed.), Treatise of Invertebrate Paleontology, part C, v. 2 ., 900 pp.

LOEBLICH, A. R. Jr., TAPPAN, H., 1987. *Foraminiferal Genera and their Classification*. Van Nostrand Rienhold Company, New York, USA, 2 vol., 970 pp.

LONGORIA, J. F., 1974. *Stratigraphic, morphologic and taxonomic studies of Aptian planktonic Foraminifera.* Rev. Espanõla Micropaleont. Num. Extraord, 150 pp..

LUCIANI, V., COBIANCHI, M., JENKYNS, H. C., 2001. *Biotic and geochemical response to anoxic events: the Aptian pelagic succession of the Gargano Promontory (southern Italy)*. Geol. Magaz., v. 138, pp. 277-298.

LUCIANI, V., COBIANCHI, M., LUPI, C., 2006. *Regional record of a global oceanic anoxic event: OAE 1a on the Apulia Platform margin, Gargano Promontory, southern Italy.* Cretaceous Res., v. 27, pp. 754-772.

MAAMOURI, A-L., SALAJ, J., 1995. *New species of foraminiferal genera Globuligerina Bignot and Guyader, 1971 and Archaeokassabella n. gen.* In: the latest Valanginian of Tunisia. Zemni Plyn a Nafta, v. 40, pp. 131-145.

MAGNIEZ-JANNIN, F., BRÉHÉRET, J. G., DELANOY, G., 1997. *Un exemple de spéciation lié à l'eustatisme: l'apparition précoce de Schackoina cabri (foraminifère planctonique mésogéen).* Comptes Rendus de l'Académie des Sciences de Paris, Sciences de la Terre et des Planètes**,** v. 325, pp. 225-230.

MAGNIEZ-JANNIN, F., 1998. *L'élongation des loges chez les foraminifères planctoniques du Crétacé inférieur: une adaptation à la sous-oxygénation des eaux?* Comptes Rendus de l'Académie des Sciences, Paris, v. 326, pp. 207-213.

MAHONEY, J., STOREY, M., DUNCAN, R. A., SPENCER, K., PRINGLE, M., 1993. *Geochemistry and age of the Ontong-Java Plateau. In: The Mesozoic Pacific: geology tectonics and volcanism.* In: Pringle, M., Sager, W., Sliter, W. and Stein, S., (eds.), American Geophysical Union, Washington, D.C., pp. 233-262.

MAHONEY, J., SINTON, J. M., MACDOUGALL, J. D., SPENCER, K. J., LUGMAIR, G.W., 1994. *Isotope and trace element characteristics of a super-fast spreading ridge: East Pacific rise, 13–23ºS*. Earth Plan. Sci. Lett., v.121, pp. 173-193.

MALINVERNO, A., ERBA, E., HERBERT, T. D., 2010. *Orbital tuning as an inverse problem: Chronology of the early Aptian oceanic anoxic event 1a (Selli Level) in the Cismon APTICORE.* Paleoceanography, v. 25, doi:10.1029/2009PA001769.

MARIANOS, A. W., ZINGULA, R. P., 1966. *Cretaceous planktic foraminifers from Dry Creek, Tehama County, California.* J. Paleontol., v. 40, pp. 328-343.

MASTERS, B. A., 1977. *Mesozoic planktonic foraminifera, a word-wide review and analysis*. In: Ramsey, A. T. S. (ed.), Oceanic Micropalaeontology 1. Academic Press, London, pp. 301-731.

McARTHUR, J. M., DONOVAN, D. T., THIRLWALL, M. F., FOUKE, B. W., MATTEY, D., 2000. *Strontium isotope profile of the early Toarcian (Jurassic) oceanic anoxic event, the duration of ammonite biozones, and belemnite palaeotemperatures.* Earth Plan.. Sci. Lett., v.179, pp. 269-285.

McARTHUR, J. M., ALGEO, T. J., VAN DE SCHOOTBRUGGE, B., LI, Q., HOWARTH, R. J., 2008. *Basinal restriction, black shales, Re-Os dating, and the early Toarcian (Jurassic) oceanic anoxic event,* Paleoceanography, v. 23, doi: 10.1029/2008PA001607.

MÉHAY, S., KELLER, C. E., BERNASCONI, S. M., WEISSERT, H., ERBA, E., BOTTINI, C., HOCHULI, P. A., 2009.: *A volcanic CO_2 pulse triggered the Cretaceous Oceanic Anoxic Event 1a and a biocalcification crisis.* Geology, v. 37, pp. 819-822.

MÉLIÈRES, F., DEROO, G., HERBIN, J. P., 1978. *Organic-matter-rich and hypersiliceous Aptian sediments from western Mid-Pacific Mountain*s. In: Initial Reports of the Deep Sea Drilling Project, v. 62, Washington (U. S. Government Printing Office), pp. 903-915.

MENEGATTI, A. P., WEISSERT, H., BROWN, R. S., TYSON, R. V., FARRIMOND, P., STRASSER, A., CARON, M., 1998. *High-resolution $\delta^{13}C$ stratigraphy through the Early Aptian "Livello Selli" of the Alpine Tethys.* Paleoceanography, v. 13, pp. 530-545.

MILLÁN, M. I., WEISSERT, H. J., FERNANDEZ-MENDIOLA, P. A., GARCIA-MONDEJAR, J., 2009. *Impact of Early Aptian carbon cycle perturbations on evolution of a marine shelf system in the Basque-Cantabrian Basin (Aralar, N Spain).* Earth Plan. Sc. Lett., v. 287, pp. 392-401.

MOULLADE, M., 1960. *Sur quelques Foraminifères du Crétacé Inférieur des Baronnies (Drome).* Rev. Micropaléont., Paris, v. 3(4), pp. 216.

MOULLADE, M., 1961. *Quelques Foraminifères et ostracodes nouveaux du Crétacé inférieur vocontiern*. Rev. Micropaléont., v. 3, pp. 213-216.

MOULLADE, M., 1966. *Etude stratigrafique et micropaléontologique du Crétacé inférieur de la ''Fosse Vocontienne''*. Documents du Laboratoire de Géologie, Faculté des Sciences, Lyon, v. 15, pp. 369.

MOULLADE, M., KUHNT, W., BERGER, J. A., MASSE, J., TRONCHETTI, G., 1998. *Correlation of biostratrigraphic and stable isotope events in the Aptian historical stratotype of La Bedoule (souther France).* Comp. Rend., v. 327, pp. 693-698.

MOULLADE M., BELLIER J. P., TRONCHETTI G., 2002. *Hierarchy of criteria, evolutionary processes and taxonomic simplification in the classification of Lower Cretaceous planktonic foraminifera*. Cretaceous Res., London, v. 23, n. 1, pp. 111-148.

MOULLADE, M., TRONCHETTI, G., BELLIER, J. P., 2008. *Associations et biostratigraphie des foraminifères benthiques et planctoniques du Bédoulien sommital et Gargasien inférieur de la Tuilière-St-Saturnin-lès-Apt (Aire stratotypique de l'Aptien, Vaucluse, SE France).* Carnets de Géologie, v. 1, pp. 32 .

MOY, A. D., HOWARD, W. R., BRAY, S. G., TRULL, T. W., 2009. *Reduced calcification in modern Southern Ocean planktonic foraminifera*. Nat. Geosc., v. 2, pp. 276-280.

MUTTERLOSE J., MALKOC, M., SCHOUTEN, S., SINNINGHE DAMSTÉ, J. S., FORSTER, A., 2010. *TEX_{86} and stable $\delta^{18}O$ paleothermometry of early Cretaceous sediments:*

Implications for belemnite ecology and palaeotemperature proxy application. Earth Plan. Sci. Lett., v. 298, pp. 286-298.

MUTTERLOSE, J., BOTTINI, C., 2013. *Early Cretaceous chalks from the North Sea giving evidence for global change*, Nat. Commun., v. 4, pp. 1686, doi:10.1038/ncomms2698.

NEAGU, T., 1975. *Monographie de la faune des foraminifères éocretacés du couloir de Dimbovicioara, de Coclea e des Monts Persani (Couches de Carhaga).* Mémoires de l'Institut de Géologie et Géophysique, Bucarest, v. 25, pp. 1-141.

NEAL, C. R., COFFIN, M. F., ARNDT, N. T., DUNCAN, R. A., ELDHOLM, O., ERBA, E., FARNETANI, C., FITTON, J. G., INGLE, S. P., OHKOUCHI, N., RAMPINO, M. R., REICHOW, M. K., SELF, S., TATSUMI, Y., 2008. *Investigating Large Igneous Province Formation and Associated Paleoenvironmental Events: A White Paper for Scientific Drilling*. Scientific Drilling, No. 6, pp. 4-18.

NORRIS, R. D., WILSON, P. A., 1998. *Low-latitude sea-surface temperature for the mid-Cretaceous and the evolution of planktonic foraminifera*. Geology, v. 26, pp. 823-826.

OBREGON DE LA PARRA, J., 1959. *Foraminiferos de la Formacion La Pena*. Bol. Asoc. Mex. Geolog. Petrol., v. 11, pp. 135-154.

PAGANI, M., CALDEIRA, K., ARCHER, D., ZACHOS, J. C., 2006. *An ancient carbon mystery*. Science, v. 314, pp. 1556-1557.

PAULY, S., MUTTERLOSE, J., WRAY, D. S., 2013. *Palaeoceanography of Lower Cretaceous (Barremian-Lower Aptian) black shales from northwest Germany evidenced by calcareous nannofossils and geochemistry*. Cretaceous Res., v. 42, pp. 28-43.

PEARSON, P. N., 1998. *Stable isotopes and the study of evolution in planktonic foraminifera*. In: Norris & Corfield 1998, (eds.), pp. 138-178.

PETRIZZO M. R., HUBER B. T., WILSON P.A., MACLEOD K. G., 2008. *Late Albian paleoceanography of the western tropical North Atlantic.* Paleoceanography, 23, PA1213, 17 pp., doi: 10.1029/2007PA001517.

PETRIZZO, M. R., HUBER, B. T., GALE, A. S., BARCHETTA, A., JENKYNS, H. C., 2012. *Abrupt planktic foraminiferal turnover across the Niveau Kilian at Col de Pré-Guittard (Vocontian Basin, southeast France): new criteria for defining the Aptian/Albian boundary.* Newsl. Stratigr., v. 45, pp.55-74.

PETRIZZO, M. R., HUBER, B. T., GALE, A. S., BARCHETTA, A., JENKYNS, H. C., 2013. *Erratum: Abrupt planktic foraminiferal turnover across the Niveau Kilian at Col de Pré-Guittard (Vocontian Basin, southeast France): new criteria for defining the Aptian/Albian boundary.* Newsl. Stratigr., v. 46, p. 93.

PEUCKER-EHRENBRINK, B., RAVIZZA, G., 2000. *The marine osmium isotope record*. Terra Nova, v. 12, pp. 205-219.

PFLAUMANN, U., KRASHENINNIKOV, V. A., 1978. *Early Cretaceous planktonic foraminifers from eastern North Atlantic, DSDP Leg 41*.In: Initial Reports of the Deep Sea Drilling Project, v. 41, Washington (U. S. Government Printing Office), pp. 539-564.

POKORNÝ, V., 1958. *Grundzüge der Zoologischen Mikropaläontologie.* Volume 1. VEB Deutscher Verlag der Wissenschaften, Berlin, 582 pp.

PREMOLI SILVA, I., ERBA, E., TORNAGHI, M., 1989. *Paleoenvironmental signals and changes in surface fertility in mid-Cretaceous C_{org}-rich facies of the Fucoidi Marls (central Italy)*. Geobios, Mémoire Spécial , v. 11, pp. 225-236.

PREMOLI SILVA, I., SLITER, W. V., 1994. *Cretaceous planktonic foraminiferal biostratigraphy and evolutionary trends from the Bottaccione section, Gubbio, Italy*. Palaeontographia Italica, v. 82 (1995), pp. 1-89.

PREMOLI SILVA, I., SLITER, W. V., 1997. *Cretaceous Paleoceanography: Evidence from planktonic foraminiferal evolution*. EUG 9, Abstract Supplement 1, Terra Nova, v. 9, p. 615.

PREMOLI SILVA, I., SLITER, W. V., 1999. *Cretaceous Paleoceanography: Evidence from planktonic foraminiferal evolution*. In: Barrera, E., & Johnson, C. C. (eds.), The Evolution of Cretaceous Ocean-Climatic System; Geol. Soc. Amer., Special Paper 332, pp. 301-328.

PREMOLI SILVA, I., ERBA, E., SALVINI, G., VERGA, D., LOCATELLI, C., 1999. *Biotic changes in Cretaceous anoxic events*. J. Foraminiferal Res., v. 29, pp. 352-370.

PRICE, G. D., 2003. *New constraints upon isotope variation during the early Cretaceous (Barremian-Cenomanian) from the Pacific Ocean*. Geolog. Magaz., v. 140, pp. 513-522.

RAVIZZA, G., NORRIS, R. N., BLUSZTAJN, J., AUBRY, M. P., 2001. *An osmium isotope excursion associated with the late Paleocene thermal maximum: Evidence of intensified chemical weathering*. Paleoceanography, v. 16, p. 155-163.

REBOULET, S., HOEDEMAEKER, P. J., AGUIRRE-URRETA, M. B., ALSEN, P., ATROPS, F., BARABOSHKIN, E. Y., COMPANY, M., DELANOY, G., DUTOUR, Y., KLEIN, J., LATIL, J. L., LUKENEDER, A., MITTA, V., MOURGUES, F. A., PLOCH, I., RAISOSSADAT, N., ROPOLO, P., SANDOVAL, J., TAVERA, J. M., VAŠIČEK, Z., VERMEULEN, J., ARNAUD, H., GRANIER, B., PREMOLI SILVA, I., 2006. *Report on the 2nd international meeting of the IUGS Lower Cretaceous Ammonite Working Group, the "Kilian Group" (Neuchâtel, Switzerland, 8 September 2005).* Cretaceous Res., v. 27, pp. 712-715.

RISCH, H., 1971. *Stratigraphie der höheren Unterkreide der bayerischen Kalkalpen mit Hilfe von Mikrofossilien*. Palaeontographica, Abteilung A, v. 138, pp. 1-80.

ROTH, P. H., 1981. *Mid-Cretaceous calcareous nannoplankton from central Pacific: implications for palaeoceanography*. In: J. Thiede, T. L. Vallier *et al.*, Initial Reports of the Deep Sea Drilling Project 62. Washington: (U.S. Government Printing House), pp. 471-89.

SABATINO, N., NERI, R., BELLANCA, A., JENKYNS, H. C., BAUDIN, F., PARISI, G., MASETTI, D., 2009. *Carbon-isotope records of the early Jurassic (Toarcian) oceanic anoxic event from the Valdorbia (Umbria–Marche Apennines) and Monte Mangart (Julian Alps) sections: Palaeoceanographic and stratigraphic implications*. Sedimentology, v. 56, pp. 1307-1328.

SALAJ, J., 1984. *Foraminifers and detailed microbiostratigraphy of the boundary beds of the Lower Cretaceous stages in the Tunisian Atlas*. Geologicky Zbornik, v. 35, pp. 583-599.

SALAJ, J., 1990. *Problematic age of Lower Cretaceous foraminiferal Zone Leupoldina cabri*. Zapadne Karpaty, Seria Paleontologia, v. 14, pp. 21-25.

SCHLANGER, S.O., JENKYNS, H.C., 1976. *Cretaceous oceanic anoxic events: causes and consequences.* Geol. Mijnb., v. 55, pp. 179-184.

SCHOLLE, P. A., ARTHUR, M. A., 1980. *Carbon isotope fluctuations in Cretaceous pelagic limestones: Potential stratigraphic and petroleum exploration tool*. AAPG Bull., v. 64, pp. 67-87.

SCHOUTEN, S., HOPMANS, S., FORSTER, A., VAN BREUGEL, Y., KUYPERS, M. M. M., SINNINGHE DAMSTÉ, J. S., 2003. *Extremely high sea-surface temperatures at low latitudes during the middle Cretaceous as revealed by archaeal membrane lipids.* Geology, v. 31, pp. 1069-1072.

SHACKLETON, N. J., OPDYKE, N. D., 1973. *Oxigen isotope and paleomagnetic stratigraphy of equatorial Pacific core* V28-238: *Oxigen isotope temperatures and ice volumes on a 10^5 year and 10^6 year scale.* Quatern. Res., v. 3, pp. 39-55.

SHANIN, A.M., 1993. *Biostratigraphy of the subsurface Lower Cretaceous succession in the Bardawli area, northern Sinai, Egypt*. Neues Jahrbuch fuer Geologie und Palaeontologie, Monatshefte 1993, pp. 413-433.

SIGAL, J., 1952. *Aperçu stratigraphique sur la micropaléontologie du Crétacé.* XIX Congrés Géologique International, Monographies Régionales, 1 série, Algérie, v. 26, pp. 1-47.

SIGAL, J., 1958. *La Classification actuelle des familles de Foraminifères plantonique du Crétacé*. C. R. Soci. Géol. Fr., v. 12, pp. 262-265.

SIGAL, J., 1959. *Notes Micropaléontologiques Alpines. Les genre Schackoina et Leupoldina dans le Gargasien Vocontien: Etude de morphogénèse*. Rev. Micropal., v. 2, pp. 68-79.

SIGAL, J., 1977. *Essai de zonation du Crétacé méditerranéen à l'aide des Foraminiféres planctoniques.* Géol. Méditer., v. 4, pp. 99-108.

SIGAL, J., 1979. *Chronostratigraphy and Ecostratigraphy of Cretaceous formations recovered on DSDP Leg 47B, Site 398*. In: Initial Reports of the Deep Sea Drilling Project, v. 47. Washington (U. S. Government Printing Office), pp. 287-326.

SINTON, C. W., DUNCAN, R. A., 1997. *Potential links between ocean plateau volcanism and global ocean anoxia at the Cenomanian-Turonian boundary*. Econ. Geol., v. 92, pp. 836-842.

SLITER, W. V., 1989. *Aptian anoxia in the Pacific Basin*. Geology, v. 17, pp. 909-912.

SLITER, W. V., 1992. *Cretaceous planktonic foraminiferal biostratigraphy and paleoceanographic events in the Pacific Ocean with emphasis on indurated sediment*. In: Ishizaki, K., Saito, T. (Eds.), Centenary of Japanese Micropaleontology. Terra Scientific Publishing Company, Tokyo, pp. 281-299.

SLUIJS, A., ROHL, U., SCHOUTEN, S., BRUMSACK, H. J., SANGIORGI, F., SINNINGHE DAMSTÉ, J. S., BRINKHUIS, H., 2008. *Arctic late Paleocene-early Eocene paleoenvironments with special emphasis on the Paleocene-Eocene thermal maximum (Lomonosov Ridge, Integrated Ocean Drilling Program Expedition 302).* Paleoceanography, v. 23, doi: 10.1029/2007PA001495.

SPEIJER, R. P., WAGNER, T., 2002. *Sea-level changes and black shales associated with the late Paleocene thermal maximum: Organic-geochemical and micropaleontologic evidence from the southern Tethyan margin (Egypt-Israel).* Geol. Soc. Amer. Special Papers, v. 356, pp. 533-549.

STEIN, M., FOLLMI, K. B., WESTERMANN, S., GODET, A., ADATTE, T., MATERA, V., FLEITMANN, D., BERNER, Z., 2011. *Progressive palaeoenvironmental change during the Late Barremian-Early Aptian as prelude to Oceanic Anoxic Event 1a: Evidence from the Gorgo a Cerbara section (Umbria-Marche basin, central Italy)*. Palaeogeogr. Palaeocl. Paleoecol., v. 302, pp. 396-406.

SUBBOTINA, N. N., 1949. *Microfauna of the Cretaceous of the southern slope of Caucasus. Microfauna of the oil fields of USSR, 2.* Trudy Vsesoyuznogo Neftyanogo Nauchnoissledovatel'skogo Geologo-razvedochnogo Instituta (VNI-GRI), new series, v. 34, pp. 1-168.

TAPPAN, H., 1940. *Foraminifera from the Grayson Formation of northern Texas*. Journal of Paleontology, v. 14, pp. 93-126.

TARDUNO, J. A., SLITER, W. V., BRALOWER, T. J., McWILLIAMS, M., PREMOLI SILVA, I., OGG., J. G., 1989. *M-sequence reversals recorded in DSDP sediment cores from the western Mid-Pacific Mountains and Magellan Rise*. Bull. Geol. Soc. Amer., v. 101, pp. 1306-1316.

TARDUNO, J. A., SLITER, W. V., KROENKE, L., LECKIE, M., MAYER, H., MAHONEY, J. J., MUSGRAVE, R., STOREY, M., WINTERER, E. L., 1991. *Rapid formation of Ontong Java Plateau by Aptian mantle plume volcanism*. Science, v. 254, pp. 399-403.

TEJADA, M. L. G., KATSUHIKO S., KURODA, J., COCCIONI, R., MAHONEY, J. J., OHKOUCHI, N., SAKAMOTO, T., TATSUMI, Y., 2009. *Ontong Java Plateau eruption as a trigger for the early Aptian oceanic anoxic event.* Geology, v. 37, pp. 855-858.

THIEDE, J., DEAN, W. E., REA, D. K., VALLIER, T. L., ADELSECK C. G., 1981. *The geologic history of the Mid-Pacific Mountains in the central North Pacific Ocean: A synthesis of deep-sea drilling studies*. In: Initial Reports of the Deep Sea Drilling Project, v. 62,. Washington (U. S. Government Printing Office), pp. 1073-1120.

TORNAGHI, M. E., PREMOLI SILVA, I., RIPEPE, M., 1989. *Lithostratigraphy and planktonic foraminiferal biostratigraphy of the Aptian-Albian "Scisti a Fucoidi" in the Piobbico core, Marche, Italy: background for cyclostratigraphy*. Riv. Ital. Paleont. Stratig., v. 95, pp. 223-264.

TURGEON S. C., CREASER R. A., 2008. *Cretaceous oceanic anoxic event 2 triggered by a massive magmatic episode.* Nature, v. 454, pp. 323.

VAN BREUGEL, Y., SCHOUTEN, S., TSIKOS, H., ERBA, E., PRICE, G. D., SINNINGHE DAMSTÉ, J. S., 2007. *Synchronous negative carbon isotope shifts in marine and terrestrial biomarkers at the onset of the early Aptian oceanic anoxic event 1a: Evidence for the release of ^{13}C-depleted carbon into the atmosphere.* Paleoceanography, v. 22, doi: 10.1029/2006PA001341.

VERGA, D., PREMOLI SILVA, I., 2002. *Early Cretaceous planktonic foraminifera from the Tethys: the genus Leupoldina*. Cretaceous Res., v. 23, pp. 189-212.

VERGA, D., PREMOLI SILVA, I., 2003a. *Early Cretaceous planktonic foraminifera from the Tethys: the small, few-chambered representatives of the genus Globigerinelloides*. Cretaceous Res., v. 24, pp. 305-334.

VERGA, D., PREMOLI SILVA, I., 2003b. *Early Cretaceous planktonic foraminifera from the Tethys: the large-sized, many-chambered representatives of the genus Globigerinelloides*. Cretaceous Res., v. 24, pp. 661-690.

VERGA, D., 2004. *The first evolutionary radiation of planktonic Foraminifera in the Valanginian-Aptian interval: taxonomical, biostratigraphical and paleocological implications.* PhD Thesis, pp. 1-134.

VERGA, D., PREMOLI SILVA, I., 2005. *Early Cretaceous planktonic foraminifera from the Tethys: the Upper Aptian, planispiral morphotypes with elongate chambers.* Cretaceous Res., v. 26, pp. 239-259.

WEISS, W., **1995**. *Aptian planktonic foraminifers from the Wiechendorf 1/86 borehole*. Geologisches Jahrbuch Hannover, v. 141, pp. 113-131.

WEISSERT, H., McKENZIE, J. A., CHANNELL, J. E. T., 1985. *Natural variations in the carbon cycle during the Early Cretaceous, in The Carbon Cycle and Atmospheric CO_2: Natural Variations Archean to Presen.* In: E. T. Sundquist & W. S. Broeker, (eds.), Geophys. Monogr. Ser., v. 32, pp. 531-545.

WEISSERT, H., 1989. *C-isotope stratigraphy, a monitor of paleoenvironmental changes: A case study from the Early Cretaceous.* Surv. Geophys., v. 10, pp. 1-61.

WEISSERT, H., LINI, A., 1991. *Ice Age interludes during the time of Cretaceous greenhouse climate?* In: D.W. Muller, J. A. McKenzie & H. Weissert, (eds.), Controversies in modern geology. Academic, San Diego, Calif., pp. 173-191.

WEISSERT, H., LINI, A., FÖLLMI, K. B., KUHN, O., 1998. *Correlation of Early Cretaceous carbon isotope stratigraphy and platform drowning events: a possible link?* Palaeogeogr., Palaeoclimatol., Palaeoecol., v. 137, pp. 189-203.

WEISSERT, H., ERBA, E., 2004. *Volcanism, CO_2 and palaeoclimate: a Late Jurassic-Early Cretaceous carbon and oxygen isotope record.* J. Geol. Soc., London, v. 161, pp. 695-702.

WEZEL, F. C., 1985. *Facies Anossiche ed episodi geotettonici globali*. Giornale di Geologia, v. 47, pp. 283–288.

WILSON, P. A., NORRIS, R. D., COOPER, M. J., 2002. *Testing the mid-Cretaceous greenhouse hypothesis using glassy foraminiferal calcite from the core of the Turonian tropics on Demerara Rise*. Geology, v. 30, pp. 607-610.

ZAKHAROV, Y. D., BARABOSHKIN, E. Y., WEISSERT, H., MICHAILOVA, I. A., SMYSHLYAEVA, O. P., SAFRONOV, P. P., 2013. *Late Barremian-early Aptian climate of the northern middle latitudes: Stable isotope evidence from bivalve and cephalopod molluscs of the Russian Platform.* Cretaceous Res., v. 44, pp. 183-201.

Plate 1

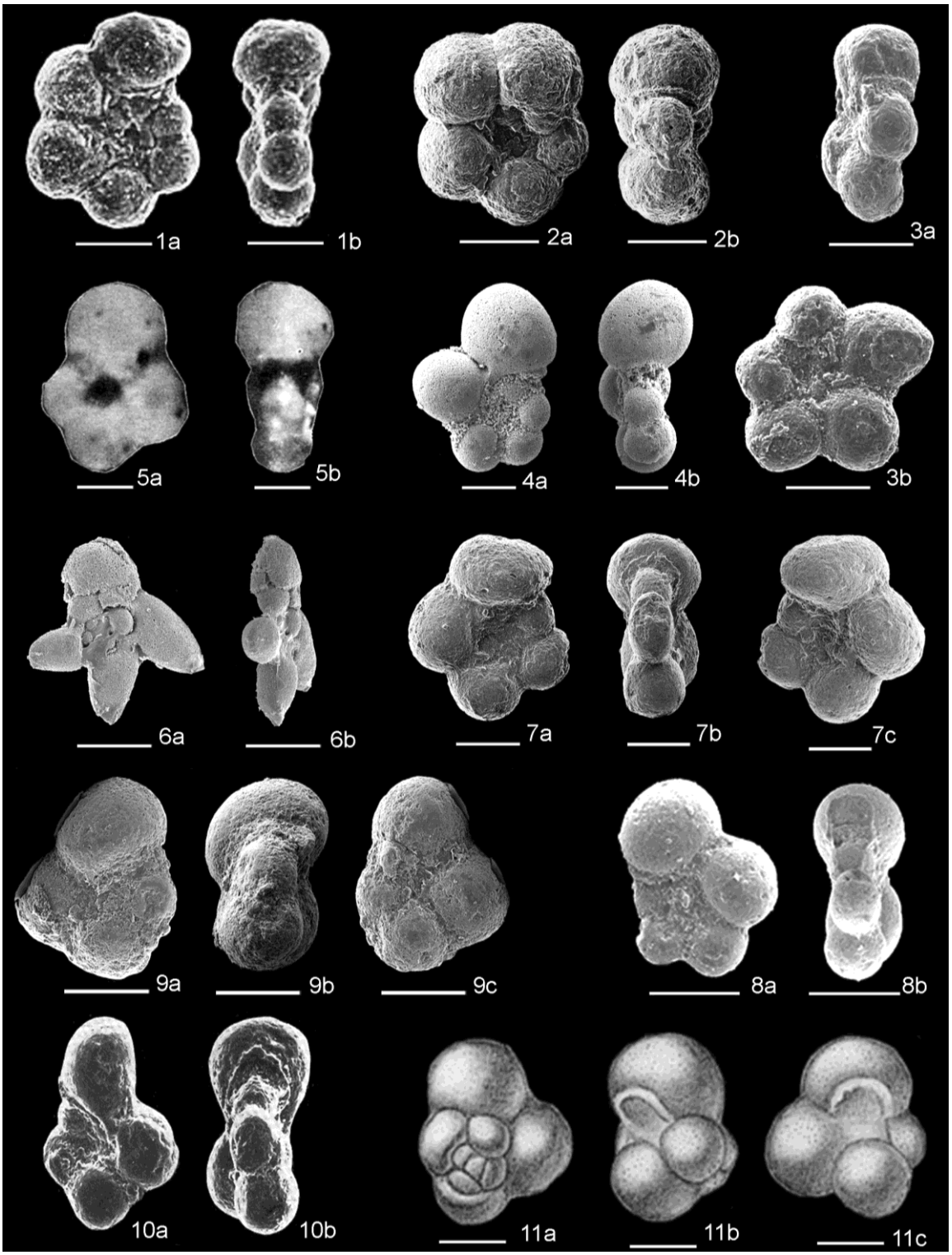

Plate 1. 1 a-b. *Globigerinelloides aptiensis* (Longoria, 1974), holotype, Gargas, France. **2 a-b.** *Globigerinelloides blowi* (Bolli, 1959), holotype, Cuche Formation, Trinidad; **3 a-b.** *Globigerinelloides blowi lobatus* (Verga & Premoli Silva, 2005), holotype, Lesches en Diois section, France; **4 a-b.** *Globigerinelloides clavatus* (Verga & Premoli Silva, 2005), holotype, Lesches en Diois section, France; **5 a-b.** *Globigerinelloides duboisi* (Chevalier, 1961), holotype, Nerthe Mountains, SE France; **6 a-b.** *Globigerinelloides elongatus* (Verga & Premoli Silva, 2005), holotype, Cismon section, Italy; **7 a-c** *Globigerinelloides maridalensis* (Bolli, 1959), holotype, Eastern Central Range, Trinidad; **8 a-b.** *Globigerinelloides paragottisi* (Verga & Premoli Silva, 2003), holotype, Lesches en Diois, France; **9 a-c.** *Globigerinelloides primitivus* (Fuchs, 1971), holotype,Vorarlberg, Austria; **10 a-b.** *Globigerinelloides sigali* (Longoria, 1974), holotype, La Boca Canyon, Mexico; **11 a-c.** *Gorbachikella kugleri* (Bolli, 1959), holotype, Cuche Formation, Trinidad. All scale bars = 100 μm.

Plate 2

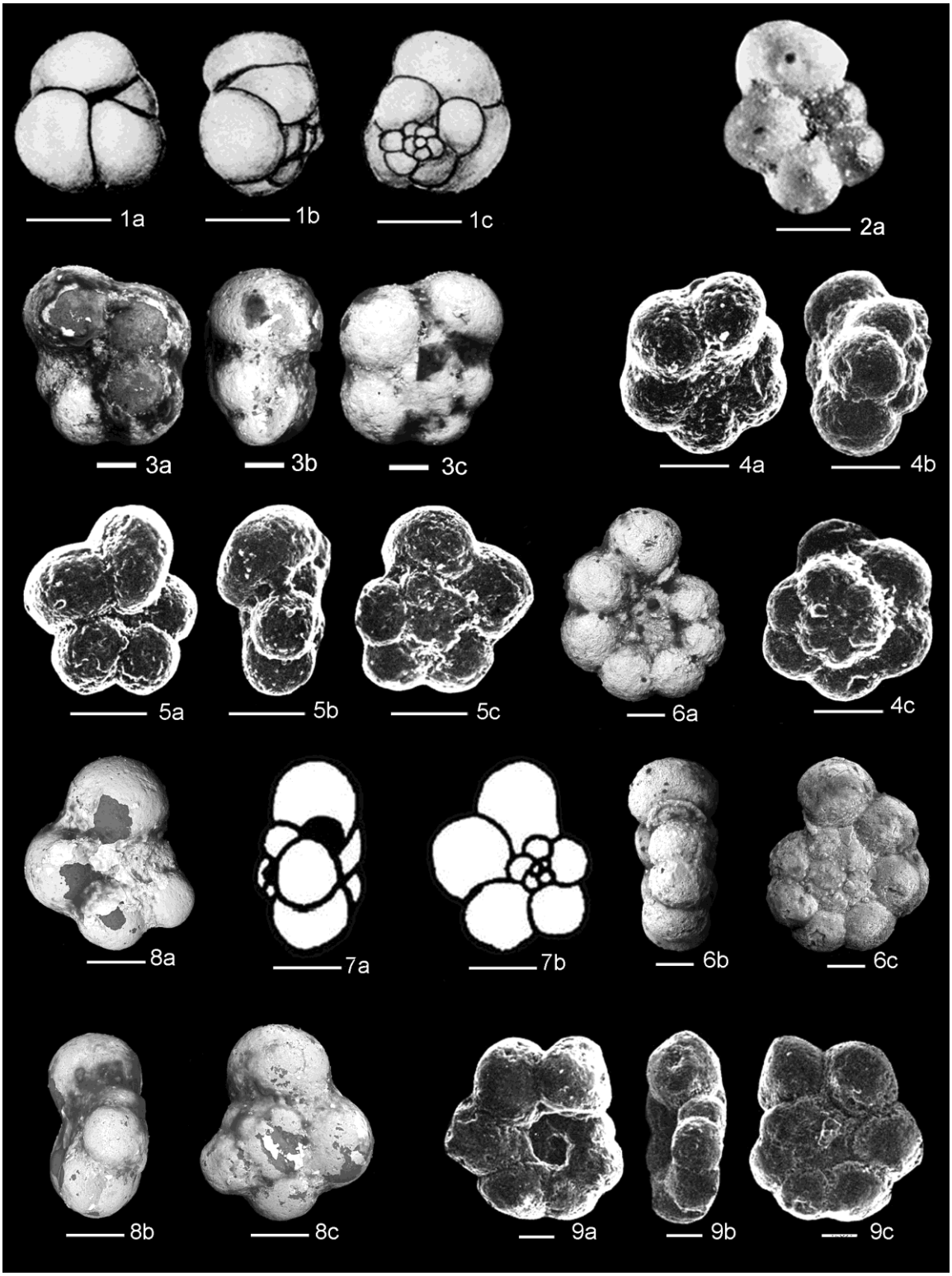

Plate 2. 1 a-c. *Gubkinella graysonensis* (Tappan, 1940), holotype, Grayson Formation, Texas. **2 a.** *Hedbergella aptiana* (Bartenstein, 1965), holotype, Mitteland-Kanal, central Germany; **3 a-c.** *Hedbergella daminiae* (Banner, Copestake & White, 1993), holotype, North Sea Well 15/30-3; **4 a-c.** *Hedbergella excelsa* (Longoria, 1974), holotype, Drome region, SE France; **5 a-c.** *Hedbergella gorbachikae* (Longoria, 1974), holotype, La Boca Canyon, Mexico; **6 a-c.** *Hedbergella kuznetsovae* (Banner & Desai, 1988), holotype, Speeton Cliffs, Filey Bay, North Yorkshire; **7 a-b** *Hedbergella infracretacea* (Glaessner, 1937), holotype, NW Caucasus; **8 a-c.** *Hedbergella laculata* (Banner, Copestake & White, 1993), holotype, Valhall Formation, central North Sea; **9 a-c.** *Hedbergella luterbacheri* (Longoria, 1974), holotype, La Boca Canyon, Mexico. All scale bars = 50 μm, except 2a, 5a-c and 7a-b = 100 μm.

Plate 3

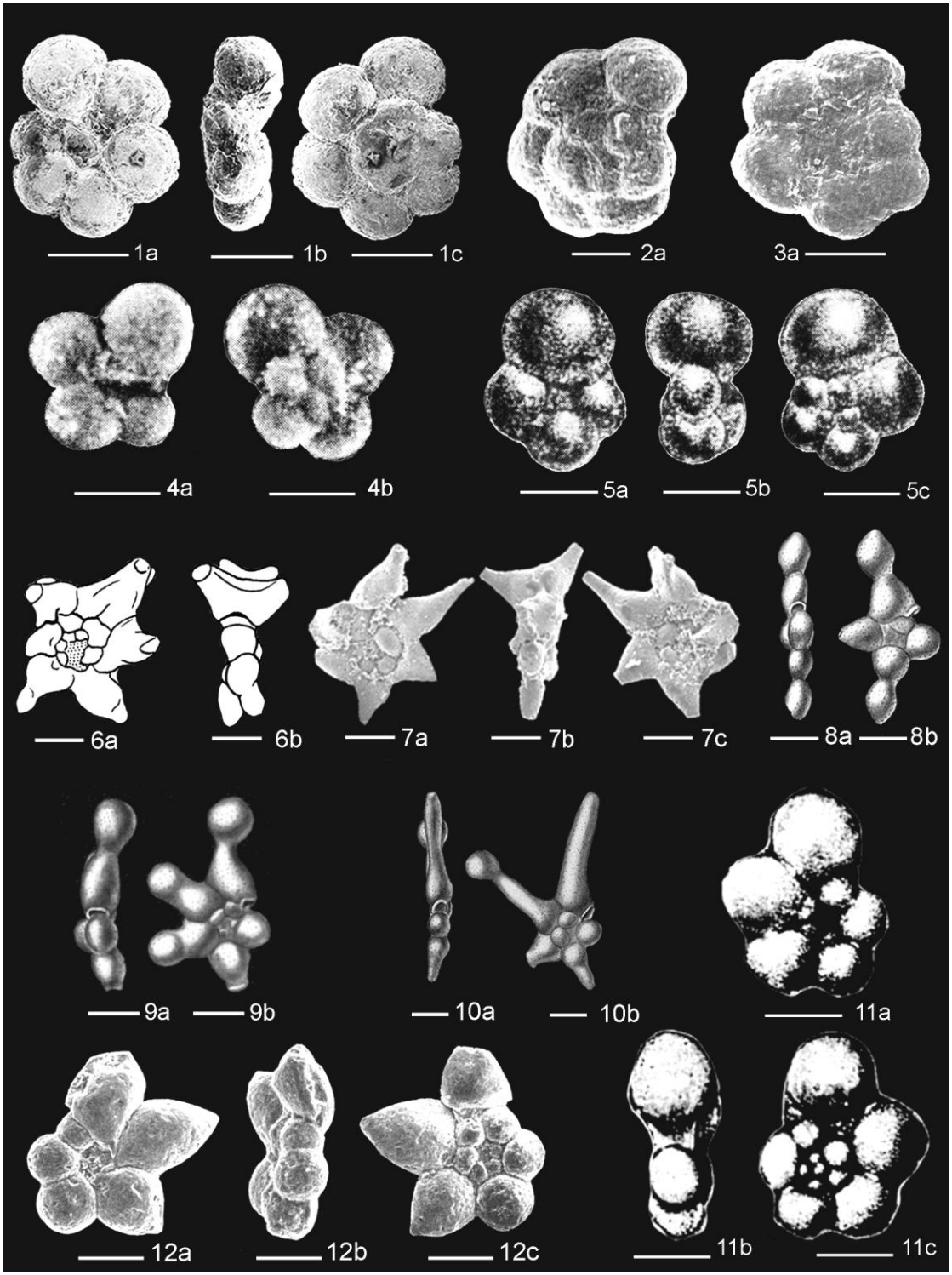

Plate 3. 1 a-c. *Hedbergella occulta* (Longoria, 1974), holotype, La Boca Canyon, Mexico; **2 a.** *Hedbergella praetrocoidea*, holotype, SW Crimea; **3 a.** *Hedbergella primare* (Bolli, 1959), holotype, Kacha River, Ukraine; **4 a-b.** *Hedbergella sigali* (Moullade, 1966), holotype, Sant-Cyrice, SE France; **5 a-c.** *Hedbergella tuschepsensis* (Antonova, 1964), holotype, Tuscheps River, NW Caucasus; **6 a-b.** *Leupoldina cabri* (Sigal, 1952), holotype Djebel Rhazouane, Tunisia; **7 a-c.** *Leupoldina hexacamerata* (Verga & Premoli Silva, 2002), holotype, Cismon core, Italy; **8 a-b.** *Leupoldina pustulans pustulans* (Bolli, 1957), holotype, Centra Range, Trinidad; **9 a-b.** *Leupoldina pustulans quinquecamerata* (Bolli, 1957), holotype, Central Range, Trinidad; **10 a-b**. *Leupoldina reicheli* (Bolli, 1957), holotype, Central Range, Trinidad; **11 a-c.** *Lilliputianella globulifera* (Kretchmar & Gorbachik, 1971), holotype, Crimea; **12 a-c.** *Lilliputianella kuhryi* (Longoria, 1974), holotype, Argos Formation, SE Spain. All scale bars = 100 μm, except 2a and 3a= 50 μm.

Plate 4

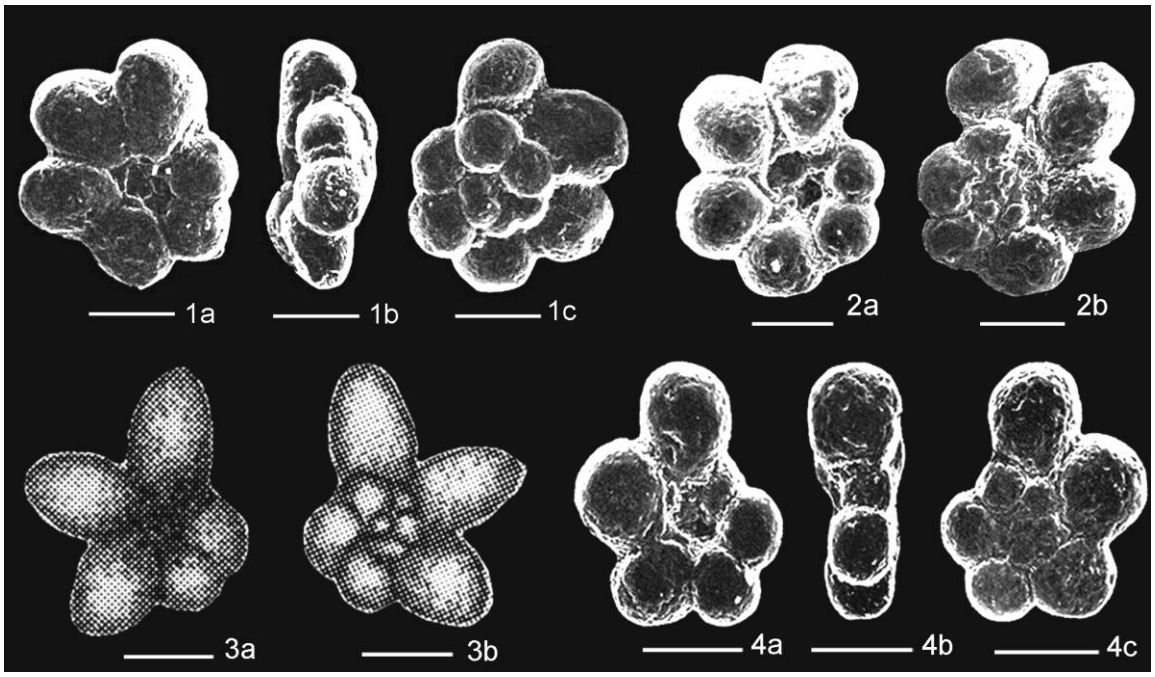

Plate 4. 1 a-c. *Lilliputianella labocaensis* (Longoria, 1974), holotype, La Boca Canyon, Mexico; **2 a-b.** *Lilliputianella maslakovae*, holotype, La Boca Canyon, Mexico; **3 a-b.** *Lilliputianella roblesae* (Obregòn de la Parra, 1959), holotype, Mexico; **4 a-c.** *Lilliputianella similis* (Longoria, 1974), holotype, La Boca Canyon, Mexico. All scale bars = 100 μm, except 3a-b = 50 μm.

Plate 5

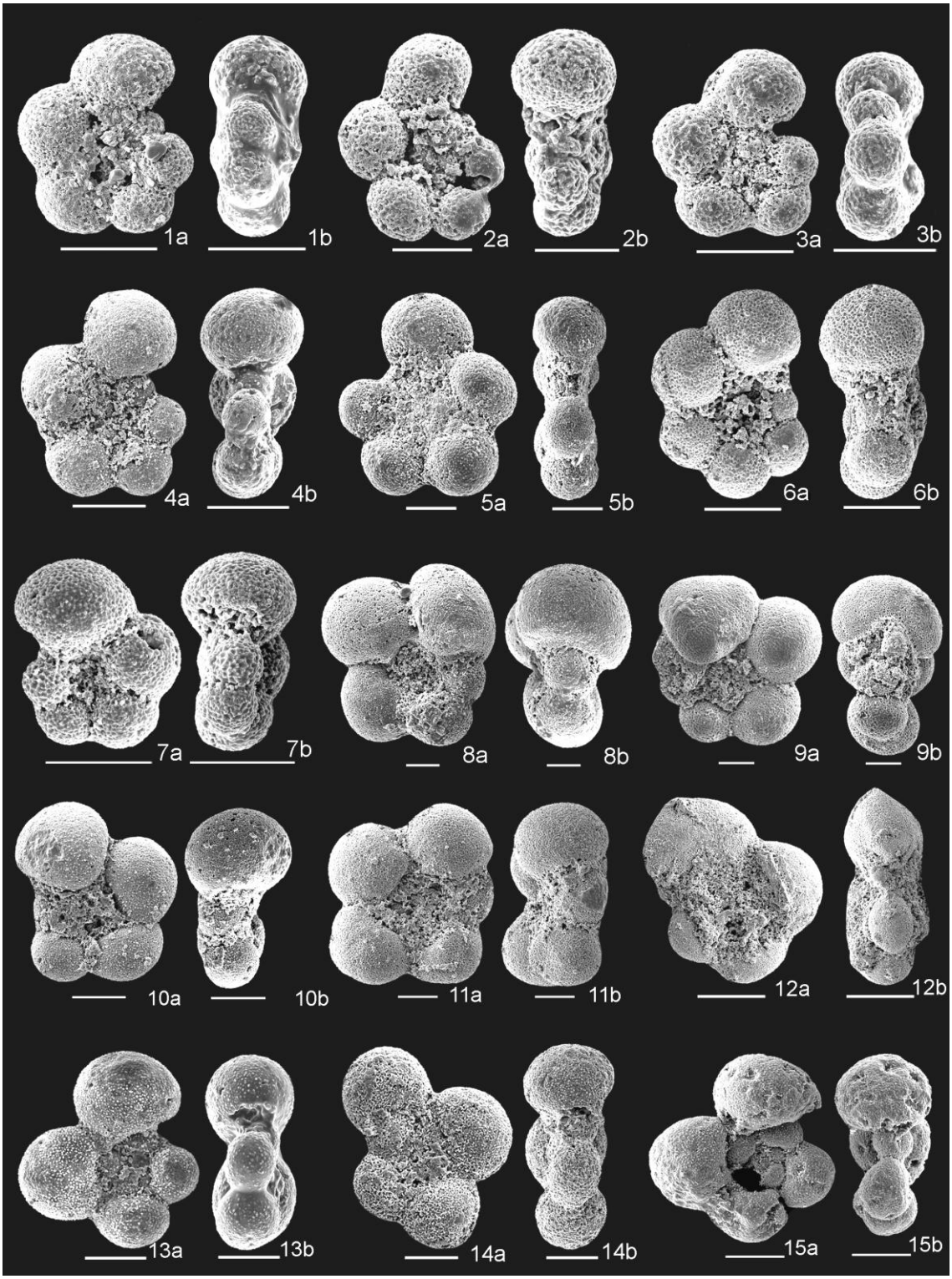

Plate 5. 1 a-b. *Globigerinelloides aptiensis*, Cismon 17/251-257 cm; **2 a-b.** *G. aptiensis*, Cismon 17/251-257 cm; **3 a-b.** *G. aptiensis*, Cismon 13/264-268 cm; **4 a-b.** *G. aptiensis*, Cismon 12/148-152 cm; **5 a-b.** *G. aptiensis*, Cismon 12/88-92 cm; **6 a-b.** *G. aptiensis*, Cismon 10/100-102 cm; **7 a-b** *Globigerinelloides blowi*, Cismon 14/141-145 cm; **8 a-b.** *G. blowi*, Cismon 12/230-234 cm; **9 a-b.** *G. blowi*, Cismon 12/209-214 cm; **10 a-b.** *G. blowi*, Cismon 12/69-71 cm; **11 a-c.** *G.* cf. *blowi*, Cismon 11/10-13 cm; **12 a-c.** *Globigerinelloides duboisi*, Cismon 13/20-24 cm; **13 a-c.** *G. duboisi*, Cismon 12/278-280 cm; **14 a-c.** *G. duboisi*, Cismon 12/148-152 cm; **15 a-c.** *G. duboisi*, Cismon 12/37-42 cm. All scale bars = 50 µm, except 12 a-c = 100 µm.

Plate 6

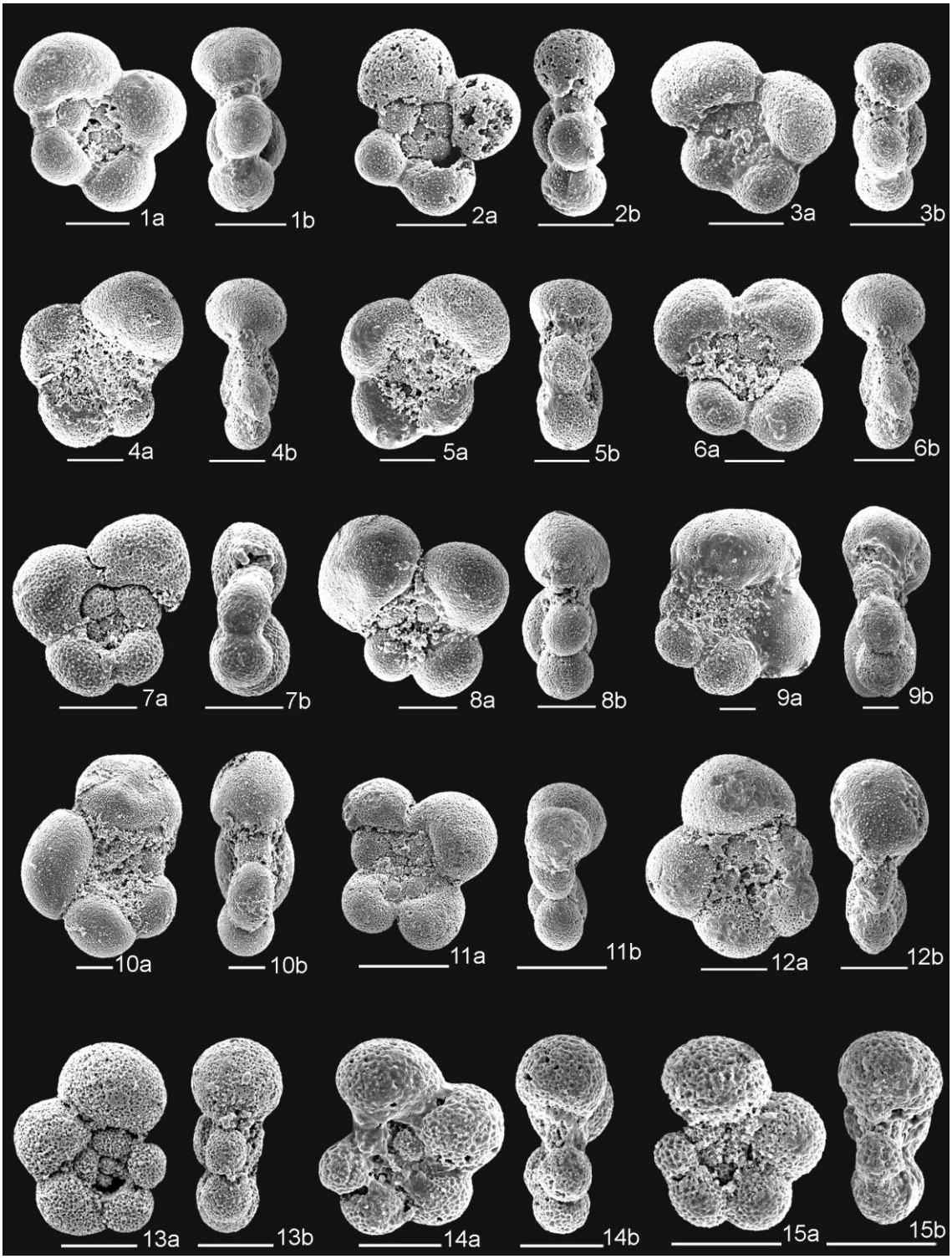

Plate 6. 1 a-b. *Globigerinelloides duboisi*, Cismon 11/281-284 cm; **2 a-b.** *G. duboisi*, Cismon 11/158-161 cm; **3 a-b.** *G. duboisi*, Cismon 11/74-76 cm; **4 a-b.** *G. duboisi*, Cismon 11/4-10 cm; **5 a-b.** *G. duboisi*, Cismon 11/1-4 cm; **6 a-b.** *G. duboisi*, Cismon 11/1-4 cm; **7 a-b** *G. duboisi*, Cismon 10/177-180 cm; **8 a-b.** *G. duboisi*, Cismon 10/177-180 cm; **9 a-b.** *Globigerinelloides maridalensis*, Cismon 12/230-234 cm; **10 a-b.** *G. maridalensis*, Cismon 12/209-214 cm; **11 a-b.** *G. maridalensis*, Cismon 12/290-293,5 cm; **12 a-b.** *G. maridalensis*, Cismon 11/143-145 cm; **13 a-b.** *Globigerinelloides paragottisi*, Cismon 15/262-271 cm; **14 a-b.** *G. paragottisi*, Cismon 15/262-271 cm; **15 a-b.** *G. paragottisi*, Cismon 14/141-145 cm. All scale bars = 50 μm.

Plate 7

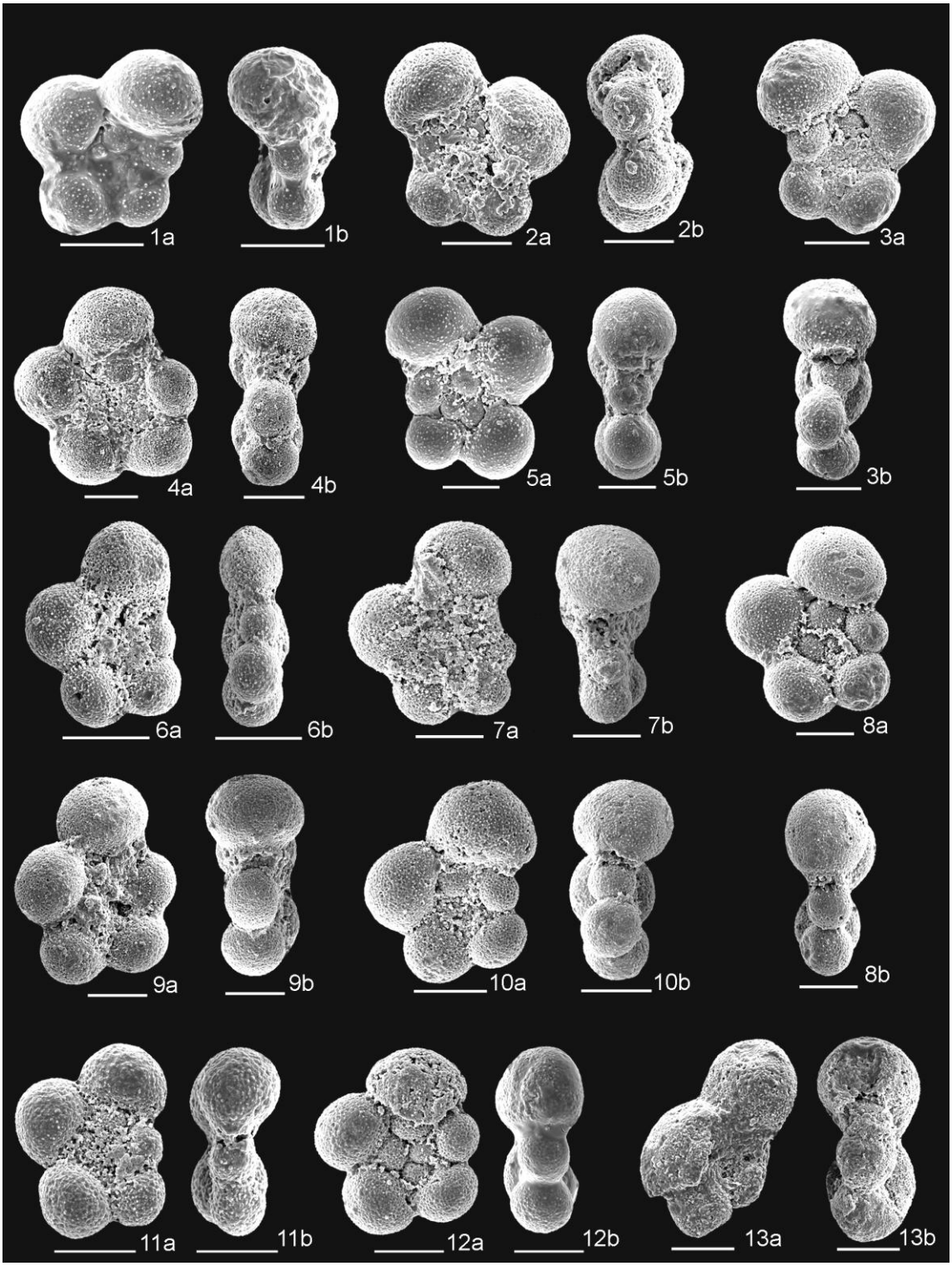

Plate 7. 1 a-b. *Globigerinelloides paragottisi*, Cismon 13/94-99 cm; **2 a-b.** *G. paragottisi*, Cismon 13/20-24 cm; **3 a-b.** *G. paragottisi*, Cismon 13/7-10 cm; **4 a-b.** *G. paragottisi*, Cismon 13/7-10 cm; **5 a-b.** *G. paragottisi*, Cismon 12/253-256,5 cm; **6 a-b.** *G. paragottisi*, Cismon 12/152-158 cm; **7 a-b** *G. paragottisi*, Cismon 12/81-84 cm; **8 a-b.** *G. paragottisi*, Cismon 12/69-71 cm; **9 a-b.** *G. paragottisi*, Cismon 11/290-293,5 cm; **10 a-b.** *G. paragottisi*, 11/281-284 cm; **11 a-b.** *G. paragottisi*, Cismon 11/184-186 cm; **12 a-b.** *G. paragottisi*, Cismon 10/177-180 cm; **13 a-b.** *Globigerinelloides primitivus*, Cismon 13/7-10 cm. All scale bars = 50 µm.

Plate 8

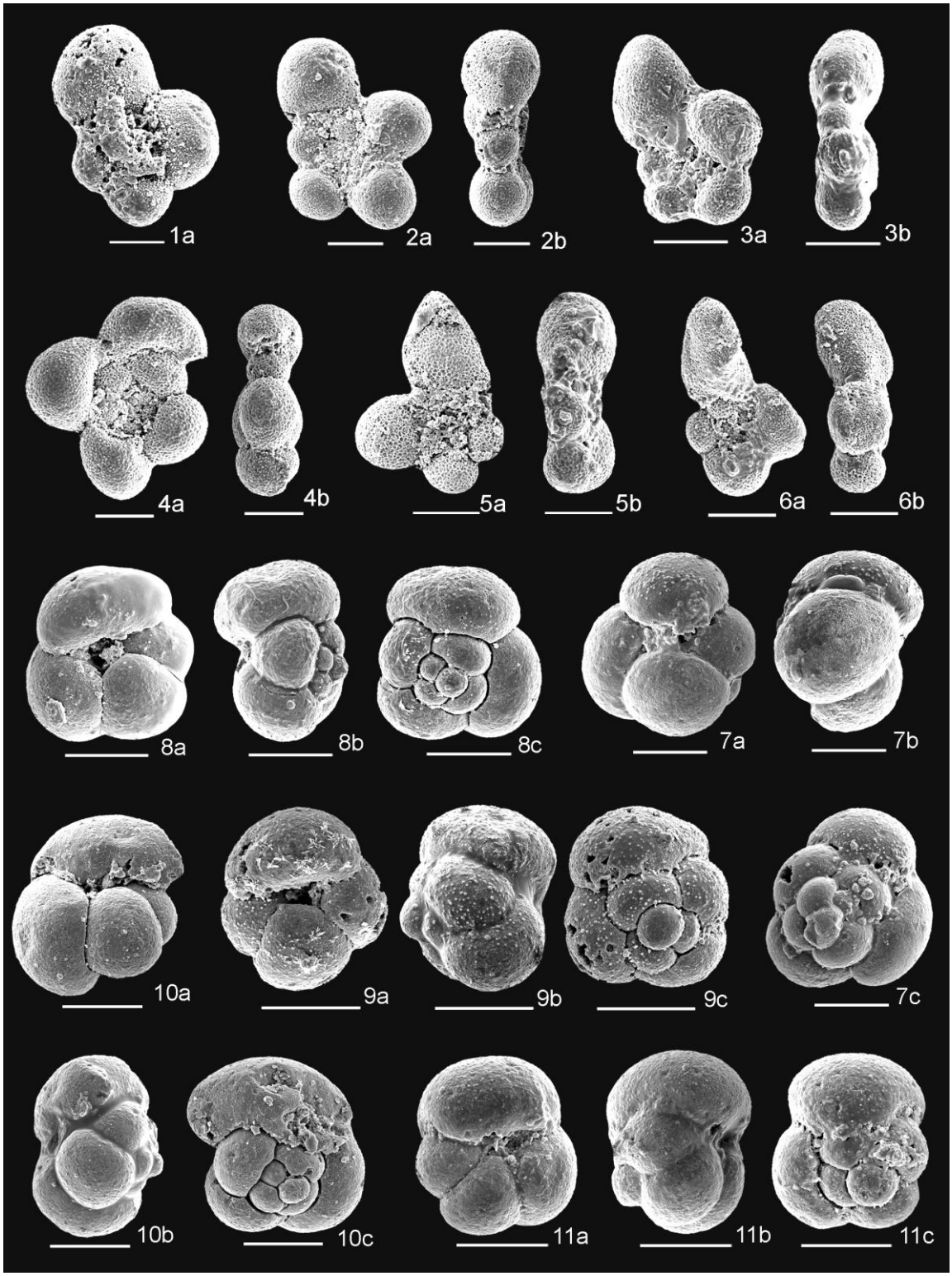

Plate 8. 1 a-b. *Globigerinelloides primitivus*, Cismon 12/69-71 cm; **2 a-b.** *Globigerinelloides clavatus*, Cismon 11/281-284 cm; **3 a-b.** *G. clavatus*, Cismon 10/177-180 cm; **4 a-b.** *Globigerinelloides elongatus*, Cismon 12/37-42 cm; **5 a-b.** *Globigerinelloides sigali*, Cismon 10/100-102 cm; **6 a-b.** *G. sigali*, Cismon 11/1-4 cm; **7 a-c.** *Gubkinella graysonensis*, Cismon 14/190-192 cm; **8 a-c.** *G. graysonensis*, Cismon 14/199-201 cm; **9 a-c.** *G. graysonensis*, Cismon 14/199-201 cm; **10 a-c.** *G. graysonensis*, Cismon 14/199-201 cm; **11 a-c.** *G. graysonensis*, Cismon 14/141-145 cm. All scale bars = 50 μm.

Plate 9

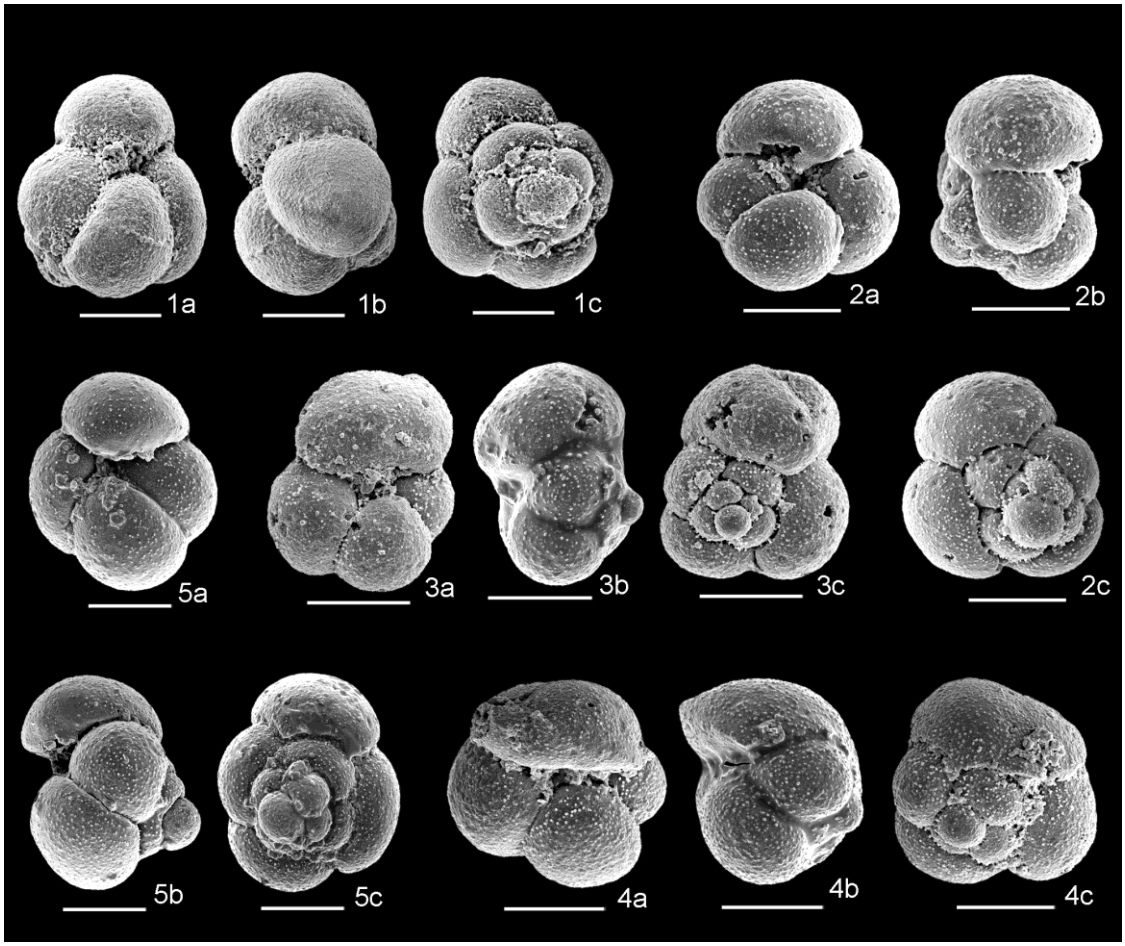

Plate 9. 1 a-b *Gubkinella graysonensis*, Cismon 14/113-115 cm; **2 a-c.** *G. graysonensis*, Cismon 14/25-30 cm; **3 a-c.** *G. graysonensis*, Cismon 13-264-268 cm; **4 a-c.** *G. graysonensis*, Cismon 13/264-268 cm; **5 a-c.** *G. graysonensis*, Cismon 12/37-42 cm. All scale bars = 50 μm.

Plate 10

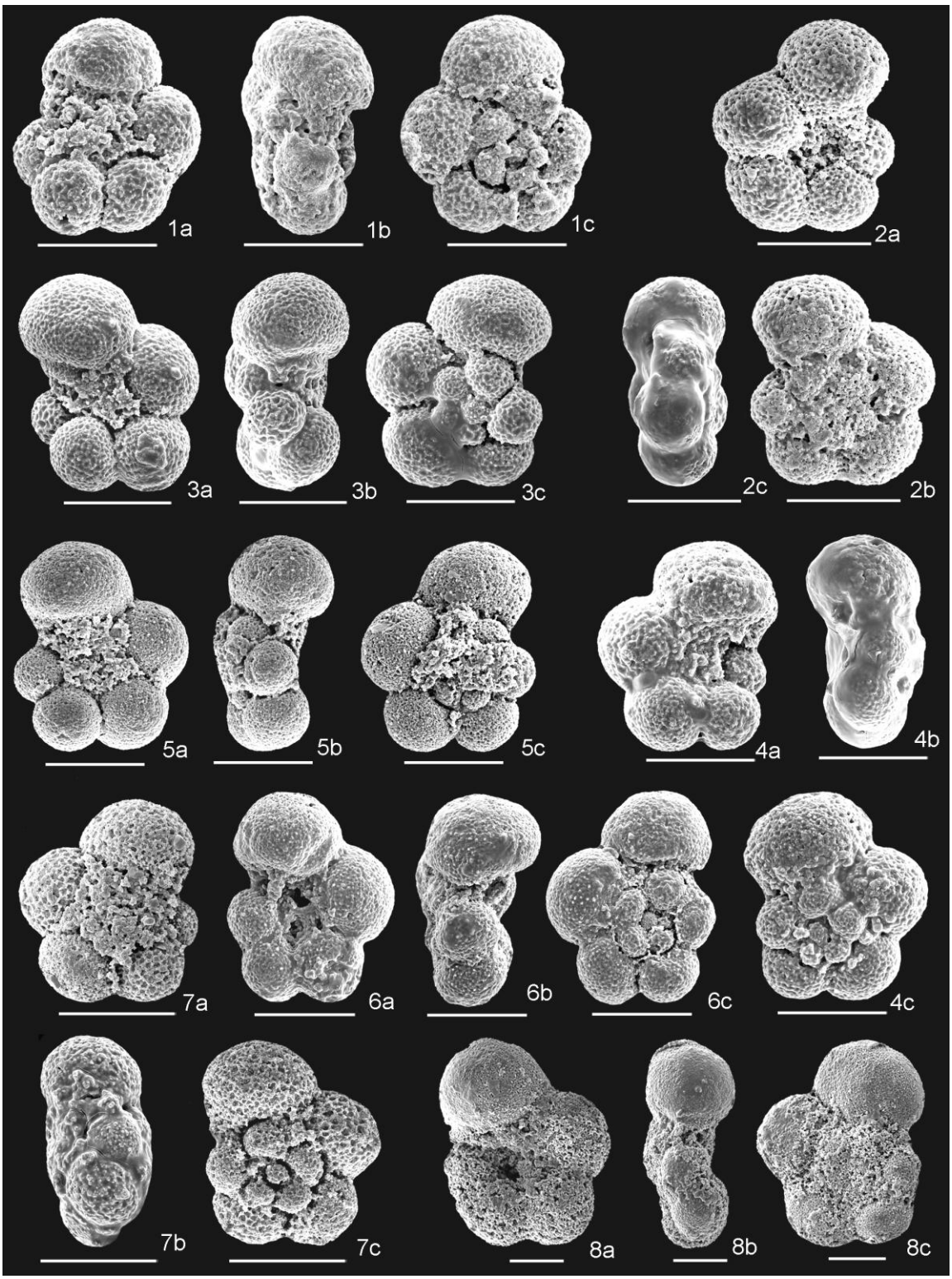

Plate 10. 1 a-c. *Hedbergella aptiana*, Cismon 15/304-307 cm; **2 a-c.** *H. aptiana*, Cismon 14/89-90 cm; **3 a-c.** *H. aptiana*, Cismon 13/183-186 cm; **4 a-c.** *H. aptiana*, Cismon 13/171-175 cm; **5 a-c.** *H. aptiana*, Cismon 13/53-57 cm; **6 a-c.** *H. aptiana*, Cismon 11/184-186 cm; **7 a-c.** *H. aptiana*, Cismon 17/32-42 cm; **8 a-c.** *H.* cf *aptiana*, Cismon 11/1-4 cm. All scale bars = 50 μm.

Plate 11

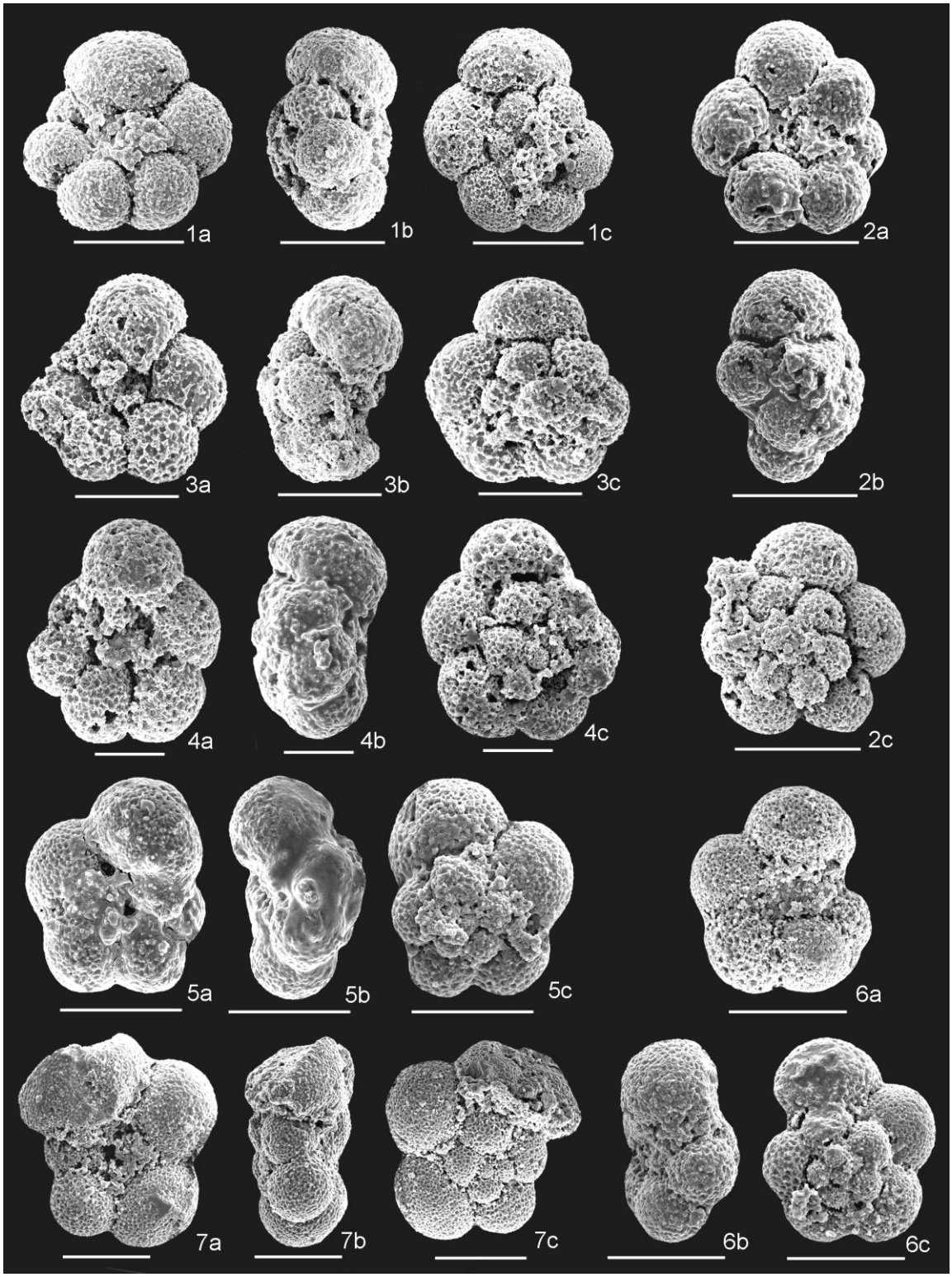

Plate 11. 1 a-c. *Hedbergella excelsa*, Cismon 17/251-257 cm; **2 a-c.** *H. excelsa*, Cismon 17/148-152 cm; **3 a-c.** *H. excelsa*, Cismon 16/120-129 cm; **4 a-c.** *H. excelsa*, Cismon 15/236-239 cm; **5 a-c.** *Hedbergella infracretacea*, Cismon 15/262-271 cm; **6 a-c.** *H. infracretacea*, Cismon 15/143-147 cm; **7 a-c.** *H. infracretacea*, Cismon 13/264-268 cm. All scale bars = 50 μm, except 4 a-c = 20 μm.

Plate 12

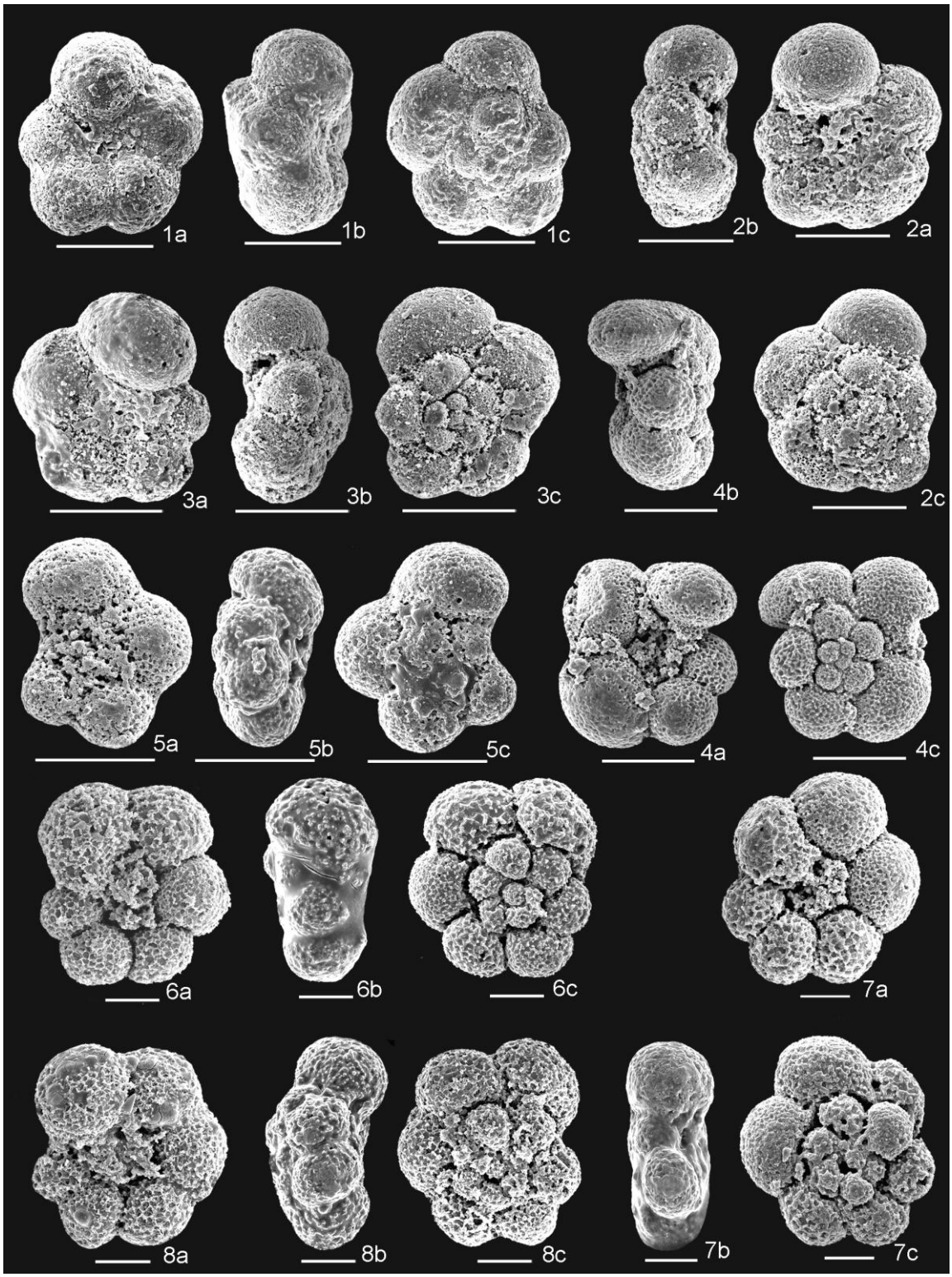

Plate 12. 1 a-c. *Hedbergella infracretacea*, Cismon 12/152-158 cm; **2 a-c.** *H. infracretacea*, Cismon 12/88-92 cm; **3 a-c.** *H. infracretacea*, Cismon 12/37-42 cm; **4 a-c.** *H.* cf. *infracretacea*, Cismon 15/262-271 cm; **5 a-c.** *Hedbergella laculata* Cismon 17/32-42 cm; **6 a-c.** *Hedbergella occulta*, Cismon 17/251-257 cm; **7 a-c.** *H. occulta*, Cismon 17/251-257 cm; **8 a-c.** *H. occulta*, Cismon 17/32-42 cm. All scale bars = 50 μm, except 6 a-c, 7 a-c and 8 a-c = 20 μm.

Plate 13

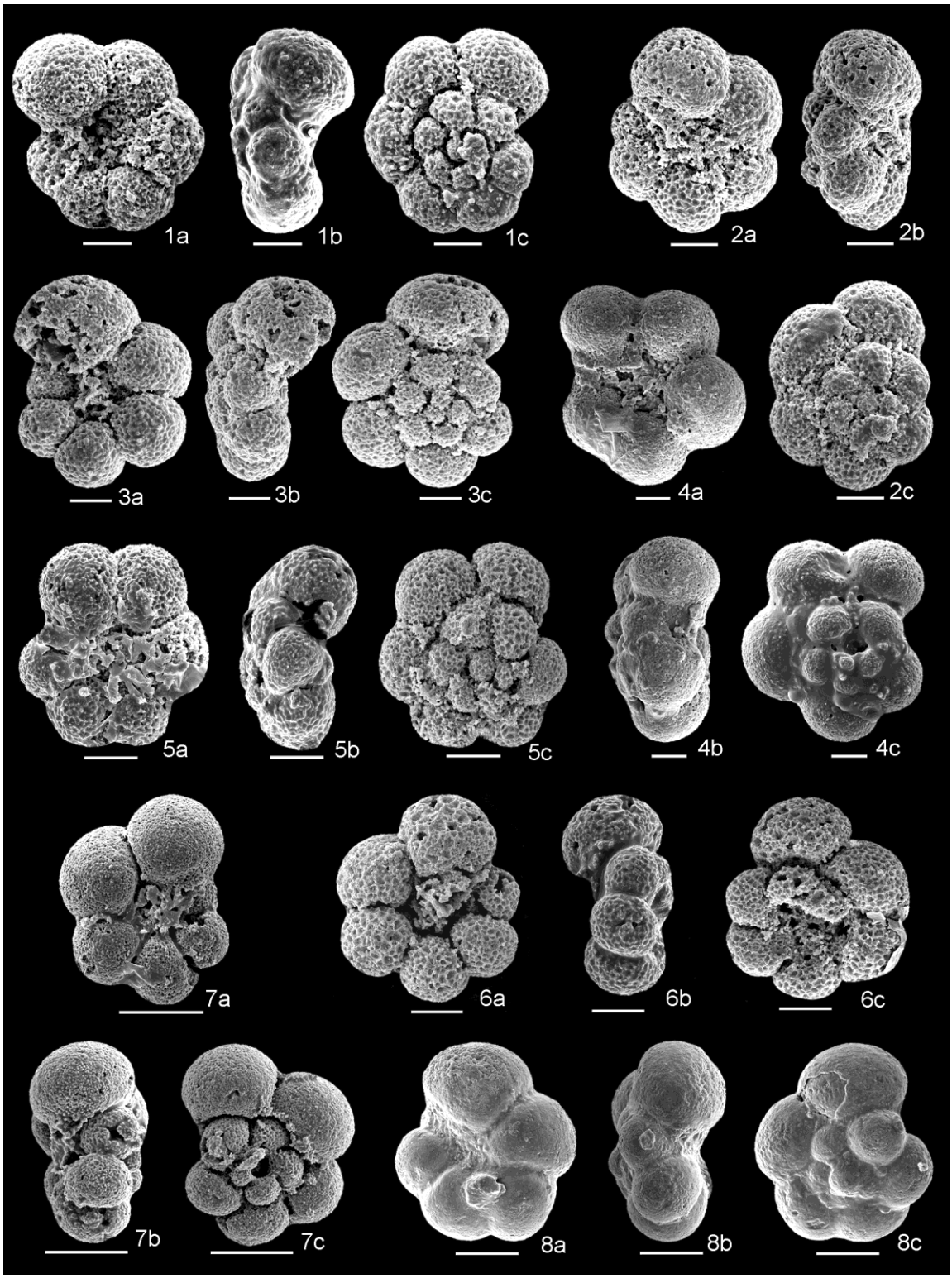

Plate 13. 1 a-c. *H. occulta*, Cismon 16/20-28 cm; **2 a-c.** *H. occulta*, Cismon 15/143-147 cm; **3 a-c.** *H. occulta*, Cismon 14/25-30 cm; **4 a-c.** *H.* cf. *occulta*, Cismon 11/1-4 cm; **5 a-c.** *Hedbergella praetrocoidea*, Cismon 16/69-75 cm; **6 a-c.** *H. praetrocoidea*, Cismon 15/236-239 cm; **7 a-c.** *H.*cf. *praetrocoidea*, Cismon 10/209-212 cm; **8 a-c.** *H.* cf. *praetrocoidea*, Cismon 11/281-284 cm. All scale bars = 20 μm, except 7a-c and 8a-c= 50 μm.

Plate 14

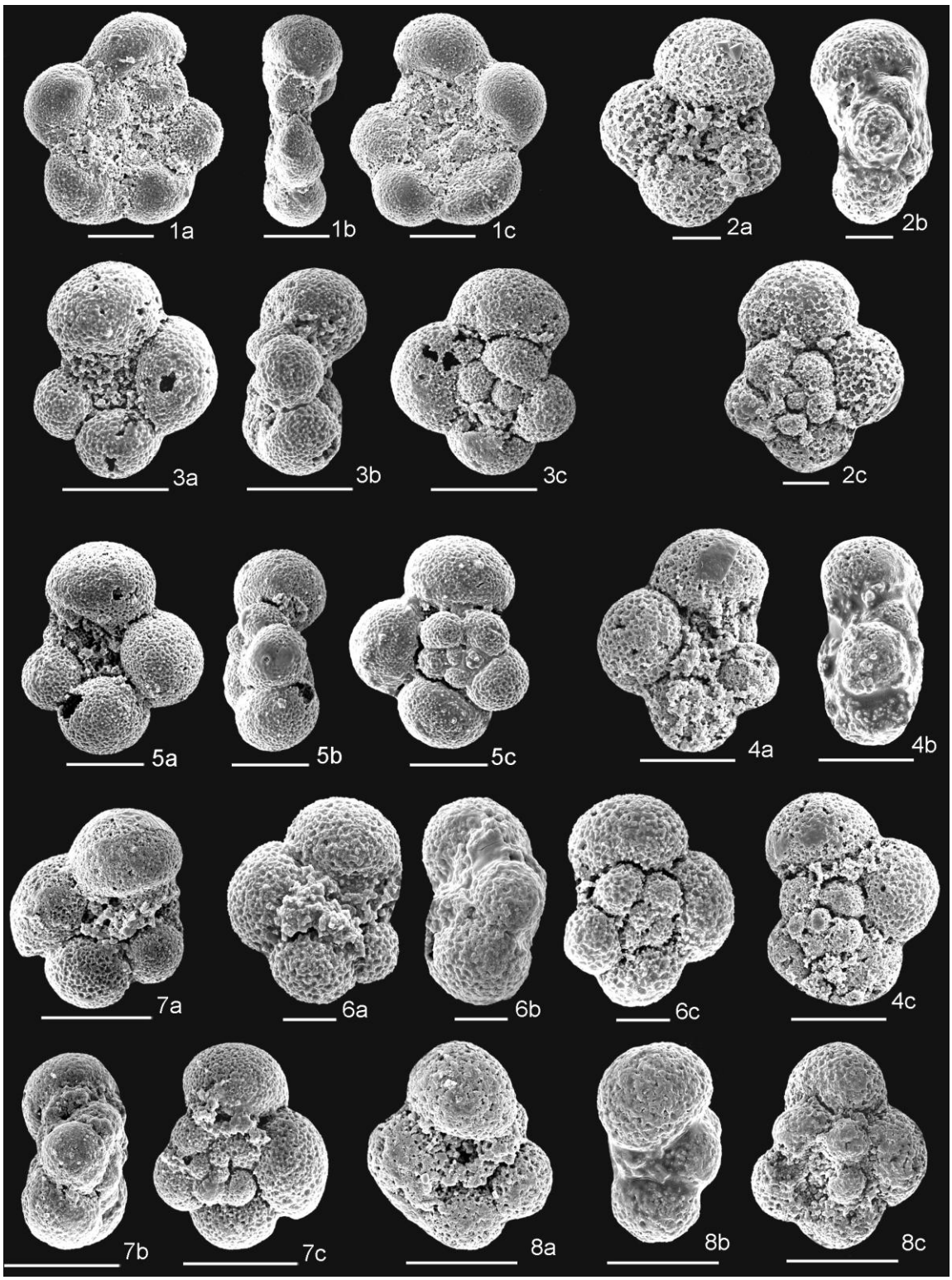

Plate 14. 1 a-c. *Hedbergella primare* Cismon 11/290-293,5 cm; **2 a-c.** *Hedbergella sigali*, Cismon 17/32-42 cm; **3 a-c.** *H. sigali*, Cismon 16/69-75 cm; **4 a-c.** *H. sigali*, Cismon 15/236-239 cm; **5 a-c.** *H. sigali*, Cismon 11/1-4 cm; **6 a-c.** *H.*cf *sigali*, Cismon 15/143-147 cm; **7 a-c.** *H.* cf *sigali*, Cismon 15/262-271 cm; **8 a-c.** *H.* cf *sigali*, Cismon 15/236-239 cm. All scale bars = 50 μm, except 6 a-c = 20 μm.

Plate 15

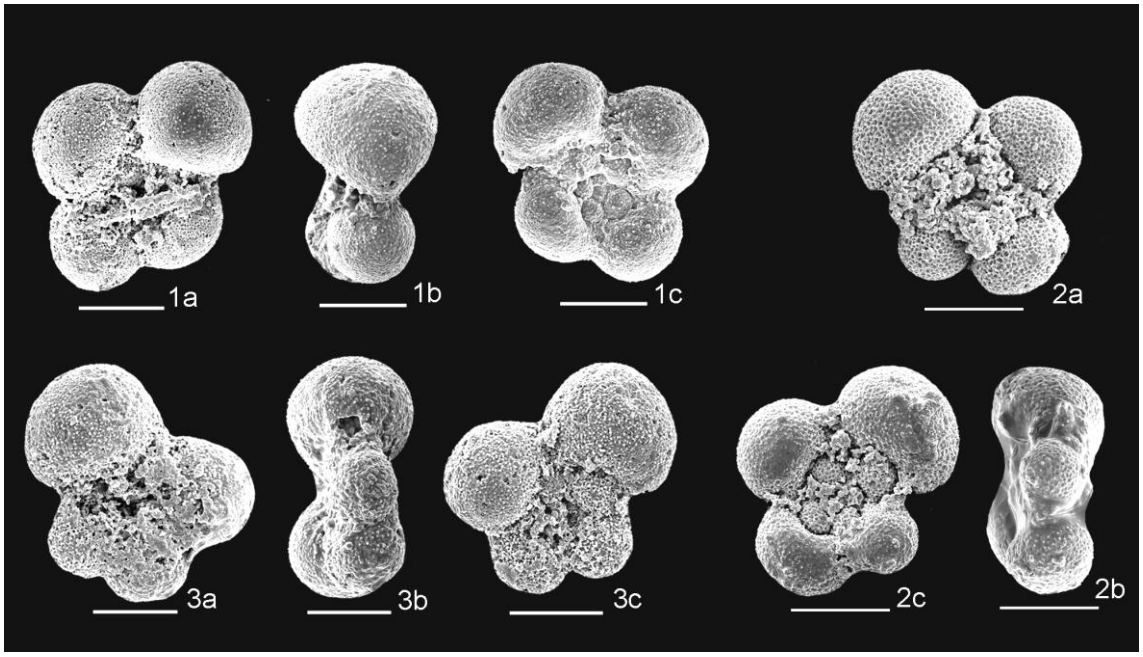

Plate 15. 1 a-c. *Hedbergella tuschepsensis*, Cismon 13/20-24 cm; **2 a-c.** *H. tuschepsensis*, Cismon 12/148-152 cm; **3 a-c.** *H. tuschepsensis*, Cismon 10/100-102 cm. All scale bars = 50 μm.

Plate 16

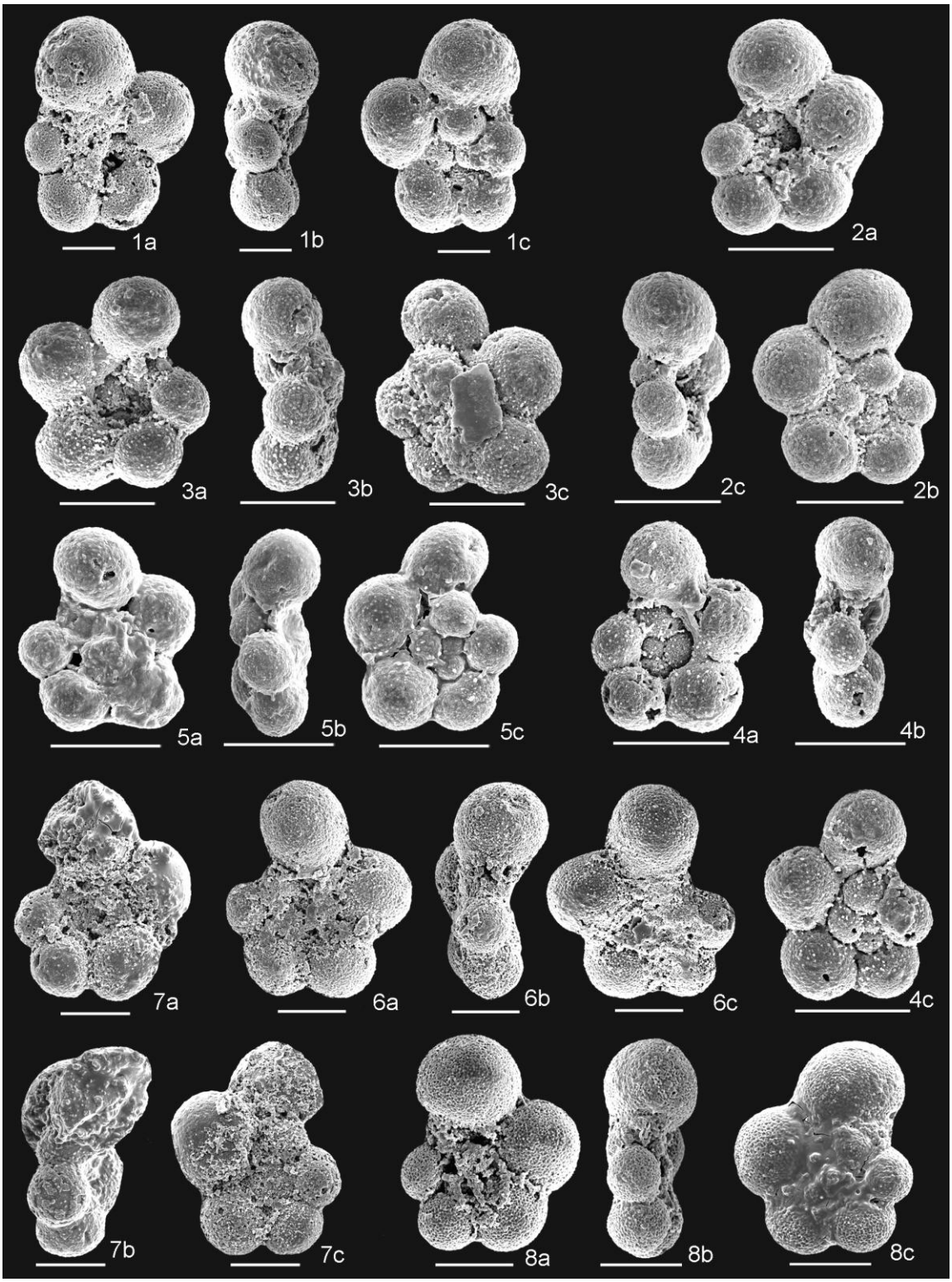

Plate 16. **1 a-c.** *Lilliputianella globulifera*, Cismon 290-293,5 cm; **2 a-c.** *L. globulifera*, Cismon 13/94-99 cm; **3 a-c.** *L. globulifera*, Cismon 12/287-292 cm; **4 a-c.** *L. globulifera*, Cismon 12/287-292 cm; **5 a-c.** *L. globulifera*, Cismon 12/253-256,5 cm; **6 a-c.** *L. globulifera*, Cismon 12/148-152 cm; **7 a-c.** *L. globulifera*, Cismon 14/199-201 cm; **8 a-c.** *L. globulifera*, Cismon 11/1-4 cm. All scale bars = 50 µm.

Plate 17

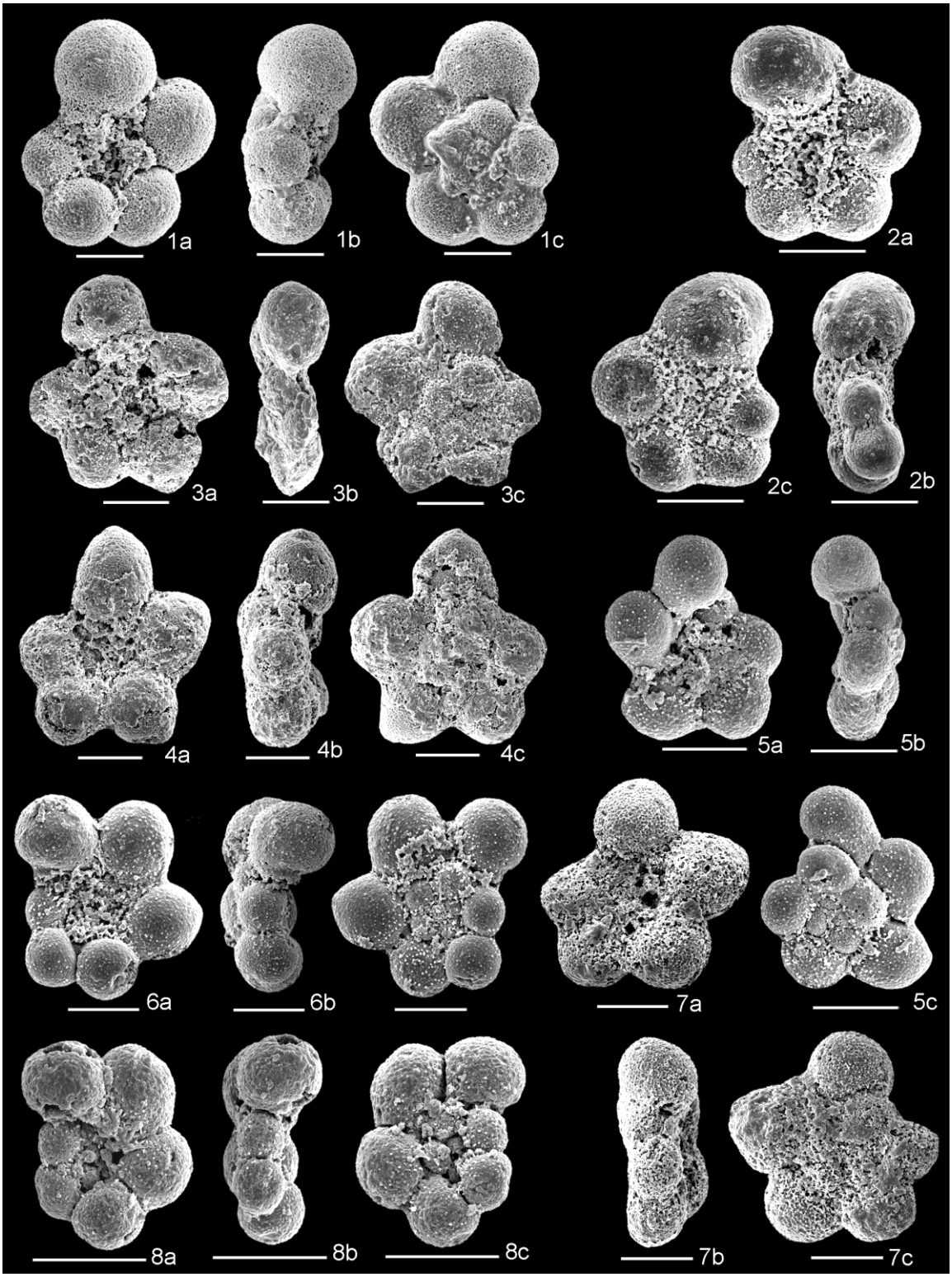

Plate 17. 1 a-c. *Lilliputianella globulifera*, Cismon 11/1-4 cm; **2 a-c.** *L.globulifera*, Cismon 13/94-99 cm; **3 a-c** *Lilliputianella kuhryi*, Cismon 12/278-280 cm; **4 a-c.** *L. kuhryi*, Cismon 11/158-161 cm.; 5 **a-c.** *Lilliputianella labocaensis*, Cismon 13/171-175 cm; **6 a-c.** *L. labocaensis*, Cismon 13/94-99 cm; **7 a-c** *Lilliputianella maslakovae*, Cismon 12/69-71 cm. All scale bars = 50 μm; **8 a-c.** *Lilliputianella* cf. *maslakovae*, Cismon 12/287-292 cm.

Plate 18

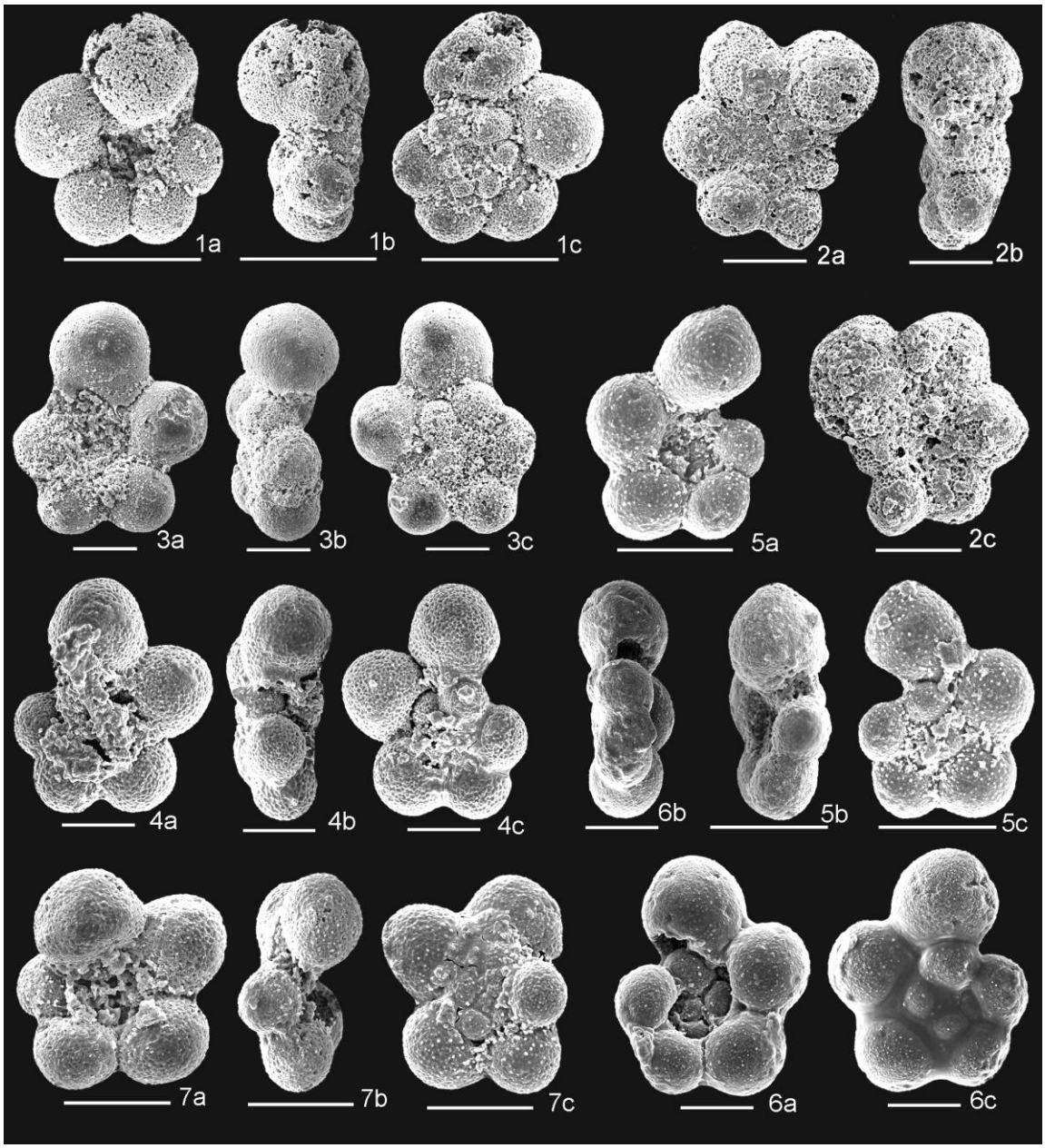

Plate 18. **1 a-c.** *L.*cf. *maslakovae*, Cismon 12/230-234 cm; **2 a-c.** *L.*cf. *maslakovae*, Cismon 10/100-102 cm; **3 a-c.** *Lilliputianella similis*, Cismon 13/94-99 cm; **4 a-c.** *L. similis*, Cismon 11/1-4 cm; **5 a-c.** *L. similis*, Cismon 13/171-175 cm; **6 a-c.** *L.* cf. *similis*, Cismon 12/253-256,5 cm; **7 a-c.** *Lilliputianella* sp., Cismon 12/88-92 cm. All scale bars = 50 μm.

Plate 19

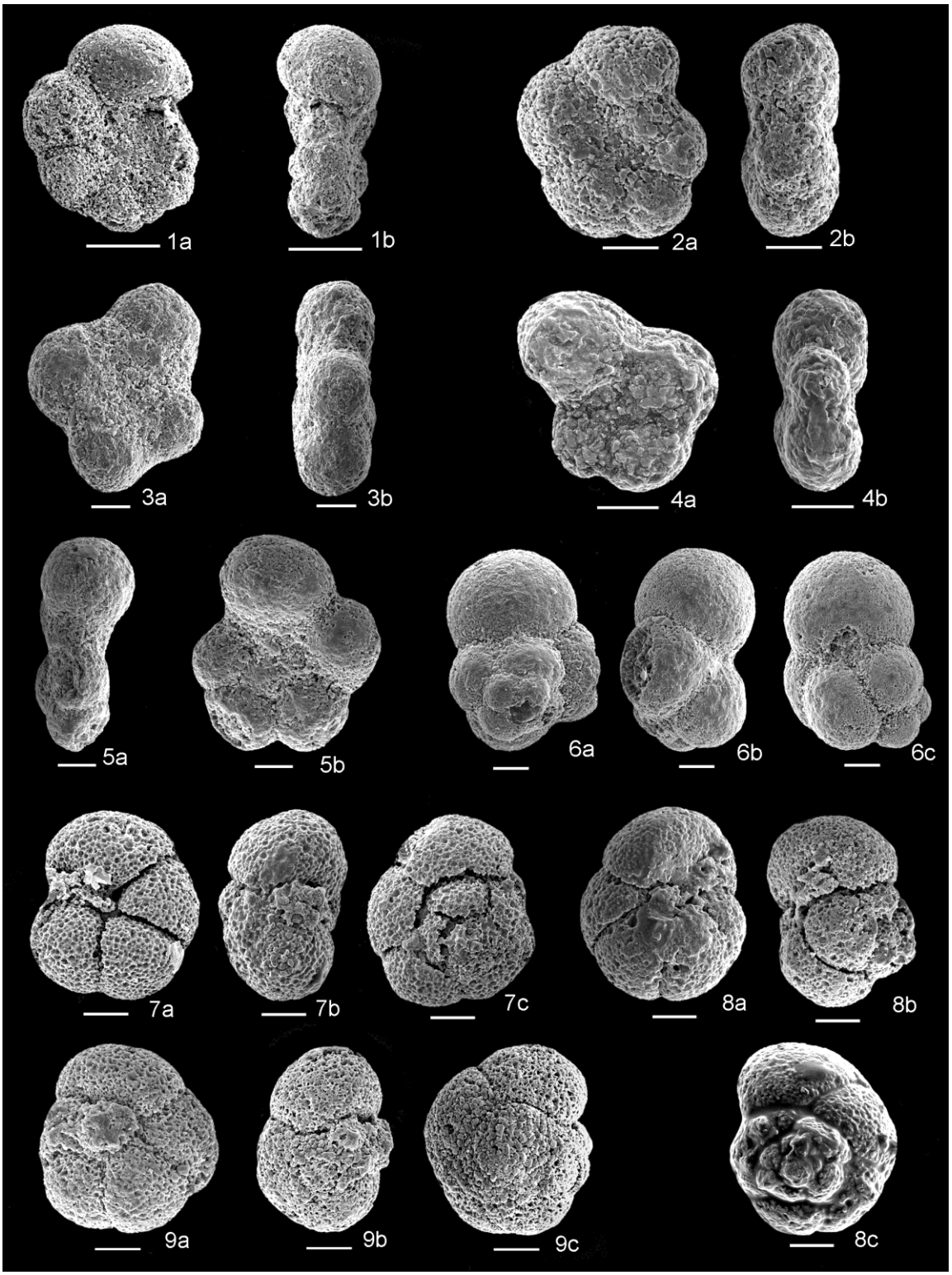

Plate 19. 1 a-b. *Globigerinelloides aptiensis*, 463-73-CC, 0-3 cm; **2 a-b.** *Globigerinelloides* cf. *blowi*, 463-72-3, 6-7 cm; **3 a-b.** *Globigerinelloides duboisi*, 463-69-3, 20-22 cm; **4 a-b.** *G. duboisi*, 463-72-3, 6-7 cm; **5 a-b.** *Globigerinelloides paragottisi*, 463-69-3, 20-22 cm; **6 a-c.** *Gorbachikella kugleri*, 463-71-2, 78-80 cm; **7 a-c.** *Gubkinella graysonensis*, 463-72-3, 100-102 cm; **8 a-c.** *G. graysonensis*, 463-72-3, 100-102 cm; **9 a-c.** *G. graysonensis*, 463-73-3, 80-82 cm. All scale bars = 20 μm, except 1 a-b= 50 μm.

Plate 20

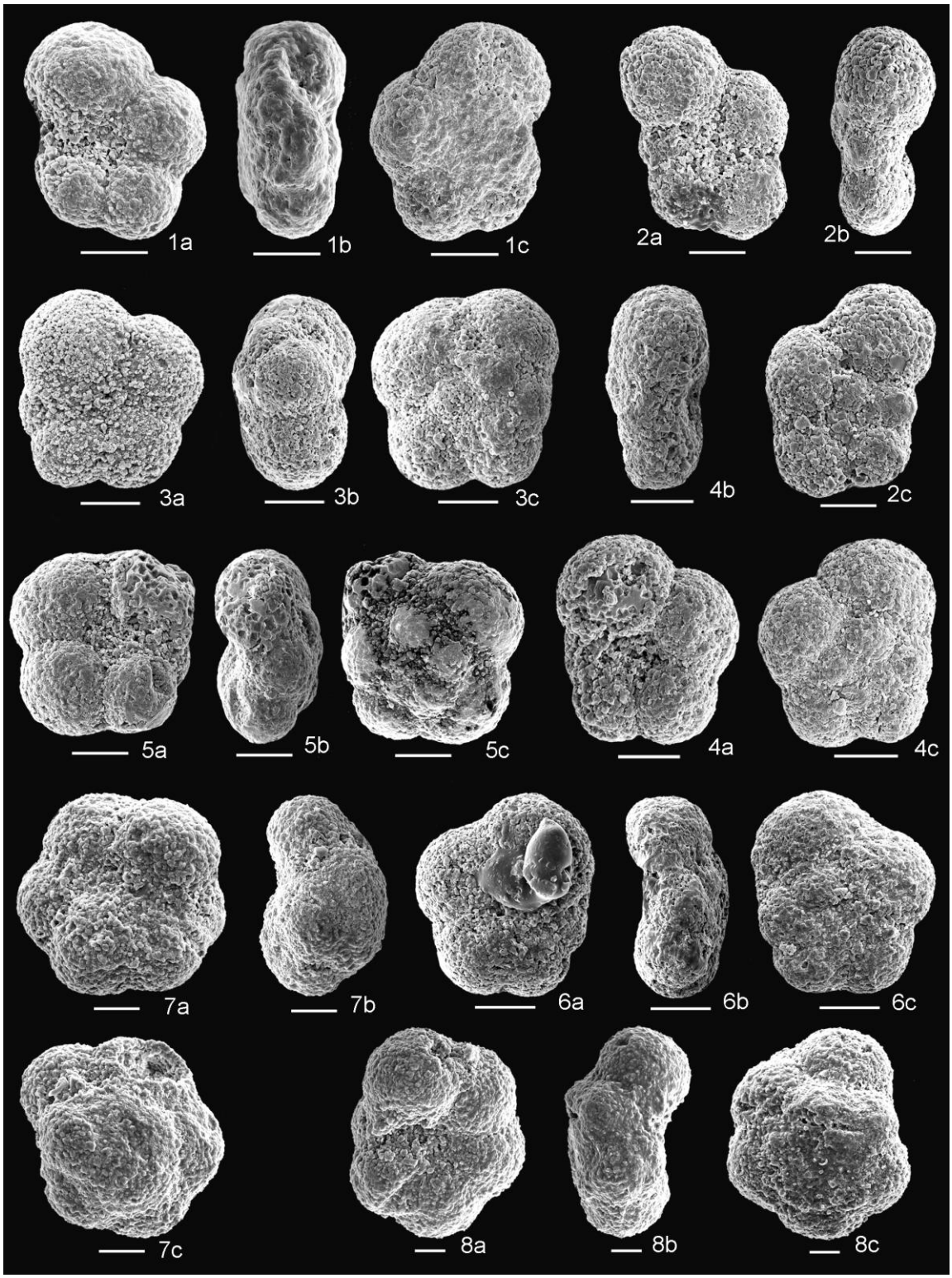

Plate 20. **1 a-c.** *Hedbergella aptiana*, 463-71-4, 39-42 cm; **2 a-c.** *H. aptiana*, 463-69-3, 20-22 cm; **3 a-c.** *Hedbergella*. *daminiae*, 463-72-4, 42-44 cm; **4 a-c.** *H. daminiae*, 463-71-4, 39-42 cm; **5 a-c.** *H. daminiae*, 463-71-4, 39-42 cm; **6 a-c.** *Hedbergella*. cf. *daminiae*, 463-72-4, 42-44 cm; **7 a-c.** *Hedbergella excelsa*, 463-67-2, 100-102 cm; **8 a-c.** *H. excelsa*, 463-67-2, 100-102 cm. All scale bars = 20 µm.

Plate 21

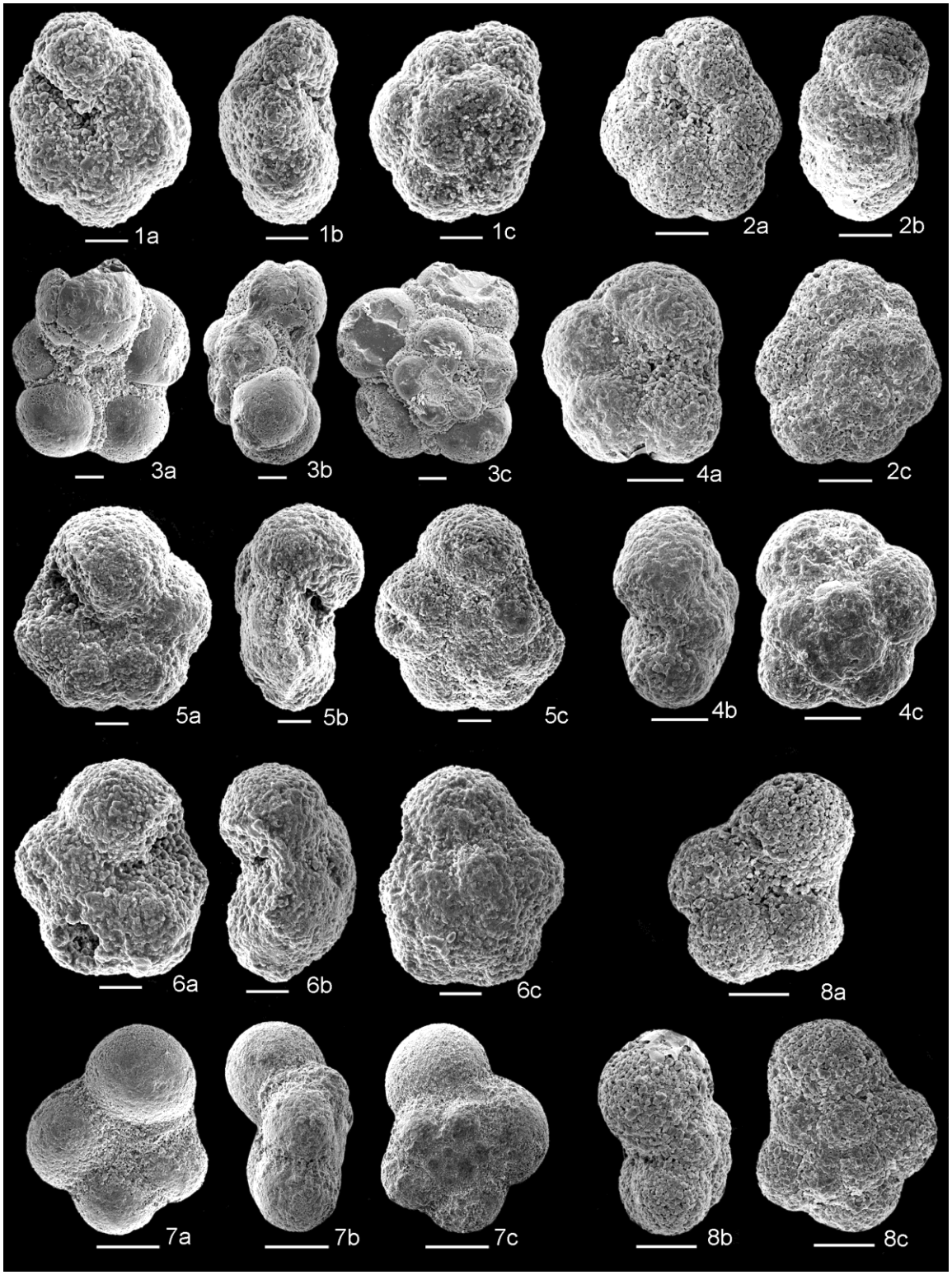

Plate 21. 1 a-c. *Hedbergella excelsa*, 463-67-2, 100-102 cm; **2 a-c.** *H. excelsa*, 463-71-4, 39-42 cm; **3 a-c** *Hedbergella infracretacea* (internal mold), 463-71-3, 137-140 cm; **4 a-c.** *H. infracretacea*, 463-71-4, 39-42 cm; **5 a-c.** *H. infracretacea*, 463-67-2, 100-102 cm; **6 a-c.** *Hedbergella infracretacea*, 463-67-2, 100-102 cm;; **7 a-c.** *Hedbergella laculata*, 463-73-CC, 0-3 cm; **8 a-c.** *H.laculata*, 463-72-3, 144-146 cm. All scale bars = 20 μm, except 7 a-c = 50 μm.

Plate 22

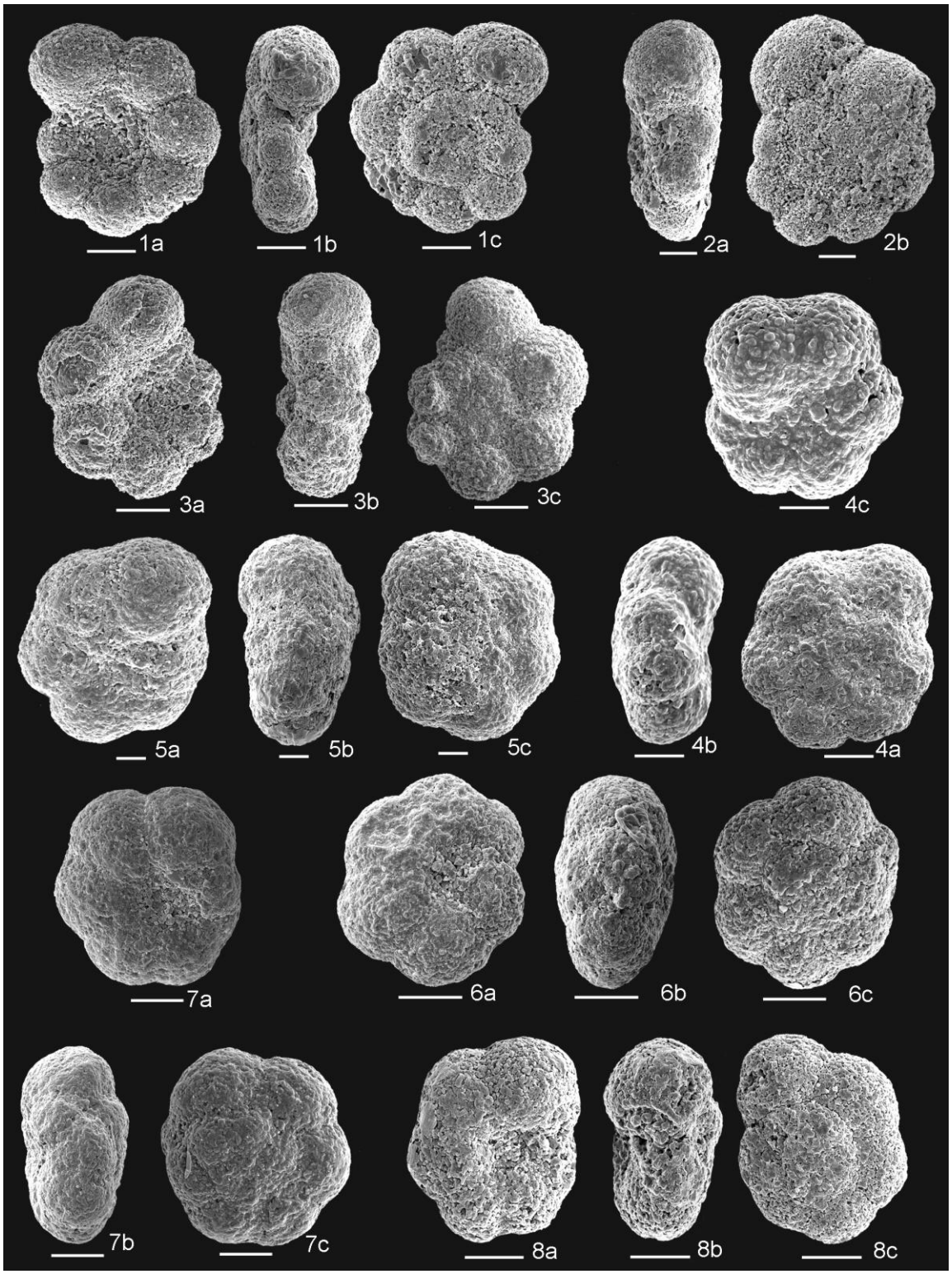

Plate 22. 1 a-c. *Hedbergella luterbacheri*, 463-71-2, 78-80 cm; **2 a-c.** *H.* cf. *luterbacheri*, 463-71-2, 78-80 cm; **3 a-c.** *H.* cf. *luterbacheri*, 463-67-2, 3-7 cm; **4 a-c.** *Hedbergella praetrocoidea*, 463-72-3, 144-146 cm; **5 a-c.** *H. praetrocoidea*, 463-71-4, 39-42 cm; **6 a-c.** *H. praetrocoidea*, 463-72-3, 144-146 cm; **7 a-c.** *H. praetrocoidea*, 463-71-4, 39-42 cm; **8 a-c.** *H. praetrocoidea*, 463-71-4, 39-42 cm. All scale bars = 20 µm.

Plate 23

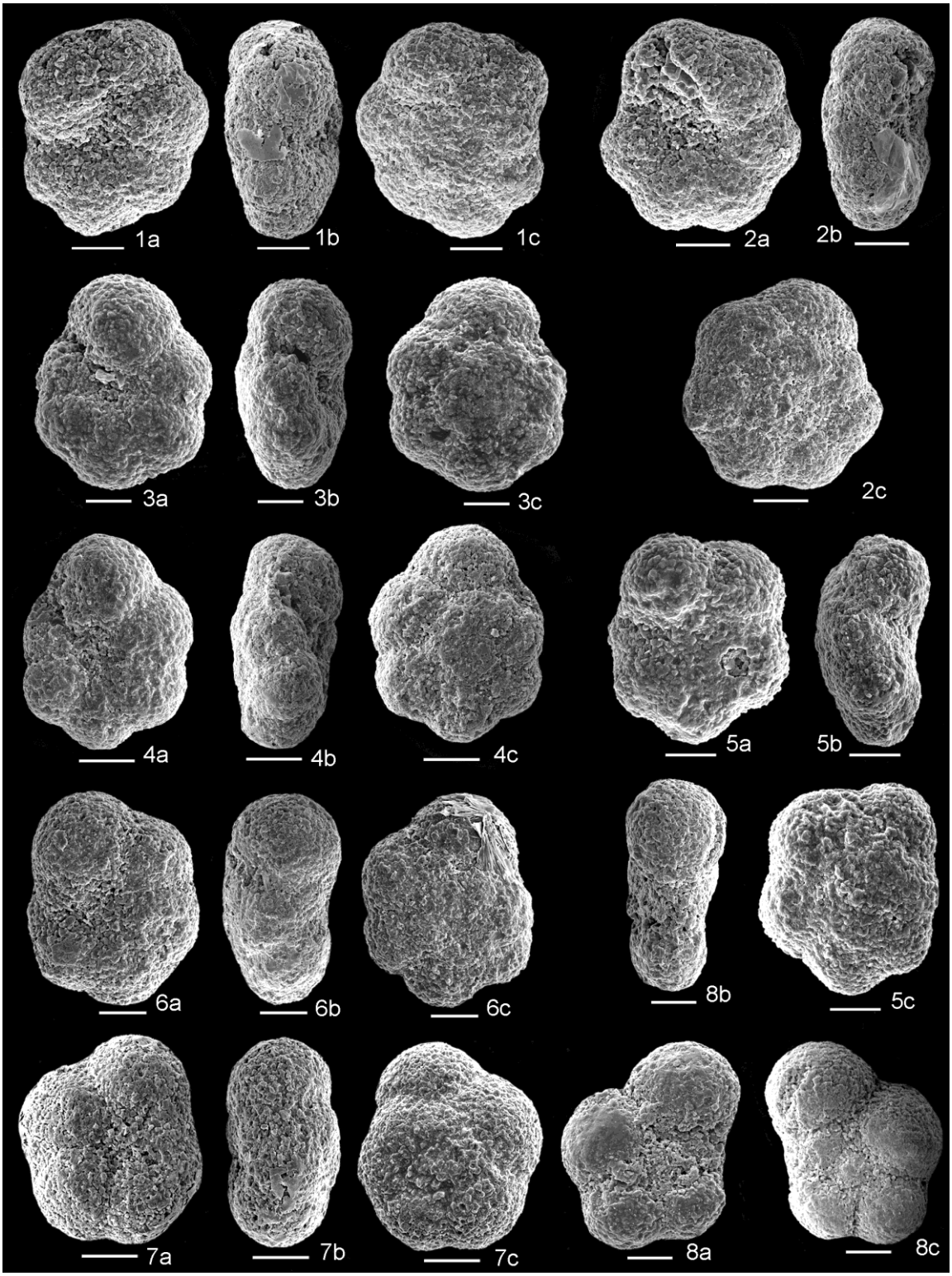

Plate 23. 1 a-c. *Hedbergella praetrocoidea*, 463-71-4, 39-42 cm; **2 a-c.** *H. praetrocoidea*, 463-71-4, 39-42 cm; **3 a-c.** *H. praetrocoidea*, 463-67-2, 100-102 cm; **4 a-c.** *H. praetrocoidea*, 463-71-4, 39-42 cm; **5 a-c.** *H. praetrocoidea*, 463-67-2, 100-102 cm; **6 a-c.** *H. praetrocoidea*, 463-71-4, 39-42 cm; **7 a-c.** *H.* cf. *praetrocoidea*, 463-72-4, 42-44 cm; **8 a-c.** *Hedbergella tuschepsensis*, 463-69-3, 20-22 cm. All scale bars = 20 µm.

Appendix

SITE	CORE	CM	METER	SAMPLE CODE	WASHED RESIDUES	THIN SECTIONS
CISMON	9	150	7.96	1,5		X
CISMON	9	176	8.2	9/176 W	X	
CISMON	10	5	8.81	0,05		X
CISMON	10	11-13	8.87	RAD 1	X	
CISMON	10	57-58,5	9.31	RAD 2	X	
CISMON	10	100-102	9.72	RAD 3	X	
CISMON	10	116	9.86	1,16		X
CISMON	10	128-134	10.00	RAD 4	X	
CISMON	10	177-180	10.44	RAD 5	X	
CISMON	10	209-212	10.76	RAD 6	X	
CISMON	10	238-240	11.02	RAD 7	X	
CISMON	10	298	11.58	2,98		X
CISMON	11	1-4	11.65	RAD 8	X	
CISMON	11	4-10	11.69	RAD 9	X	
CISMON	11	10-13	11.73	RAD 10	X	
CISMON	11	74-76	12.34	RAD 11	X	
CISMON	11	84-84,1	12.42	RAD 12	X	
CISMON	11	100	12.57	1,00		X
CISMON	11	143-145	12.99	RAD 13	X	
CISMON	11	158-161	13.13	RAD 14/ 15,9	X	X
CISMON	11	184-186	13.38	RAD 15	X	
CISMON	11	245	13.94	2,45		X
CISMON	11	281-284	14.29	RAD 16	X	
CISMON	11	290-293,5	14.39	RAD 17	X	
CISMON	12	8	14.52	0,08		X
CISMON	12	37-42	14.82	RAD 18	X	
CISMON	12	64	15.05	0,64		X
CISMON	12	69-71	15.11	RAD 19	X	
CISMON	12	81-84	15.22	RAD 20	X	
CISMON	12	88-92	15.30	RAD 21	X	
CISMON	12	112	15.50	1,12		X
CISMON	12	148-152	15.86	RAD 22	X	
CISMON	12	152-158	15.91	RAD 23	X	
CISMON	12	173	16.08	1,73		X
CISMON	12	209-214	16.44	RAD 24	X	
CISMON	12	222-225	16.56	RAD 25	X	
CISMON	12	228	16.60	2,28		X
CISMON	12	230-234	16.64	RAD 26	X	
CISMON	12	247-248	16.78	RAD 27	X	
CISMON	12	253-256,5	16.86	RAD 28	X	
CISMON	12	256,5-265	16.91	RAD 29	X	
CISMON	12	278-280	17.08	RAD 30	X	
CISMON	12	287-292	17.18	RAD 31	X	
CISMON	12	290	17.19	2,90		X
CISMON	13	7-10	17.34	RAD 32	X	
CISMON	13	9	17.35	5		X
CISMON	13	13-17	17.41	RAD 33 / 8	X	X
CISMON	13	26	17.51	12		X
CISMON	13	34	17.59	0,34		X
CISMON	13	39	17.63	16		X
CISMON	13	20-24	17.47	RAD 34	X	
CISMON	13	50	17.74	21		X
CISMON	13	53-57	17.78	RAD 35	X	
CISMON	13	66	17.89	29		X
CISMON	13	70	17.93	31		X
CISMON	13	79	18.01	34		X
CISMON	13	93	18.14	41		X
CISMON	13	94-99	18.17	RAD 36	X	
CISMON	13	101	18.22	46		X
CISMON	13	109	18.30	54		X
CISMON	13	115	18.35	56		X
CISMON	13	119-127	18.43	RAD 37	X	
CISMON	13	126	18.46	61		X
CISMON	13	135	18.54	65		X
CISMON	13	148	18.66	69		X
CISMON	13	154	18.72	1,54		X
CISMON	13	159	18.77	73		X
CISMON	13	163	18.81	77		X
CISMON	13	164-169	18.83	RAD 38	X	
CISMON	13	170	18.87	82		X
CISMON	13	171-175	18.9	RAD 39	X	
CISMON	13	176	18.93	86		X
CISMON	13	180	18.97	90		X
CISMON	13	183-186	19.01	RAD 40	X	
CISMON	13	191	19.07	97		X
CISMON	13	196-199	19.14	RAD 41 / 101	X	X
CISMON	13	202-206	19.2	RAD 42 / 2,05	X	X
CISMON	13	210	19.25	106		X
CISMON	13	215	19.3	111		X
CISMON	13	220	19.35	115		X
CISMON	13	235	19.49	123		X
CISMON	13	240-241	19.53	RAD 43 / 128	X	X
CISMON	13	244	19.57	130		X
CISMON	13	253-258	19.68	RAD 44 / 2,55	X	X
CISMON	13	260	19.72	139		X
CISMON	13	264-268	19.79	RAD 45	X	
CISMON	13	271	19.83	145		X
CISMON	13	275	19.87	147		X
CISMON	14	5	19.92	150		X
CISMON	14	15	20.02	158		X
CISMON	14	22	20.08	160		X
CISMON	14	25-30	20.13	RAD 46	X	
CISMON	14	32	20.18	168		X
CISMON	14	38	20.23	0,38		X
CISMON	14	42	20.27	14/42 W	X	
CISMON	14	45	20.3	176		X
CISMON	14	48-49,5	20.34	RAD 47	X	
CISMON	14	52	20.37	182		X
CISMON	14	59	20.43	189		X
CISMON	14	68-70	20.53	RAD 48	X	
CISMON	14	70	20.54	198		X
CISMON	14	80	20.63	206		X
CISMON	14	89-90	20.73	RAD 49 / 215	X	X
CISMON	14	103-108	20.87	RAD 50	X	
CISMON	14	113-115	20.95	RAD 51	X	
CISMON	14	116	20.97	14/116 W	X	
CISMON	14	124	21.05	240		X
CISMON	14	127-128	21.08	RAD 52	X	
CISMON	14	131	21.11	14/131 W	X	
CISMON	14	140	21.2	249		X
CISMON	14	141-145	21.23	RAD 53	X	
CISMON	14	150	21.29	256		X
CISMON	14	167	21.46	14/167 W	X	
CISMON	14	175	21.53	14/175 W / 271	X	X
CISMON	14	190-192	21.67	RAD 54	X	
CISMON	14	197	21.74	287		X
CISMON	14	199-201	21.77	RAD 55	X	
CISMON	14	201	21.78	289		X
CISMON	14	209	21.85	293		X
CISMON	14	211	21.87	294		X
CISMON	14	213	21.89	14/213 W	X	
CISMON	14	216	21.92	298		X
CISMON	14	222-224	21.98	RAD 56	X	
CISMON	14	225	22	14/225 W	X	
CISMON	14	235	22.1	311		X
CISMON	14	238-242	22.15	RAD 57	X	
CISMON	14	242	22.16	316		X
CISMON	14	252-256	22.28	RAD 58	X	
CISMON	14	257-261	22.33	RAD 59	X	
CISMON	14	261	22.34	329		X
CISMON	14	269	22.42	336		X
CISMON	14	280	22.52	345		X
CISMON	14	281	22.53	14/281 W	X	
CISMON	14	290	22.62	354		X
CISMON	14	293-295	22.64	RAD 60	X	
CISMON	14	298	22.69	361		X
CISMON	14	298-301	22.71	RAD 61	X	
CISMON	15	1-3	22.77	RAD 63	X	
CISMON	15	3	22.78	367		X
CISMON	15	5-7	22.81	RAD 64	X	
CISMON	15	9-10	22.84	RAD 65	X	
CISMON	15	15-17	22.9	RAD 66	X	
CISMON	15	22-25	23	RAD 67	X	
CISMON	15	29	23.03	386		X
CISMON	15	30-35	23.06	RAD 68	X	
CISMON	15	35	23.08	392		X
CISMON	15	37	23.1	15/37 W	X	
CISMON	15	45	23.18	397		X
CISMON	15	47	23.2	15/47 W	X	
CISMON	15	50-52	23.23	RAD 69	X	
CISMON	15	52	23.24	403		X
CISMON	15	60	23.32	410		X
CISMON	15	57-70	23.35	RAD 70	X	
CISMON	15	70	23.41	15/70 W	X	
CISMON	15	72	23.43	RAD 71 / 416	X	X
CISMON	15	74	23.45	RAD 72	X	
CISMON	15	75	23.46	15/75 W	X	
CISMON	15	76-78	23.47	RAD 73	X	
CISMON	15	83	23.54	424		X
CISMON	15	87	23.57	428		X
CISMON	15	93-95	23.63	RAD 74	X	
CISMON	15	95	23.65	434		X
CISMON	15	96	23.66	15/96 W	X	
CISMON	15	97	23.67	435		X
CISMON	15	105	23.74	442		X
CISMON	15	108	23.77	445		X
CISMON	15	120	23.89	455		X
CISMON	15	135	24.03	468		X
CISMON	15	140	24.08	472		X
CISMON	15	143-147	24.12	RAD 75	X	
CISMON	15	164-170	24.33	RAD 76	X	
CISMON	15	175	24.41	498		X
CISMON	15	180,5-181,5	24.45	RAD 77 / 503	X	X
CISMON	15	184	24.49	507		X
CISMON	15	199,5-200,5	24.64	RAD 78	X	
CISMON	15	236-239	24.99	RAD 79	X	
CISMON	15	262-271	25.25	RAD 80	X	
CISMON	15	304-307	25.65	RAD 81	X	
CISMON	15	310	25.68	3,10		X
CISMON	16	19	26.02	0,19		X
CISMON	16	20-28	26.07	RAD 82	X	
CISMON	16	69-75	26.53	RAD 83	X	
CISMON	16	121	26.99	1,21		X
CISMON	16	120-129	27.02	RAD 84	X	
CISMON	16	157-160	27.34	RAD 85	X	
CISMON	16	212	27.85	16/212 W	X	
CISMON	16	229	28.01	2,29		X
CISMON	16	285	28.54	2,85		X
CISMON	17	19-27	28.85	RAD 86	X	
CISMON	17	32-42	28.99	RAD 87	X	
CISMON	17	75.83	29.36	RAD 89	X	
CISMON	17	99	29.57	0,99		X
CISMON	17	112-114	29.7	RAD 90	X	
CISMON	17	126-130	29.85	RAD 91	X	
CISMON	17	148-152	30.05	RAD 92	X	
CISMON	17	159	30.14	1,59		X
CISMON	17	177-185	30.33	RAD 93	X	
CISMON	17	195-199	30.5	RAD 94	X	
CISMON	17	204-210	30.59	RAD 95	X	
CISMON	17	211	30.63	17/211	X	
CISMON	17	230	30.81	2,30		X
CISMON	17	234-235	30.85	RAD 96	X	
CISMON	17	251-257	31.04	RAD 97	X	
CISMON	17	261	31.1	2,61		X
CISMON	17	279-284	31.29	RAD 98	X	
CISMON	18	59	31.94	0,59		X
CISMON	18	117	32.49	1,17		X

Table 1. Cismon core sample list. Green band = Selli Level equivalent.

SITE	CORE	SECTION	CM	METER	SAMPLE CODE	WASHED RESIDUES	THIN SECTIONS
463	67	2	3-7	586.53	66	X	
463	67	2	24-26	586.74	65	X	X
463	67	2	100-102	587.50	61	X	X
463	67	2	140-150	587.90	59		X
463	67	CC	20-22	589.80	57		X
463	68	1	3-6	594.53	56		X
463	68	CC	0-2	594.82	54	X	X
463	68	CC	20-22	595.02	53		X
463	69	2	38-40	605.88	42		X
463	69	2	105-106	606.55	39	X	X
463	69	2	143-144	606.93	37	X	
463	69	3	7-9	607.07	36		X
463	69	3	20-22	607.20	35	X	
463	69	CC	7-9	607.57	33		X
463	70	1	0-2	613.50	32	X	X
463	70	1	20-22	613.70	31		X
463	70	1	41-43	613.91	30	X	X
463	70	1	58-60	614.08	29		X
463	70	1	77-79	614.27	28	X	X
463	70	1	96-98	614.46	27		X
463	70	1	125-126	614.75	26		X
463	70	1	140-142	614.90	25		X
463	70	2	6-8	615.06	24		X
463	70	2	20-22	615.20	23		X
463	70	2	40-42	615.40	22		X
463	70	2	65-67	615.65	21	X	X
463	70	2	80-82	615.80	20		X
463	70	2	123-125	616.23	18		X
463	70	2	140-142	616.40	17	X	X
463	70	3	4-5	616.54	16		X
463	70	3	18-20	616.68	15		X
463	70	3	39-40	616.89	14		X
463	70	3	62-64	617.12	13		X
463	70	3	85-87	617.35	12		X
463	70	3	100-103	617.50	11		X
463	70	3	124-125	617.74	10		X
463	70	3	140-141	617.90	9		X
463	70	4	5-6	618.05	8		X
463	70	4	19-20	618.19	7		X
463	70	4	62-63	618.61	5		X
463	70	4	100-102	619.00	3	X	X
463	70	4	120-121	619.20	2		X
463	70	4	139-141	619.39	1		X
463	70	5	6-7	619.56	28a	X	X
463	70	5	20-21	619.70	27a	X	X
463	70	5	40-41	619.90	26a	X	X
463	70	5	60-61	620.10	25a	X	X
463	70	5	80-81	620.30	24a	X	X
463	70	5	101-102	620.51	23a	X	X
463	70	5	123-124	620.73	22a	X	X
463	70	5	140-141	620.90	21a	X	X
463	70	6	2-3	621.02	20a	X	X
463	70	6	20-22	621.20	19a	X	X
463	70	6	39-41	621.39	18a	X	X
463	70	6	59-61	621.59	17a	X	X
463	70	6	81-82	621.81	16a	X	X
463	70	6	100-101	622.00	15a	X	X
463	70	6	122-123	622.22	14a	X	X
463	70	6	141-142	622.41	13a	X	X
463	70	7	7-8	622.57	12a	X	X
463	70	7	19-20	622.69	11a	X	X
463	70	CC	19-20	623.00	9a	X	
463	71	1	61-62	623.61	5a	X	X
463	71	1	76-78	623.76	4a		X
463	71	1	96-97	623.96	3a	X	X
463	71	1	124-125	624.24	2a	X	X
463	71	1	138-141	624.38	1a	X	X
463	71	2	1-3	624.51	78c	X	X
463	71	2	19-20	624.69	77c	X	X
463	71	2	39-40	624.89	76c		X
463	71	2	58-59	625.08	75c	X	X
463	71	2	78-80	625.28	74c	X	X
463	71	2	100-102	625.50	73c		X
463	71	2	120-121	625.70	72c		X
463	71	2	140-142	625.90	71c	X	X
463	71	3	0-3	626.00	70c		X
463	71	3	24-26	626.24	69c	X	
463	71	3	59-61	626.59	67c	X	X
463	71	3	79-81	626.79	66c	X	X
463	71	3	137-140	627.37	63c	X	X
463	71	4	19-20	627.69	61c		X
463	71	4	39-42	627.89	60c	X	
463	71	4	60-62	628.10	59c		X
463	71	CC	7-8	628.56	57c	X	
463	71	CC	21-22	628.71	56c	X	X
463	72	1	20-22	632.70	54c	X	X
463	72	1	60-62	633.10	52c	X	X
463	72	1	116-117	633.66	49c	X	X
463	72	2	15-16	634.15	46c	X	X
463	72	2	39-41	634.39	45c	X	
463	72	2	66-68	634.66	44c		X
463	72	2	98-100	634.98	42c	X	
463	72	2	118-120	635.18	41c		X
463	72	3	6-7	635.56	39c	X	
463	72	3	17-19	635.67	38c	X	X
463	72	3	60-62	636.10	36c	X	X
463	72	3	100-102	636.50	34c	X	
463	72	3	118-120	636.68	33c		X
463	72	3	144-146	636.94	32c	X	
463	72	4	0-3	637.00	31c	X	
463	72	4	20-26	637.24	30c		X
463	72	4	42-44	637.42	29c	X	
463	72	4	64-65	637.64	28c	X	X
463	72	CC	0-3	638.40	26c		X
463	72	CC	23-25	638.63	25c	X	X
463	73	1	0-4	642.00	24c	X	
463	73	1	38-40	642.38	22c	X	
463	73	1	61-63	642.61	21c	X	
463	73	1	78-80	642.78	20c	X	X
463	73	1	101-104	643.01	19c	X	X
463	73	2	0-3	643.50	16c	X	X
463	73	2	41-43	643.91	14c		X
463	73	2	59-60	644.09	13c	X	
463	73	2	104-105	644.54	11c		X
463	73	2	138-139	644.88	9c	X	X
463	73	3	20-22	645.20	7c	X	
463	73	3	42-44	645.42	6c		X
463	73	3	60-62	645.60	5c	X	
463	73	3	80-82	645.80	4c	X	X
463	73	3	143-144	646.43	2c	X	X
463	73	CC	0-3	648.00	1c	X	X

Table 2. DSDP Site 463 sample list. Green band = Selli Level equivalent.

SITE	CORE	CM	METERS	SAMPLE CODE (washed residues)	HEDBERGELLIDS													LILLIPUTIANELLIDS							GLOBIGERINELLOIDIDS											LEUPOLDINIDS						GORBACHIKELLIDS		PLANKTONIC FORAMINIFERA ABUNDANCE
					H. aptiana	*H. excelsa*	*H. gorbachikae*	*H. kuznetsovae*	*H. infracretacea*	*H. laculata*	*H. luterbacheri*	*H. occulta*	*H. praetrocoidea*	*H. primare*	*H. sigali*	*H. tuschepsensis*	*H. sp*	*L. globulifera*	*L. kuhryi*	*L. labocaensis*	*L. maslakovae*	*L. roblesae*	*L. similis*	*L. sp.*	*G. aptiensis*	*G. blowi*	*G. blowi lobatus*	*G.clavatus*	*G. duboisi*	*G. elongatus*	*G. paragottisi*	*G. maridalensis*	*G. primitivus*	*G. sigali*	*G. sp.*	*L. Pustulans pust.*	*L. cabri*	*L. reicheli*	*L. pustulans quinq.*	*L. pustulans hexacam.*	*L. sp.*	*Gorbachikella kugleri*	*Gubkinella graysonensis*	
CISMON	9	176	8.2	9/176 W	X?												X																											f
CISMON	10	11-13	8.87	RAD 1																																								b
CISMON	10	57-58,5	9.31	RAD 2													X												X					X	X									f
CISMON	10	100-102	9.72	RAD 3	X				X			X	X			X	X	X			cf				X				X					X		X	X							va
CISMON	10	128-134	10.00	RAD 4													X	X																										r
CISMON	10	177-180	10.44	RAD 5	X				X		X	X					X					X	X					X	X		X	X	X	X	X	X	X	X	X					va
CISMON	10	10/209-212	10.76	RAD 6		X			X				cf			X	X				X	X			X	X			X		X	X	X			X	X						X	va
CISMON	10	238-240	11.02	RAD 7																																								b
CISMON	11	1-4	11.65	RAD 8	cf	X	X		X			cf			X		X	X					X			X			X		X	X		X		X	X	X	X				X	va
CISMON	11	4-10	11.69	RAD 9	X				X						X		X	X								X			X				X	X		X	X							va
CISMON	11	10-13	11.73	RAD 10	X	X			X			X					X	X								cf			X			X	X	X		X	X	X	X					va
CISMON	11	74-76	12.34	RAD 11	X				X								X	X										X	X		X					X	X	X	X					va
CISMON	11	84-84,1	12.42	RAD 12			X		X								X								X				X						X	X	X							f/c
CISMON	11	143-145	12.99	RAD 13															X										X			X				X	X							f/c
CISMON	11	158-161	13.13	RAD 14									X						X	X	X		X			X			X		X	X	X			X	X						X	va
CISMON	11	184-186	13.38	RAD 15	X				X												X								X		X	X	X			X	X	X	X					va
CISMON	11	281-284	14.29	RAD 16	X							cf	cf		X		X						X		X	X			X		X		X	X		X	X	X			X			va
CISMON	11	290-293,5	14.39	RAD 17	X				X					X			X	X							X			X	X	X	X	X		X		X	X	X	X					va
CISMON	12	37-42	14.82	RAD 18	X				X						X		X									X			X		X	X		X		X	X	X					X	va
CISMON	12	69-71	15.11	RAD 19													X				X	X	X		X	X			X		X	X	X	X		X	X	X	X				X	va
CISMON	12	81-84	15.22	RAD 20		X			X				X					X					X		X						X		X			X	X	X	X			X		va
CISMON	12	88-92	15.30	RAD 21	X	X	X		X											X			X	X	X				X		X			X		X	X		X					va
CISMON	12	148-152	15.86	RAD 22												X	X	X					X		X				X		X	X		X		X								va
CISMON	12	152-158	15.91	RAD 23					X						X		X					X				X			X		X	X				X							X	va
CISMON	12	209-214	16.44	RAD 24	X						X	X				X			X	X	X	X	X			X	X	X	X	X	X	X	X	X		X		X	X	X	X			va
CISMON	12	222-225	16.56	RAD 25													X												X												X			f
CISMON	12	230-234	16.64	RAD 26		X	X		X			X			X		X				cf		X			X	X		X		X	X	X			X	X	X	X	X				va
CISMON	12	247-248	16.78	RAD 27												X										X			X							X							X	c
CISMON	12	253-256,5	16.86	RAD 28				X										X					cf						X		X													f/c
CISMON	12	256,5-265	16.91	RAD 29													X																			X							X	c/a
CISMON	12	278-280	17.08	RAD 30	X				X						X		X		X		X	X			X				X		X	X	X					X			X		X	va
CISMON	12	287-292	17.18	RAD 31					X							X		X			cf	X	X?		X				X		X		X										X	va
CISMON	13	7-10	17.34	RAD 32					X						X		X												X		X	X	X			X	X	X	X			X	X	va
CISMON	13	13-17	17.41	RAD 33												X						X			X		X		X		X	X	X	X		X	X	X	X	X		X		va
CISMON	13	20-24	17.47	RAD 34					X							X	X	X					X			X			X		X					X	X	X	X					va
CISMON	13	53-57	17.78	RAD 35	X	X			X				X				X								X	X			X		X		X			X	X	X	X					va
CISMON	13	94-99	18.17	RAD 36				X									X	X		X			X						X		X				X						X		X	va
CISMON	13	119-127	18.43	RAD 37	cf				X		X	X				X	X	X	X	X	X	X	X		X	X	X	X	X	X		X	X	X		X		X	X				X	va
CISMON	13	164-169	18.83	RAD 38													X																											vr
CISMON	13	171-175	18.9	RAD 39	X												X			X			X																					f/c
CISMON	13	183-186	19.01	RAD 40	X												X																										X	f/c
CISMON	13	196-199	19.14	RAD 41													X																											r
CISMON	13	202-206	19.2	RAD 42																																								b
CISMON	13	240-241	19.53	RAD 43																																					X			vr
CISMON	13	253-258	19.68	RAD 44																																								b
CISMON	13	264-268	19.79	RAD 45	X				X						X	X	X								X											X							X	c/a
CISMON	14	25-30	20.13	RAD 46								X					X																								X		X	r/f
CISMON	14	42	20.27	14/42 W											X		X																											r
CISMON	14	48-49,5	20.34	RAD 47																																								b
CISMON	14	68-70	20.53	RAD 48													X																											vr
CISMON	14	89-90	20.73	RAD 49	X																																				X			f
CISMON	14	103-108	20.87	RAD 50																																								b
CISMON	14	113-115	20.95	RAD 51																																					X		X	f
CISMON	14	116	20.97	14/116 W					X						X		X																											f/c
CISMON	14	127-128	21.08	RAD 52																																								b
CISMON	14	131	21.11	14/131 W	X?				X								X																								X			c/a
CISMON	14	141-145	21.23	RAD 53											X?											X					X												X	f
CISMON	14	167	21.46	14/167 W	X?				X						X		X																								X			va
CISMON	14	175	21.53	14/175 W													X																								X		X	c/a
CISMON	14	190-192	21.67	RAD 54																																							X	r
CISMON	14	199-201	21.77	RAD 55									X			X	X	X											X												X		X	f
CISMON	14	213	21.89	14/213 W	X?				X?			X?			X		X																								X		X	c/a
CISMON	14	222-224	21.98	RAD 56																																								b
CISMON	14	225	22	14/225 W					X?						X		X																								X		X	a
CISMON	14	238-242	22.15	RAD 57																																								b
CISMON	14	252-256	22.28	RAD 58																																								b
CISMON	14	257-261	22.33	RAD 59																																								b
CISMON	14	281	22.53	14/281 W	X				X			X			X		X														X				X									va
CISMON	14	293-295	22.64	RAD 60																																					X			r
CISMON	14	298-301	22.71	RAD 61																																	X				X			r
CISMON	15	1-3	22.77	RAD 63																																					X			vr
CISMON	15	5-7	22.81	RAD 64																																	X				X			f
CISMON	15	9-10	22.84	RAD 65																																	X				X			r
CISMON	15	15-17	22.9	RAD 66																																	X				X			r
CISMON	15	22-25	23	RAD 67																																								b
CISMON	15	30-35	23.06	RAD 68																																								b
CISMON	15	37	23.1	15/37 W																																					X		X	c
CISMON	15	47	23.2	15/47 W																																					X		X	f/c
CISMON	15	50-52	23.23	RAD 69																																								b
CISMON	15	57-70	23.35	RAD 70																																	X							vr
CISMON	15	70	23.41	15/70 W					X			X					X																								X			va
CISMON	15	72	23.43	RAD 71																						X																		vr
CISMON	15	74	23.45	RAD 72																																								b
CISMON	15	75	23.46	15/75 W	X	X?			X						X?																X?										X			va
CISMON	15	76-78	23.47	RAD 73																																								b
CISMON	15	93-95	23.63	RAD 74													X																											vr
CISMON	15	96	23.66	15/96 W	X							X	X		X?		X																	X							X		X	va
CISMON	15	143-147	24.12	RAD 75	X	X			X			X			cf		X						cf																				X	va
CISMON	15	164-170	24.33	RAD 76		X			X								X																				X							r/f
CISMON	15	180,5-181,5	24.45	RAD 77																																								b
CISMON	15	199,5-200,5	24.64	RAD 78																																								b
CISMON	15	236-239	24.99	RAD 79	X	X						X	X		cf	X	X															X												f/c
CISMON	15	262-271	25.25	RAD 80	X	X			cf				X		cf		X	X							X	X					X												X	va
CISMON	15	304-307	25.65	RAD 81	X										X		X																											r
CISMON	15	20-28	26.07	RAD 82	X							X	X				X																										X	c
CISMON	15	69-75	26.53	RAD 83	X	X			X				X		X	X																												a
CISMON	15	120-129	27.02	RAD 84		X			X			X			X	X																												va
CISMON	15	157-160	27.34	RAD 85																																								b
CISMON	16	212	27.85	16/212 W											X		X																											c/a
CISMON	17	19-27	28.85	RAD 86								X?					X								X																			f/c
CISMON	17	32-42	28.99	RAD 87	X	X			X	X		X	X		X	X	X															X											X	va
CISMON	17	75-83	29.36	RAD 89	X								X		X	X																												f
CISMON	17	112-114	29.7	RAD 90																																								b
CISMON	17	126-130	29.85	RAD 91													X																											r
CISMON	17	148-152	30.05	RAD 92		X						X	X		X		X																											f/c
CISMON	17	177-185	30.33	RAD 93																																								b
CISMON	17	195-199	30.5	RAD 94									X																															vr
CISMON	17	204-210	30.59	RAD 95					X				X				X																											f/c
CISMON	17	211	30.63	17/211													X						X																		X			r
CISMON	17	234-235	30.85	RAD 96																																								b
CISMON	17	251-257	31.04	RAD 97		X			X			X	X		X		X								X							X												va
CISMON	17	279-284	31.29	RAD 98																																X								vr

Table 3. Cismon core. Stratigraphic distribution and relative abundances of planktonic foraminiferal species. Green band = Selli Level equivalent.

SITE	CORE	SECTION	CM	METER	SAMPLE CODE	HEDBERGELLIDS									GLOBIGERINELLOIDIDS					GORBACHIKELLIDS	LEUPOLDINIDS		PLANKTONIC FORAMINIFERA ABUNDANCE
						H. aptiana	*H. daminiae*	*H. excelsa*	*H. infracretacea*	*H. laculata*	*H. luterbacheri*	*H. praetrocoidea*	*H. tuschepsensis*	*H. sp*	*G. aptiensis*	*G. blowi*	*G. duboisi*	*G. paragottisi*	*G. sp.*	*G. kugleri*	*Leupoldina* sp.	*G. graysonensis*	
463	67	2	3-7	586.53	66						X	X		X									a
463	67	2	24-26	586.74	65									X									r
463	67	2	100-102	587.50	61			X	X			X		X									a
463	67	CC	0-2	588.00	58																		b
463	68	CC	0-2	594.82	54									X									r
463	69	2	105-106	606.55	39																		b
463	69	2	143-144	606.93	37									X									vr
463	69	3	20-22	607.20	35	X						X	X	X			X	X	X				a
463	70	1	0-2	613.5	32																		b
463	70	1	41-43	613.91	30																		b
463	70	1	77-79	614.27	28																		b
463	70	1	96-98	614.46	27																	*?	vr
463	70	2	65-67	615.65	21																		b
463	70	2	140-142	616.4	17																		b
463	70	4	100-102	619	3																		b
463	70	5	6-7	619.56	28a																		b
463	70	5	20-21	619.7	27a																		b
463	70	5	40-41	619.9	26a																		b
463	70	5	60-61	620.1	25a																		b
463	70	5	80-81	620.3	24a																		b
463	70	5	101-102	620.51	23a																		b
463	70	5	123-124	620.73	22a																		b
463	70	5	140-141	620.9	21a																		b
463	70	6	2-3	621.02	20a																		b
463	70	6	20-22	621.2	19a																		b
463	70	6	39-41	621.39	18a																		b
463	70	6	59-61	621.59	17a																		b
463	70	6	81-82	621.81	16a																		b
463	70	6	100-101	622	15a																		b
463	70	6	122-123	622.22	14a																		b
463	70	6	141-142	622.41	13a									X									vr
463	70	7	7-8	622.57	12a																		b
463	70	7	19-20	622.69	11a																		b
463	70	CC	19-20	623	9a																		b
463	71	1	61-62	623.61	5a																		b
463	71	1	96-97	623.96	3a																		b
463	71	1	124-125	624.24	2a																		b
463	71	1	138-141	624.38	1a																		b
463	71	2	1-3	624.51	78c																		b
463	71	2	19-20	624.69	77c																		b
463	71	2	58-59	625.08	75c																		b
463	71	2	78-80	625.28	74c							X								X			r
463	71	2	140-142	625.9	71c																		b
463	71	3	24-26	626.24	69c																		b
463	71	3	59-61	626.59	67c																	*?	vr
463	71	3	79-81	626.79	66c									X									vr
463	71	3	137-140	627.37	63c				X					X									r
463	71	4	39-42	627.89	60c	X	X	X	X			X		X					X				va
463	71	4	60-62	628.10	59c																	*?	vr
463	71	CC	7-8	628.56	57c																		b
463	71	CC	21-22	628.71	56c																	*?	vr
463	72	1	20-22	632.70	54c																		b
463	72	1	60-62	633.10	52c																		b
463	72	1	116-117	633.66	49c									X								*	vr
463	72	2	15-16	634.15	46c																		b
463	72	2	39-41	634.39	45c									X							X		r
463	72	2	98-100	634.98	42c									X									vr
463	72	3	6-7	635.56	39c			X						X		cf	X		X				c
463	72	3	17-19	635.67	38c																		b
463	72	3	60-62	636.10	36c																		b
463	72	3	100-102	636.50	34c																X		r
463	72	3	118-120	636.68	33c																	*	vr
463	72	3	144-146	636.94	32c		cf					X		X									c
463	72	4	0-3	637.00	31c			cf						X									r/f
463	72	4	42-44	637.42	29c		X					cf		X									c
463	72	4	64-65	637.64	28c		cf					cf		X									f
463	73	1	0-4	642.00	24c		cf							X									f/c
463	73	1	38-40	642.38	22c									X									r
463	73	1	61-63	642.61	21c																		b
463	73	1	101-104	643.01	19c																		b
463	73	2	0-3	643.50	16c																		b
463	73	2	59-60	644.09	13c																		b
463	73	2	104-105	644.54	11c																	*	r
463	73	2	138-139	644.88	9c																		b
463	73	3	20-22	645.20	7c																		b
463	73	3	60-62	645.60	5c																		b
463	73	3	80-82	645.80	4c																		b
463	73	3	143-144	646.43	2c									X									r
463	73	CC	0-3	648.00	1c					X				X	X				X			*?	r/f

Table 4. DSDP Site 463. Stratigraphic distribution and relative abundances of planktonic foraminiferal species. Green band = Selli Level equivalent.

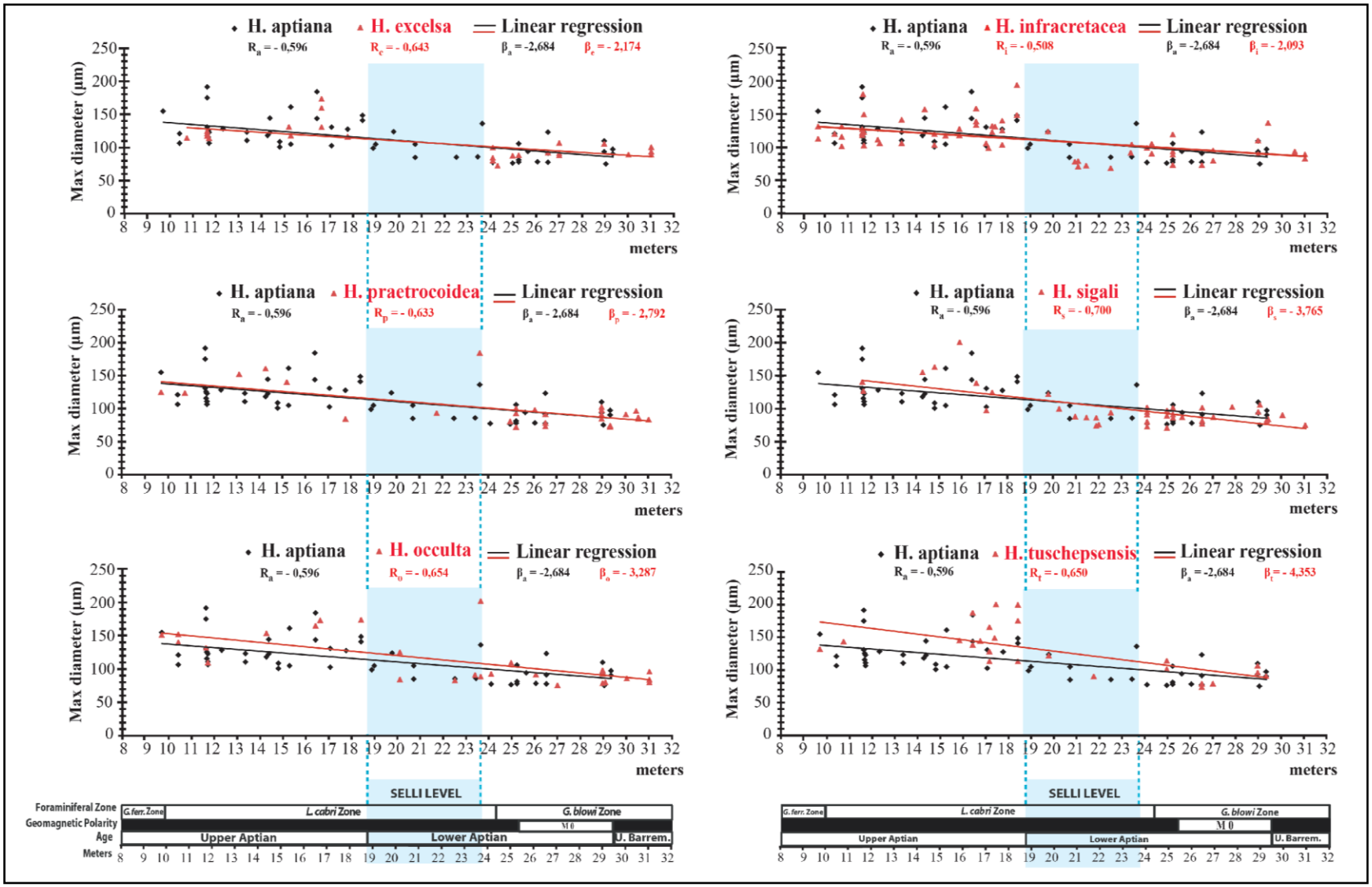

Graph 1. Cismon core. Relationship between test size variations of Hedbergellids and depth. R = Pearson's coefficient, β = angular coefficient.

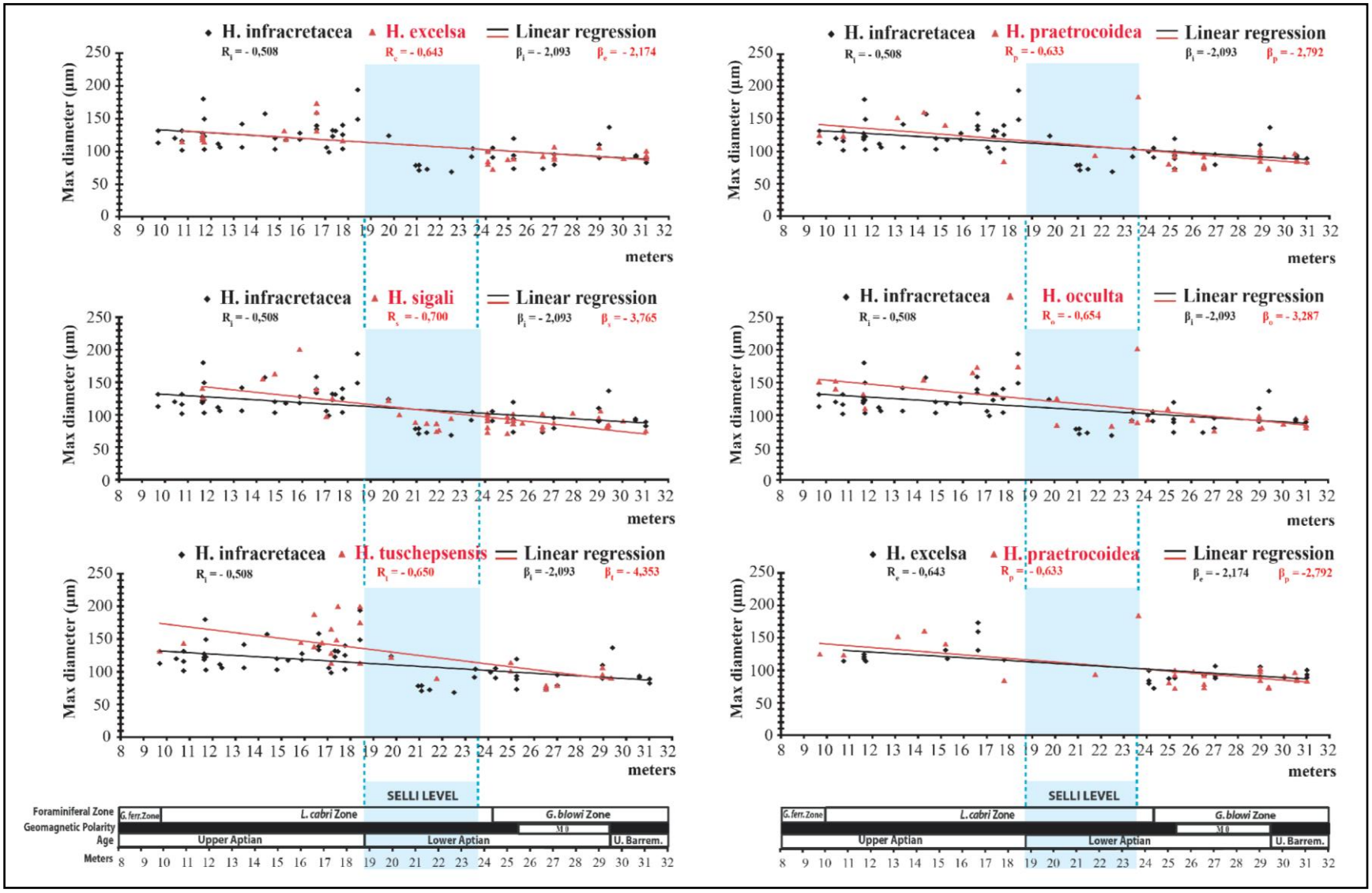

Graph 2. Cismon core. Relationship between test size variations of Hedbergellids and depth. R = Pearson's coefficient, β = angular coefficient.

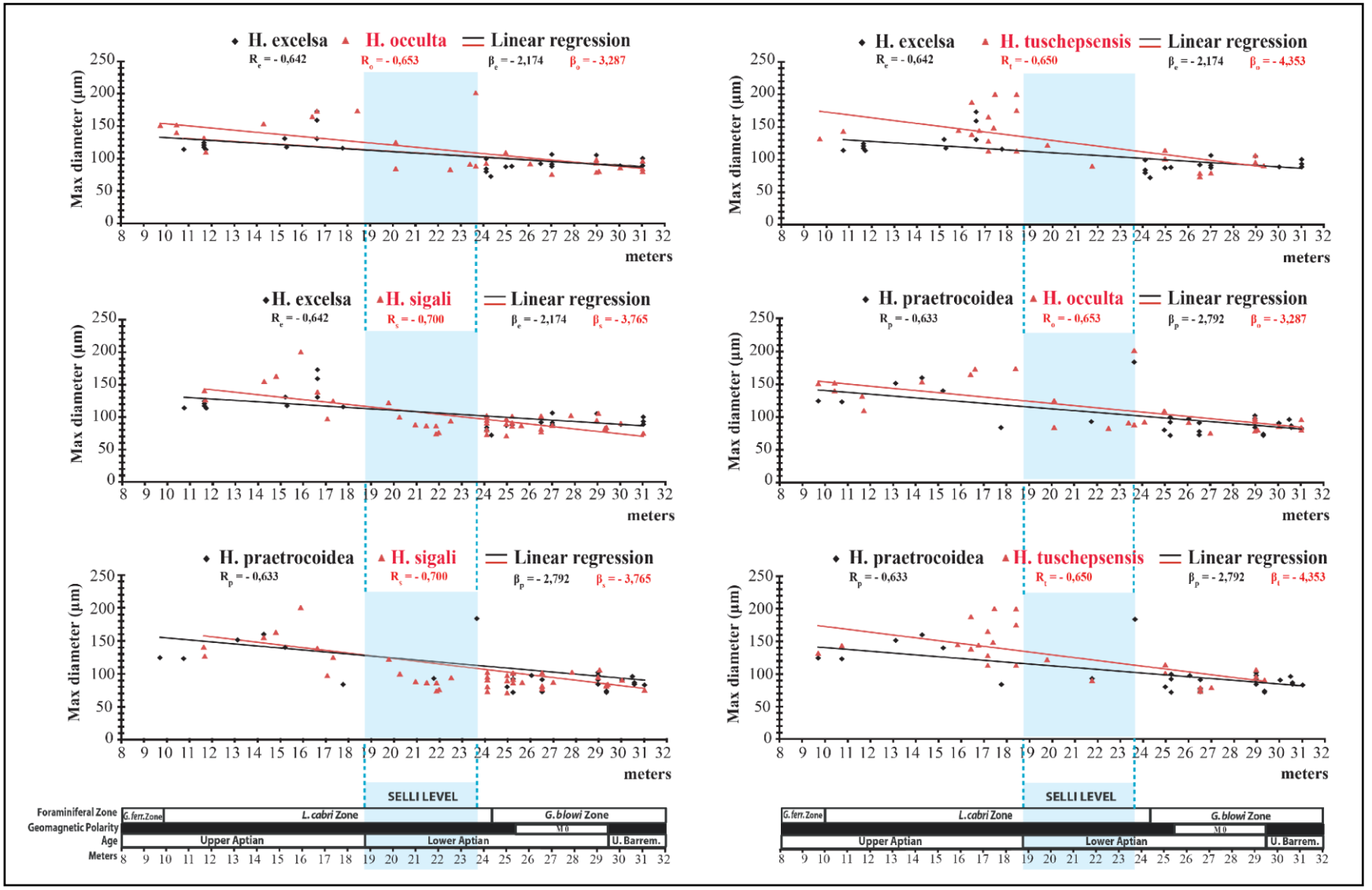

Graph 3. Cismon core. Relationship between test size variations of Hedbergellids and depth. R = Pearson's coefficient, β = angular coefficient.

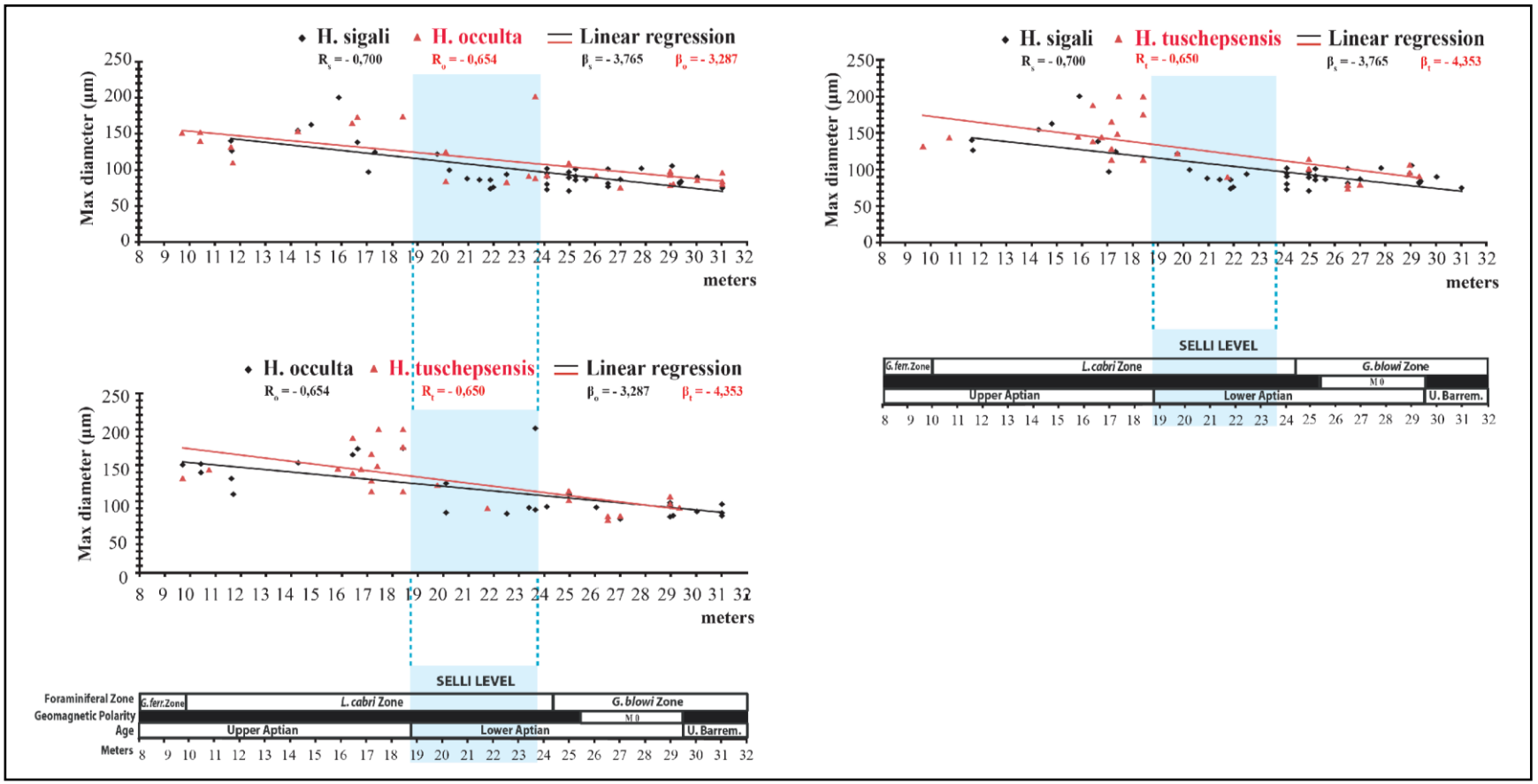

Graph 4. Cismon core. Relationship between test size variations of Hedbergellids and depth. R = Pearson's coefficient, β = angular coefficient.

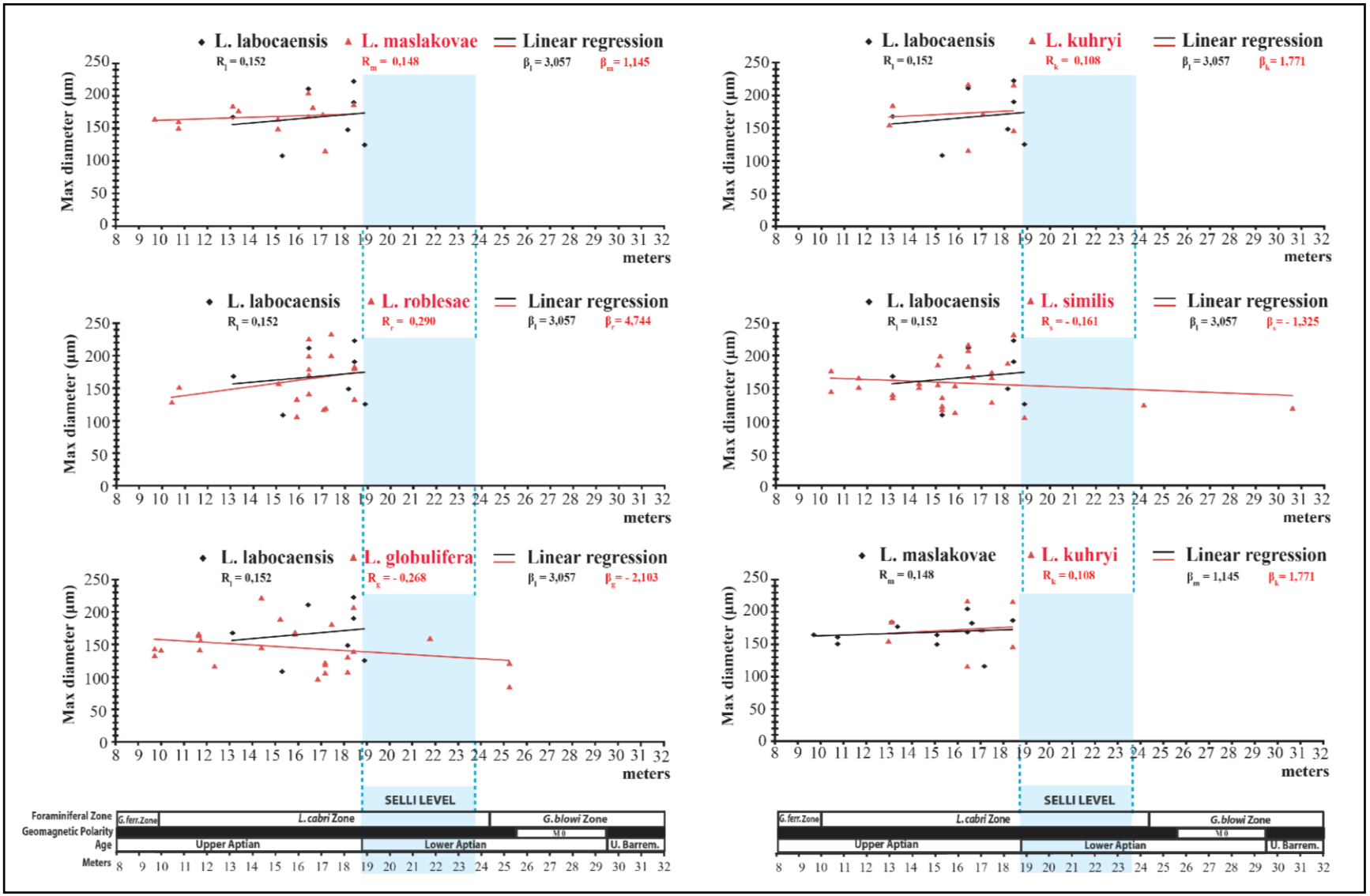

Graph 5. Cismon core. Relationship between test size variations of Lilliputianellids and depth. R = Pearson's coefficient, β = angular coefficient.

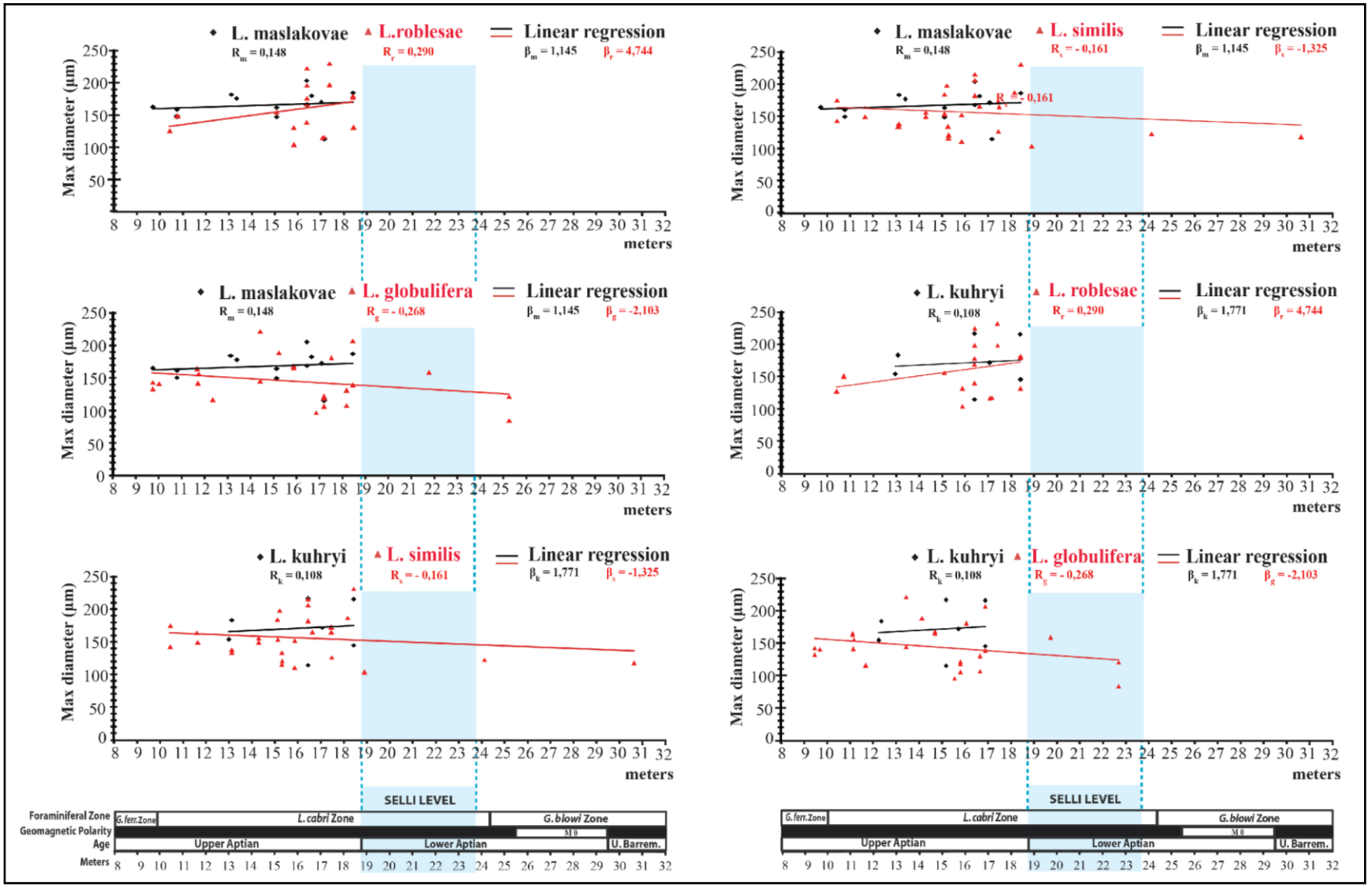

Graph 6. Cismon core. Relationship between test size variations of Lilliputianellids and depth. R = Pearson's coefficient, β = angular coefficient.

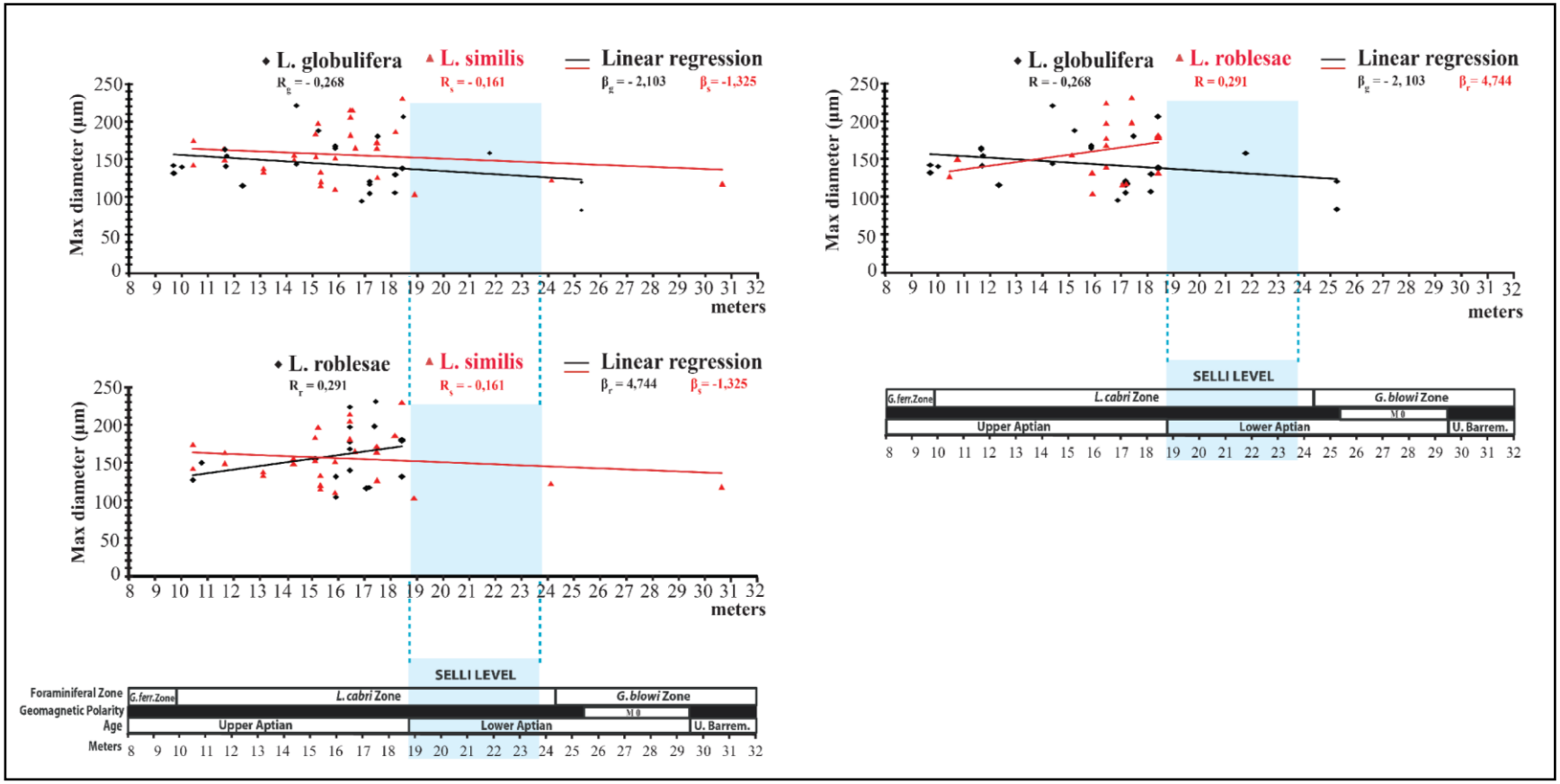

Graph 7. Cismon core. Relationship between test size variations of Lilliputianellids and depth. R = Pearson's coefficient, β = angular coefficient.

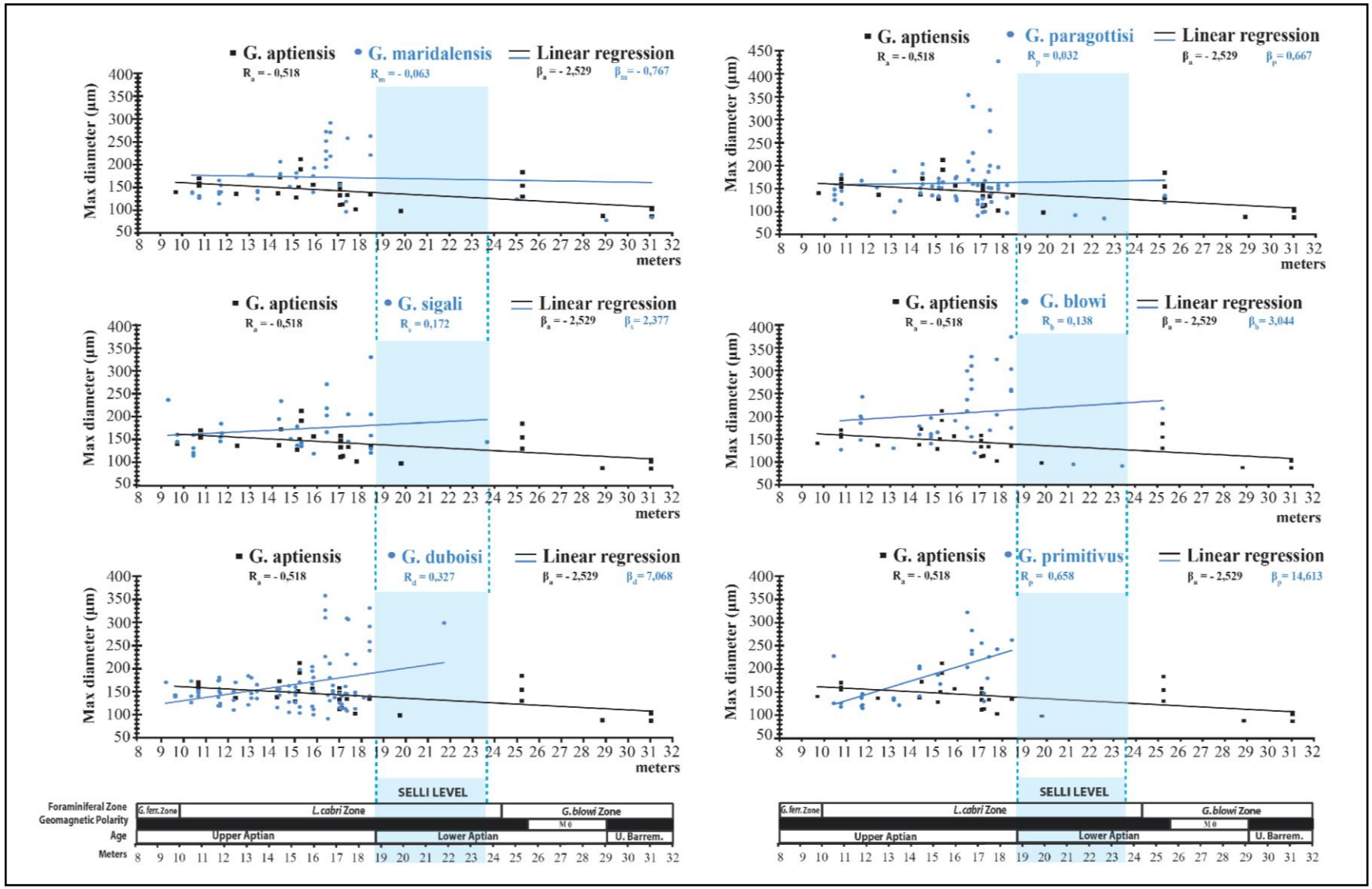

Graph 8. Cismon core. Relationship between test size variations of Globigerinelloidids and depth. R = Pearson's coefficient, β = angular coefficient.

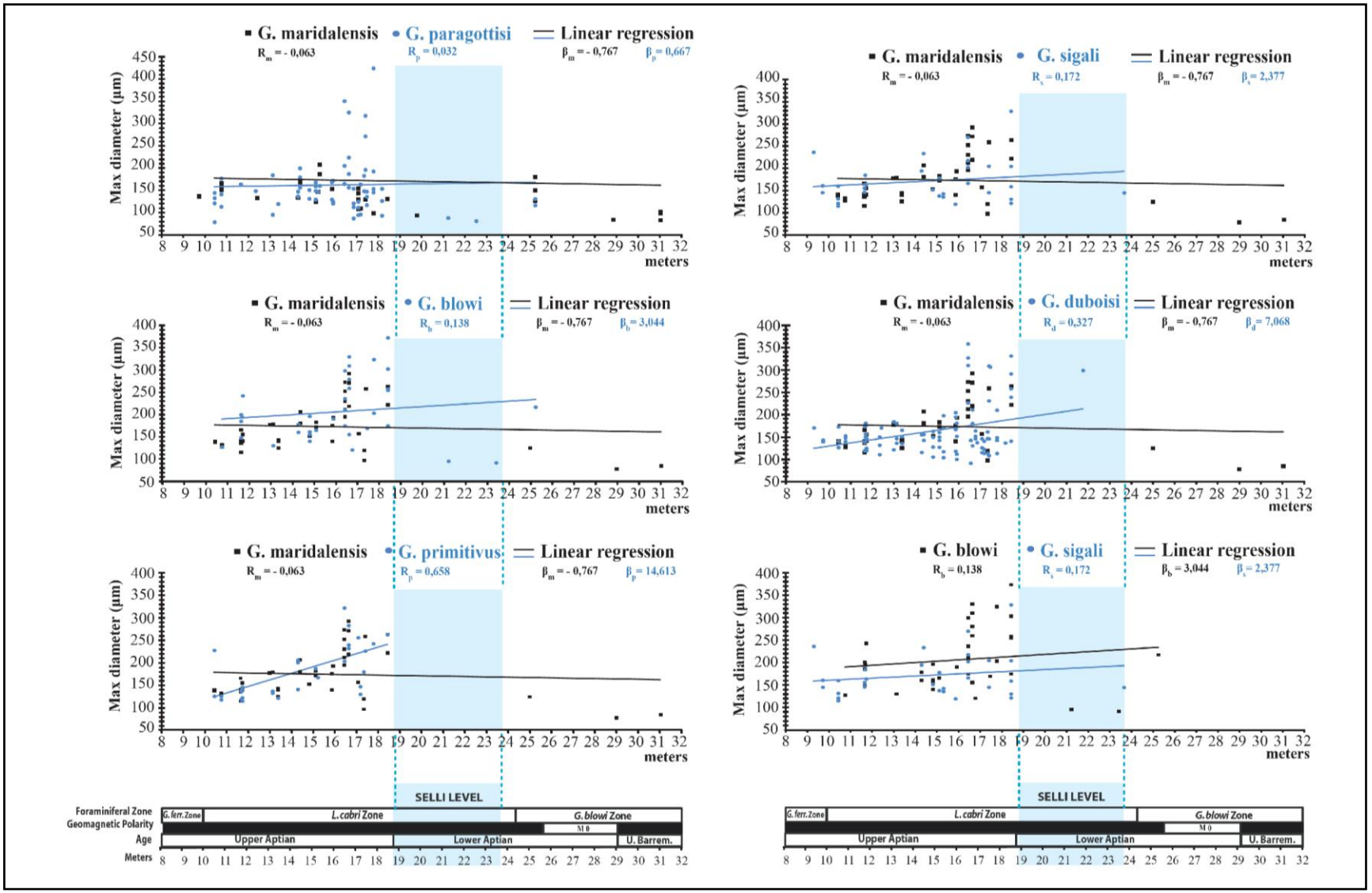

Graph 9. Cismon core. Relationship between test size variations of Globigerinelloidids and depth. R = Pearson's coefficient, β = angular coefficient.

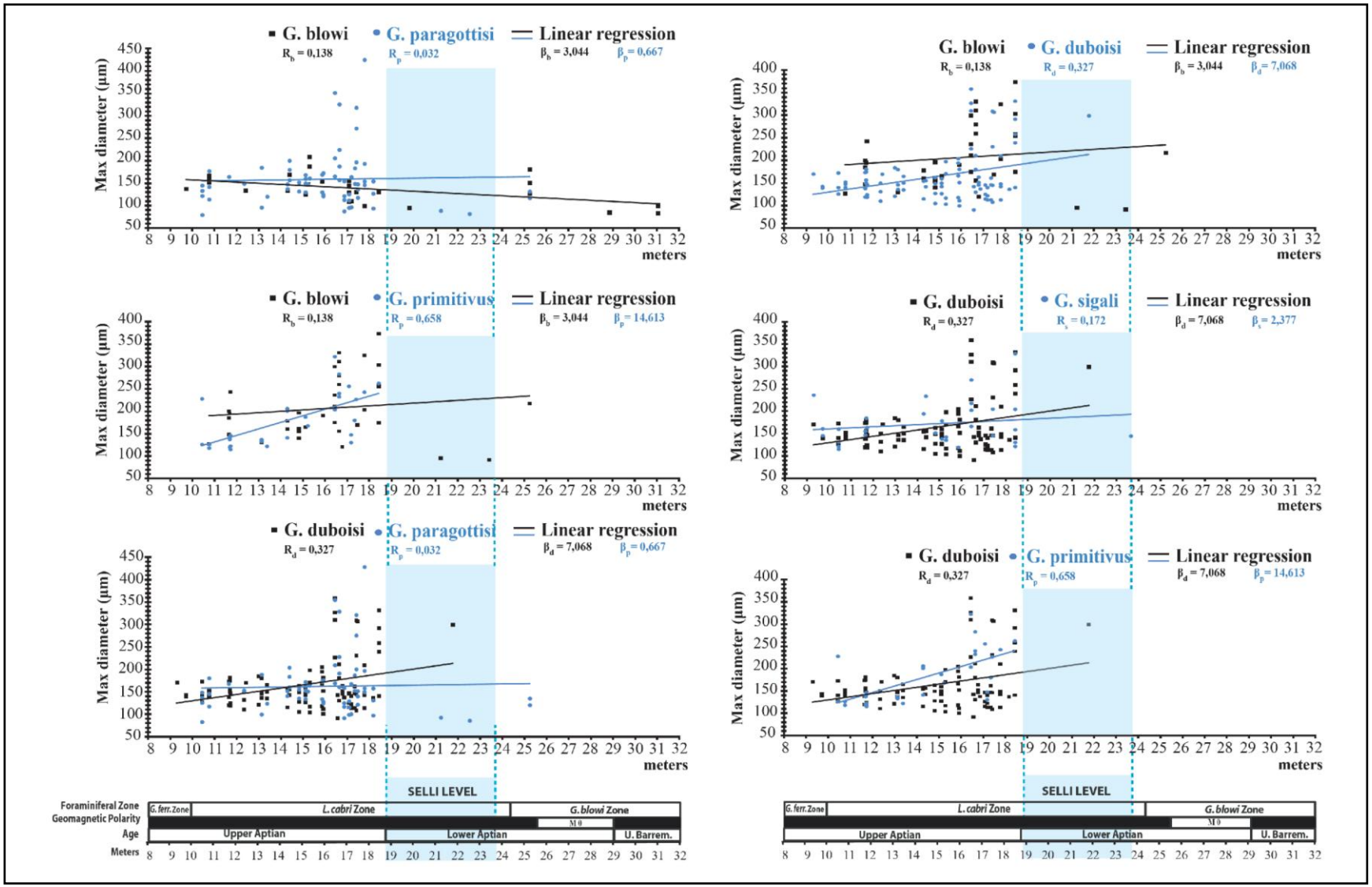

Graph 10. Cismon core. Relationship between test size variations of Globigerinelloidids and depth. R = Pearson's coefficient, β = angular coefficient.

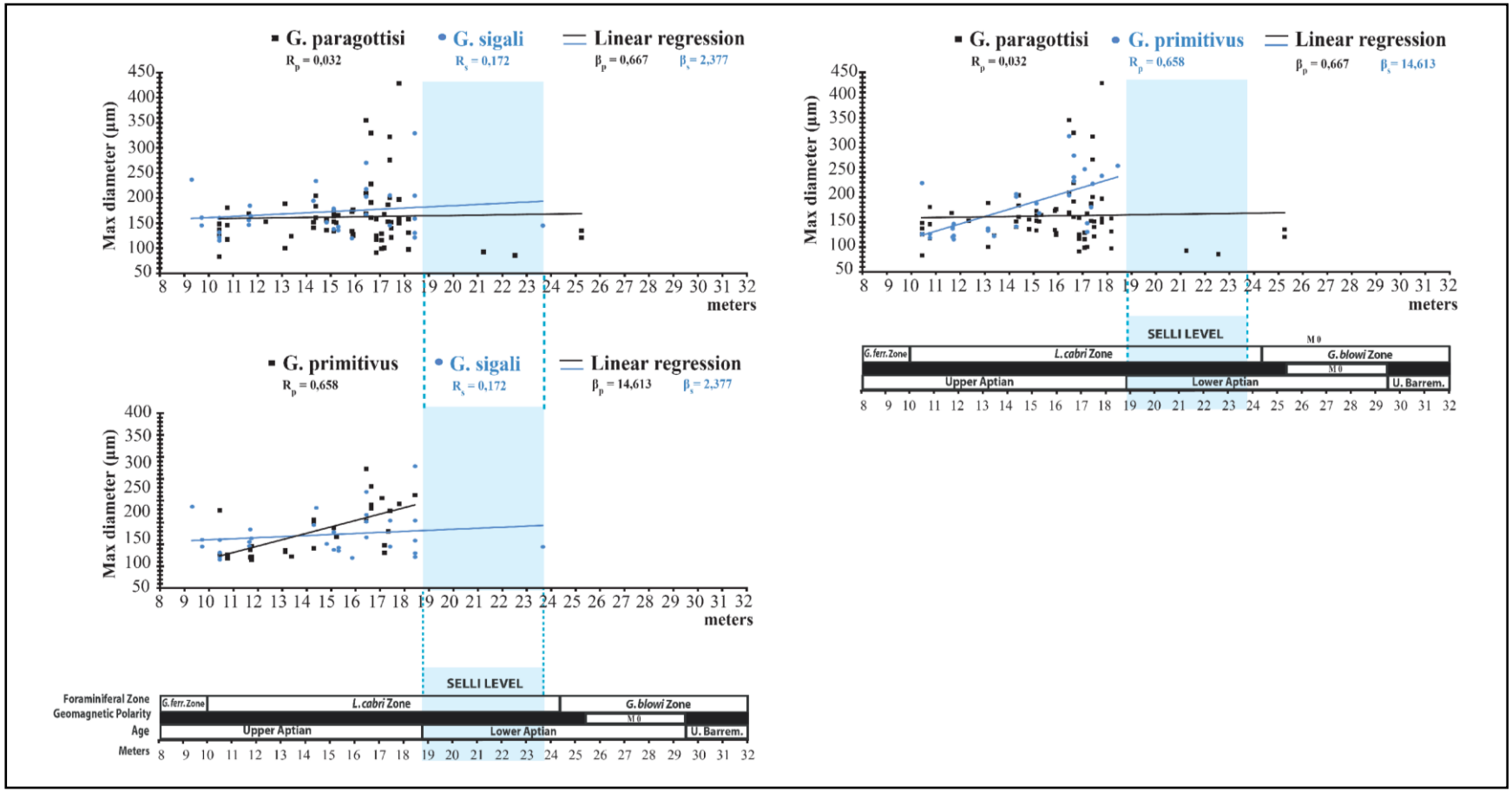

Graph 11. Cismon core. Relationship between test size variations of Globigerinelloidids and depth. R = Pearson's coefficient, β = angular coefficient.

Acknowledgments

First, I would like to warmly thank my supervisor Dr. Maria Rose Petrizzo, who supported me throughout my thesis, sharing her knowledge with passion, patience and constancy. I am truly grateful for being worthy of your trust and for all the beautiful working adventures of the last 3 years, experiences I will never forget.

A deep thank goes to Prof. Isabella Premoli Silva, for her precious and helpful suggestions at every step of my research.

My thanks go to Prof. Elisabetta Erba for her support, knowledge and useful advices.

I would like to thank Fabrizio Felletti for his suggestions.

My thanks go to Cinzia for her availability and advices.

I want to thank Agostino Rizzi for the SEM images and Curzio Malinverno for all the thin sections prepared for this thesis.

The Cushman Foundation for Foraminiferal Research (William V. Sliter Research Award) is warmly thanked for financial support.

During my period as a Ph.D. student I had the opportunity to meet a lot of people who made this experience a great one. My special thanks go to my wonderful workmates Irene, Giulia and Gaia for all these years together in our room (Office n° 70), the best in the world. You made my time unforgettable.

I would like to thank Francesca for sharing with me my daily work in Milan and almost all of my working adventures, without you they would not have been so memorable and funny.

Special thanks go to Federica for supporting me every time and sharing very funny and unforgettable moments.

My thanks go to Silvia, Cristina, Fabio, Michele, Claudio, Dario, Andrea, Irene B., Gabriele and Sara for all the time spent together on the 2th floor of our Department.

Thanks to my long-standing best friends Paola and Rosalia, for teaching me that true friendship doesn't know any distance.

I would like to truly thank Benedetta for her constant support during these months, it has been so precious to me.

Thanks to Marina for her advices, knowledge, teachings and support during these years.

Thanks to my roommates Teresa, Valeria, Silvia and my friends, Giuseppe (known as Maestro), Stella, Ludovica, Nilesh, Harsh, Giulia, Giacomo and Giuseppe R. for all the enjoyable moments.

A special and deep thank goes to Anna, Luigi, Daniel and Xiomara: you have been and will always be like a family to me.

Finally, I am deeply and forever indebted to my family to have supported me during these long years in many ways, since I came in Milan as a Master student.